The Role of Cytokinin Signalling in Rice Root Vascular Patterning

John Vaughan-Hirsch B.Sc. (Hons)

Thesis submitted to the University of Nottingham for the degree of Doctor of Philosophy

September 2017

Abstract

The vascular anatomy of rice roots is an important factor in drought tolerance, but little is known about the mechanisms governing its patterning. The *Arabidopsis thaliana* root vascular tissues are patterned by a mutually inhibitory feedback loop between auxin and cytokinin signalling (Mähönen et al. 2006). Cytokinin signalling in the procambium promotes accumulation of auxin in neighbouring cells which consequently differentiate as xylem. In these cells, high auxin levels promote expression of the pseudo-histidine phosphotransfer protein (PHP) AHP6, an inhibitor of cytokinin signalling (Bishopp et al. 2011). Whereas the root vasculature of *Arabidopsis* consists of a single xylem axis with phloem poles on either side, that of rice roots show a central metaxylem vessel surrounded by multiple xylem poles, between which are phloem. I hypothesised that the basic interaction between auxin and cytokinin in vascular patterning is conserved between *Arabidopsis* and rice, but is adapted to enable development of these different tissue patterns.

Chemical treatments revealed that auxin and cytokinin are central regulators of root vascular patterning in rice, as is the case in *Arabidopsis*. In an effort to test whether this conservation extended to individual components of the molecular circuitry, I examined the role of the three OsPHPs, homologues of AHP6. These genes are not auxin inducible and are not able to rescue the *Arabidopsis* AHP6 mutant, suggesting they do not function in rice root vascular patterning. However, screening known inhibitors of cytokinin signalling for

auxin inducibility in the root tip revealed a subset of the type-A RRs (OsRR1, OsRR6 and OsRR7) are auxin inducible, and were able to rescue the *Arabidopsis ahp6* mutant, suggesting these genes may have been recruited to function in the hormonal crosstalk regulating root vascular patterning.

Phylogenetic analyses revealed a single amino acid substitution in a conserved region of the PHPs which differs between the dicots and the monocots. To directly determine activity of the OsPHPs, and the relevance of these substitutions, in-vitro phosphotransfer assays were performed. Preliminary results suggest these substitutions do not affect protein function. To characterise candidate genes, transcriptional reporters and mutant plants were generated. Reporters show expression of most candidate genes in the root, with some localised to root protoxylem. Mutants were generated using CRISPR and homozygous and heterozygous mutants were identified. Together, results described here give insight into how regulatory networks may be adapted to bring about differing responses.

Acknowledgements

I would like to thank my supervisor, Tony Bishopp, for his direction in the project and encouragement throughout. Thanks also to Malcolm Bennett, all those in CPIB, and my lab mates, George Janes, Ben Goodall, Britta Kümpers and Jekaterina Truskina, who have made Sutton Bonington a genuinely lovely place to work for four years. Special mention goes to Kamal Swarup who did all the useful bits in the lab and behind the scenes.

I am extremely grateful for all the collaborators who I was able to work with during this project. Erik Murchie and Umar Mohammed (UoN) provided seed and physiological data on the African rice cultivars used, Ian Kerr and his lab (UoN) helped hugely in protein expression and purification for the phosphotransfer assays, Christophe Perin's lab (CIRAD, Montpellier) gave me advice on CRISPR construct design, provided plasmids and welcomed me into their lab for a few weeks, and Wanqi Liang (SJTU, Shanghai) and her students did an enormous amount of rice transformation for the reporter and CRISPR constructs. I am also grateful to Jonathan Lynch and his lab group for providing me with the opportunity to carry out a 3 month placement with them.

I would like to thank all the friends I have met here in Nottingham over the last four years, and my family for their continual support throughout. Finally, I would like to thank Dorien, who I met after a more successful than anticipated internship in Arizona, and whose support made all of this much easier and more enjoyable.

Contents

Abstract..... i

Acknowledgements..... iii

Contents..... iv

List of figures..... vii

Abbreviations..... xii

Chapter 1. Introduction 1

1.1 Summary 1

1.2 Structure of vascular tissues 2

1.3 The role of model organisms 3

1.4 The role of plant hormones 6

1.5 Hormonal crosstalk 7

1.6 AHP6 function: Diverse developmental roles 10

1.7 Cytokinin biosynthesis 12

1.8 Cytokinin signalling 16

1.9 Cytokinin transport 22

1.10 Evolution of two-component signalling systems 24

1.11 Specification of the procambium 27

1.12 Maintenance of the procambium 31

1.13 Differentiation of procambial cells 33

1.14 Secondary cell wall development 37

1.15 Communication between pathways 38

1.16 Understanding complex pathways - modelling 40

1.17 Patterning of vascular tissues 42

1.18 *Arabidopsis* vs rice: root architecture 48

1.19 *Arabidopsis* vs rice: root anatomy 49

1.20 Rice: understanding a complex vascular pattern 58

1.21 Project aims 61

Chapter 2. Materials and Methods 62

2.1 Plant material 62

2.2 Growth conditions 62

2.3 qRT-PCR protocol 63

2.4 Genomic DNA extraction 64
2.5 Competent cell preparation 65
2.6 Molecular cloning 67
2.7 Rice transformations 70
2.8 GUS staining 71
2.9 Sectioning and microscopy 72
2.10 Protein expression in bacteria 73
2.11 Protein expression in insect cells 74
2.12 Protein purification 77
2.13 Running PAGE 79
2.14 Performing Western blots 79
2.15 Phosphotransfer assays 80
2.16 Phylogenetic analysis 81

Chapter 3: Auxin and cytokinin function in rice root vascular patterning 82
3.1 Introduction 82
3.2 Root anatomical diversity across cultivars 85
3.3 Root anatomical diversity across different root types 96
3.4 Root anatomic plasticity in response to drought 96
3.5 Root anatomical responses to cytokinin and auxin 103
3.6 Discussion 111
3.7 Summary 114

Chapter 4: OsRR1, OsRR6 and OsRR7 are auxin inducible in the root tip 115
4.1 Introduction 115
4.2 Phylogeny of the HPTs and PHPs 117
4.3 The OsPHPs as candidates for AHP6 function proteins 128
4.4 Candidate genes response to auxin 137
4.5 Candidate genes response to cytokinin 139
4.6 Discussion 144
4.7 Summary 148

Chapter 5. OsRR1, OsRR6 and OsRR7 can rescue *Arabidopsis ahp6* mutants 149
5.1 Introduction 149
5.2 In planta analysis of candidate gene function: Complementation of *ahp6* mutants 151
5.3 In vitro analysis of OsPHP function: Phosphotransfer assays 166

5.4 Bacterial protein expression and purification 168
5.5 Insect cell protein expression and purification 172
5.6 SLN1 kinase domain troubleshooting 175
5.7 Preliminary results of phosphotransfer experiments 177
5.8 Discussion 178
5.9 Summary 180

Chapter 6. Reporters and CRISPR constructs 181
6.1 Introduction 181
6.2 Expression patterns of candidate genes 183
6.3 OsPHP1 expression patterns 186
6.4 OsPHP2 expression patterns 191
6.5 OsPHP3 expression patterns 194
6.6 OsRR1 expression patterns 198
6.7 OsRR3 expression patterns 202
6.8 OsRR7 expression patterns 202
6.9 CRISPR construct design 206
6.10 Genotyping CRISPR transformants 214
6.11 CRISPR mutant phenotyping 220
6.12 Discussion 224
6.13 Summary 227

7. Discussion 228
7.1 Vascular anatomy is primarily dependent on cultivar rather than the environment 228
7.2 Vascular pattern is dependent on stele size 231
7.3 Auxin and cytokinin influence rice root vascular development 234
7.4 OsPHPs are unlikely to function in an AHP6-like manner in rice roots 238
7.5 OsRR1, OsRR6 and OsRR7 may function in an AHP6-like manner in rice roots 244
7.6 Future work 252

References 256

Appendix 289

List of figures:

Figure 1.1. The major pathways of cytokinin biosynthesis in plants 15
Figure 1.2. The *Arabidopsis* two component signalling system 18
Figure 1.3. The organisation of vascular tissues 44
Figure 1.4. Radial sections in *Arabidopsis* reveal the diversity of tissue specific vascular patterns 45
Figure 1.5. Radial sections in rice reveal different vascular organisation 46
Figure 1.6. The diversity of radial anatomy between different rice tissues. 47
Figure 1.7. The root radial vascular patterning of *Arabidopsis* and rice 51
Figure 1.8. The diversity of radial anatomy within different rice root types 53
Figure 1.9. Root types with larger steles show more vascular poles 54
Figure 1.10. Radial sections showing details of *Arabidopsis* and rice root vasculature 56
Figure 3.1. Upland and lowland cultivars root radial sections 88
Figure 3.2. Pipeline of radial anatomy analysis using PHIV Rootcell software 89
Figure 3.3. Upland and lowland cultivars anatomical analyses 91
Figure 3.4. Upland and lowland cultivars physiological measurements 94
Figure 3.5. Upland and lowland cultivars physiological measurements in response to drought 95
Figure 3.6. The number of vascular poles is dependent on stele diameter 97
Figure 3.7. The number of vascular poles changes along the root length 98
Figure 3.8. Root radial anatomy after sorbitol treatment 100
Figure 3.9. Root radial anatomy analyses after sorbitol treatment 101
Figure 3.10. Treatment with BA and NPA lead to changes in vascular anatomy 104
Figure 3.11. Treatment with BA significantly reduces root length and peripheral metaxylem areas 106
Figure 3.12. Primary root radial sections of the rice DR5-GFP reporter 109
Figure 3.13. Stem radial sections of the rice DR5-GFP reporter 110
Figure 4.1. An alignment of the HPTs and PHPs of *Arabidopsis* and rice 118
Figure 4.2. Phylogenetic relationships between the HPTs and PHPs of 38 different species 120
Figure 4.3. Details of phylogenetic relationships between the two core PHP clades of the eudicots and the monocots 121
Figure 4.4. An amino acid identity matrix for the *Arabidopsis* and rice HPTs and PHPs. 124
Figure 4.5. Expression data reveals OsPHPs are not responsive to cytokinin or auxin in roots whereas some type-A RRs show much greater response 129
Figure 4.6. Experimental outline and output from RiceXPro microarray database 134
Figure 4.7. Expression domains of the OsPHPs and a sub set of the type-A RRs 135
Figure 4.8. OsRR1, OsRR6 and OsRR7 are induced by 2 µM IAA in the root tip 138

Figure 4.9. OsRR1, OsRR6 and OsRR7 are induced by 10 µM IAA in the root tip 140

Figure 4.10. OsRR1, OsRR6 and OsRR7 are induced by 1 µM BA in the root tip 141

Figure 4.11. OsRR1, OsRR6 and OsRR7 are induced by 5 µM BA in the root tip 142

Figure 5.1. Fuchsin stained Col-0 showing the presence of two continuous protoxylem poles 154

Figure 5.2. Fuchsin stained *ahp6-1* showing protoxylem developmental defects 155

Figure 5.3. Fuchsin stained *ahp6-2* showing protoxylem developmental defects 156

Figure 5.4. Longitudinal and corresponding radial confocal images of fuchsin stained roots, showing details of variations in protoxylem defects 157

Figure 5.5. Expressing rice candidate genes under the AHP6 promoter in the *ahp6-1* mutant reveals only OsRR1 and OsRR6 partially rescue 159

Figure 5.6. Expressing rice candidate genes under the AHP6 promoter in the *ahp6-2* mutant reveals OsRR1, OsRR6 and OsRR7 partially rescue 160

Figure 5.7. Preliminary bacterial expression experiments 170

Figure 5.8. Purification of proteins expressed in bacteria 171

Figure 5.9. Protein gels and corresponding Western blots showing expression of protein in insect cells 174

Figure 5.10. Glutathione sepharose bead-bound SLN1-HK and SLN1-HK-Rec is functional in preliminary phosphotransfer assays 176

Figure 6.1. GUS activity in roots driven by the OsPHP1 promoter 187

Figure 6.2. GUS activity showing OsPHP1 expression in response to hormonal treatment 189

Figure 6.3. Expression of PHP1 and GUS in the roots of the PHP1 reporter 190

Figure 6.4. GUS activity showing OsPHP1 expression in leaves 192

Figure 6.5. GUS activity in roots driven by the OsPHP2 promoter 193

Figure 6.6. GUS activity showing OsPHP2 expression in response to hormonal treatment 195

Figure 6.7. GUS activity showing OsPHP2 expression in leaves 196

Figure 6.8. GUS activity in roots driven by the OsPHP3 promoter 197

Figure 6.9. GUS activity showing OsPHP3 expression in leaves 199

Figure 6.10. GUS activity in roots driven by the OsRR1 promoter, and under hormonal treatment 200

Figure 6.11. GUS activity showing OsRR1 expression in leaves 201

Figure 6.12. GUS activity in roots driven by the OsRR3 promoter 203

Figure 6.13. GUS activity in roots driven by the OsRR3 promoter in response to hormonal treatment 204

Figure 6.14. GUS activity showing OsRR3 expression in leaves 205

Figure 6.15. GUS activity in roots driven by the OsRR7 promoter 207

Figure 6.16. GUS activity showing OsRR7 expression in response to hormonal treatment 208

Figure 6.17. GUS activity showing OsRR7 expression in leaves 209

Figure 6.18. The CRISPR-Cas9 sgRNA system and off-target predictions 211

Figure 6.19. Details of sequencing of homozygous mutants in OsPHP3 and OsRR7 216

Figure 6.20. Details of the homozygous mutations generated through CRISPR 217

Figure 6.21. Electropherograms showing the four independent heterozygous mutants identified in OsPHP3 218

Figure 6.22. Electropherograms showing the two independent heterozygous mutants identified in OsRR7 219

Figure 6.23. Radial sections of CRISPR mutants show no obvious differences in vascular anatomy 221

Figure 6.24. Plastic sectioning of CRISPR mutants 223

Figure 7.1. The barley *pin1* mutant phenocopies the NPA treatment phenotype seen in rice 236

Figure 7.2. The number of AuxRE sequences in the promoters of AHP6 and the OsPHPs and type-A OsRRs studied 243

Figure 7.3. Phylogenetic relationships between the type-A RRs of 38 different species 247

Figure 7.4. The type-A RR AtARR17 is induced by auxin and cytokinin treatment 250

Appendix figures/tables:

Appendix Figure 1. Plasmid maps of pDONR_221 and pDONR_P4P1R_AHP6 289

Appendix Figure 2. Plasmid maps of p2Rp3-nosT2 and pHm34GW 290

Appendix Figure 3. Plasmid map of pGEX-6p-1 291

Appendix Figure 4. Plasmid maps of pJET1.2 and pCAMBIA1305.1 292

Appendix Figure 5. Plasmid maps of pOssgRNA and pHUBIcas9-7 293

Appendix Figure 6. The list of species used in the phylogenetic study, along with the corresponding two letter identifiers used 294

Appendix Figure 7. Tissue expression profile data for a subset of the rice PHPs and type-A RRs 295

Appendix Figure 8. Tissue specific expression patterns of candidate genes in rice 298

Appendix Figure 9. Expression of the OsAHPs in response to auxin or cytokinin treatment 300

Appendix Figure 10. Biological replicates for expression levels determined by qRT-PCR indicate the same trends in gene expression 301

Appendix Figure 11. Scores for multiple independent transgenic lines for trans-complementation of *ahp6-1* and *ahp6-2* with AHP6 302

Appendix Figure 12. Amino acid sequence similarity between the type-A RRs of *Arabidopsis* and rice 303

Appendix Table 1. qRT-PCR primers 304

Appendix Table 2. Gateway cloning primers 305

Appendix Table 3. Gibson cloning primers 305

Appendix Table 4. Phosphotransfer assay cloning 306

Appendix Table 5. Site directed mutagenesis primers 306

Appendix Table 6. Promoter amplification primers 307

Appendix Table 7. CRISPR protospacer oligos 308

Appendix Table 8. CRISPR genotyping primers 308

Appendix Table 9. Sequencing primers 309

Mellor et al. paper (in review) 310

Abbreviations:

µl	Micro liter
µm	Micro meter
µM	Micro Molar
ARR	Type-A Response Regulator
At	*Arabidopsis thaliana*
BA	6-Benzylaminopurine
bp	Base pair
cDNA	Complementary DNA
CK	Cytokinin
ddH2O	Double-distilled water
DNA	Deoxyribonucleic Acid
GFP	Green Fluorescent Protein
GUS	Beta-glucuronidase
HK	Histidine Kinase
HPT	Histidine Phosphotransfer protein
IAA	Indole-3-acetic acid
mRNA	Messenger RNA
NPA	1-naphthylphthalamic acid
OD600	Optical Density at 600 nm
Os	*Oryza sativa*
PCR	Polymerase Chain Reaction
PHP	Pseudo-Histidine Phosphotransfer protein
PIN	Pin-Formed
qRT-PCR	Quantitative Reverse Transcription- PCR
RNA	Ribonucleic Acid
RR	Response Regulator
SDS	Sodium Dodecyl Sulphate
T-DNA	Transfer-DNA

Chapter 1. Introduction

1.1 Summary

The evolution of vascular tissues was one of several major factors which enabled expansion of land plants (Kenrick and Crane, 1997). The importance of this change can be seen by considering the dominance of vascular plants (tracheophytes) over nonvascular plants (which include green algae and mosses). With domination of land comes diversity, and this can be seen in the structure of the vasculature itself. The patterning of vascular tissues is adapted to serve particular organs, and these patterns differ across the Tracheophyta. In roots, vascular pattern ranges from the simple diarch pattern of *Arabidopsis thaliana* roots to the complex polyarch pattern of rice roots. There are numerous molecular mechanisms involved in development of root vascular tissues, and among them a mutually inhibitory feedback loop between the plant hormones cytokinin and auxin was discovered as crucial in setting up tissue boundaries in the *Arabidopsis* vasculature. Given the importance of this conductive tissue, it might be expected that the principles underpinning these mechanisms would be evolutionarily conserved. This project investigates the level of conservation shared between vascular patterning in rice and *Arabidopsis*. Studying development of the *Arabidopsis* vascular pattern aids an understanding of development of more complex vascular patterns such as that of rice, and may offer an understanding of how regulatory networks can produce a diversity of different patterns.

1.2 Structure of vascular tissues

The vasculature consists of three main tissue types; xylem, phloem and the meristematic tissues which give rise to the conductive tissues, the procambium and vascular cambium. The xylem has a dual function of transporting water, minerals and plant hormones from roots to shoots, and providing the plant with a mechanical support structure. The phloem transports carbohydrates produced by photosynthesis as well as additional hormones, proteins and mRNAs involved in development (De Lucas and Brady, 2013). Within the xylem it is the tracheary elements, which at maturity are emptied entirely of their cell contents, which form the lignified hollow vessels that transport liquids (Turner, Gallois, & Brown, 2007). Together with tracheary elements, the xylem parenchyma (which provides metabolic support) and xylem fibres (responsible for the load bearing strength of the vasculature) form the xylem. The sieve elements are the conducting cells of the phloem and unlike xylem tracheary elements, they remain alive and are supported by non-conducting companion cells, which are also involved in transport of photoassimilates between sieve elements and source or sink organs (Heo et al., 2014). In addition, the phloem is supported by phloem fibres and phloem parenchyma cells which provide mechanical and metabolic support. The procambium consists of vascular stem cells which are derived from the apical meristems, and differentiate to form vascular tissues in primary vascular development. Procambial cells lie parallel to the developing vascular bundle and undergo characteristic divisions parallel to this axis, unlike surrounding cells which usually divide perpendicular to the axis of growth (Smith, 2001). The vascular cambium is the meristematic tissue

responsible for maintenance of the secondary or lateral vasculature. One key difference in growth patterns between the major plant groups is the absence of vascular cambium in monocots, which do not undergo secondary thickening. In dicots and gymnosperms the vascular cambium (which derives from the procambium in roots and hypocotyl, or parenchyma and endodermis in shoots) forms a lateral tissue layer which gives rise to the secondary vasculature, consequently leading to thickening of tissues (reviewed by Nieminen, Blomster, Helariutta, & Mähönen, 2015). Extensive development of secondary vasculature in woody plants lends enormous structural support to these plants and enables development of diverse growth types (reviewed by Spicer & Groover, 2010). The visually comparative thickening seen in some monocots (such as *Aloe*, *Agave*, *Yucca*, *Dracaena* and *Cordyline*) usually arises from parenchyma cells of the cortex or pericycle (Rudall, 1991). Primary vascular development however, refers to the initial development of vascular tissues at the apical meristems which occurs in all vascular plants. It is the patterning of the primary vasculature that is the major theme in this thesis.

1.3 The role of model organisms

As is the case with many developmental processes, the understanding of how development of the vasculature is controlled has been greatly aided through studies using *Arabidopsis* as a model experimental system. The relatively small genome size, ease of growth and short life span meant *Arabidopsis* became a popular plant to work on, and the growing body of research and corresponding

resources secured its role as a model plant. Despite the diversity within the plant kingdom, *Arabidopsis* has proven useful in transferring knowledge to many other species, including high value crops. Two examples of how the basic molecular mechanisms controlling radial root patterning in *Arabidopsis* have been translated into other species include the development of vascular cambium in poplar, and the endodermis in rice. The use of *Arabidopsis* as a model to study the secondary thickening which leads to wood formation in dicots has proven fruitful (reviewed by Zhang et al., 2011a). Previous studies demonstrated that the phytohormone cytokinin plays a crucial role in the proliferation of the *Arabidopsis* vascular cambium (Werner et al., 2003, Matsumoto-Kitano et al., 2008). Armed with this knowledge, Nieminen et al. (2008) showed that cytokinin is required for activity of the vascular cambium in poplar trees by overexpressing an *Arabidopsis* cytokinin oxidase (which irreversibly inactivates bioactive cytokinins) in the vascular cambium of poplar. Phenotypic analysis of the resulting cytokinin deficient trees showed that the reduced cytokinin levels in the cambium were associated with a reduced number of cambial cells, indicating the role of cytokinin in vascular cambium proliferation is evolutionarily conserved. Knowledge from *Arabidopsis* has also been translated to more distantly related species. An elegant study by Cui et al. (2007) made use of *Arabidopsis* to unpick the molecular mechanisms controlling development of the root endodermis, the cell layer surrounding the stele. The two primary transcription factors involved in this process are SHORT ROOT (SHR) and SCARECROW (SCR). It had already been shown that SHR is expressed in the stele and localises to nuclei in the adjacent cell layer where it

controls SCR expression, which consequently promotes cell division and specification of the endodermis (Nakajima et al., 2001). Cui et al. (2007) confirmed this and found that the direct binding of SHR and SCR causes sequestration of SHR in endodermal nuclei. They also found that a positive feedback loop of the SHR/SCR dimer promoting SCR expression provides a pool of SCR in the endodermis, which ensures sequestration of SHR only in endodermal nuclei. The observation that most plants have a single endodermal layer led researchers to consider whether the mechanism of *Arabidopsis* endodermis specification is evolutionarily conserved. Remarkably, two of the four rice homologues of SHR and SCR (OsSHR1 and OsSCR1) showed analogous expression patterns and binding specificity as the *Arabidopsis* genes, and these genes were observed to bind to *Arabidopsis* SCR and SHR, respectively (Cui et al., 2007). This study provides support for the hypothesis that this mechanism is highly evolutionarily conserved. However, some differences in the mechanism of action of the SHR/SCR from *Arabidopsis* and rice have been observed. In *Arabidopsis*, the binding of SHR to SCR (and consequent sequestration of SHR in endodermal nuclei) prevents SHR movement beyond the endodermis (Cui et al., 2007). However, when expressed in *Arabidopsis* the SHR homologues in rice and *Brachypodium distachyon* (all of which bind *Arabidopsis* SCR) move out from the stele to several cell layers beyond the endodermis, where they lead to the development of supernumerary cortex cell layers (Wu et al., 2014). Since SHR homologues bind AtSCR (with similar interaction levels as AtSHR-AtSCR) and are nuclear localised upon binding, yet are not restricted to the endodermal layer like AtSHR, the authors proposed

the existence of an unknown SCR-dependent factor which restricts movement of AtSHR but not the homologues (Wu et al., 2014). This hypothesis is supported by previous studies which showed that upon inclusion of a nuclear export signal, cytoplasmic AtSHR-GFP is still restricted to the endodermis (Gallagher & Benfey., 2009). In addition, when AtSHR is expressed in the epidermis, it shows little movement into the cortex unless in the absence of functional AtSCR (Sena et al., 2004). As well as controlling ground tissue development in *Arabidopsis*, it was recently found that overexpression of AtSHR and OsSHR2 leads to the development of supernumerary cortex cell layers in rice, suggesting a conserved function of SHR genes in cortex development (Henry et al., 2017). While SHR is necessary for endodermis and cortex development, SHR alone is not sufficient for development of these tissues, implying the existence of other regulatory factors which function in consort with SHR and SCR signalling (Yu et al., 2017). In this example, the initial transfer of knowledge from *Arabidopsis* to rice may enable a better understanding of AtSHR function, showing the importance of studying multiple species.

1.4 The role of plant hormones

As signalling molecules which regulate just about every aspect of plant growth and development imaginable, the plant hormones have a rich history of research. The first of the major plant hormone classes to be studied in any detail was the auxins in the early 1900s (reviewed in the seminal book

'Phytohormones' by Went and Thimann, 1937). Assays developed by Went (1928), involving placing an agar block containing test compounds on an excised coleoptile to measure a physiological response (coleoptile elongation or curving), led to the identification of auxins as important regulators of plant growth. Since then, a number of classic experiments revealed the importance of auxins in a number of developmental processes (reviewed by Enders & Strader, 2015). Soon after the chemical characterisation of auxin as indole-3-acetic acid (IAA) by Thimann & Koepfli (1935), it was discovered that another compound in coconut milk promoted cell division in tissue culture (Van Overbeek, Conklin, & Blakeslee, 1941). Efforts to understand this effect led to the identification of a breakdown product of DNA as the first cytokinin in 1955 (Miller et al., 1955). This compound was named kinetin for its effect of promoting cytokinesis. Identification of other cytokinins soon followed (Letham, 1963; Miller, 1961;). As was the case with our understanding of the role of auxin, cytokinin was soon discovered to be involved in many different developmental processes aside from cell division (reviewed by Hwang et al., 2012). Aside from auxin and cytokinin, a number of other plant hormones have been discovered, each involved in regulation of a sub-set of diverse developmental processes.

1.5 Hormonal crosstalk

As is the case for many plant hormones, cytokinin often interacts with other phytohormone pathways in a complex network of crosstalk, one notable

example being with auxin (reviewed by El-Showk et al., 2013). Auxin and cytokinin signalling pathways have been known to interact at many levels, often in an antagonistic manner. Skoog and Miller (1957) demonstrated in their classic tobacco callus experiment that the ratio of auxin:cytokinin regulates organogenesis, with higher auxin levels favouring root development and higher cytokinin levels favouring shoot development. Since then, many other examples of crosstalk between auxin and cytokinin have been discovered (reviewed by El-Showk et al., 2013). A number of studies have shown certain cytokinin biosynthesis genes are upregulated by auxin (Miyawaki et al., 2004), while others are negatively regulated by auxin (Takei et al., 2004, Nordström et al., 2004). As well as cytokinin biosynthesis, auxin has also been shown to influence cytokinin signalling at various levels. During the formation of the root apical meristem (RAM), it was shown that auxin induces expression of the type-A RRs *ARR7* and *ARR15* in the basal cell lineage, whereas in the SAM auxin represses expression of these genes (Muller and Sheen, 2008, Zhao et al., 2010). Expression of *ARR7* and *ARR15* in both locations leads to a reduction in cytokinin signalling, which in turn influences the existing meristem maintenance machinery. This suggests auxin and cytokinin signalling pathways interact in an antagonistic manner in the RAM, but a synergistic manner in the SAM to enable proper development of the apical meristems (Zhao et al., 2010).

Cytokinin has also been shown to induce auxin biosynthesis (Jones et al., 2010) and affect auxin signalling in a number of ways. Most of the auxin signalling responses to cytokinin are mediated through the effects of cytokinin on the PIN auxin efflux transporters. Dello Ioio et al. (2008) proposed a mechanism

whereby auxin and cytokinin signalling pathways converge on the Aux/IAA protein *SHY2*, an auxin response inhibitor, to regulate cell differentiation and division in the RAM. In this pathway, the type-B RR ARR1 (a positive regulator of cytokinin signalling) induces expression of *SHY2* which in turn represses expression of PIN proteins as well as cytokinin biosynthesis genes, leading to redistribution of auxin and consequent cell differentiation. Auxin signalling, on the other hand, leads to the proteosomal degradation of *SHY2*, enabling maintenance of PIN protein expression and consequent auxin mediated cell division. These negative feedback loops, which are set up by the antagonistic relationship between auxin and cytokinin, therefore allow careful regulation of RAM size (Dello Ioio et al., 2008). More detailed studies have shown that cytokinin regulates PINs post-transcriptionally (Zhang et al., 2011b) via PIN endocytic trafficking to lytic vacuoles where they are degraded, resulting in rapid changes in auxin distribution in response to cytokinin (Marhavy et al., 2011). More recently, it has been shown that cytokinin is capable of promoting degradation of PIN1 at specific polar locations, according to the degree of phosphorylation of PIN1 (Marhavy et al., 2014). This has important implications for developmental systems which require rapid redirection of auxin flow, such as lateral root organogenesis (Marhavy et al., 2014).

The involvement of cytokinin in the maintenance of the procambium can be clearly seen by considering the cytokinin receptor mutant *wol*, or the *cre1 ahk2 ahk3* triple mutant, both of which show development of ectopic protoxylem in place of procambium in *Arabidopsis* roots (Mähönen et al., 2006, Mähönen et al., 2000). On the other hand, application of exogenous cytokinin or a mutation

in the inhibitor of cytokinin signalling *ARABIDOPSIS HISTIDINE PHOSPHOTRANSFER PROTEIN 6* (*AHP6*) results in loss of protoxylem development (Mähönen et al., 2006). Cytokinin has also been shown to interact with auxin to pattern the root vasculature. While a lack of cytokinin signalling leads to protoxylem development, a lack of auxin signalling due to a dominant *axr3-1* mutation, or treatment with the auxin transport inhibitor NPA, inhibits protoxylem development in the proximal meristem (Bishopp et al., 2011). The molecular mechanisms governing this mutual inhibitory feedback loop have been uncovered by Bishopp et al. (2011). In this loop, cytokinin promotes lateral localisation of the PIN auxin efflux carriers PIN1 and PIN7 in procambial cells, possibly via phosphorylation of particular residues within the PIN proteins themselves (Weller et al., 2017; Zhang et al., 2010). This leads to an accumulation of auxin in a central axis of meristematic cells in the protoxylem position. A high level of auxin signalling at this location specifies protoxylem cell fate and induces expression of the pseudo-histidine phosphotransfer protein (PHP) AHP6, which in turn inhibits cytokinin signalling and is itself inhibited by cytokinin. This results in a clear boundary between the procambial cells which show high levels of cytokinin signalling, and the protoxylem cells which show high levels of auxin signalling.

1.6 AHP6 function: Diverse developmental roles

As an auxin inducible inhibitor of cytokinin signalling, AHP6 plays a clear role in mediating the relationship between auxin and cytokinin signalling in root

protoxylem patterning (Bishopp et al., 2011; Mähönen et al., 2006). As mentioned, auxin and cytokinin have been shown to act in consort to regulate many developmental processes. In *Arabidopsis* pseudo HPTs are represented by one member (AHP6) which has been shown to function in many of these diverse developmental roles. In *Arabidopsis*, lateral root primordia develop from specific pericycle cells in a process dependent on auxin and cytokinin signalling. AHP6 plays a crucial role in this process, demonstrated by the mutant phenotype displaying abnormal orientations of pericycle cell divisions (Moreira et al., 2013). AHP6 was also shown to influence localisation of PIN1, which is required for correct patterning of lateral root primordia. The roles of AHP6 may correlate with the roles of orthologues of AHP6 in other species. To understand this, Moreira et al., (2013) drove GUS expression under the AHP6 promoter in *Medicago* and found that the promoter was active in lateral roots and in developing root nodules. This suggests that the *Medicago* homologues of AHP6, which were subsequently identified and are yet to be examined in detail, may function in lateral root development and possibly in root nodule development, an organ absent in *Arabidopsis*.

Aside from its involvement in patterning processes in roots, AHP6 has also been shown to function in patterning processes in the shoot apical meristem (SAM), which were previously thought to be regulated primarily by auxin distribution. Patterns of AHP6 expression within the SAM enable optimisation of organ initiation temporally, thereby enabling better control of phyllotactic development (Besnard et al., 2014). In addition, it is likely that auxin and cytokinin act in a synergistic manner in the SAM during organ initiation

(Besnard et al., 2014). More recently, a role for AHP6 in development of the gynoecium has been revealed. Cytokinin activity is restricted to the gynoecium 'medial domain' via the inhibitory action of AHP6 (and possibly the type-A RR ARR16) which is expressed in the lateral domains (Reyes-Olalde et al., 2017). In the medial domain, cytokinin signalling (via action of the bHLH SPATULA) is required for maintenance of the carpel margin meristem, the meristematic tissue from which internal gynoecium structures arise (Reyes-Olalde et al., 2017).

1.7 Cytokinin biosynthesis

In order to understand the role of cytokinin in vascular patterning, it is helpful to consider the cytokinin biosynthesis and signalling pathway as a whole. The cytokinins comprise a family of N^6-substituted adenine derivatives which are involved in a wide variety of developmental processes, often interacting with auxin (reviewed by Vanstraelen and Benkova, 2012). The naturally occurring bioactive cytokinins can be divided into two groups based on the species at the N^6 position, which will be either an isoprenoid (branched-chain unsaturated hydrocarbon) or an aromatic (cyclic and planar) moiety. Bioactive cytokinins may also be metabolised to a number of biologically inactive conjugates, allowing the level of active cytokinins to be carefully controlled. In plants, isoprenoid cytokinins are found in much higher abundance than aromatic cytokinins, with the two major bioactive derivatives being N^6-(Δ^2-isopentenyl)-adenine (iP) and *trans*-zeatin (tZ) (reviewed by Mok and Mok, 2001). The

isoprenoid cytokinins tZ and *cis*-zeatin (cZ) are isomers formed by hydroxylation of the isoprenoid side chain at the *trans*- or *cis*- terminal region respectively. Despite high abundance in some species, cZ has been consistently shown to have little or no biological activity in a number of bioassays in various species (Schmitz and Skoog, 1972, Mok et al., 1978, Kamínek et al., 1987). However, more recent studies have revealed that levels of cZ in *Arabidopsis* increase during conditions which restrict growth, including both abiotic and biotic stresses (Gajdošová et al., 2011; Großkinsky et al., 2013). This suggests cZ may play a role in maintaining basal levels of cytokinin signalling required for survival under growth limiting conditions (reviewed by Schäfer et al., 2015). Indeed, in some species cZ has been shown to have clear physiological roles. Kudo et al. (2012) demonstrated through various bioassays that cZ impacts growth and development of rice in a similar manner to tZ.

Biosynthesis of isoprenoid type cytokinins is thought to take place via two interconnected pathways. In the first, the transfer of an isopentenyl side chain from the donor molecules dimethylallyldiphosphate (DMAPP) or 4-hydroxy-3-methyl-2-(*E*)-butenyl diphosphate (HMBDP), to ATP, ADP or AMP (catalysed by isopentenyl transferase, IPT) results in iP riboside 5'-triphosphate (iPRTP), iP riboside 5'-diphosphate (iPRDP) or iP riboside 5'-monophosphate (iPRMP) products. These products may be subsequently converted to iP, or can be further hydroxylated by P450 monooxygenases to zeatin-type cytokinins (reviewed by Sakakibara, 2006). In the second pathway, the direct transfer of a hydroxylated isopentenyl side chain from the donor HMBDP to the adenine ring can result in production of the zeatin type cytokinins, although little evidence

of this pathway in vivo suggests the former pathway is the major contributor (Sakakibara et al., 2005). These two pathways are summarised in Figure 1.1.

It is also important to consider the biosynthesis of the donor molecules DMAPP and HMBDP. DMAPP can be produced via two different pathways; the mevalonate (MVA) pathway, or the methylerythritol (MEP) pathway. The MVA pathway, which is common to all plants, fungi and animals (and some bacteria) makes use of acetyl-CoA as a precursor which is taken through a series of condensation and reduction reactions to generate mevalonate, which is then phosphorylated and isomerised to produce DMAPP (reviewed by Frebort et al., 2011). The methylerythritol (MEP) pathway however, is bacteria and plastid specific, and uses pyruvate and glyceraldehyde-3-phosphate as precursors which undergo condensation reactions and modifications to produce methylerythritol phosphate. This product is then conjugated to the cytidylphosphate moiety and undergoes various modifications to produce HMBDP. HMBDP can be reduced to another isoprenoid precursor, isopentenyl pyrophosphate, or to a lesser extent, DMAPP (reviewed by Frebort et al., 2011).

For many years the aromatic cytokinins were thought to be synthetic artefacts which do not occur naturally in plants. Indeed, many compounds commonly used in cytokinin research, such as BAP, are synthetic aromatic cytokinins. Research into derivatives of these compounds is ongoing, with the aim of identifying new compounds of biotechnological use (Plíhalová et al., 2016). However, many different aromatic cytokinins (including BAP) have been identified in various species (Horgan et al., 1975; Nandi et al., 1989; Strnad et

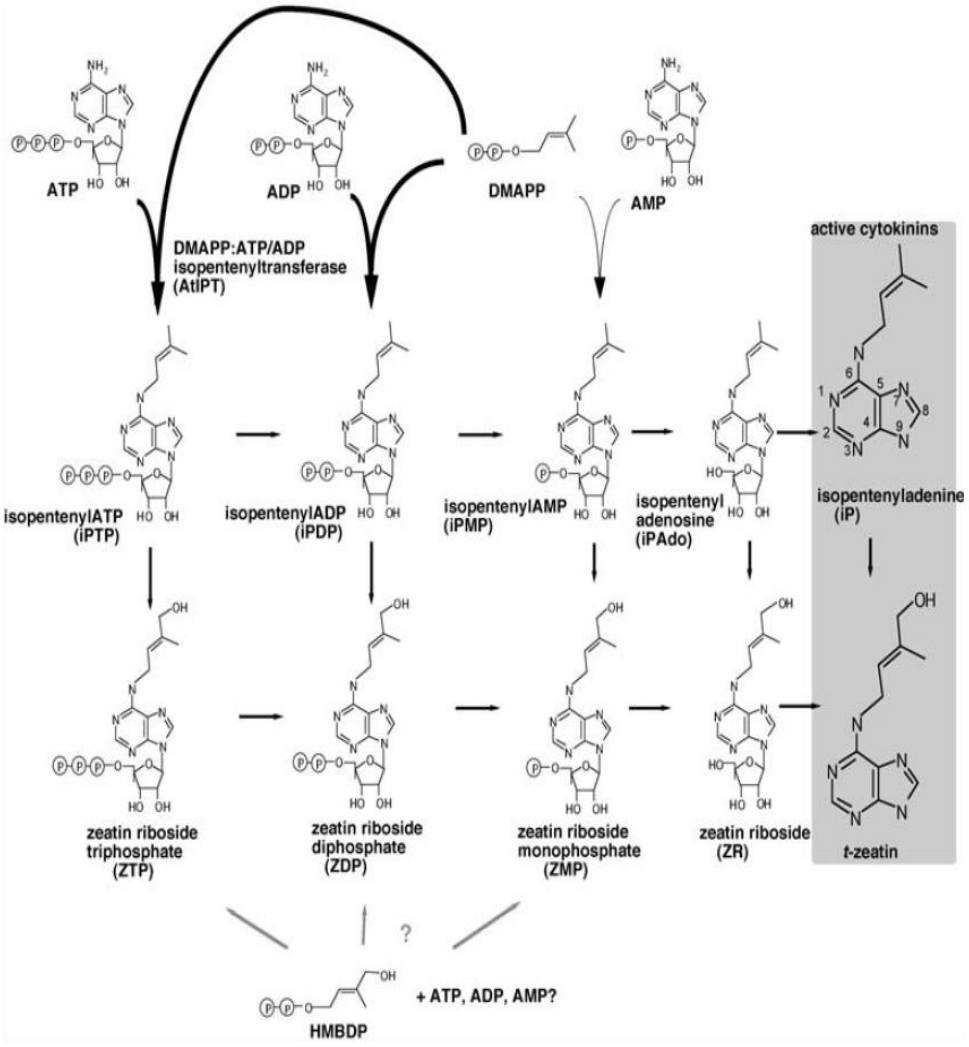


Figure 1.1. The major pathways of cytokinin biosynthesis in plants. Taken from Kakimoto (2003).

al., 1997; Strnad et al., 1994; Tarkowská et al., 2003). This indicates that, despite probable low tissue concentrations in comparison to the isoprenoid cytokinins for most species, the aromatic cytokinins are naturally occurring bioactive cytokinins. Despite this being known for many years now, much of the focus of cytokinin biosynthesis research has been into the isoprenoid-type cytokinins due to their higher abundance. Consequently, we know comparatively little about biosynthesis of aromatic cytokinins (reviewed by Strnad, 1997).

1.8 Cytokinin signalling

Cytokinin signalling occurs via what is known as the two-component signalling system, or the His-Asp phosphorelay. These signalling systems are common in bacteria, and in their most simple form consist of a histidine kinase receptor, which is phosphorylated at a His residue upon activation, and a response regulator protein which receives the phosphoryl group from the receptor at a conserved Asp residue (reviewed by Hwang et al., 2002). Activation of the response regulator in this way leads to further downstream signalling to bring about the appropriate response. In many species this simple system has developed into a more complicated network with hybrid histidine kinases and multiple phosphotransfer steps. This is demonstrated nicely in the *Arabidopsis* two-component system (Figure 1.2). In *Arabidopsis* there are three histidine kinase (HK) cytokinin receptors (AHK2, AHK3 and AHK4/CRE1/WOL1) along with CKI1 which shows constitutive histidine kinase activity independent of cytokinin and lacks the cytokinin binding domain (Hejatko et al., 2009, Deng et al., 2010).

These transmembrane receptors have a common hybrid histidine kinase structure consisting of a cytokinin binding domain known as the CHASE (Cyclases/Histidine kinases Associated Sensory Extracellular) domain, a histidine kinase domain which contains a conserved His residue (which is autophosphorylated upon cytokinin binding to the CHASE domain), and a receiver domain which contains a conserved Asp residue (which receives the phosphoryl group) (reviewed by Steklov et al., 2013). It has been shown that ligand binding specificity differs amongst receptors, and that side chain modifications of cytokinin species directly affect this specificity (Yonekura-Sakakibara et al., 2004). This enables another level of control of the cytokinin signalling pathway.

Downstream of the HK cytokinin receptors, the phosphoryl group is transferred to the conserved His residue of the histidine phosphotransfer proteins (HPTs), which in *Arabidopsis* consist of a family of five proteins (AHP1-5), all of which function to transfer the signal from the cytoplasm to response regulator proteins (RRs) in the nucleus, with the possible exception of AHP4 (Hutchison et al., 2006). AHP4 forms its own clade distinct from the other four HPTs indicating significant protein sequence differences, and the quintuple *ahp1,2,3,4,5* mutant appears to be no more severe than the quadruple *ahp1,2,3,5* suggesting AHP4 is not functional in phosphotransfer (Hutchison et al., 2006). AHP6 is a pseudo HPT (PHP) as it lacks the conserved His domain and consequently cannot function in phosphotransfer. Instead, it has been shown to act as an inhibitor of cytokinin signalling, presumably by competing with the other HPTs to bind the receptor HKs and downstream components (Mähönen

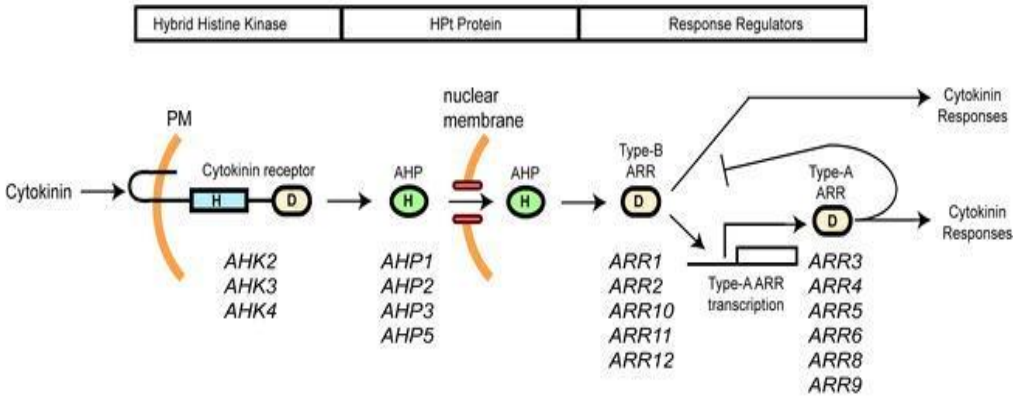


Figure 1.2. The *Arabidopsis* two component signalling system consists of HK receptors, HPts and RRs. Taken from Schaller et al. (2008)

et al., 2006). Restoring the conserved phosphoaccepting histidine domain in AHP6 does allow it to function in phosphotransfer, indicating that this single amino acid substitution is sufficient to change AHP6 from a negative to a positive regulator of cytokinin signalling (Mähönen et al., 2006).

The final components of the two component cytokinin signal transduction pathway are the RRs, which accept the phosphoryl group from the HPTs at a conserved Asp residue and control the diverse responses to cytokinin signalling. The *Arabidopsis* two-component signalling system has 33 RRs which are grouped together into 4 classes based on protein domain organisation and phylogenetic analysis: type-A, type-B, type-C and the pseudo-response-regulators (PRRs) (Hwang, Chen, Sheen, & Hwang, 2002). The 11 type-B RRs are DNA-binding transcription factors which positively regulate cytokinin signalling responses, and also induce expression of the cytokinin inducible type-A RRs. The type-A RRs are a family of 10 proteins which negatively regulate cytokinin signalling, thereby forming a negative feedback loop. This has been confirmed by a number of studies which analysed loss-of-function RR mutants and RR overexpressors (Hwang & Sheen, 2001). It was originally thought the type-A RRs would function simply by sequestering phosphate groups, thereby preventing activation of the type-B RRs and consequent cytokinin dependent gene regulation. However, a mutant version of the type-A RR ARR5 with the receiver Asp substituted to a Glu (a phosphomimic) is able to partially rescue the *arr3,4,5,6* mutant phenotype (To et al., 2007). This indicates ARR5 functions, at least in part, via unknown downstream protein-protein interactions which are dependent on phosphorylation status. It may be the case that some ARRs only

function to sequester phosphate groups, while others may interact with many other unknown proteins to bring about their responses. In addition, for a subset of type-A RRs, phosphorylation increases stability of these proteins (Ren et al., 2009; To et al., 2007). Enabling differences in protein turnover in response to cytokinin signalling in this way may enable functional specificity amongst the type-A RRs. *Arabidopsis* also has two members of the type-C RRs (along with another which is missing the receiver domain) which show structural similarity to the type-A RRs but are phylogenetically and functionally distinct. Despite poor understanding of the exact function of type-C RRs, it is known that they are expressed mainly in flowers and siliques, and overexpression results in inhibition of cytokinin signalling. In addition to these components, *Arabidopsis* also has nine pseudo-response regulators (PRRs), all of which have the receiver domain but are missing components essential for phosphorelay activity (Makino et al., 2000). Many of these proteins are involved in regulation of circadian rhythms. Perhaps the best characterised member is *PRR1/TOC1* which was identified as a component involved in maintenance of circadian rhythms through analysis of the semi-dominant mutation *timing of cab 1-1*, which displayed shortened circadian rhythms in expression of chlorophyll a/b-binding protein (CAB) and leaf movements (Millar et al., 1995).

In addition to this classic view of cytokinin signalling as a single phosphotransfer chain ending with activation of the type-A or B response regulators, a parallel signalling pathway has been discovered. Rashotte et al., (2006) characterised members of the AP2/ERF transcription factor family which are up-regulated in response to cytokinin, to find they transcriptionally regulate cytokinin response

along with the type-B RRs. Consequently, this family of transcription factors was termed the cytokinin response factors (CRFs). The CRFs are up-regulated by the type-B RRs and upon activation (by accepting a phosphate group from the HPTs) they localise to the nucleus where they regulate expression of cytokinin responsive genes, most of which are also regulated by the type-B RRs (Rashotte et al., 2006). Phylogenetic studies have since shown CRFs are present in all land plant lineages and are characterised by having a unique conserved CRF domain (Rashotte & Goertzen, 2010). The CRFs have been shown to function in various aspects of plant development, in part through their interaction with cytokinin signalling (Raines et al., 2016). In addition, they are involved in cross-talk between cytokinin and auxin. The CRFs are able to transcriptionally regulate PIN1 expression in response to cytokinin signalling (Šimášková et al., 2015). This occurs through direct binding of CRFs to the PIN1 Cytokinin Responsive Element (PCRE1) in the PIN1 promoter, confirmed by plants lacking the PCRE1 domain phenocopying the *crf2 crf3 crf6* triple mutant (Cucinotta et al., 2016). CRFs may also link cytokinin signalling with other pathways. Zwack et al., (2016) found CRF6 is induced by oxidative stress, and by comparing transcriptomic changes in response to oxidative stress in wild type plants or the *crf6* mutant background, authors identified many genes down-regulated by oxidative stress in a CRF6-dependent manner. These genes include components of cytokinin biosynthesis, signalling and transport, and thus provide a link between cytokinin and the response to oxidative stress (Zwack et al., 2016).

1.9 Cytokinin transport

The details of auxin movement, including its transport via PIN protein efflux transporters, has been studied in great detail yet comparatively little is known about the distribution of cytokinin and the role of transporters. Early studies showing long distance movement of cytokinin shootward through the xylem and rootward through the phloem implied the existence of cytokinin transporters, which would allow transport into these conductive tissues (Letham & Palni, 1983; Weiler & Ziegler, 1981). It has since been shown there is a bias in distribution of different cytokinin species in these different conductive tissues, with tZ type cytokinins being more abundant in xylem and iP type cytokinins more abundant in phloem (reviewed by Hirose et al., 2008). This suggests specificity in the cytokinin transport systems. To date, three classes of cytokinin transporters have been identified; the purine permeases (PUPs), the equilibrative nucleoside transporters (ENTs) and the ATP-binding cassette (ABC) transporter ABCG14 (reviwed by Kang et al., 2017).

The first cytokinin transporter characterised was AtPUP1, discovered by screening a yeast mutant with deficient adenine uptake with a cDNA expression library from *Arabidopsis* (Gillissen et al., 2000). This study indicated AtPUP1 is able to transport adenine, cytosine, cytokinins and similar compounds such as some purine derivatives and alkaloids into cells. Members of the PUP family have been shown to have differential expression in both *Arabidopsis* and rice, with mutant phenotypes associated with aberrant accumulation of cytokinin (Bürkle et al., 2003; Qi & Xiong, 2013). More recently, a study into cytokinin

distribution in developing embryos revealed AtPUP14 is expressed in the embryonic cotyledons, a region where activity of the TCS reporter is not seen (Zürcher et al., 2016). It was determined that the reason for this lack of cytokinin signalling is due to AtPUP14 importing cytokinins into cells, thereby preventing binding to the plasma membrane localised cytokinin receptors. As a consequence of this a cytokinin sink is produced, which the authors suggest is a critical component regulating morphogenesis (Zürcher et al., 2016). However, many cytokinin receptors are thought to be localised on the endoplasmic reticulum, not the plasma membrane (Ding et al., 2017; Wulfetange et al., 2011). It remains to be seen whether these internal receptors can function in cytokinin signalling.

The other class of proteins involved in cytokinin import are the ENTs. OsENT2 from rice was the first of this class characterised, and it was later shown that *Arabidopsis* AtENT3, AtENT6 and AtENT8 show similar activity (Hirose et al., 2005; Qi & Xiong, 2013; Sun et al., 2005). These proteins function to import nucleosides and nucleoside-type cytokinins, which include the riboside forms (precursors to the bioactive forms) of IPT and tZ. This may suggest accumulation of these compounds can enable a rapid production of bioactive cytokinins when needed.

While the PUP and ENT families are both cytokinin importers, AtABCG14 is the only cytokinin exporter in *Arabidopsis* currently known. This protein is involved in export of cytokinin from sites of biosynthesis and loading them into the xylem (Ko et al., 2014; Zhang et al., 2014). Mutants for *abcg14* accumulate

cytokinin in the root with depletion in the shoot, which leads to slowed shoot growth (Zhang et al., 2014). Grafting *abcg14* mutant shoots onto wild type roots rescues the mutant shoot phenotype, indicating the root derived cytokinins are critical in shoot development (Ko et al., 2014). This implicates ABCG14 in long distance transport of cytokinins.

1.10 Evolution of two-component signalling systems

Linking detailed biochemical studies with phylogenetic analyses enables an understanding of functional changes of proteins throughout evolutionary history, and in turn can shed light on the evolution of hormonal signalling pathways as a whole and the diverse roles they fulfil. Two-component signalling pathways arose in bacteria where they regulate a diverse range of responses, not least involving environmental adaptations (Schaller et al. 2011). These pathways consist of a receptor histidine kinase and a response regulator. The histidine kinase, when activated by binding to its ligand, autophosphorylates and then passes the phosphoryl group onto a conserved aspartate residue within the receiver domain of the response regulator. This activates the response regulator which can then fulfil its function, which is often transcriptional regulation. The signal stops when the phosphoryl group is removed from the response regulator, either spontaneously or when cleaved by an enzyme. Most bacteria utilise two-component signalling systems and many such systems may exist in a single bacterium, all of which have histidine kinases which respond to particular inputs and response regulators which bring

about particular outputs. Despite the diversity of two-component signalling systems and the structural similarity between conserved domains of histidine kinases and response regulators, there appears to be little cross talk between signalling systems in bacteria (Capra & Laub, 2012). Biochemical studies have revealed particular regions within binding domains responsible for this specificity, and coevolution of histidine kinase and response regulator pairs has been widely observed by computational studies (Capra & Laub, 2012). Such a high degree of structural specificity as this is often not seen in eukaryotic signalling systems, possibly in part due to more complex regulation (such as regulating domains of expression) negating the requirement for such specificity.

Within the eukaryotes, it is only plants and fungi which make use of two-component signalling systems. Eukaryotes are likely to have obtained two-component signalling systems via horizontal gene transfer, and these signalling systems have diversified hugely such that the system no longer contains only two-components. Because animals lack TCS components it is not clear whether the eukaryotes acquired this signalling system multiple times, or whether they were lost in animals. However, eukaryotes such as *Dictyostelium discoideum* which diverged before the metazoans, do contain TCS components, suggesting they were present but were lost in animals (Eichinger et al., 2005). The most basal land plant known to contain all four major components of cytokinin signalling (receptor, HPT, type-A and B RRs) is the moss *Physcomitrella patens* (Pils & Heyl, 2009). Interestingly, the Chlorophyceae algae contain only HPTs and type-B RRs (Pils & Heyl, 2009). The function of these proteins in these algae,

and how they were recruited to cytokinin signalling in the basal land plants, remains to be fully understood.

As well as following evolution of particular signalling components, it is interesting to consider the changing function of signalling pathways as a whole. The cytokinin signalling pathway as defined in *Arabidopsis* came together in basic form in *P. patens*, and it is likely this is one change of many which played a crucial role in the colonisation of land by plants. Given the enormous differences between *P. patens* and *Arabidopsis*, it is no surprise that cytokinin signalling will have hugely diverse functions between the two groups. One obvious difference between these two species is the presence of vascular tissue in *Arabidopsis*, which was a critical factor enabling the enormous diversification of the Tracheophytes seen today. In *Arabidopsis* roots, cytokinin signalling is a key pathway which works antagonistically with auxin to specify and maintain development of vascular tissues. Given the importance of properly regulated development of the vascular tissues it may be thought that the molecular mechanisms governing vascular development would be highly evolutionarily conserved amongst the Tracheophytes. However, there is great diversity in vascular plants so this may not necessarily be the case. Whilst the role of cytokinin in vascular development of *Arabidopsis* roots has been well studied, that of other species such as rice is lacking in research. Research in this direction will enable an understanding of how signalling pathways can be adapted throughout evolutionary history, to change or extend the functions they fulfil.

The following sections describe the molecular mechanisms governing specification, maintenance and differentiation of vascular tissues in *Arabidopsis*. Given that the mechanisms and components controlling development of vascular tissues in shoots are different from that of roots, here I focus only on root vascular development unless specifically stated.

1.11 Specification of the procambium

Plant hormones have been shown to regulate many aspects of development including development of the vascular tissues. It has been known since the 1950s that auxin is a crucial factor in development of the vasculature. Early studies demonstrated that excision of a leaf primordia below a wound has no effect on regeneration of vasculature, whereas excision of primordia above a wound dramatically reduces the development of new vascular structures (Jacobs, 1952). Since auxin is predominantly synthesised in leaf primordia and transported basipetally (Rubery and Sheldrake, 1974, Raven, 1975), this study provided the first link between auxin transport and vascular development. Further studies showed that application of auxin to the side of a growing hypocotyl can promote development of new vascular bundles to link the source of auxin to the existing vascular system (Sachs, 1981). More recent characterisation of auxin efflux carriers has provided support for this auxin canalisation hypothesis. The efflux carrier PIN1, for example, is polarly localised and sets up a flow of auxin before the differentiation of the procambium in leaf vein development (Scarpella et al., 2006). The specification of vascular stem

cells is initiated during early embryogenesis in *Arabidopsis*, in the globular stage embryo (De Rybel et al., 2013). At this stage four provascular initial cells can be seen, which differentiate to form vascular tissues and ground tissues. Detailed analysis has revealed the presence of a cell-cell junction between two of these cells, and combining experimental data with mathematical modelling has shown the importance of this initial junction in orienting later cell divisions as vascular tissues differentiate (De Rybel et al., 2014). At this stage of embryonic development expression of the transcription factor MONOPTEROUS (MP)/AUXIN RESPONSE FACTOR5 (ARF5) and its regulator BODENLOS (BDL)/IAA12, is seen in a pattern following auxin accumulation (in the proembryo cells but not the adjacent hypophysis) (Hamann et al., 2002, Hardtke and Berleth, 1998). It has been suggested that this initial asymmetry in auxin accumulation, derived from the developing cotyledons, is the critical symmetry breaking step in embryogenesis (Bishopp et al., 2011; De Rybel et al., 2014). Cells with highest auxin response in the developing embryo eventually differentiate to form xylem, and the influence of cotyledon derived auxin in this process is evidenced by mutants with altered numbers of cotyledons displaying corresponding numbers of vascular poles in the hypocotyl (Help et al., 2011).

Many targets of MP/ARF5 have been identified, such as the bHLH transcription factor *TARGET OF MP 5* (*TMO5*) and the Dof-type transcription factor *TMO6*, both of which are expressed in procambial cells (Schlereth et al., 2010). It was found that successive bHLH loss of function mutants show increasingly severe phenotypes characterised by lack of periclinal cell divisions of the vascular tissues, which results in eventual loss of the vascular tissues (De Rybel et al.,

2013; Ohashi-Ito & Bergmann, 2007; Ohashi-Ito et al., 2013). Overexpression of TMO5 and the bHLH transcription factor LONESOME HIGHWAY (LHW), on the other hand, leads to dramatic increases in cell number (Ohashi-Ito et al., 2014). Expression of *TMO5* in the *MP* domain of an *mp* mutant suppresses vascular defects of the mutant, suggesting one role of TMO5 is mediating the function of MP (De Rybel et al., 2013). TMO5 has also been shown to interact with *LHW*, which was identified in an *Arabidopsis* mutant showing a monoarch root vascular pattern instead of the wild type diarch pattern (Ohashi-Ito and Bergmann, 2007, De Rybel et al., 2013). Through careful mutant analysis it was demonstrated that the interaction between *LHW* and *TMO5* is necessary and sufficient to regulate the size of the vasculature (De Rybel et al., 2013). In addition, the TMO5-LHW dimer promotes expression of LOG4 in the stele, one member of a class of proteins involved in the biosynthesis of cytokinin (De Rybel et al., 2014; Kuroha et al., 2009; Kyoko Ohashi-Ito et al., 2014). Cells expressing LOG4 are non-responsive to cytokinin due to expression of a cytokinin signalling inhibitor (AHP6) in this domain, but induction of cytokinin biosynthesis in the stele has been shown to promote periclinal cell divisions outside of the stele, as it diffuses out (De Rybel et al., 2014; Ohashi-Ito et al., 2014). The activity of the TMO5-LHW dimer is also influenced by activity of the polyamine signalling molecule thermospermine. Previously, thermospermine was known to be implicated in vascular development as mutants of ACL5 (which is involved in thermospermine biosynthesis) results in dwarf plants with altered xylem patterning (Hanzawa, Takahashi, & Komeda, 1997; Imai et al., 2006; Knott, Römer, & Sumper, 2007; Muñiz et al., 2008). Thermospermine promotes the

accumulation of the SUPPRESSOR OF ACAULIS51-LIKE (SACL) family of bHLH transcription factors (Takano, Kakehi, & Takahashi, 2012; Yamamoto & Takahashi, 2017). Members of this family can dimerise with LHW, therefore restricting TMO5-LHW dimer dependent processes (Katayama et al., 2015; Vera-Sirera et al., 2015). ACL5 and SACL3 have been identified as downstream targets up-regulated by the TMO5-LHW dimer, suggesting a feedback loop which prevents over-proliferation of vascular cells (Kyoko Ohashi-Ito et al., 2014).

Another target of MP is the class III HD-ZIP transcription factor *ATHB8*, which is regarded as an early marker of procambium cell identity (Baima et al., 1995, Donner et al., 2009). The *Arabidopsis* genome encodes 5 HD-ZIP class III genes: *PHABULOSA* (*PHB*), *PHAVOLUTA* (*PHV*), *REVOLUTA* (*REV*), *ATHB15*/*CORONA*, and *ATHB8*. These transcription factors are involved in both specification of the procambium, as well as differentiation of procambial cells to xylem and development of the secondary cell wall in xylem vessels at a later developmental stage (Baima et al., 2001; Carlsbecker et al., 2010; Du & Wang, 2015; Taylor-Teeples et al., 2015; Zhong & Ye, 1999). MP binds directly to the auxin response element (ARE) in the promoter of *ATHB8*, positively regulating the expression of ATHB8 (Donner et al., 2009). The other HD-ZIP III proteins may also be regulated by MP indirectly, as indicated by reduced expression of these genes in the *mp* mutant (Mattsson et al., 2003). Another way HD-ZIP III genes are involved in specification of the procambium is by antagonism with the phloem expressed transcription factors *KANADI* (*KAN*) *1-4* (Emery et al., 2003). In the *kan1-4* quadruple mutant the procambium is enhanced in a similar

manner to plants overexpressing *REV* or *PHB*, whereas overexpression of *KANADI* in the procambium precursor cells suppresses formation of the procambium through reduced *PIN1* expression (Ilegems et al., 2010, Izhaki and Bowman, 2007). This supports the hypothesis that *KANADI* indirectly acts on HD-ZIP III genes through inhibition of PIN proteins and therefore auxin transport (Ilegems et al., 2010).

1.12 Maintenance of the procambium

As well as dividing to give rise to daughter cells which differentiate to other vascular cell types, procambial cells must also maintain a pool of meristematic tissue. Once the procambium has been specified there are various mechanisms in place which control its maintenance. It is known that maintenance of the meristematic tissues in the shoot apical meristem (SAM) and root apical meristem (RAM) is controlled in part by small signalling peptides and their receptors restricting expression of homeobox transcription factors (Sarkar et al., 2007). In the SAM, a feedback loop is set up between the homeobox transcription factor WUSCHEL (WUS) which is required for stem cell specification and is expressed in a cell layer below the stem cells, and the CLE peptide CLV3 which is expressed in the stem cells (Schoof et al., 2000, Brand et al., 2000). WUS promotes the expression of CLV3 in the overlying stem cells, which in turn interacts with leucine-rich-repeat receptor-like-kinases (LRR-RLKs) to restrict the area of the *WUS* expression domain (Schoof et al., 2000). Recently, a number of studies have shown WUS is directly regulated by the

type-B RRs, providing a link between cytokinin signalling and maintenance of the SAM (Meng et al., 2017; Wang et al., 2017; Zhang et al., 2017; Zhang et al., 2017; Zubo et al., 2017). In the RAM the CLE40 peptide expressed in columella cells binds the LRR-RLK ACR4, which in turn regulates the expression of *WUS-related homeobox 5* (*WOX5*) leading to its confinement to the quiescent centre (QC) (Stahl et al., 2009). *WOX5* expression in the QC is essential for maintenance of stem cells distal to the QC. Maintenance of the procambium also makes use of a similar WUS-CLV like regulatory feedback loop. The CLE peptide TDIF (tracheary element differentiation inhibitory factor)/CLE41/44 is secreted from phloem cells and binds to the LRR-RLK TDR/PXY in procambial cells which in turn regulates the expression of *WOX4*, a *WUS* homolog which promotes procambial cell maintenance (Fisher and Turner, 2007, Etchells and Turner, 2010, Hirakawa et al., 2010, Hirakawa et al., 2008).

A number of other factors have been implicated in maintenance and organisation of the procambium, including the plant hormone cytokinin. Increased cytokinin signalling results in ectopic protoxylem in the procambium domain, whereas decreased cytokinin signalling results in loss of protoxylem (Mähönen et al., 2006, Mähönen et al., 2000), demonstrating the importance of cytokinin in maintenance of the procambium and proper specification of the vascular tissues.

1.13 Differentiation of procambial cells

As well as being involved in specification of the procambium, the HD-ZIP III transcription factors also function in controlling cell fate decisions of proto or metaxylem cell types. Although the *phb phv rev cna athb8* mutant results in loss of protoxylem and proliferation of procambium, the quadruple mutants *phb phv rev cna* and *phb phv cna athb8* result in a protoxylem axis without the development of metaxylem, showing these genes function in a dose dependent manner (Carlsbecker et al., 2010). The regulatory mechanism governing HD-ZIP III control of xylem differentiation has recently been uncovered. This process involves bidirectional transport of the transcription factor SHORT ROOT (SHR) and miRNA. As mentioned earlier, SHR is produced in the stele and is transported via plasmodesmata to the endodermis where it forms a complex with the transcription factor SCARECROW (SCR) (Nakajima et al 2001, Vaten et al., 2011). This complex leads to the upregulation of miR165/166, which then diffuses (again via plasmodesmata) into the stele, where it degrades the target mRNAs of the HD-ZIP III transcription factors (Carlsbecker et al., 2010, Vaten et al., 2011). The consequent differential distribution in HD-ZIP III proteins specifies xylem cell differentiation, and differentiation of various other vascular tissues, in a dose dependent manner (Miyashima et al., 2011). Higher levels of HD-ZIP III activity (in the central position) inhibit protoxylem development but enhance metaxylem development whereas lower levels (at the peripheral position) promotes protoxylem development (Carlsbecker et al., 2010). The HD-ZIP III members also act redundantly to repress expression of the cytokinin signalling inhibitor *AHP6*, therefore restricting localisation to more marginal

positions (Carlsbecker et al., 2010). As well as feeding back on cytokinin signalling in this way, PHB also feeds back on the auxin response by inducing expression of both MP/ARF5 and its inhibitor IAA20 (Müller et al., 2016). IAA20 and its homologue IAA30 are stable in the presence of auxin (unlike other AUX/IAAs which are degraded and consequently allow transcription of ARFs), suggesting they function to constituitively dampen the auxin response (Sato & Yamamoto, 2008a, 2008b). The importance of this level of inhibition of auxin response is indicated by the *iaa20 iaa30* double mutant, which develops aberrant protoxylem. This shows PHB also functions, through activation of MP/ARF5 and IAA20 and IAA30, in focussing auxin response to enable proper protoxylem development. In contrast to this, various auxin biosynthesis mutants develop defects in metaxylem which are partially rescued by increasing expression of HD-ZIP IIIs (Ursache et al., 2014). This indicates that auxin biosynthesis in the root is essential for proper HD-ZIP III mediated metaxylem differentiation. In addition, crosstalk between various hormones regulates expression of miRNA165/166 as well as HD-ZIP IIIs (Singh et al., 2017). Taken together, these results reveal complicated regulatory networks which converge on the HD-ZIPs, which feed back into both auxin and cytokinin responses.

Another factor which regulates the activity of the HD-ZIP III genes are the plant hormones brassinosteroids, which have been shown to induce expression of some HD-ZIP III genes (Ohashi-Ito and Fukuda, 2003). This suggests that brassinosteroids play a role in xylem differentiation, although the authors warn that an interaction with auxin may also be important given the observation that

both hormones are required for differentiation of procambial cells to tracheary elements in *Zinnia* tissue culture (Iwasaki and Shibaoka, 1991). More recently, a study by Ibanes et al. (2009) made use of a mathematical model to investigate the role of auxin and brassinosteroids in shoot vascular patterning. This, supported by experimental observations, demonstrated that brassinosteroids enhance the number of provascular cells, which leads to an increase in vascular bundle number (Ibanes et al., 2009).

Aside from hormonal based specification of vascular domains, the AT-HOOK MOTIF NUCLEAR LOCALISED PROTEIN 3 (AHL3) and AHL4 transcription factors play a role in this process, as indicated by ectopic protoxylem development in the procambium domain of the mutants (Zhou, Wang, & Lee, 2013). The AT-hook protein motif is highly conserved, and in plants AT-hook proteins are involved in a diverse range of developmental processes (Yun et al., 2012, Matsushita et al., 2007, Lim et al., 2007, Street et al., 2008). *AHL3* and *AHL4* are closely related members in the AT-hook family of transcription factors, and have been shown to interact in vivo (Zhou et al., 2013). This dimerisation facilitates the movement of the *AHL3*/*AHL4* complex via plasmodesmata from the procambium, where they are expressed, to the other stele tissues in a non-directional manner. The importance of the mobility of these proteins in developmental function was demonstrated by impairing their movement by fusing the coding region of AHL4 with multiple tandem copies of YFP, which greatly restricts movement due to the large size of the protein fusion. This resulted in the inability to complement the *ahl4* mutant xylem phenotype. Taken together, these data support the hypothesis that *AHL3* and *AHL4* are

involved in specifying a boundary between the xylem and procambium. Although genes regulated by these transcription factors remain unknown, they appear to function independently of cytokinin signalling (Zhou et al., 2013).

A number of other factors have been characterised due to their involvement in the development of particular vascular tissue types. One such group of factors are members of the NAC domain transcription factors. The NAC (NAM, ATAF1,2 and CUC1) domain proteins are a family of plant specific transcription factors which have been shown to be involved in a diverse range of developmental processes. The development of a tracheary element inducible system in *Arabidopsis* suspension cells enabled a detailed microarray analysis to be performed, which eventually led to the discovery of a gene family related to a gene upregulated during tracheary element differentiation discovered in a similar *Zinnia* system (Demura et al., 2002, Kubo et al., 2005). This family of 7 NAC domain transcription factors were named VASCULAR-RELATED NAC-DOMAIN PROTEIN 1 (VND1) – VND7. VND6 and VND7 in particular are thought to act as master regulators of metaxylem and protoxylem differentiation respectively, as their overexpression leads to ectopic development of these tissues. A loss of function *vnd6 vnd7* mutant, however, shows no obvious vascular defects, suggesting the other VND family proteins act in a functionally redundant manner with VND6 and VND7 (Kubo et al., 2005). Interestingly, the multiple *vnd* loss of function mutant also shows no phenotype, indicating other regulatory mechanisms may overcome this (Kubo et al., 2005). The activity of VND6 and VND7 is also regulated by other transcription factors. ASL20/LBD18 and ASL19/LBD30 were shown to positively regulate VND7 expression, whereas

another NAC-domain transcription factor, VNI2, acts as a transcriptional repressor through its interaction with VND7 (Soyano et al., 2008, Yamaguchi et al., 2010). More recently, Endo et al., (2015) identified 14 transcription factors which up-regulate VND7, including the entire VND family themselves (along with many transcription factors previously associated with vascular development). This work indicates the existence of a wider signalling network which integrates multiple developmental signals which converge on VND7.

1.14 Secondary cell wall development

Whilst the signalling pathways described are crucial in the patterning process, development of the secondary cell wall of xylem vessels is largely dependent on separate signalling mechanisms (although a degree of cross talk with some pathways mentioned has recently been uncovered) (Du & Wang, 2015; Taylor-Teeples et al., 2015). The secondary cell wall, composed mainly of cellulose, hemicelluloses and lignin, is crucial for tissue function as it forms a waterproof layer and provides mechanical support to vessels. While VND6 and VND7 regulate xylem cell type differentiation, other members of the NAC domain transcription factors function in secondary cell wall development. The SECONDARY WALL ASSOCIATED NAC DOMAIN PROTEIN 1 (SND1), NAC SECONDARY WALL THICKENING PROMOTING FACTOR 1 (NST1) and NST3 function as master regulators of secondary thickening, shown by repression reducing secondary thickening and overexpression leading to ectopic secondary thickening (Zhong et al., 2006, Mitsuda et al., 2007). These master

regulators act on a number of factors downstream to control differentiation, including up-regulating a number of genes involved in secondary cell wall biosynthesis (Taylor-Teeples et al., 2015). In addition, SND1 up-regulates KNAT7, which functions to inhibit secondary cell wall formation. Recently another NAC-domain transcription factor, ANAC005, has been suggested to function in a similar manner as it up-regulates some secondary cell wall biosynthesis genes in common with SND1, and mutant and over-expressor phenotypes show similarity to those of KNAT7 (Zhao et al., 2016).

Whilst SND1, NST1 and NST3 appear to be master regulators of secondary cell wall development, many other signalling pathways are involved too and many proteins involved in secondary cell wall biosynthesis, deposition and transcriptional regulation of related genes have been described, as reviewed by Ruiqin Zhong & Ye, (2015). Some proteins involved in secondary cell wall development play roles in xylem development and patterning as previously described. For example, HD-ZIP IIIs and their targeted degradation by miRNA165/166 have been shown to function in secondary cell wall development, by interacting with regulatory pathways governing secondary cell wall development (Du & Wang, 2015; Taylor-Teeples et al., 2015).

1.15 Communication between pathways

A number of recent studies have identified various factors which have an effect on xylem development, but likely are involved in many developmental contexts, indicated by pleitropic mutant phenotypes. For example,

Grienenberger & Douglas (2014) identified VASCULAR-RELATED UNKOWN PROTEIN1 (VUP1), a protein with no annotated functional domains which is expressed in the vascular tissues and with a mutant phenotype showing collapsed xylem. Although the mechanism of action remains unknown, the VUP1 over-expressor resembles BR and GA deficient mutants indicating its possible role in secondary cell wall formation by modulating these signalling pathways. Some factors with pleitropic mutant phenotypes function at the level of mRNA transcription or post-transcriptional modification. Recently, it has been shown that N6-adenosine methylation of mRNA plays a role in root vascular patterning (Růžička et al., 2017), and the translation elongation factor eIF5A has been shown to regulate root protoxylem development by modulating cytokinin signalling (Ren et al., 2013). The polyamine spermidine (a precursor to thermospermine) is essential for activation of eIF5A by post translational modification (hypusination), and eIF5A has also been implicated in ABA signalling (Belda-Palazón et al., 2014; Belda-Palazón et al., 2016). As well as regulation of RNA processing, changing patterns of gene expression via chromatin remodelling have also been described to enable vascular differentiation. The Polycomb Repressive Complex 2 (PRC2), involved in repressive chromatin formation via histone methylation, is expressed in a tissue-specific manner allowing differential gene regulation in non-vascular and vascular cells and thereby enabling another level of developmental control (de Lucas et al., 2016).

1.16 Understanding complex pathways - modelling

One way to aid understanding of the various complex molecular interactions which collectively govern patterning of the vasculature is through the use of mathematical modelling. Mathematical models have been developed to describe a wide range of parameters within the research area of root development, and experimental evidence which agrees with the models predictions enables confirmation of the models validity. Much of this research has been focussed on auxin transport. Grieneisen et al. (2007) developed a 2D model describing diffusion and PIN facilitated flux of auxin and concluded, with support from experimental evidence, that these auxin flux patterns are sufficient to generate auxin maxima and gradients which drive tissue patterning and development. Mironova et al. (2010) expanded upon this by developing a model which combined auxin flux with the action of cytokinin and ethylene on cell division, to describe the effect of these factors on root patterning. Swarup et al. (2005) used a 3D model to show that AUX1 mediated influx of auxin is required for auxin transport through the lateral root cap to elongating epidermal cells. The model predicted that this process is required for gravitropism, and this was confirmed by the agravitropic dominant *axr 3-1* mutation.

More recently, root vascular patterning has seen attention with the development of three independent models. The first was a multicellular model developed by Muraro et al. (2014) which combined a number of factors known to be involved in *Arabidopsis* root vascular patterning, with the aim of

identifying a minimum set of these components required for maintenance of vascular pattern. This resulted in identification of auxin and cytokinin signalling along with signalling through PHB, miRNA165/6 and SHR as the minimal components required for maintaining a stable vascular pattern. The model also suggests the existence of an unknown component involved in negative regulation of cytokinin signalling, which when included in the model, results in predicted patterns of gene expression which correspond with experimental data (Muraro et al., 2014). In the second model of root vascular patterning, a growing model was developed by De Rybel et al., (2014) which demonstrated the importance of initial asymmetry in auxin, derived from the cotyledons during embryogenesis. In addition, the model predicted the two 'source cells' which show initial high levels of auxin must share a cell wall for correct patterning, an observation which was subsequently confirmed experimentally. This study also demonstrated that auxin (via the activity of the TMO5/LHW dimer) induces expression of LOG4 (an enzyme involved in cytokinin biosynthesis) in the xylem. Due to expression of AHP6 in this domain, the xylem cells are nonresponsive to cytokinin, but as it diffuses out of the stele it is involved in orienting cells divisions and therefore acts as a tissue organiser. The third model, developed by, el-Showk et al., (2015), focussed on hormonal activation of auxin transport by modelling the AUX/LAX auxin importers, as well as the PIN auxin exporters. In this detailed model the localisation of auxin transporters was placed according to experimental observations. While activity of PINs was previously known to be important in the patterning process, this study predicted a role for AUX1, LAX1 and LAX2 in vascular patterning, and this

was confirmed experimentally by the triple mutant displaying an unstable vascular pattern.

Given the importance of proper patterning of the vascular tissues, it is not surprising that mechanisms have evolved which enable careful control of the development of pattern in these tissues. With this in mind, it is reasonable to suggest that similar mechanisms may be in place to enable development of the diverse patterns of vascular tissues seen in other species. It will likely be beneficial to use modified versions of mathematical models to identify whether a system similar to that seen in *Arabidopsis* is capable of generating more complicated vascular patterns, such as that of rice roots.

1.17 Patterning of vascular tissues

The spatial organisation of the vasculature can be thought of at two levels: the longitudinal pattern, which describes the vascular bundle arrangement in a certain organ, and the radial, which describes the arrangement of the particular vascular cell types within the vascular bundles (Esau, 1977). The stele has traditionally been used to refer to the combination of vascular tissue with pericycle cells (a ring of cells forming the outer edge of the stele), and three main stele types (the prostele, eustele and atactostele) have been described based on the patterning of the vascular bundles within the stele (Figure 1.3). The patterning of individual vascular bundles has also been classified into four major groups, based on location of phloem and xylem within the bundle: the collateral pattern (xylem develops on the inside and phloem the outside of the

bundle); amphivasal (phloem surrounded by xylem); amphicribal (xylem surrounded by phloem); and bicollateral (two phloem poles either side of the central xylem). However, it is important to consider how organ specific the various patterns are. The functions of different plant organs require that there are differences in spatial patterning of the vasculature, and this often differs throughout the plant kingdom. For example, in shoot tissue the prostele pattern is commonly seen in nonseed vascular plants, the eustele pattern in dicots, and the atactostele pattern in monocots. In roots, the prostele pattern is seen in many dicots and the eustele in monocots (Figures 1.4 and 1.5). Leaves also have a complex and varied vascular patterning, with dicots often presenting a midvein and a network of diverging veins, and monocots typically presenting multiple parallel veins.

Arabidopsis, as the model plant, has been well anatomically characterised. In roots, *Arabidopsis* shows a diarch vascular pattern consisting of a central axis of xylem with a phloem pole on either side of this axis, in between which is the procambial tissue. In shoots, the eustele pattern is seen with individual vascular bundles organised in a single ring, with the inner xylem and outer phloem separated by a strip of procambial tissue. In leaves, xylem develops above the phloem and these domains are, again, separated by procambial tissue. As is common in dicots, the vascular bundles within the leaves are highly branched forming complex patterns.

As compared to *Arabidopsis*, the vascular tissues of rice have very different organisational patterns (Figures 1.5 and 1.6). In rice roots a polyarch pattern is

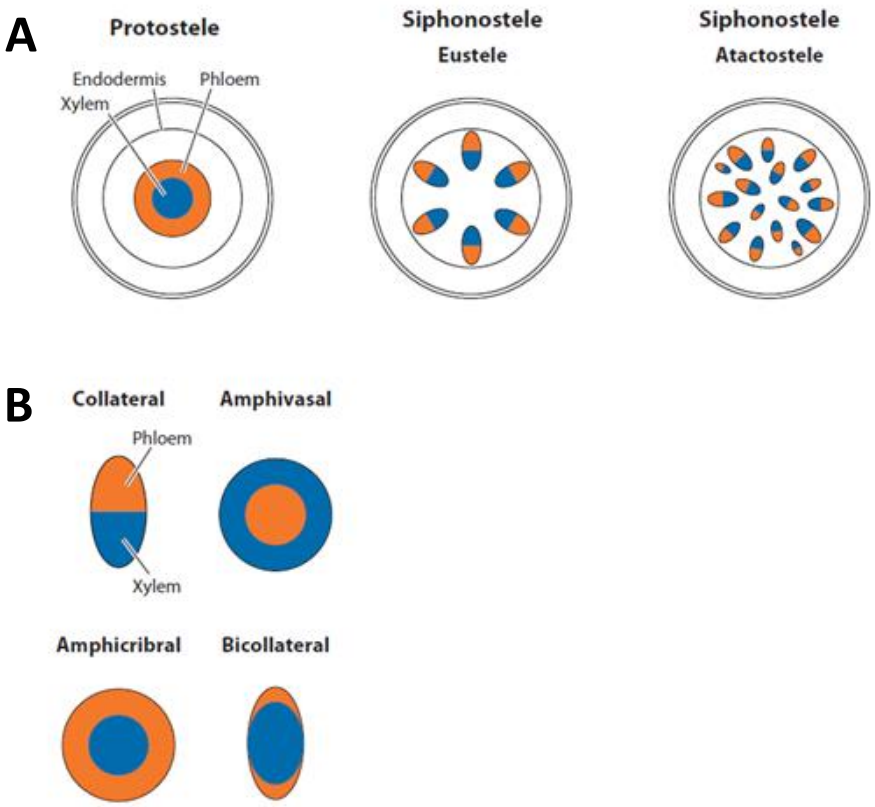


Figure 1.3. The organisation of vascular bundles within the stele (A) and the organisation of vascular tissues within vascular bundles (B) is highly variable between species. Modified from Furuta et al., (2014).

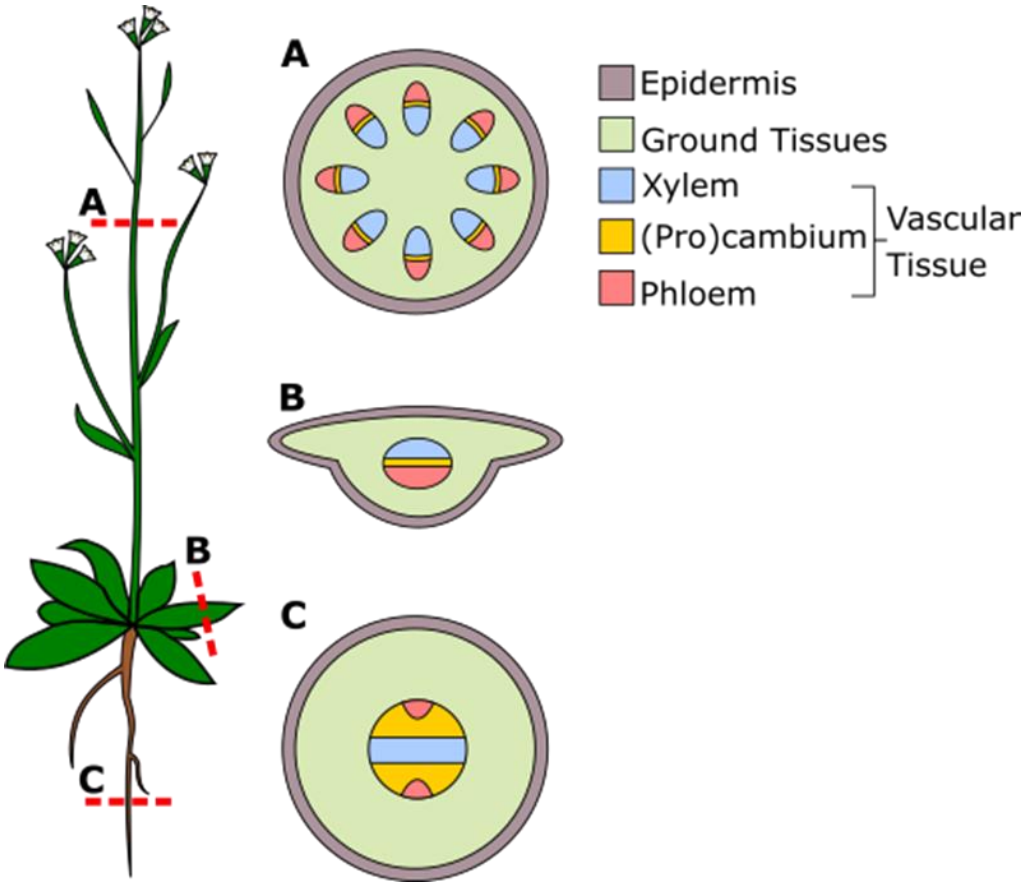


Figure 1.4. Radial sections through an *Arabidopsis* stem (A) leaf (B) and root (C) reveal the diversity of tissue specific vascular patterns. Diagram drawn by Ben Goodall.

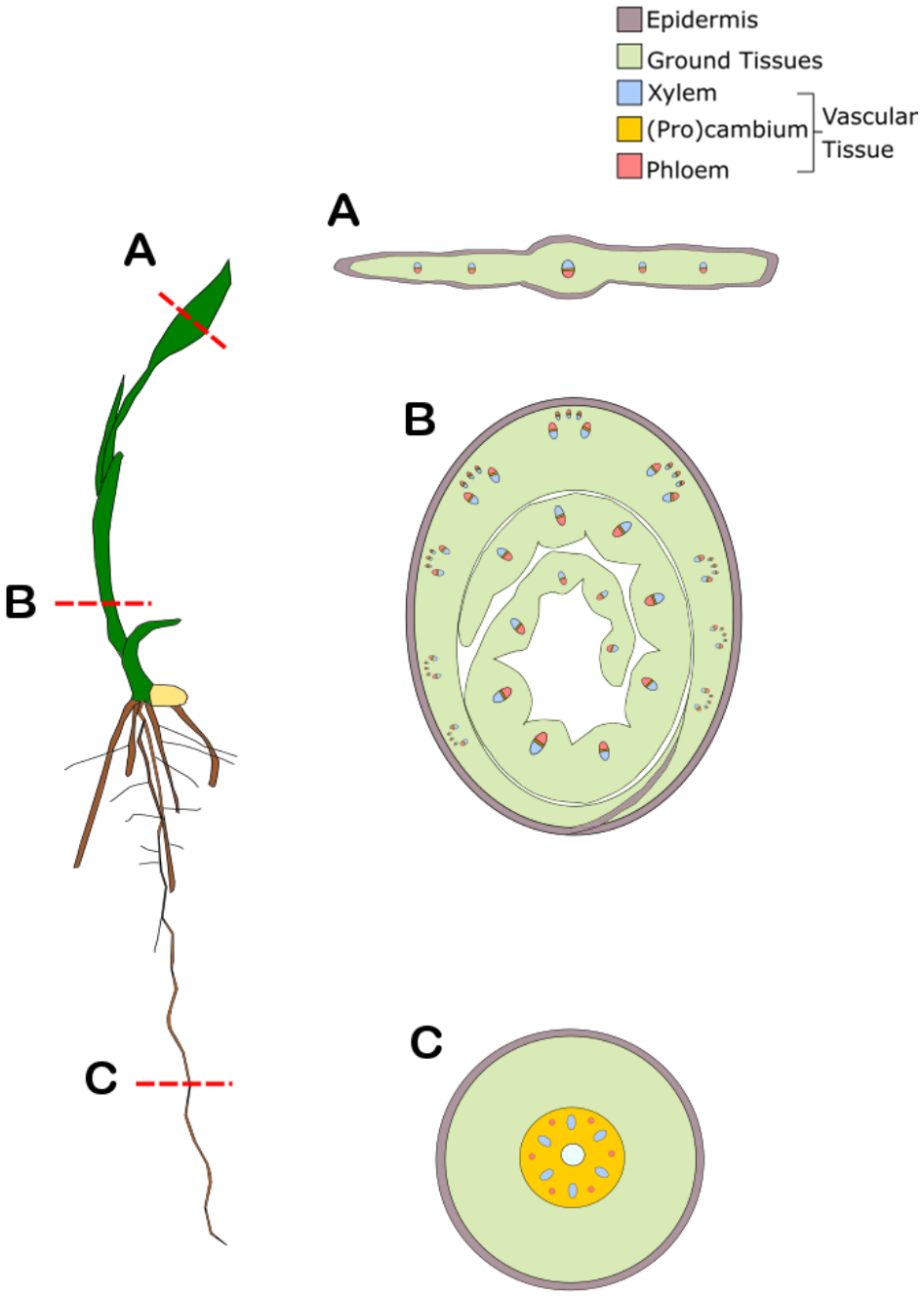


Figure 1.5. Radial sections through a rice leaf (A) stem (B) and root (C) reveal different vascular organisation as compared to that of *Arabidopsis*.

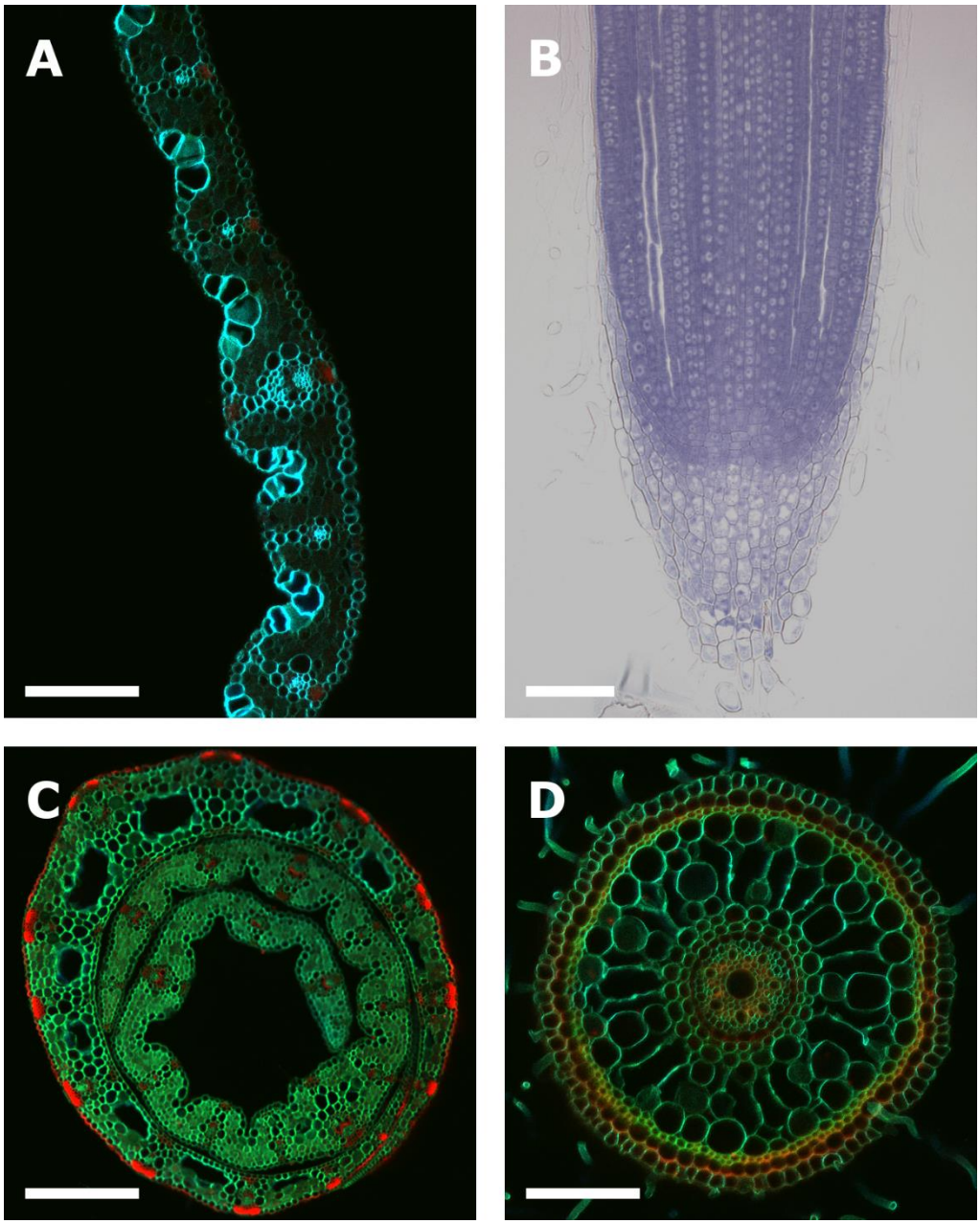


Figure 1.6. The diversity of radial anatomy between different rice tissues. (A) leaf, (B) crown root longitudinal section, (C) stem and (D) crown root radial sections. Sections were taken from Kitaake seedlings 14 days after germination. A, C and D are stained with calcofluor and imaged using a confocal microscope to differentiate between lignified tissue (in red) and cell walls (green). B was stained with toluidine blue. Scale bars are 100 µm.

seen, consisting of a central metaxylem vessel surrounded by a variable number of xylem poles, between which are phloem poles, with procambium in between. In stems, an atactostele pattern is seen with multiple vascular bundles arranged throughout the stem, with phloem on the outer and xylem the inner edge of the bundle, between which is procambial tissue. Often, radial sections reveal the inner folded leaf developing within the stem. In leaves, vascular bundles are arranged with xylem on top and phloem on bottom, with these two tissues being separated by a strip of procambium. As is characteristic of monocot leaves, the vascular bundles are arranged in multiple parallel vessels rather than being branched as is seen in dicots.

1.18 *Arabidopsis* vs rice: root architecture

Whilst *Arabidopsis* has a simple root structure consisting of a single primary root with branching lateral roots, most cereals have many different types of branching root. For example, rice has 4 major distinct root types: the radicle or primary root (which is the first to emerge after germination), the embryonic crown roots (which emerge from the coleoptilar node), the postembryonic crown roots (which emerge from the stem and tiller nodes and form the bulk of the fibrous root structure), and lateral roots. Lateral roots have been further divided into several classes. Early studies described lateral root classes based purely on morphological traits, and termed them L-type (large) and S-type (small) lateral roots (Kono & Yamada, 1972; Yamauchi, Kono, & Tatsumi, 1987). As the names indicate, L-type LRs are longer, thicker and capable of further

branching, whereas S-type LRs are shorter, thinner and non-branching. For many years these classes were considered the only genuine distinctions between lateral root types (Rebouillat et al., 2009, Coudert et al., 2010). However, a more recent detailed study by Henry et al (2016) further sub-divided the L-type LRs into L-LLRs (large-large lateral roots) and T-LLRs (thin-large lateral roots) based on the presence of sclerenchyma only in L-LRRs. Frequency of formation of these different lateral root types seems to be heavily influenced by method of growth, and consequently some authors still only consider the two classes of L-type or S-type lateral roots. Indeed, detailed studies have shown differences in root hair density and length across different root types, which show enormous variation depending on growth conditions (Nestler, Keyes, & Wissuwa, 2016). Growth in nutrient media leads to a higher density of longer root hairs on the primary and crown roots, and a much lower density on lateral roots, as compared to growth in soil. This demonstrates nicely the caution needed when interpreting phenotypes based on one growth method.

1.19 *Arabidopsis* vs rice: root anatomy

There are few differences in radial anatomy between *Arabidopsis* primary and lateral roots. Surrounding the stele are two layers of ground tissue (endodermis and cortex), which are surrounded by the epidermis. Each tissue type surrounding the stele consists of only one cell layer and there is little variation even in cell number. For example, unless under nutrient stress, the cortex

always consists of 8 cells (Ma et al., 2001). Within the stele, *Arabidopsis* roots have a simple diarch vascular pattern with two planes of symmetry, consisting of a central xylem axis flanked by phloem cells on either side with procambium in between (Mähönen et al., 2006) (Figure 1.7). The xylem axis consists of two xylem cell types; protoxylem (located at the distal ends) and metaxylem (located in a central position). Protoxylem matures while surrounding tissue is still elongating whereas metaxylem matures after surrounding tissues, and these distinct cell types are associated with characteristic differences in secondary thickening. Protoxylem develops spiral thickenings to allow further cell elongation, whereas metaxylem develops evenly spaced pits in the cell wall.

Despite a much greater diversity of distinct root types in rice, the radial anatomies of these root types is broadly similar, consisting of the central stele surrounded by at least three layers of ground tissue (endodermis, cortex, and exodermis, with sclerenchyma present between cortex and exodermis layers in some root types) and the epidermis (Figure 1.7) (Rebouillat et al., 2009). Whilst the cortex certainly is the major contributor to variation in root diameter across different root types, representing only 1 cell layer in small lateral roots to around 10 cell layers in mature crown roots (depending on the genotype and growth conditions) there are also interesting anatomical differences in other tissue types (Figure 1.8). Detailed internal tissue organisation of rice roots, and lateral roots in particular, is not well defined. In an effort to better describe particular tissue layers, (Henry et al., 2016) screened a library of cell wall antibodies linked to fluorochromes to find suitable tissue specific markers. Immunolabelling of sectioned roots with these markers enabled the

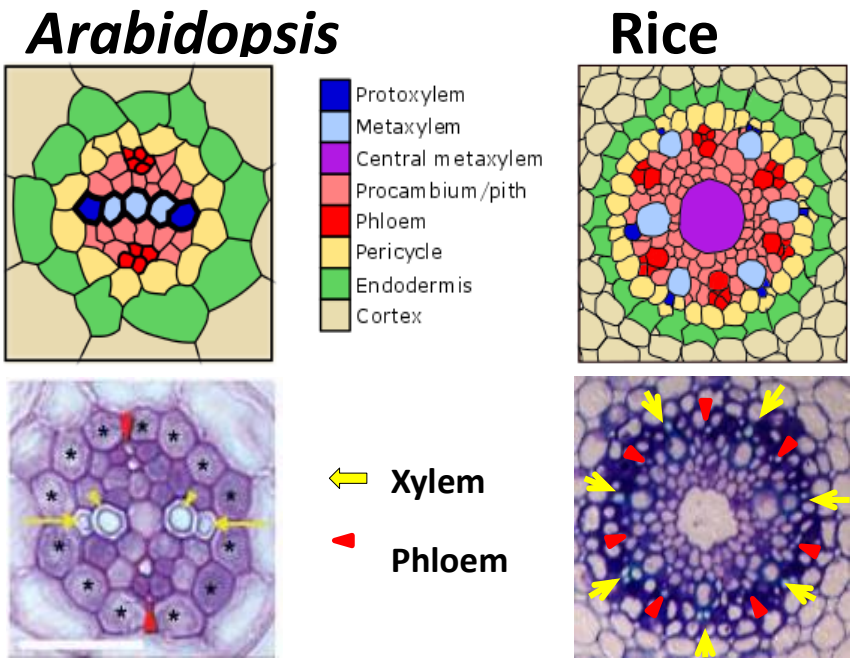


Figure 1.7. The root radial vascular patterning of *Arabidopsis* and rice. The diarch vascular pattern of *Arabidopsis* is simple in comparison with that of rice, which can have up to 10 xylem and 10 phloem poles. Yellow arrows indicate protoxylem, yellow arrowheads indicate metaxylem and red arrowheads indicate phloem. Scale bars are 20 µm. *Arabidopsis* cross section image adapted from Mähönen et al (2006) and *Arabidopsis* section cartoon drawn by Ben Goodall.

identification of two distinct cortical cell zones referred to as ‘inner cortex’ and outer cortex’. Interestingly, immunolabelling of lateral roots with the same markers revealed cortical cells of all lateral root types only have ‘outer cortex’ identity (Henry et al., 2016). In addition to differences in ground tissues between different root types, there are also differences in tissue organisation within the stele. The most obvious difference is the lack (or reduction) of a central metaxylem vessel in the small lateral roots, whereas all other root types have at least one (with mature crown roots often developing several) (Henry et al., 2016; Rebouillat et al., 2008). In addition, it appears the pericycle layer is absent in small lateral roots. Without pericycle specific markers it is difficult to make certain claims about tissue identity, but tissue domains can be derived by examining autofluorescence of lignified or suberized tissues, which is easily observed (namely the casparian strip in the endodermis and the xylem vessels). Displaying confocal images of all channels alongside the autofluorescence channel only, enables easy identification of endodermis, xylem vessels and surrounding tissues. In the cultivar Kitaake, small lateral roots have 2 or 3 metaxylem poles, large lateral roots have 4 metaxylem poles and primary and crown roots have 6 to 10 metaxylem poles (Figure 1.9). For small lateral roots the inner cell layer to the endodermis is interrupted by xylem vessels, suggesting it does not have pericycle identity. Given the function of the pericycle as a tissue layer essential for lateral root formation, it is perhaps not surprising that the pericycle should be absent in small lateral roots themselves, the only root type which never develops other lateral root branching. The root vascular pattern of rice also differs greatly from the simple diarch pattern seen

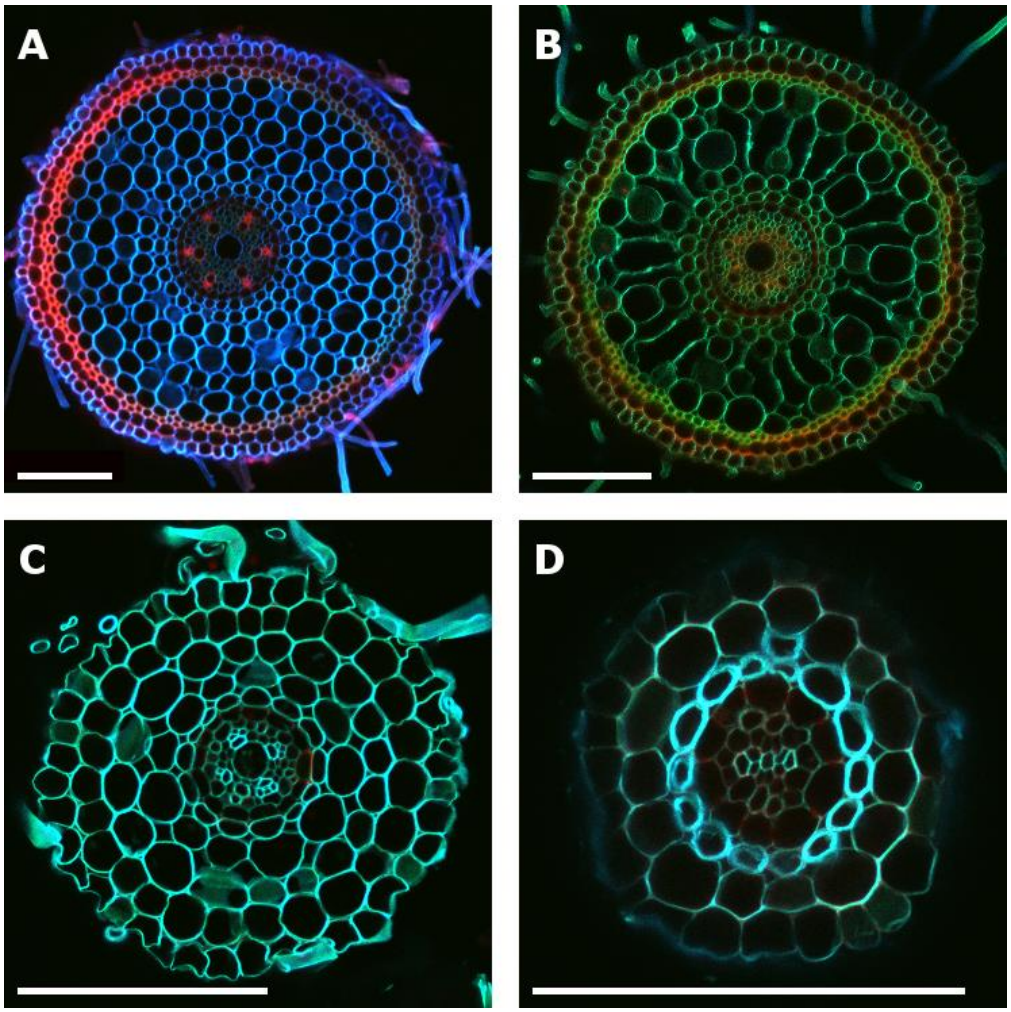


Figure 1.8. The diversity of radial anatomy within different rice root types. Images show representative radial sections from (A) radicle, (B) crown, (C) large lateral and (D) small lateral roots. Scale bars are 100 µm.

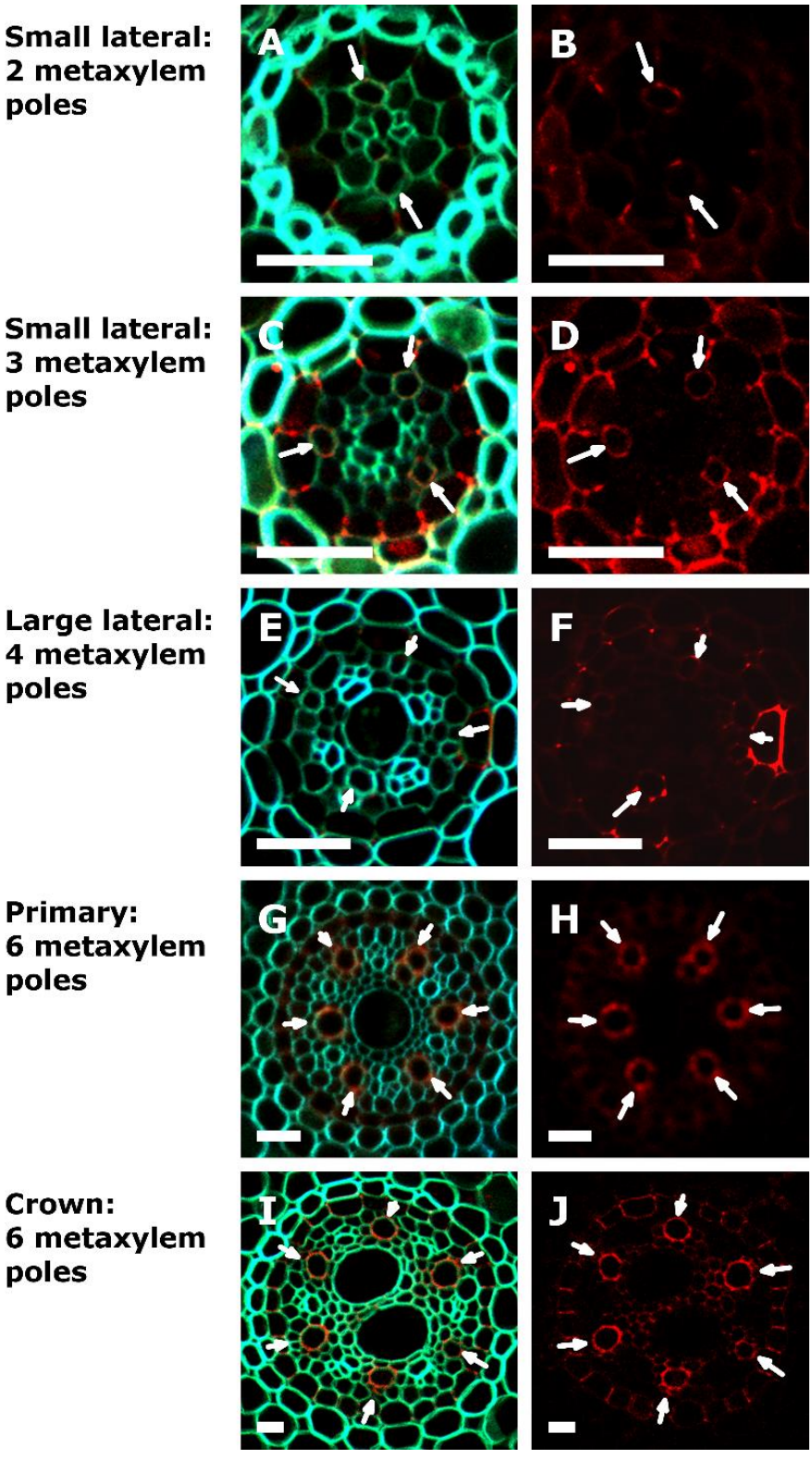


Figure 1.9. Root types with larger steles show more vascular poles. Confocal imaging of calcofluor stained rice root sections showing channel overlay (A,C,E, G and I) and autofluorescence only (B, D, F, H and J), allowing for easier identification of xylem and endodermal cells. Sections are from small lateral roots (A-D), thin large lateral roots (E-F), primary roots (G-H) and crown roots (I-J). White arrows indicate xylem vessels. Scale bars are 20 µm.

in *Arabidopsis*, with rice roots having a polyarch pattern consisting of one or several central metaxylem vessels surrounded by up to 10 xylem poles (depending on the root type and cultivar), between which are the phloem poles (Figure 1.7). The large peripheral metaxylem vessels are adjacent to protoxylem vessels and have a more central position, with the protoxylem at a more distal position (Figure 1.10). Whilst the procambium of *Arabidopsis* roots can be visualised by tissue specific reporters, tools such as this are less widely utilised in rice. Consequently, it is difficult to be totally sure of procambial cell identity within the stele, and there appears to be some confusion about the true identity of what can be referred to in the literature as pith or medulla. The use of tissue specific reporters, or RNA in-situ hybridisations with suitable reporter genes, may enable clarification of the anatomical details of the rice root.

The root apical meristem (RAM) structure of rice is also different from that of *Arabidopsis*. The RAM was originally divided into two groups amongst different species, based on morphological characteristics, referred to as open or closed (von Guttenberg, 1968). In the closed RAM, cell files of particular tissue types can be traced back to the distinct tiers of initial cells which they originate from. The alternative open RAM structure describes cell files which derive from a large zone of initial cells which are not organised in clonally derived tiers. Although these were the major organisational patterns originally described, recent work has shown there is a huge diversity of RAM organisation which is complicated by organisational changes through development (Heimsch & Seago, 2008). In the *Arabidopsis* RAM, which in early development begins with a closed meristem structure, the quiescent centre (QC), which is the organising

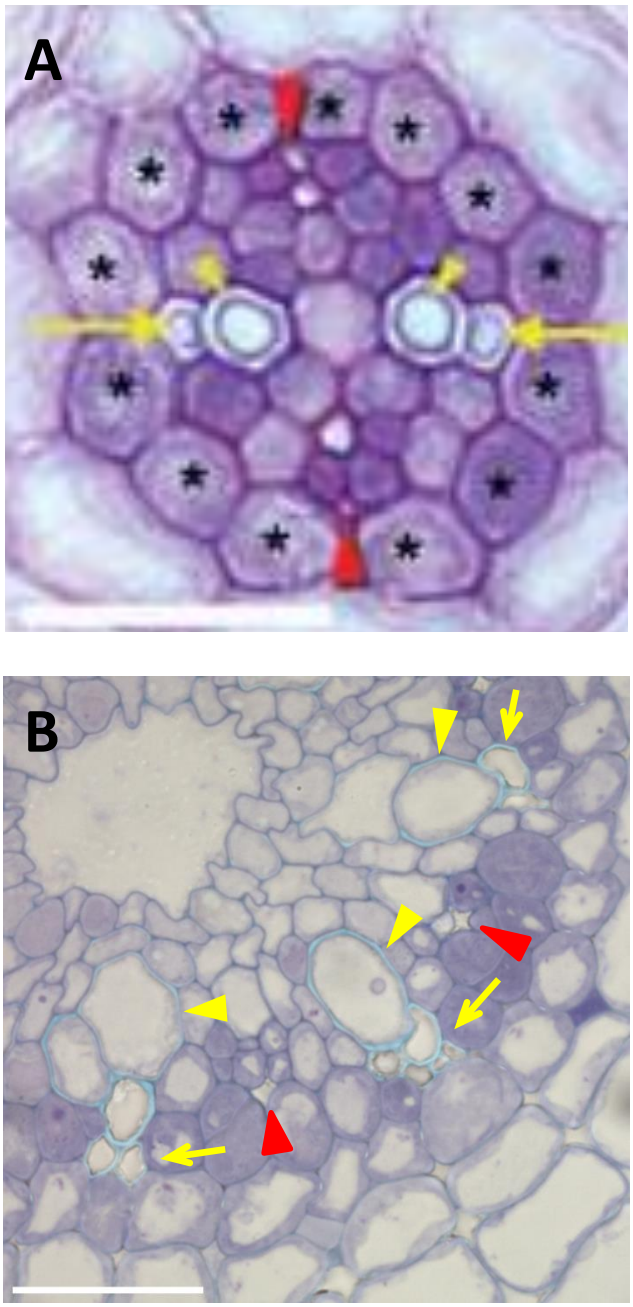


Figure 1.10. Radial sections showing details of *Arabidopsis* (A) and rice (B) root vasculature. Xylem poles are differentiated by staining with toluidine blue. Yellow arrowheads indicate metaxylem, yellow arrows indicated protoxylem and red arrowheads indicate phloem poles. *Arabidopsis* cross section image adapted from Mähönen et al (2006). Scale bars are 20 µm.

centre of the RAM cells, consists of four founder cells surrounded by three layers of initials (Dolan et al., 1993). These three tiers of initial cells divide asymmetrically to give rise to stele, endodermis and cortex, and epidermis and root cap tissues respectively, with cells which remain in contact with the QC retaining initial identity. The rice RAM, like that of *Arabidopsis*, comprises the QC with three tiers of initial cells in a closed meristem structure. However, the initial cells of the rice RAM give rise to different tissue types from that of *Arabidopsis*. In rice, the root cap and columella differentiate from a common initial (a feature common to all monocots), as do all tissue layers from the epidermis to the endodermis, and the stele tissues (Clowes, 1994; Rebouillat et al., 2008; Coudert et al., 2010). Above the QC, and adjacent to the epidermis-endodermis initial cells, are a group of large cells distinct from other meristematic cells known as central cells (CCs). Initials surrounding the CCs divide asymmetrically to give rise to the stele tissues (Rebouillat et al., 2008). Unlike *Arabidopsis*, it appears that the metaxylem differentiates before protoxylem in rice roots. Detailed anatomical analysis revealed that the metaxylem originates from an initial cell which is in contact with two pericycle (outer) cells. After this, a series of divisions of adjacent pericycle cells leads to development of a small group of cells which differentiate as protoxylem (Rebouillat et al., 2008). Although detailed anatomical study has been carried out on the rice RAM, the use of tissue specific reporters (or, as previously mentioned, RNA in-situ hybridisations) would enable clearer distinction between tissue types which may not otherwise be obvious, particularly upon hormonal treatment.

In recent years many more research groups have been answering molecular developmental questions in crop plants. However, we still have vastly more information about vascular development in *Arabidopsis* than any crop plant.

1.20 Rice: understanding a complex vascular pattern

Rice is a major world crop which forms a staple diet for nearly half the world's population, and provides around 19% of dietary energy globally (Ray et al., 2013). In addition, it is also of great scientific value and is considered a model cereal due to its relatively small genome size and the wide range of molecular genetic resources available. The genomes of the two main subspecies of cultivated rice, *Oryza sativa* spp. *japonica* and spp. *indica*, have been sequenced, annotated, and brought together in central databases (International Rice Genome Sequencing Project,. 2005; Sakai et al., 2013). In the same way that knowledge gained from studying *Arabidopsis* has proven useful in rice research, knowledge gained from studying rice may lead to further discoveries in the other major cereal crops such as wheat, maize and barley. Given the huge dependence on rice, it is of great benefit to develop varieties which increase productivity to enable a secure food supply, even under environmental stresses. Despite lowland rice being grown in flooded paddy fields, drought is often a problem in environments where irrigation is restricted and rainfall is unpredictable. A number of traits have been associated with water uptake in rice, including the size and number of xylem vessels and the size of the stele as a whole (Henry et al., 2012). Drought tolerant rice varieties

have been shown to have reduced numbers of xylem vessels which are smaller in diameter than drought susceptible varieties, and to develop more narrow xylem vessel diameter under more severe drought conditions (Henry et al., 2012). It is thought that the benefit of narrower xylem vessels is to reduce the risk of vessel cavitation, a process where the reduced tissue water potential resulting from water stress leads to entry of air from surrounding tissues into xylem vessels, which consequently lose hydraulic conductivity (Stiller et al., 2003). In addition, smaller and less numerous xylem vessels promote increased water use efficiency by increasing hydraulic resistance. Indeed, a breeding program to reduce the xylem vessel diameter in wheat enabled yield increases of between 3 and 11% in plants grown under water stressed conditions, with no yield penalty when grown under well-watered conditions (Richards and Passioura, 1989). This demonstrates the importance of an understanding of vascular development in future crop breeding.

Manipulating cytokinin signalling can have a huge impact on yield in rice, demonstrated by down-regulation of cytokinin oxidase/dehydrogenase 2 (OsCKX2), and consequent increased cytokinin levels in stems and inflorescences, increasing yield primarily as a result of increased tiller number (Ashikari et al., 2005; Yeh et al., 2015). Manipulating cytokinin signalling may also have the potential to regulate root xylem anatomy, therefore changing how plants respond to water stress. To understand whether cytokinin may play a similar role in setting up pattern of the vasculature in rice roots as it does in *Arabidopsis*, it is necessary to first detail the components of the two-component signalling system present in rice. These signalling elements have

been characterised in large part by comparing the sequences of conserved domains of known two-component signalling elements from *Arabidopsis* with genomic sequence data from rice, accompanied by a number of phylogenetic studies (Jain et al., 2006, Pareek et al., 2006, Du et al., 2007, Pils and Heyl, 2009). More recently, Tsai et al. (2012) provided a detailed characterisation of the rice two-component signalling elements through the use of a number of experimental systems. The rice genome encodes 5 HK cytokinin receptors (OsHK3-6 and OsCRL4), 2 HPTs (OsAHP1 and OsAHP2), 3 PHPs (OsPHP1-3), 28 RRs (represented by type-A, B and C as in *Arabidopsis*) and 8 pseudo-RRs (Tsai et al., 2012). While phylogenetic analysis revealed an orthologous relationship between most HKs and HPts in *Arabidopsis* and rice, it was determined that the rice type-A and type-B RRs have undergone significant lineage-specific expansion. In *Arabidopsis,* AHP6 represents a major component involved in specifying the vascular tissues through negative regulation of cytokinin signalling. There are three OsPHPs in rice, and it has been suggested that they function in a similar manner to AHP6 (Tsai et al., 2012).

1.21 Project aims

The major aim of this project is to investigate whether the mutually inhibitory feedback loop governing vascular patterning in *Arabidopsis* is also conserved in rice roots. Since *Arabidopsis* and rice roots display very different vascular patterns, it is of interest to understand whether similar signalling mechanisms can be used to bring about a different pattern, or whether signalling systems must be adapted to enable this. Because AHP6 is a central component in this process in *Arabidopsis*, it is a priority to find a cytokinin signalling inhibitor which fulfils an AHP6 like function in rice (i.e. an auxin inducible inhibitor of cytokinin signalling). Since the OsPHPs are homologues of AHP6, these are promising candidate genes which may function in a similar manner. To determine whether this is the case or whether another inhibitor of cytokinin signalling may be involved, the following questions will be considered.

1. Do the OsPHPs function in inhibition of cytokinin signalling?
2. Are the OsPHPs auxin inducible?
3. Do the OsPHPs function in root vascular patterning, and what are the other functions of the OsPHPs throughout the plant?
4. Can any other inhibitor of cytokinin signalling function in vascular development?

Chapter 2. Materials and Methods

2.1 Plant material

Arabidopsis thaliana Col-0 was obtained from CPIB (the University of Nottingham). The *Arabidopsis ahp6-1* and *ahp6-2* mutants were obtained from seed collections at the University of Helsinki. Rice (*Oryza sativa japonica*) cultivar ''Nipponbare'' was obtained from Erik Murchie (the University of Nottingham), and cultivar ''Kitaake'' was obtained from Christophe Perin (CIRAD, Montpellier). The cultivars used to study anatomical variation across genotypes (CG14O.g., Faro 52, IR64, Kaybonnet, Nerica L41, Nerica 2, Nerica 6, Nerica 7, Nerica 8, WAB 56, WAB 181 and WAB 759) were obtained from Umar Mohammed, the University of Nottingham.

2.2 Growth conditions

Arabidopsis seeds were surface sterilised with 70% ethanol for 2 minutes with inversion, and then 5% hypochlorite with 0.1% Tween 20 for 5 minutes with inversion. Seeds were then washed at least 5 times with sterile distilled water and directly plated onto ½ strength MS agar plates. All *Arabidopsis* seeds were imbibed at 4˚C for two days on plates before being transferred to the growth room.

Rice seeds were threshed by hand, and surface sterilized with 70% ethanol for 2 minutes with inversion, and then 5% hypochlorite with 0.1% Tween 20 for

30 minutes with inversion. Seeds were then washed with sterile distilled water at least 5 times, and imbibed in sterile distilled water for 1 day at room temperature before plating onto ½ strength MS agar plates.

For growth on ½ strength MS agar plates, 2.15 g/l MS basal salts (Sigma-Aldrich) with 1% (w/v) Bacto agar (Appleton Woods) was adjusted to pH 5.8 with 1 M KOH and autoclaved before pouring plates.

Plants were grown in the growth room with 24 hours light with an intensity of 150 uE m^{-2} s^{-2} at 23 ˚C, and all analyses were carried out on plants grown under such conditions. Rice to grow to maturity was potted in 3 L pots with compost of 1:1 (w:w) ratio of John Innes No1 (John Innes, Norwich UK) : Levington M3 (JFC Monro, Devon, UK) and transferred to a glasshouse. Glasshouse conditions were 12 h light (30 ˚C)/ 12 h dark (25 ˚C), supplemented with sodium lighting which was activated when external irradiance fell below 200 µmol m^{-2} s^{-1}, located at Sutton Bonington Campus, the University of Nottingham (52°49’59”N, 1°14’50”W).

2.3 qRT-PCR

Rice grown on ½ strength MS agar for 7 days were transferred to liquid ½ MS (prepared without addition of Bacto agar), with two concentrations (2 µM or 10 µM) of IAA and BAP with a control of DMSO, and incubated for the amount of time indicated in the figures in a growth room with a light intensity of 150 uE m^{-2} s^{-2} at 23 ˚C. Ten plants from each treatment were collected and roots dissected to three sections; 1 mm, 1 to 3 mm, 3 to 6 mm from the root tip.

Whole RNA was extracted from these separate sections using TRIzol (Life Technologies) according to manufacturer's instructions, and 100ng RNA was used for cDNA synthesis using SuperScriptIII reverse transcriptase (Life Technologies) according to manufacturer's instructions. qRT-PCR was performed using SensiMix SYBR Hi-ROX kit (Bioline) in a LightCycler 480 (Roche) according to manufacturer's instructions. OsUBQ and Os40S were used as internal controls to normalise all data, and primers are listed in Appendix Table 1.

2.4 Genomic DNA extraction

For genotyping purposes a rough genomic DNA extraction protocol was employed. This involved grinding a single leaf in an Eppendorf tube with a plastic grinder for 15 seconds, adding 400 µl extraction buffer (200 mM Tris-HCl pH 7.5, 250 mM NaCl, 25 mM EDTA, 0.5% SDS) and grinding a further 15 seconds. Samples were centrifuged 13000 g for 1 minute, and 300 µl of supernatant added to a new tube with 300 µl isopropanol. Samples were mixed by inversion and incubated for 2 minutes at room temperature. Samples were then centrifuged at 13000 g for 15 minutes at 4 ˚C, supernatant removed and pellet rinsed with 500 µl 70 % ethanol. Samples were centrifuged a further 5 minutes at 13000 g at 4 ˚C, supernatant removed and pellet dried. Pellets were resuspended in 50 µl TE buffer pH 8.

For promoter amplification genomic DNA of better quality was preferred and the CTAB extraction protocol was used. Leaf tissue was ground using plastic

grinders in Eppendorfs with liquid nitrogen and when powdered 400 µl of CTAB extraction buffer (100 mM Tris-HCl pH 8, 1.4 M NaCl, 20 mM EDTA, 2 % CTAB, 0.2 % BME) was added. Samples were incubated in extraction buffer at 65 ˚C for 10 minutes. 400 µl of phenol: chloroform: isoamyl alcohol (25: 24: 1) was added, samples mixed by inversion and centrifuged 13000 g for 15 minutes at room temperature. The aqueous upper layer was then mixed with an equal volume of chloroform, and samples centrifuged for a further 15 minutes at 13000 g at room temperature. The aqueous phase was then taken to a new tube and 0.7 volume of isopropanol and 0.1 volume of 3 M sodium acetate pH 5.7 was added and samples mixed by inversion. Genomic DNA was precipitated at -20 ˚C overnight. Samples were then centrifuged at 13000 g for 15 minutes at 4 ˚C, supernatant removed and pellet rinsed with 500 µl 70 % ethanol. Samples were centrifuged a further 10 minutes at 13000 g at 4 ˚C, supernatant removed and pellet dried. Pellets were resuspended in 50 µl TE buffer pH 8.

2.5 Competent cell preparation

Escherichia coli strains DH5a, Origami 2(DE3)pLysS and DH10Bac cells were made as chemically competent stocks and *Agrobacterium tumefaciens* strains GV3101 and AGL1 were made as electro-competent stocks.

To make chemically competent cells 10 ml LB cultures from a single colony were grown shaking at 150 rpm at 37 ˚C overnight. 5 ml of the starter culture was used to inoculate 100 ml pre-warmed LB media, and the culture grown in

the same conditions to an OD_{600} of 0.37 to 0.4. Once at the correct OD_{600}, the culture was chilled on ice for 15 minutes, centrifuged at 3000 rpm for 15 minutes at 4 ˚C, the supernatant removed and the pellet resuspended in 50 ml RF1 solution (100 mM RbCl, 50 mM $MgCl_2.4H_2O$, 30 mM potassium acetate, 10 mM CaCl2.$2H_2O$, 15 % glycerol w/v, pH to 5.8 with acetic acid). Cell suspensions were incubated on ice for 15 minutes and cells pelleted by centrifuging at 3000 rpm for 15 minutes at 4 ˚C. The pellet was resuspended in 8 ml RF2 solution (10 mM RbCl, 10 mM MOPS, 75 mM $CaCl_2.2H_2O$, 15 % glycerol w/v, pH to 6.8 with NaOH). Cells were incubated on ice for 15 minutes before being separated to 50 µl aliquots, flash frozen in liquid nitrogen and stored at -80 ˚C.

To make electro-competent cells 100 ml of LB was inoculated with a single colony and grown shaking at 200 rpm at 28 ˚C overnight. 500 ml LB media was inoculated with 50 ml of the overnight culture and grown to an OD_{600} of 1 to 1.5. At the correct OD_{600} the culture was chilled on ice for 20 minutes and then centrifuged at 4000 g for 15 minutes at 4 ˚C. Supernatant was removed, the pellet resuspended in 250 ml of chilled sterile H_2O and the cell suspension centrifuged at 4000 g for 15 minutes at 4 ˚C. This was step was repeated four more times and the cell pellet resuspended in 50 ml chilled sterile 10 % glycerol. The cell suspension was centrifuged 4000 g for 15 minutes at 4 ˚C, supernatant removed and the pellet resuspended in 4 ml 10 % glycerol. Cells were separated to 40 µl aliquots, flash frozen in liquid nitrogen and stored at -80 ˚C.

2.6 Molecular cloning

Vectors for trans-complementation experiments were created through MultiSite Gateway (Life Technologies) according to manufacturer's instructions (for a review see Karimi, Depicker, & Hilson, 2007). CDS of OsPHP1, OsPHP2, OsPHP3, OsRR1, OsRR3, OsRR6, OsRR7 were amplified from rice 'Nipponbare' cDNA and AHP6 and ARR5 amplified from *Arabidopsis thaliana* (Columbia-0) cDNA using gene specific primers (Appendix Table 2) by PCR using Phusion DNA polymerase (New England Biolabs), and cloned into pDONR_221 (Appendix Figure 1) through the BP reaction following manufacturer's instructions. Resulting entry clones were recombined with the entry clones pDONR_P4P1R_AHP6 and p2RP3_nosT2 (already in use in the lab) into the destination vector pHm34GW through the LR reaction (Appendix Figures 1 and 2). OsRR6 pDONR221 was recombined into destination vector pK7m34GW. Resulting constructs were checked to be correct via diagnostic restriction digests and confirmed via sequencing.

Vectors for bacterial protein expression were created by restriction enzyme cloning and ligation with T4 DNA ligase (New England Biolabs) according to manufacturer's instructions. Plasmids were obtained from Tatsuo Kakimoto (Osaka University). Plasmids obtained included SLN1 HK, SLN1 Rec and ARR1 Rec in pMAL-c2x (New England Biolabs), AtAHP1 in pGEX6p1 (GE Healthcare Life Sciences), and AtAHP6 and AtAHP6(NH) in pFAST-BAC1-GST (Thermo Fischer Scientific). The CDS of OsAHP1, OsAHP2, OsPHP1, OsPHP2 and OsPHP3 were amplified from rice 'Nipponbare' cDNA using primer sets described in

Appendix Table 4 by PCR using Phusion DNA polymerase (New England Biolabs). OsAHP1 and OsAHP2 were cloned into pGEX-6p1 (Appendix Figure 3) at the BamHI and SalI, and BamHI and EcoRI restriction sites respectively. Constructs for expression of SLN1-HK and SLN1-HK-Rec with GST tags were obtained from Ann West, the University of Oklahoma.

For plasmids for insect cell expression, CDS of OsPHP1, OsPHP2 and OsPHP3 were cloned into pFAST-BAC1-GST at the BamHI and SalI restriction sites. Site directed mutagenesis was performed to change the conserved phosphoaccepting histidine (H) residue of OsAHP1 and OsAHP2 to both an aspartamine (N) and a glutamine (Q) residue, and to restore the phosphoaccepting H residue in OsPHP1, OsPHP2 and OsPHP3. This was done using the Quickchange II XL kit (Agilent) according to manufacturer's instructions. AtAHP6(NQ) was created by site directed mutagenesis using the Quickchange II XL kit (Agilent). Primer lists for SDM are shown in Appendix Table 5.

Promoter::GUS reporter constructs were created by restriction enzyme cloning into pCAMBIA 1305.1 (Appendix Figure 4) using T4 DNA ligase (New England Biolabs) according to manufacturer's instructions. Promoter regions 3-4 kb immediately upstream of the start codon for OsPHP1, OsPHP2 , OsPHP3, OsRR1, OsRR3, OsRR6 and OsRR7 were amplified from rice 'Kitaake' gDNA by PCR using Phusion DNA polymerase (New England Biolabs) and cloned into pCAMBIA 1305.1 using primers and restriction enzyme combinations described in Appendix Table 6. Promoter sequences were first

sub-cloned to pJET1.2 (Thermo Fischer Scientific) (Appendix Figure 4), sequenced (primers in Appendix Table 9) and then cloned into specific restriction sites of pCAMBIA 1305.1 after treatment of the cut vector with calf intestinal alkaline phosphatase (Promega) according to manufacturer's instructions.

Regions of genes of interest to target as sgRNA for CRISPR were chosen with help from CasOT software (Xiao et al., 2014) and the OryGenes database (CIRAD). Regions chosen were from the CDS and had the lowest number of estimated off-target recognition. Two sgRNA constructs were designed for each gene. Constructs for CRISPR were created by cloning sgRNA regions (ordered as complementary oligos and annealed by diluting to 100 uM in a buffer with 100 mM potassium acetate and 30 mM HEPES at pH 7.5, heating to 92 ˚C for 2 minutes in a water bath and allowing to cool slowly) into the BsaI restriction enzymes sites of the pOssgRNA vector (Appendix Figure 5). This construct was then cloned into the pH-Ubi-Cas9-7 vector (Appendix Figure 5) via Gateway (Life Technologies) LR reaction, according to manufacturer's instructions. sgRNA oligos ordered and annealed are listed in Appendix Table 7. Resulting transformants were genotyped by amplifying target regions using primers in Appendix Table 8 and sending PCR product for sequencing.

2.7 Rice transformations

Rice was transformed through infection of callus induced from mature embryos, and the method was based on Hiei and Komari (2008). Callus formation was induced by incubating dehusked surface sterilised seeds on induction media (2N6). Seeds were incubated at 32 ˚C in the dark for 10 days. Scutellar calli were then dissected and moved to new 2N6 media and incubated for a further 10 days. Four days before infection calli were cut to 2-4 mm pieces and subcultured to new 2N6 media. *Agrobacterium tumefaciens* strain AGL1 were transformed with appropriate vectors and grown on YEP plates with appropriate antibiotic at 28 ˚C for 2 days. One colony was used to inoculate a 5 ml overnight culture in liquid YEP with appropriate antibiotic shaking at 28 ˚C. 100 ul of this culture was then used to inoculate a 15 ml overnight culture in liquid YEP shaking at 28 ˚C. These cultures were centrifuged at 5000 g for 10 minutes, and pellets were resuspended in infection media (AAM) to an OD_{600} of 0.3-0.5. Calli were washed in sterile ddH_2O, drained and incubated with *Agrobacterium* infection cultures for 2 minutes with gentle shaking. Calli were blotted dry on filter paper, transferred to co-cultivation media (2N6-As) with filter paper and incubated in the dark at 25 ˚C for 3 days. After 3 days calli were washed in sterile ddH_2O supplemented with 200 mg/l timentin and without acetosyringone, blotted dry on sterile filter paper for at least 15 minutes, transferred to selection I plates (2NBKCH40) and incubated for 2 weeks at 32 ˚C in the dark. Actively growing calli were then transferred to new selection II media (nN6CH50) and incubated at 32 ˚C in the light for 5 days. Proliferating calli were then

transferred to regeneration I media (N6RH50) and grown at 28 ˚C in the light until shoots appear (changing to new media every 2 weeks if needed). Plants with shoots around 5 cm were then transferred to regeneration II media (N6FH50) and grown in the same conditions another 2 to 3 weeks. Plants were then transferred to the greenhouse, planted in soil (making sure to keep them humid for the first few days) and grown to maturity. Compositions of all media used is described as seen in (Hiei & Komari, 2008).

This protocol, including compositions of media used, went through a number of optimisation steps. The main major changes to media was hormone concentrations in the first regeneration media. Initially, 2 mg/l kinetin and 1 mg/l NAA were used which gave poor regeneration efficiency. This was eventually changed to 2 mg/l kinetin and 0.2 mg/l NAA. In addition a major problem initially was overgrowth of Agrobacterium at all stages after co-cultivation. This was resolved by making washing and drying calli more thoroughly after co-cultivation, and including two antibiotics in the selection media. Although initial transformations were carried out at the University of Nottingham, subsequent transformations were carried out by the lab of Wanqi Liang, Shanghai Jiao Tong University, due to greater capacity.

2.8 GUS staining

For GUS staining, tissue was harvested and fixed in cold acetone for 1 hour on ice. Acetone was washed out of tissue with multiple washes of sodium phosphate buffer monobasic (100 mM, pH 7). Tissue was then placed in GUS

stain solution (1 mM EDTA pH 8, 5 mM potassium ferricyanide, 5 mM potassium ferrocyanide, 0.1 % Triton-X-100, 1 mg/ml X-gluc) and incubated at 37 °C in the dark until staining appeared. After an appropriate amount of staining was seen, GUS stain solution was removed and replaced with 70 % ethanol for 1 day. Tissue was then mounted in chloral hydrate and imaged.

2.9 Sectioning and microscopy

For embedding and sectioning in plastic resin, dissected roots were fixed in 5 ml fixation solution (1 ml 25% glutaraldehyde, 2.7 ml 37% formaldehyde, 2.5 ml 0.5M NaPi pH 7.2, 18.8 ml ddH2O) overnight at 4˚C. Tissue was then taken through an ethanol dilution series of 10%, 30%, 50%, 70%, 96%, 100%, 100% ethanol with incubations of 30 minutes at each dilution. Tissue was then incubated in 1:1 100% ethanol:Solution A (Leica HistoResin embedding kit) and incubated at room temperature overnight. Tissue was then incubated in Solution A for 4 hours, transferred to moulds and moulds filled with 15:1 Solution A:Hardener (Leica HistoResin embedding kit). Moulds were left to fully set for four days. Plastic sections were then removed from moulds and sectioned (4 um sections) using a Leica Ultracut EM UC6 microtome according to manufacturer's instructions. Glass blades for use with the microtome were made using a Leica Glass Knifemaker EM KMR2 according to manufacturer's instructions. Sections were stained with 0.05 % toluidine blue in 0.1M sodium phosphate buffer and imaged using a Leica DM5000 B microscope.

For rice root sections cut using a vibratome, roots were first harvested and embedded in hot 3 % agarose using an Eppendorf tube box as a mould to keep roots straight. Once solidified, the agarose block with roots embedded is cut to an appropriate shape for the vibratome and glued onto a vibratome mounting block. This is secured into a water filled well in position for cutting on the vibratome. Sections were cut. Sections were stained with calcofluor for 30 seconds, washed by dipping in water and mounted on slides. A Nikon confocal microscope was used to image sections by using three passages with different laser and detector combinations to create three images which are overlayed (1: laser 488 and 543, detector 605/75; 2: laser 408, detector 450/35; 3: laser 408, detector 515/30).

For screening of protoxylem defects in *Arabidopsis* complementation lines, plants were mounted in chloral hydrate and imaged using a Leica DM5000 B microscope.

2.10 Protein expression in bacteria

For bacterial expression, constructs with CDS in pGEX6p1 or pMALc2x were transformed into Origami 2(DE3)pLysS competent cells (Novagen) and plated on LB agar with 100 mg/ml ampicillin, 30 mg/l kanamycin and 34 mg/l chloramphenicol, according to manufacturer's instructions. Individual colonies were picked and grown in 5 ml LB cultures with 100 mg/ml ampicillin, 30 mg/l kanamycin and 34 mg/l chloramphenicol shaking at 200 rpm at 37 ˚C overnight. Glycerol stocks were made from these same cultures by combining

1 ml of culture with 500 µl of 50 % glycerol, flash freezing in liquid nitrogen and storing at -80˚C. Plasmid was extracted from the same cultures using GeneJET Plasmid Miniprep Kit (Thermo Fischer Scientific) according to manufactures instructions, and diagnostic digests performed to check for the presence of the corrects plasmids. For stocks with the correct plasmid in, glycerol stocks were streaked onto new LB agar plates with 100 mg/ml ampicillin, 30 mg/l kanamycin and 34 mg/l chloramphenicol and incubated overnight at 37 ˚C. Individual colonies were taken to inoculate new 5 ml LB cultures with 100 mg/ml ampicillin, 30 mg/l kanamycin and 34 mg/l chloramphenicol shaking at 200 rpm at 37 ˚C overnight. The full 5 ml of these starter cultures were used to inoculate 500 ml cultures in the same media. These were grown in the same conditions to an OD_{600} of 0.5 and IPTG was then added to a final concentration of 0.2 mM to induce protein expression. Cells were grown for a further 2 hours after induction, were harvested by centrifugation at 4000 x g for 15 minutes, and pellets stored at -80.

2.11 Protein expression in insect cells

For insect cell expression, recombinant bacmid first needs to be produced and isolated. To do this, DH10Bac cells (Thermo Fischer Scientific) were transformed with the appropriate pFAST-BAC-GST plasmid containing the CDS of genes to be expressed. For the transformation, 1 ng of plasmid was added to 100 ul of thawed DH10Bac cells which were incubated on ice. Cells were heat-shocked at 42 for 45 seconds and returned to ice for two minutes. Cells

were then transferred to 1 ml LB media and incubated at 37 ˚C shaking at 225 rpm for 4 hours. For each transformation, 1/10 and 9/10 of the cell volume was plated on LB agar plates with 50 ug/ml kanamycin, 7 ug/ml gentamycin, 10 ug/ml tetracycline, 100 ug/ml, 100 ug/ml X-gal and 40 ug/ml IPTG, and incubated at 37 for 2 days. For each transformation 10 white colonies were picked and restreaked onto fresh plates (with the same antibiotic, X-gal and IPTG concentrations) and incubated at 37 for 2 days. A single white colony per transformation from these plates was then used to inoculate a 5 ml liquid LB culture containing 50 ug/ml kanamycin, 7ug/ml gentamycin and 10 ug/ml tetracycline, which was grown at 37 ˚C shaking at 225 rpm for 2 days. Cells were pelleted by centrifugation at 13,000 x g for 2 minutes, supernatant removed and cell pellet resuspended in 300 ul of Solution I added (15 mM Tris-HCl pH 8, 10 mM EDTA, 100 ug/ml RNase A). 300 ul of Solution II (0.2 N NaOH, 1% SDS) was then added and cells gently mixed. 300 ul of 3 M potassium acetate pH 5.5 was added and the samples incubated on ice for 10 minutes. Samples were then centrifuged 13,000 x g for 10 minutes and supernatant transferred to a new tube with 800 ul cold isopropanol, samples gently mixed and incubated on ice for 10 minutes. Samples were centrifuged at 13,000 x g for 15 minutes, supernatant removed, and the pellet washed with 500 ul of 70% ethanol. Samples were centrifuged again at 13,000 for 5 minutes, supernatant removed, the pellet dried and resuspended in 40 ul 1X TE buffer, pH 8. The presence of the gene of interest in recombinant bacmid DNA was checked by PCR using the primers M13 Forward (-40) and M13 Reverse (see Appendix). PCR was performed according to Phusion taq

protocol (New England Biolabs) with 100 ng of Bacmid DNA as the template. Bacmid DNA was stored at 4 ˚C in darkness.

Insect cells used were *Spodoptera frugiperda* Sf9 cells which were maintained in mid-log phase and grown in Insect X-Press protein-free media with L-glutamine (Lonza), and supplemented with penicillin (100 U/ml) and streptomycin (100 ug/ml) at 28 ˚C. All insect cell work was carried out using sterile technique in appropriate laminar flow hoods. For initial infection with recombinant bacmid, insect cells were grown as a monolayer adhered to the bottom of 6-well plates and for all other infections cells were grown in media shaking at 150 rpm with 10% foetal calf serum (FCS). Infections were carried out according to instructions in Bac-to-Bac baculovirus expression system manual (Invitrogen), with few changes (10 ug bacmid was used for initial infection and Insect X-press media was used). After protein gels and Western blots were run to check for expression of protein of interest (summarized in Chapter 4), BIIC stocks were made. To make BIIC stocks, 50 ml cells (0.5 X 106 cells/ml) in shaking culture were infected with 500 ul P1 virus, and after growing for 16 hours cell size was monitored using a cell counter (Orflow). Once cells increase in size from around 15 um to 18-19 um, cells are harvested by centrifuging at 1500 rpm for 5 minutes and resuspended in 2.5 ml Insect X-press media with the same concentration of antibiotics and 10% DMSO. The cells are then split to aliquots of 300 ul and slowly frozen to -80 ˚C. To infect large cultures for scaling up protein purification, 200 ml cultures (seeded at 0.5 X 106 cell/ml and grown for 24 hours before infection) were infected with 100 ul BIIC stock. After expression of protein in insect cells, cultures were

pelleted by centrifuging at 4000 x g for 15 minutes and cell pellets stored at -80 ˚C.

2.12 Protein purification

Purification of protein from bacterial or insect cell pellets followed the same protocol, except that cells were lysed in different ways. Cell pellets were resuspended in 40 ml (for bacterial pellets) or 20 ml (for insect cell pellets) of GST buffer for GST-tagged proteins (50 mM Tris-HCl pH 8, 150 mM NaCl, 1 mM EDTA, 10 % v/v glycerol, 10 mM BME, 1 mM AEBSF, 10 µg/ml leupeptin hemisulphate) or MBP buffer for MBP-tagged proteins (20 mM Tris-HCl pH 7.4, 200 mM NaCl, 1 mM EDTA, 10 % v/v glycerol, 10 mM BME, 1 mM AEBSF, 10 µg/ml leupeptin hemisulphate). For bacteria, cells were lysed by using a cell disruptor at 35 Kpa according to manufacturer's instructions. For insect cells, cells were lysed using a probe sonicator according to manufacturer's instructions. Cell lysate was centrifuged 4000 g for 15 minutes at 4 ˚C. Supernatant was decanted to ultracentrifuge tubes and centrifuged at 45000 g for 1 hour at 4 ˚C. For GST tagged proteins 500 µl glutathione sepharose 4B resin (GE Healthcare Life Sciences) was washed in 50 ml GST buffer, and for MBP tagged proteins 500 µl amylose resin (New England Biolabs) was washed in 50 ml MBP buffer for 5 minutes. After washing, tubes with glutathione sepharose 4B or amylose resin were centrifuged at 800 g for 5 minutes, buffer removed and the wash step repeated. Cell lysate was added to the appropriate resin and rotated at 4 ˚C for 1 hour. Samples were then

centrifuged at 800 g for 5 minutes at 4 ˚C, supernatant removed the resin was washed in 20 ml of the appropriate buffer. Samples were centrifuged again, supernatant removed and 5 µl mixed with 60 µl coomassie reagent (Sigma-Aldrich) to test how much protein comes off during the washes. Washes in appropriate buffer were repeated until no more protein was observed to come off. After washing, resins were transferred to Eppendorf tubes, centrifuged 800 g a further 5 minutes at 4 ˚C and supernatant removed. GST tagged proteins were eluted with 500 µl of 40 mM glutathione in GST buffer and MBP tagged proteins eluted with 500 µl of 40 mM maltose in MBP buffer, by mixing and incubating on ice for 1 minute, centrifuging 800 g for 5 minutes and keeping supernatant with protein. For GST tagged SLN1-HK and SLN1-HK-Rec protein was left bound to glutathione sepharose 4B beads, and used in assays as such. Elutions were carried out until no more protein was observed in the supernatant by testing 5 µl in 60 µl coomassie reagent. Successful purification was observed by running 20 µl of each eluted fraction on a SDS PAGE gel and staining with Instant Blue. Buffer was exchanged in purified protein fractions for phosphotransfer buffer (50 mM Tris-HCl pH 8, 50 mM KCl, 10 % v/v glycerol, 2 mM BME, 0.1 mM AEBSF) by dialysis using 10 mm cellulose dialysis tubing (Sigma-Aldrich) according to manufacturer's instructions. After dialysis, proteins were separated to 100 µl aliquots and stored at -80 ˚C.

2.13 Running PAGE

PAGE gels were poured using 10 % resolving gel and 4 % stacking gel. For two resolving gels, 8.5 ml ddH2O was combined with 4.5 ml 1.5 M Tris HCl pH 8.8, 4.5 ml 40 % acrylamide, 135 µl 10 % SDS, 270 µl 10 % ammonium persulfate and 5 µl TEMED. For two stacking gels, 7.5 ml ddH2O was combined with 3 ml 0.5 M Tris-HCl pH 6.8, 1.2 ml 40 % acrylamide, 90 µl 10 % SDS, 180 µl 10 % ammonium persulfate and 7.5 µl TEMED. For resolving and stacking gels, APS and TEMED was added immediately before pouring. Before loading, protein sample was mixed with 6 X Protein loading buffer (375 mM Tris-HCl pH 6.8, 9 % SDS, 50 % glycerol, 0.03 % bromophenol blue, 5 % β-mercaptoethanol). Samples were then heated to 99 °C for 5 minutes, and gels loaded at 120 V until the leading protein band was seen to run off the gel. All steps were carried out using the Bio-Rad MiniProtean system.

2.14 Performing Western blots

For Western blots, protein gels were run as described above. After running, the gel was assembled next to a nitrocellulose sheet, with layers of filter paper and sponge on either side of it, in a clamp in the transfer chamber placed and submerged in transfer buffer (5 mM Tris, 50 mM glycine, 20 % methanol). Transfer was run at 250 mA for 90 minutes. Successful transfer was determined by staining the nitrocellulose sheet with Ponceau stain. After confirmation of successful transfer, Ponceau stain was washed off with ddH_2O and the sheet put in blocking buffer (5 % Marvel dry skimmed milk in PBST

buffer) on a roller for 1 hour. After blocking, solution was removed and primary antibody (anti-GST goat) was introduced in the same blocking solution at a concentration of 1:800 for 2 hours. The antibody solution was then removed and the membrane washed in PBST buffer for 5 minutes 3 times. After washing solution was removed secondary antibody (donkey anti-goat IgG IR800) was introduced at a concentration of 1:10,000 and incubated on a roller for 1 hour. Secondary antibody solution was removed, the membrane washed 5 minutes 3 times in PBST buffer and the membrane imaged using a LI-COR imager (according to manufacturers protocols).

2.15 Phosphotransfer assays

Phosphotransfer assays were carried out according to methods described by Fassler & West, (2010). For phosphorylation of bead-bound SLN1-HK or SLN1-HK-Rec, 3 uM of bead bound protein was combined with 7 uM [y-32P]-ATP (30 Ci/mmol) in phosphotransfer buffer (50 mM Tris-HCl pH 8, 100 mM KCl, 10 mM $MgCl_2$, 2 mM DTT, 20 % glycerol) and incubated at room temperature for 1 hour. Resin bound phosphorylated protein was pelleted by centrifuging at 100 X g for 1 minute and washed 3 times with wash buffer (50 mM Tris HCl pH 8, 50 mM KCl, 10 mM $MgCl_2$, 1 mM DTT). The pellet was resuspended in 100 µl of wash buffer and used in phosphotransfer experiments immediately.

To follow transfer of the phosphate group from SLN1-HK-Rec to HPTs, P~SLN1-HK-Rec was incubated with HPT in equimolar amounts in a total

reaction volume of 15 ul in reaction buffer (50 mM Tris-HCl pH 8, 30 mM KCl, 10 mM $MgCl_2$, 1 mM DTT) for 10 minutes at room temperature. Reactions were stopped by adding 5 ul of 4 X stop buffer (250 mM Tris-HCl pH 6.8, 8% SDS, 60 mM EDTA, 40% glycerol, 0.008 % bromophenol blue), samples run by PAGE as described above and the wet gel sealed and exposed to a BAS-IP-MS storage phosphor sheet (GE Healthcare) and imaged using the molecular imager FX (Bio-Rad).

2.16 Phylogenetic analysis

To obtain the amino acid sequences of histidine phosphotransfer proteins for multiple species, BLAST searches were performed using the Phytozome database. Searches were performed using each of the *Arabidopsis* and rice HPTs to ensure all related proteins would be included, and the proteomes of 38 species were searched each time. Species used for phylogenetic analysis are listed in Supplementary. Phylogenetic analysis and bootstrapping (using 100 bootstrap replicates) was performed using PHYLIP (Joe Felsenstein, University of Washington) programmes Seqboot, Protdist, Neigbour and Consense to generate unrooted neighbour-joining trees. Consensus trees from PHYLIP were visualised using FigTree (Andrew Rambaut, University of Edinburgh) and iTOL.

Chapter 3: Auxin and cytokinin function in rice root vascular patterning

3.1 Introduction

There are numerous environmental stresses which plants must be able to cope with and phenotypic plasticity is key to survival. Plasticity in developmental traits can be thought of at various levels, and as such there are some important distinctions to be made. Phenotypic plasticity, defined as 'the ability of a single genotype to exhibit variable phenotypes in different environmental conditions', refers only to individual genotypes within a species (Fusco & Minelli 2010). However, it is also useful to consider the degree of plasticity exhibited by different genotypes within a species, and also across species. Studies at this level are able to indicate species or cultivars which are better able to survive particular environmental stresses, which in turn may lead to understanding of why and how these differences occur. For example, a quantitative trait loci (QTL) mapping study using the progeny of a cross between two rice cultivars with very different root architecture (shallow or deep rooting) led to the identification of DEEPER ROOTING 1 (DRO1) as a QTL involved in root growth angle (Uga et al. 2011). Further characterisation of DRO1 showed this QTL can lead to deeper rooting when introduced into a shallow rooting cultivar (by altering crown root gravitropism), enabling the resulting line to maintain yield under drought stress (Uga et al. 2013).

Phenotypic plasticity itself can also be studied at multiple levels, depending on the particular phenotypic aspect under scrutiny, be it physiological,

architectural or anatomical. Recently, research into phenotypic plasticity has largely been driven by a desire to understand adaptive responses of plants to climate change. This has largely focussed on responses to elevated CO_2, temperature, drought and a combination of these stresses (as reviewed by Gray & Brady 2016). These studies have enabled identification of a number of traits for which plasticity in development is important for adaptation, and in many cases provided insight into the molecular mechanisms governing development of these traits. In rice, much of the focus has been on the implications of C3 photosynthesis (Hamim et al. 2016). Detailed study has also been able to link physiological measurements such as rates of photosynthesis with anatomical differences seen. For example, two back-crossed inbred lines from a cross between a high-yielding indica and a japonica cultivar were observed to have much higher photosynthetic rates. Through detailed study of both physiology and anatomy, He et al. (2017) were able to show the reason for higher photosynthetic rates was increased conductance of mesophyll cells, which results from increased lobing of these cells.

Cellular anatomy has been fairly well studied in this respect, particularly in the major food crops. In rice, there is huge variation in leaf anatomy across cultivars and analysis of this diversity has revealed evolutionary trends in anatomical changes (Chatterjee et al. 2016). In roots, the focus on research into anatomy is largely with respect to drought stress. As mentioned in the introduction, drought tolerant rice varieties are associated with fewer, more narrow xylem vessels (Henry et al. 2012). While much work has been done to compare these anatomic traits across cultivars, relatively few studies have focussed exclusively

on plasticity of root anatomy within a single cultivar. Greater plasticity in terms of root aerenchyma development in rice has been associated with development of longer and more branched lateral roots, enabling increased shoot development (Niones et al. 2013). In addition, a screen of plasticity of various anatomic traits of rice and wheat suggested that the greater plasticity observed in wheat roots is a key reason for its superior ability to tolerate drought (Kadam et al. 2015). Recently, research into root architectural plasticity in response to drought and phosphate stress led to the identification of genetic loci related to multiple root architectural plasticity traits (Sandhu et al. 2016). Similar studies to identify loci related to anatomical plasticity may also be useful, to allow development of cultivars with greater plasticity in various traits and consequent improved adaptability to drought prone environments. An additional consideration is the importance of anatomical plasticity in different root types. The bulk of the rice root mass is composed of crown roots and as such, many studies have focussed only on this root type. However, recently the importance of other root types has become apparent. For example, comparing root architectural traits of different root types and in different growth conditions, revealed it is the lateral roots which provide the majority of the root hair surface area – a trait associated with phosphate uptake (Nestler et al. 2016). This study also nicely demonstrates the importance of developmental plasticity, as authors show great differences in root hair formation in different growth conditions, in addition to in different root types (Nestler et al. 2016).

Plasticity in anatomical development has been fairly well studied but the underlying molecular causes which enable plasticity have not. During

development plants need to integrate multiple environmental signals to enable them to make these developmental decisions. Therefore, understanding how these signalling pathways interact to modify development is critical in understanding phenotypic plasticity.

This chapter is divided into three sections. Firstly, root anatomical traits of rice cultivars which are favoured for use in different environments are compared, and possible links with physiological measurements examined. Secondly, plasticity in root anatomical traits in response to drought is considered. Finally, the role of cytokinin and auxin in rice root vascular development is discussed.

3.2 Root anatomical diversity across cultivars

Rice is a major world crop and also serves as a model monocot. As such it has been intensively studied for many years, which has led to a wealth of research material as well as breeding of many cultivars of commercial importance. Since many areas of the world are dependent on rice as a staple crop, breeding has resulted in a huge number of cultivars which are well adapted to their local ecology. Rice has traditionally been grown in two major ways: in flooded paddy fields (or lowlands) or in rain-fed upland environments (Parameswari et al. 2014). In addition, many areas also grow deep rice, in flooded conditions at least 50 cm deep in water. Generally, paddy rice requires much greater input in terms of water and fertilisers, but also has much greater yields. Upland rice, while not performing as well in terms of yield, is often more tolerant to drought and so has traits of interest to breeders. It is also worth considering that while

paddy rice is generally grown in a similar manner regardless of the location, for upland rice there is a great diversity of farming practises which is largely dependent on local climate, and consequently a great diversity of upland rice cultivars. More recently, the System of Rice Intensification (SRI) has been put into practice to increase productivity and reduce dependence on costly agricultural technologies (Sridevi et al. 2011). The major components of SRI include growth with intermittent irrigation, rather than flooded paddy fields, and careful choosing of cultivars appropriate to the local environment.

There is a large body of work comparing upland and paddy rice cultivars. All this has largely concluded differences in both anatomy and physiology are important for drought tolerance, but that the major differences are between genotypes (Uga et al. 2009). Large scale phylogenetic analyses may be useful in understanding the selection of drought tolerant traits in different cultivars rather than assuming differences in tolerance between upland or lowland rice, which encompass great variation. Recent genome sequencing efforts have led to the sequences of 3000 rice genomes to become available, enabling these sorts of analyses in the future (the 3000 rice genomes project., 2014). While it might be expected that upland cultivars would consistently show traits we associate with drought tolerance, this is not true across all genotypes. It may be the case that the drought tolerant cultivars have mechanisms to enable survival in drought other than those that have been studied so far. GWAS and QTL analysis is an extremely important tool to uncover elements that may be important but are not as visible (Uga et al. 2008). In addition, different cultivars may have different strategies to tolerate drought, with some neglecting to

improve water use efficiency in an attempt to complete their life cycle as quickly as possible.

One anatomical aspect known to be important in a plants response to drought is xylem vessel number and size. This has been seen in many previous studies (Henry et al. 2012; Yambao et al. 1992; Stiller et al. 2003). In order to see whether xylem anatomies differ between upland and lowland cultivars, and the potential influence this may have on physiological measurements, a number of upland and lowland cultivars were chosen for analysis. These cultivars were chosen for study because they were already being analysed for physiological differences by Umar Mohammed (the University of Nottingham). The cultivars used include the African rice (*Oryza glaberrima*) accession CG14 (a separate rice species domesticated in Africa (Wang et al. 2014)), the widely used Asian rice (*Oryza sativa*) cultivars FARO52 (developed in Nigeria (Toungos 2016)), IR64 (developed in the Philippines (Datta & Datta 2006)) and Kaybonnet (developed in the US (Wells et al. 1995)), and a number of improved cultivars developed by crossing African and Asian rice cultivars (developed by the Africa Rice Centre, Ivory Coast (Fukuta et al. 2012)). Primary roots of 7 day old plants were sectioned at the same distance from the root tip, imaged by confocal microscopy (Figure 3.1) and analysed using PHIV-Rootcell software (Lartaud et al. 2015) (Figure 3.2). Anatomical data was correlated with physiological data obtained by Umar Mohammed (the University of Nottingham).

Major anatomical differences between cultivars can be seen from images of representative sections, such as the upland cultivar WAB 759 having a much

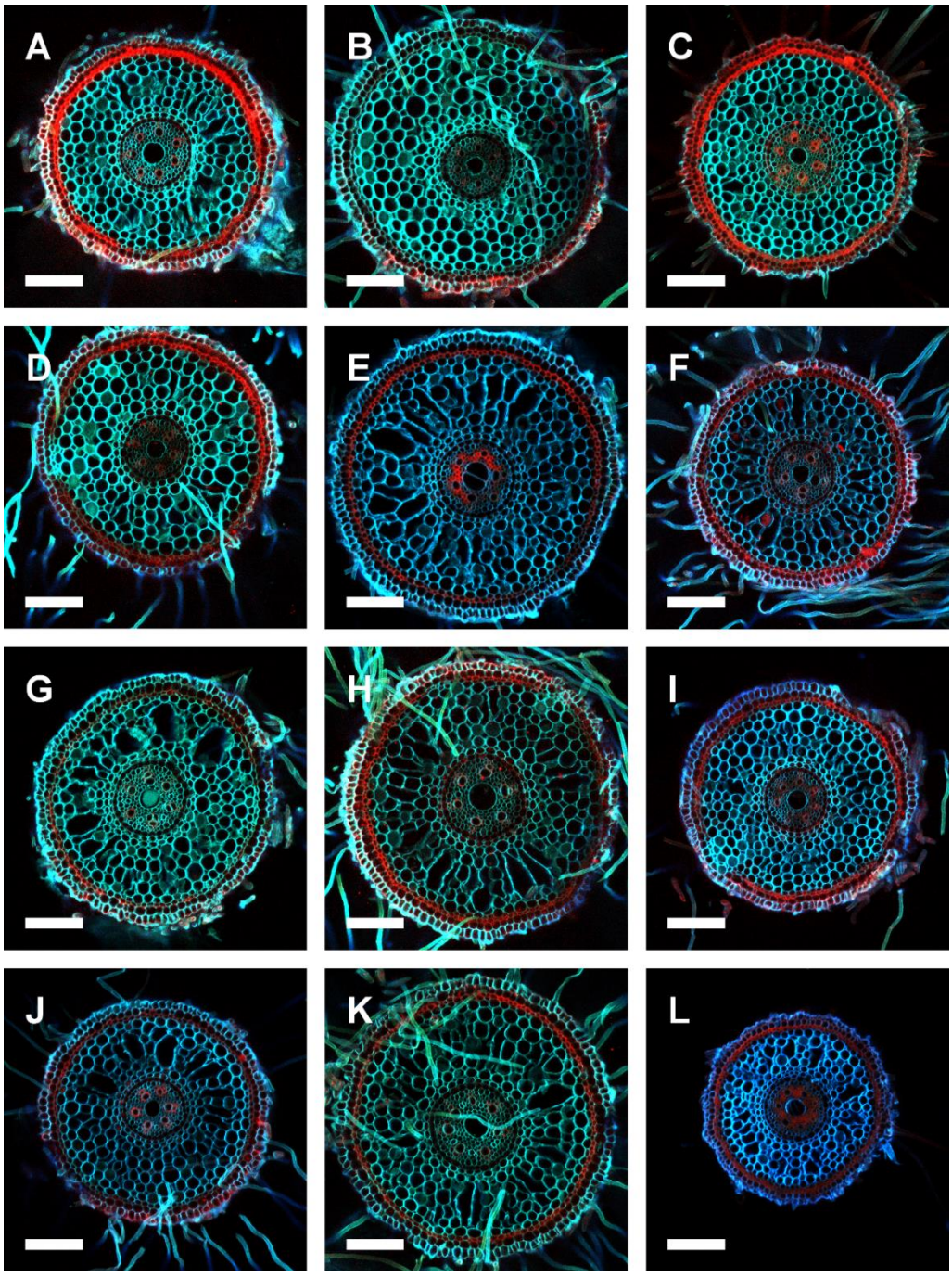


Figure 3.1. Upland and lowland cultivars exhibit a wide variation in root anatomical traits. Radial sections of representative samples grown on plates from (A) CG14O.g., the lowland cultivars (B) Faro 52, (C) IR64, (D) Kaybonnet and (E) Nerica L41, and the upland cultivars (F) Nerica 2, (G) Nerica 6, (H) Nerica 7, (I) Nerica 8, (J) WAB 56, (K) WAB 181 and (L) WAB 759. Sections were taken 3 cm from the root tip, stained with calcofluor white and imaged with differential confocal laser setting to enable identification of autofluorescence from lignified tissues (in red) and all cell walls (in blue). For details of this method see materials and methods. Scale bars are 100 µm.

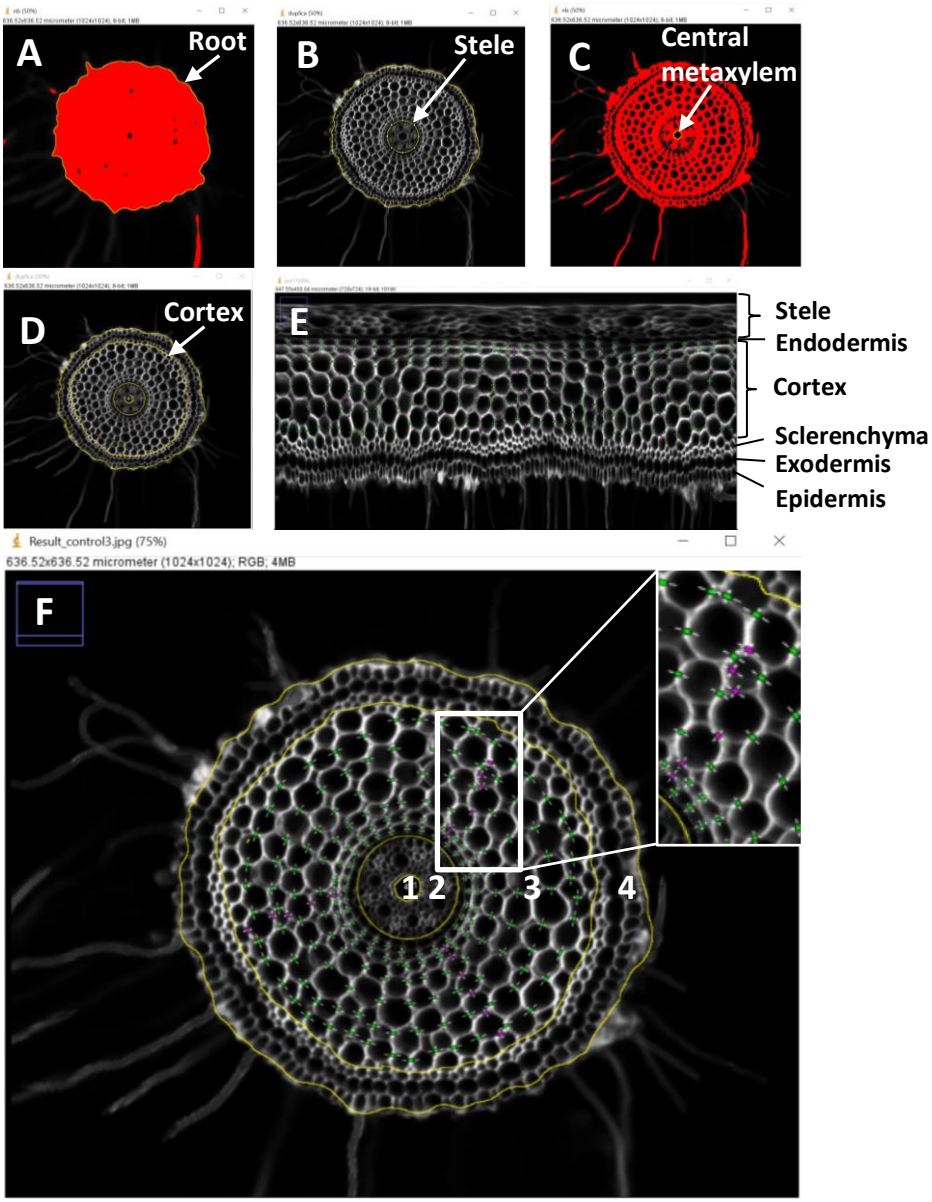


Figure 3.2. Pipeline of radial anatomy analysis using PHIV Rootcell software (Lartaud et al. 2015). (A) Images are converted to greyscale and thresholding used to highlight total root area (yellow outline). (B) Stele is selected. (C) Thresholding is used to select central metaxylem. (D) Cortex is selected. (E) The image undergoes polar transformation to allow for easier cell counts to be made. Lines are drawn vertically to count radial cell file number (magenta dots) and then horizontally to count cell number per file (green dots). (F) Output of the analysis gives area of (1) central metaxylem, (2) stele, (3) cortex, (4) external cell layers consisting of sclerenchyma, exodermis and epidermis, total root area, peripheral metaxylem counts and cell counts for cell files selected. The expanded box in the image allows easier viewing of green and magenta dots.

smaller whole root area than the others (Figure 3.1). However, to quantify this and understand more subtle differences, as well as variability within a cultivar, detailed anatomical analysis is required. PHIV-Rootcell, a FIJI plugin (Lartaud et al. 2015), is a good tool for this as it can easily give a range of tissue areas as well as cell counts for any tissue type required (Figure 3.2). This was a preliminary study, and as such only primary roots of seedlings grown on ½ MS agar plates were taken seven days after germination for sectioning and anatomical analysis, and only sectioned at one location (3 cm from root tip) per root. Although this causes some limitations in data interpretation, there are still some major differences seen between cultivars. It is likely that anatomical differences seen in young primary roots will translate to form equivalent differences in crown roots, which are of greater importance to the mature plant. Previous work has shown similar patterns in primary and crown roots (reviewed by Rebouillat et al. 2008). However, from this study we cannot be sure if this is the case. Further work will be important in revealing if anatomical differences seen in young plants primary roots can give indication of similar differences in crown root of mature plants.

Anatomical analysis indicates there are no differences in general trends seen between the 8 upland (including *Oryza glabberima.* CG14) and 4 lowland cultivars studied. However, there are significant differences in some measurements between different cultivars (Figure 3.3). When considering whole root, cortex and external cell layer (epidermis, exodermis and sclerenchyma) areas, the ratios between these tissue areas remain broadly the same between the different cultivars. This means that cultivars which have a

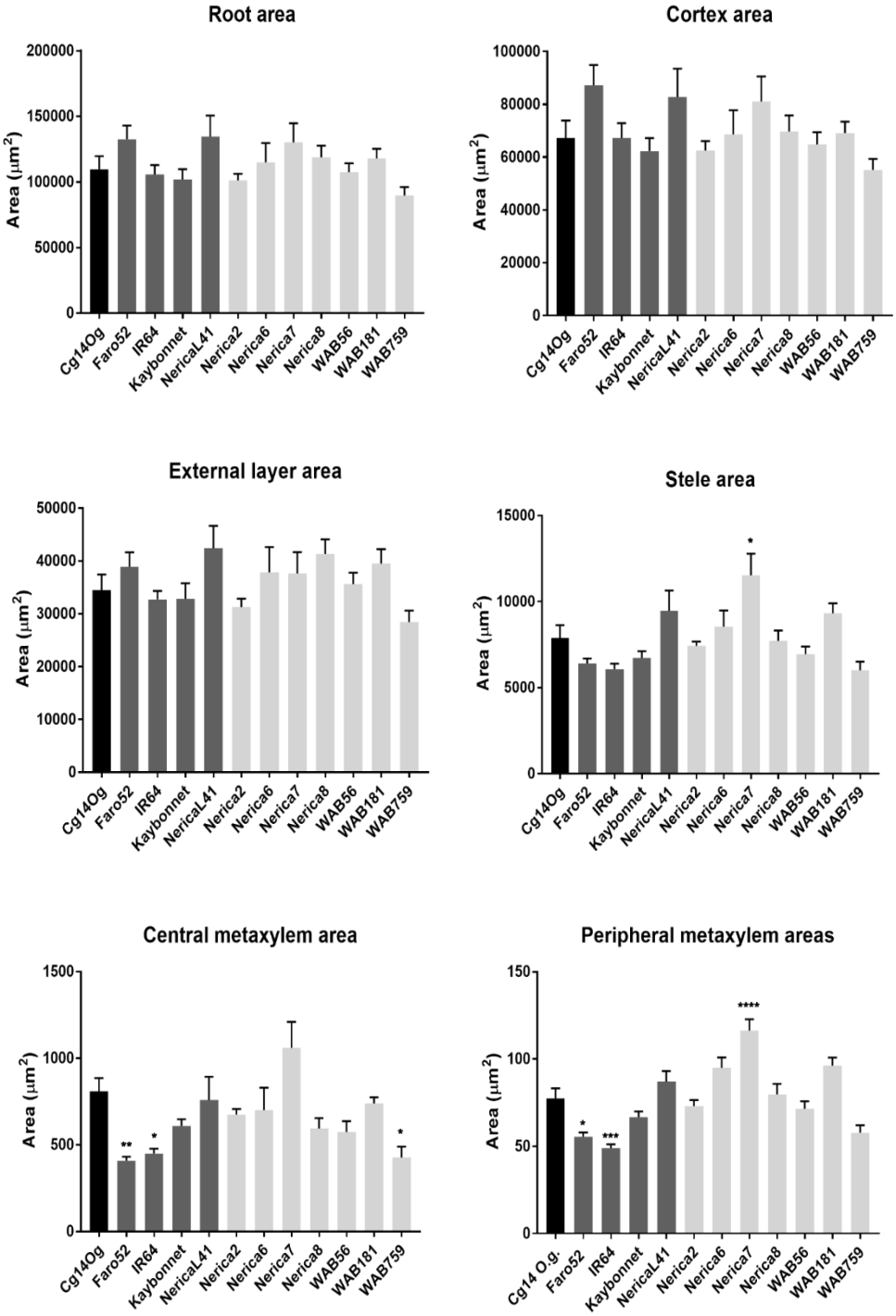


Figure 3.3. Upland and lowland cultivars do not show general differences in anatomical traits. Analyses of primary root radial anatomy measurements from *Oryza glaberrima* upland accession CG14 (black bars), lowland cultivars (dark grey bars) and upland cultivars (light grey bars). One-way ANOVA and Tukey tests were performed to test for significant differences as compared to CG14. Asterisks indicate significance (* $P \leq 0.05$, ** $P \leq 0.01$, *** $P \leq 0.001$, **** $P \leq 0.0001$).

higher whole root area also have higher cortex and external tissue areas. In these tissues there are no significant differences between areas of the different cultivars from that of *Oryza glabberima* CG14. When considering stele, central metaxylem and peripheral metaxylem areas different ratios are observed between the different cultivars but, again, these patterns follow the same trends for these three tissue types. However, the trends seen in tissue areas for the whole root, cortex and outer tissues do not follow exactly the same pattern as stele, central metaxylem and peripheral metaxylem areas. Comparing tissue area ratios in this manner indicates the major anatomical factors which may lead to increased whole root, or increased stele area. For example, whereas the whole root area of Faro52 is bigger than that of *O.g*. CG14, the stele area of Faro52 is smaller. This suggests the cortex area, external tissue area, or both, must be greater than that of *O.g.* CG14, and analysis shows that both tissue layers are larger.

When considering water uptake it is important to consider the roles of each tissue layer and the effect variation of cell size or number may have. The radial anatomy of root xylem vessels is of particular importance as manipulation of size and number can have dramatic effects on the whole plant response to drought. Generally, upland cultivars are much more tolerant to drought than paddy rice, and it may be expected that this tolerance may be, in part, a result of root xylem anatomy. This appears, generally, not to be the case (at least not for the cultivars studied here). Tolerance to drought is a complex trait which may be associated with a number of variable phenotypes. One factor limiting how much photosynthesis can occur in a plant, and consequently how much

biomass it can produce, is availability of water. Although there will be many confounding factors, it may be the case that (in some cultivars at least) root xylem anatomy is directly related to measures of photosynthesis. In the cultivars studied here, Nerica 7 (an upland cultivar), has significantly the largest stele, central and peripheral metaxylem areas. It is interesting to note that in glasshouse studies Nerica 7 has one of the highest rates of transpiration, stomatal conductance and photosynthesis (Figure 3.4). This particular cultivar also responds most severely to drought stress with a huge drop in photosynthetic rate when grown under drought conditions (Figure 3.5). Although more detailed analysis is required to understand the influence of root xylem anatomy on photosynthetic rate, it may be the case that, at least in Nerica 7, they are closely linked. Larger xylem vessels would allow for greater availability of water for photosynthesis, but would also potentially leave plants more susceptible to drought (due to less efficient use of water and greater risk of vessel cavitation). As anatomical analyses were conducted on young seedlings whereas physiological measurements were taken from mature plants, the fact that relationships could still be found suggest the early anatomical patterning is maintained through to mature plants. Although photosynthetic rates do not necessarily indicate plant fitness or resulting yield, a plant with lower photosynthetic rates will not be able to build as much biomass as one which photosynthesises more, purely due to lowered carbon fixing ability. It may be the case therefore, at least for some cultivars, that limiting water conductivity by manipulating root xylem anatomy could have a huge impact on photosynthetic output and consequently yield.

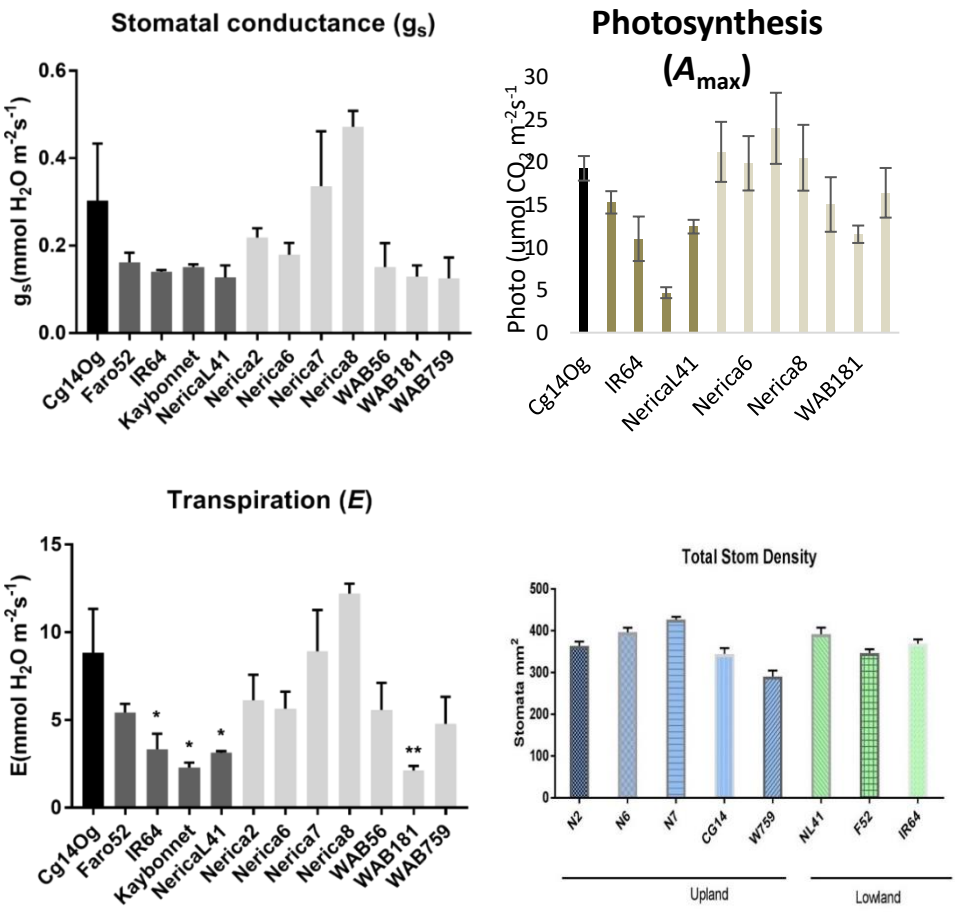
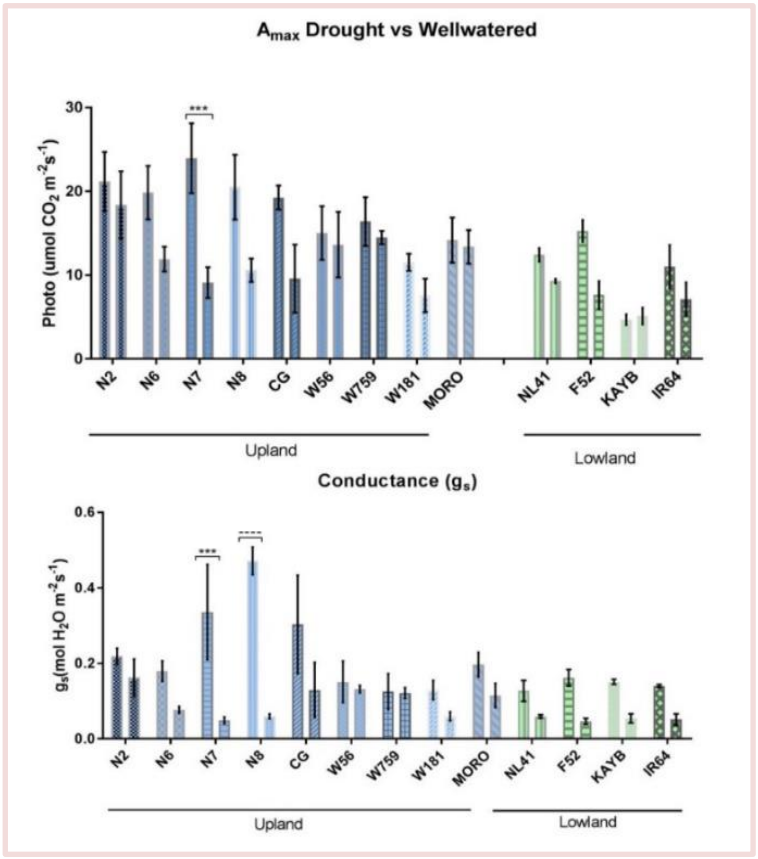


Figure 3.4. Upland and lowland cultivars do not show general differences in physiological measurements. Analyses of photosynthesis (A_{max}), stomatal conductance (g_s) and transpiration (*E*) from *Oryza glaberrima* upland accession CG14 (black bars), lowland cultivars (dark grey bars) and upland cultivars (light grey bars). One-way ANOVA and Tukey tests were performed to test for significant differences as compared to CG14. Asterisks indicate significance (* $P \leq 0.05$, ** $P \leq 0.01$, *** $P \leq 0.001$, **** $P \leq 0.0001$). Data from plants grown in soil. Data from Umar Mohammed (University of Nottingham thesis 2017).



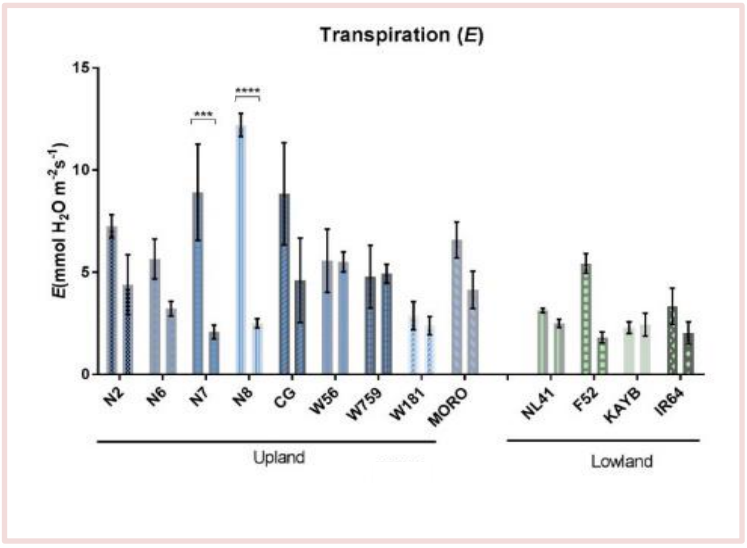


Figure 3.5. Upland and lowland cultivars do not show general differences in physiological measurements in response to drought stress. Physiological analyses within upland and lowland cultivars. (A) CO_2 assimilation, (B) stomatal conductance, (C) transpiration rates and (D) total stomatal density. Data from plants grown in Hydroleca with imposed drought. Data from Umar Mohammed (University of Nottingham thesis 2017).

3.3 Root anatomical diversity across different root types

As previously mentioned, the extensive branching of the rice root system leads to different root types which show diverse radial anatomies, especially when considering vascular pattern. Diverse root types enable rice to adequately explore soil and harness water and nutrients. These different root types show both larger scale architectural differences, as well as differences in details of anatomy. There are clear differences in terms of vascular pattern across the different root types. While there is a degree of variability, it is generally true that larger the root area, the more vascular poles that develop. In mature zones of the root, the primary root of Kitaake plants usually has 5 or 6 vascular poles, crown roots between 6 and 9, and the lateral roots between 2 and 4 (Figure 3.6). However, there is not a constant number of vascular poles throughout the whole length of the root. As roots get smaller towards the root tip, the number of vascular poles decreases (Figure 3.7).

3.4 Root anatomic plasticity in response to drought

When stressed with poor water availability, there are many responses plants can adopt in order to survive. As well as slowing costly physiological processes to improve water use efficiency, plants can also adapt to the environment through new growth. This can take place by combining the two major aspects of root development discussed in this chapter; changing root architecture as well as anatomy. While different cultivars may be genetically predisposed to certain root architectures and anatomies, developmental plasticity allows

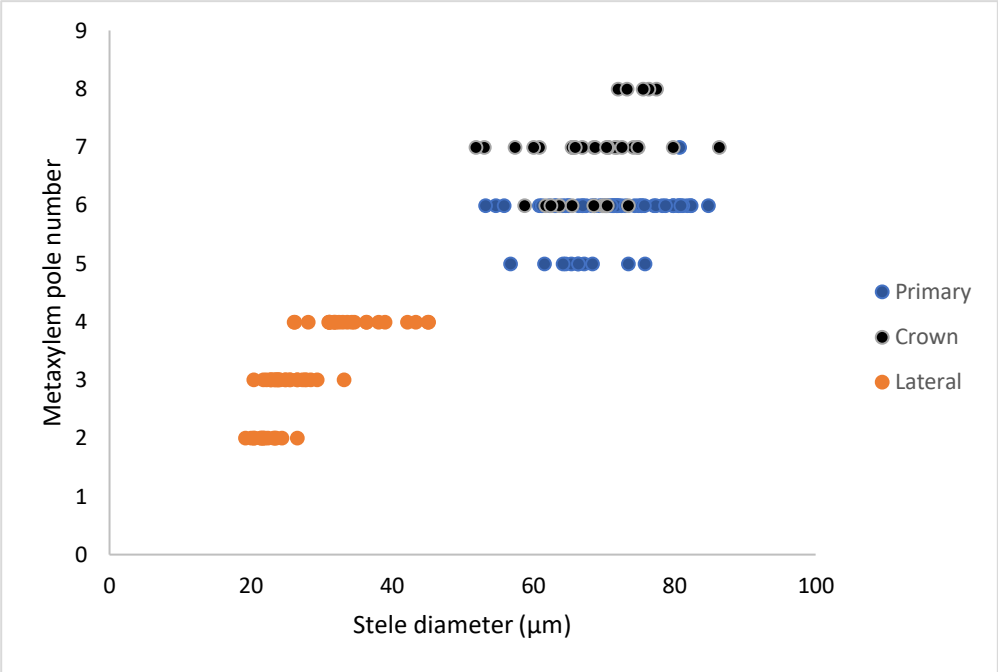


Figure 3.6. The number of vascular poles is dependent on stele diameter. Scatter plots showing the variation in number of metaxylem poles and the stele diameter (from outer metaxylem to opposite outer metaxylem), for different root types. Data was obtained from sections of 67 primary roots, 37 crown roots and 62 lateral roots from Kitaake plants grown on plates for 14 days. Roots were sectioned 1 cm from root tip, sectioned, imaged and analysed using ImageJ.

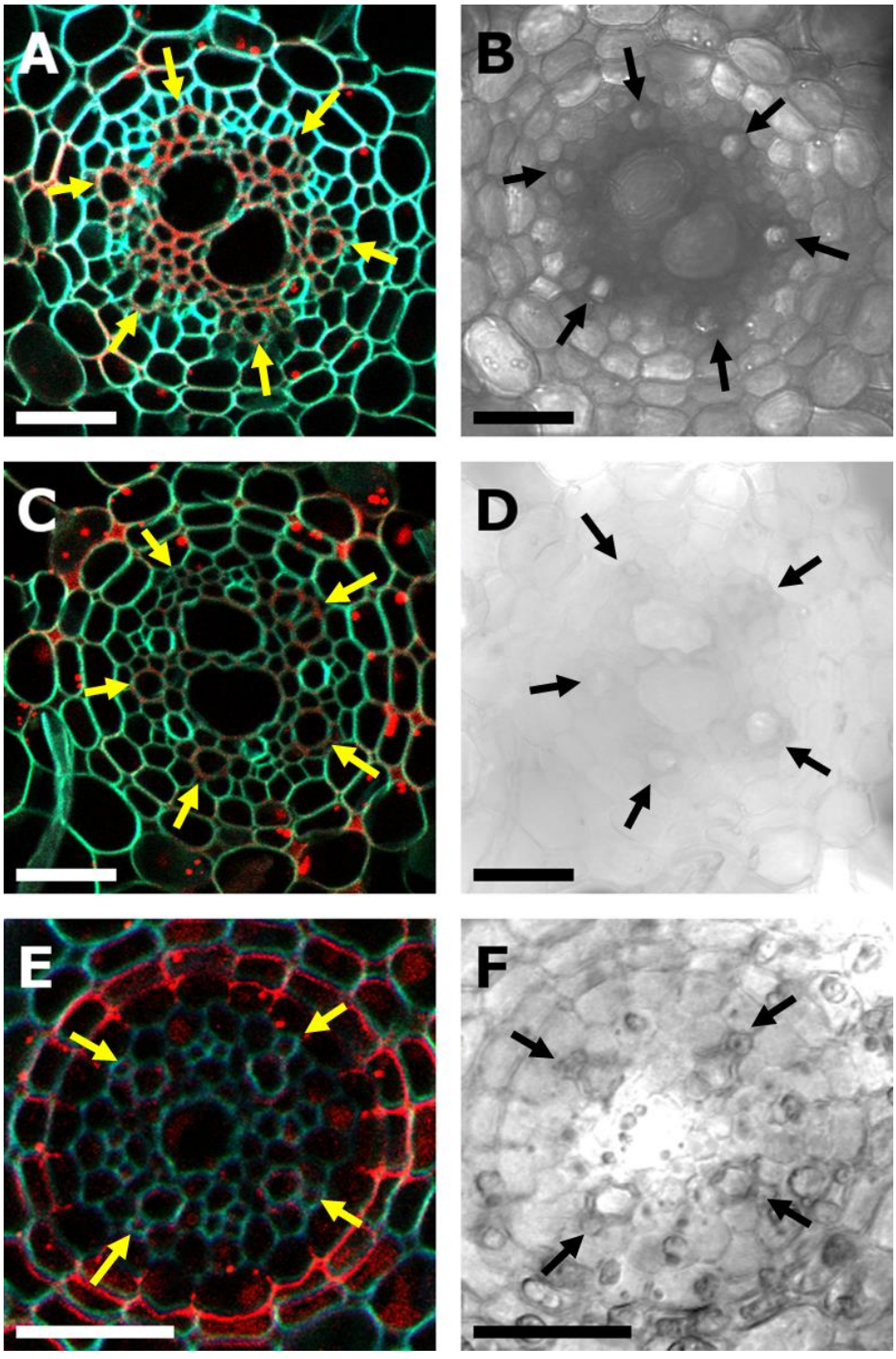


Figure 3.7. The number of vascular poles changes along the root length. Sectioning a single crown root 5 mm (A and B), 30 mm (C and D) and 65 mm (E and F) from the root-coleoptile junction shows a decrease of vascular pole number from six, to five, to four in the sections respectively. Calcofluor fluorescence (A,C and E) is shown alongside false brightfield images (B, D and F). Yellow and black arrows indicate xylem vessels. Scale bars are 50 µm.

plants to grow in response to their environment and so the genetic predisposition for a certain phenotype may be overcome. In response to drought, plants may be able to change angle of growth of new roots in order to reach deeper into the soil, as indicated by studies on the DRO1 QTL (Uga et al., 2011). In addition, new roots may be able to develop fewer, narrower xylem vessels to improve water use efficiency and reduce the risk of vessel cavitation. The plasticity of response is also highly dependent on the particular cultivar, and this is likely something that varies greatly across cultivars.

In order to test anatomical changes in adaptation to drought stress in a single cultivar and a single root type, Kitaake seedlings were grown on ½ MS agar plates with differing concentrations of sorbitol and primary root radial sections taken 1 cm from the root tip were analysed for differences in anatomy. While use of sorbitol in media does not entirely represent drought stress, it does impose osmotic stress upon the plants and lowers water potential of the media, thereby simulating dry soil. Anatomical differences are subtle and consequently it is difficult to see any obvious differences when comparing representative radial sections (Figure 3.8). In these representative sections, there appear to be much higher quantities of lignin or suberin in the 'outer tissues' of the sclerenchyma, exodermis and epidermis, as indicated by increased autofluorescence. Autofluorescnece was not quantified because gain and focus could not be kept the same between sections while maintaining high quality images. While there are few obvious anatomical effects of sorbitol treatment, the major impact is on growth rate with growth on 100 mM sorbitol significantly decreasing root length in seven day old seedlings (Figure 3.9).

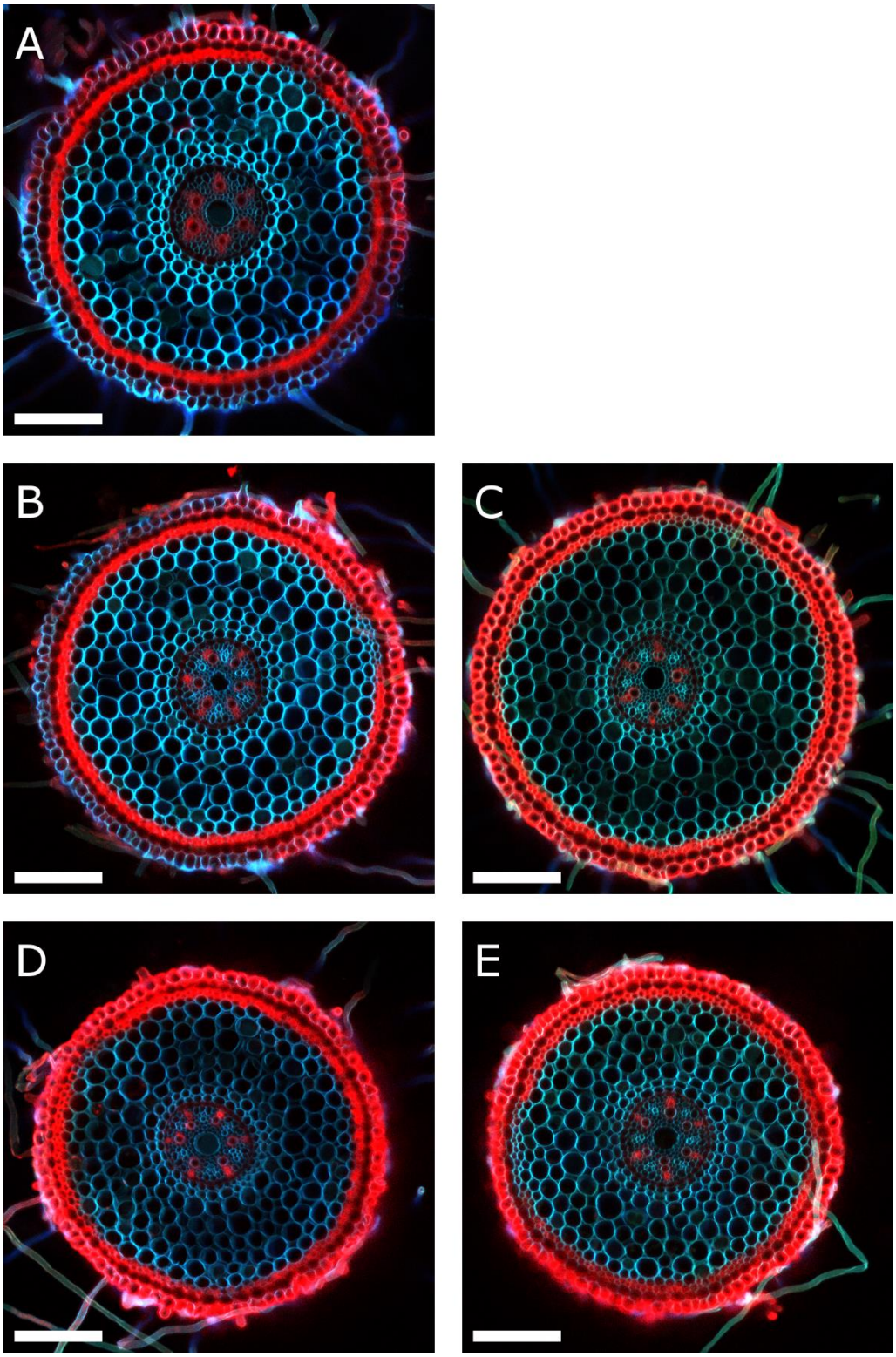


Figure 3.8. Treatment with sorbitol to induce osmotic stress increases lignification and suberization of epidermis, sclerenchyma and exodermis, but anatomical changes are too small to be seen by eye. Representative radial section images of 7 day old Kitaake primary roots treated with (A) control, (B) 50 mM, (C) 100 mM, (D) 200 mM and (E) 300 mM sorbitol. Scale bars are 100 µm.

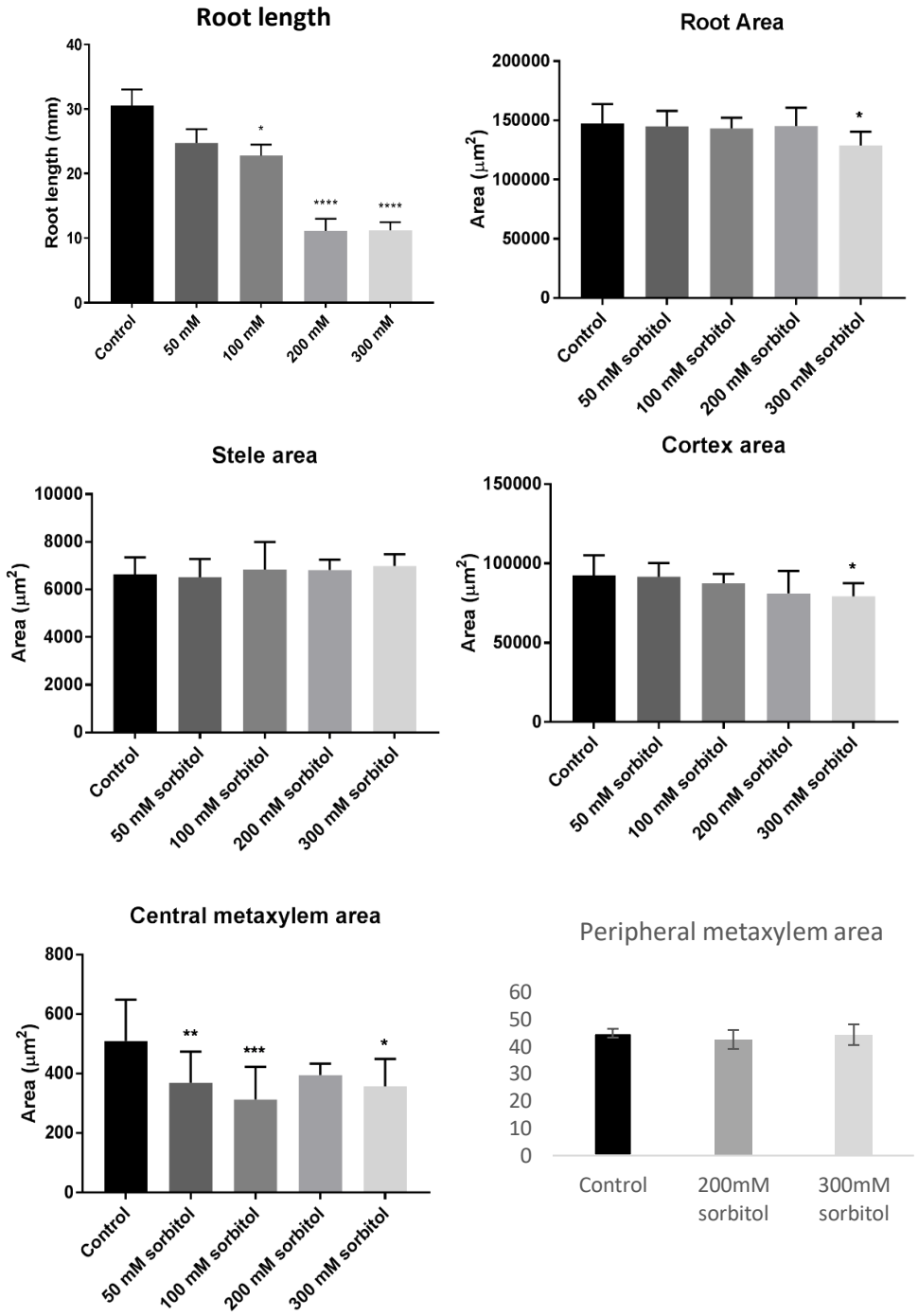


Figure 3.9. Induction of osmotic stress results in a significant reduction in root length but only subtle changes in root anatomy. Analyses of 7 day old Kitaake primary root radial anatomy measurements treated with control, 50 mM, 100 mM, 200 mM and 300 mM sorbitol. One-way ANOVA and Tukey tests were performed to test for significant differences as compared to the control. Asterisks indicate significance (* $P \leq 0.05$, ** $P \leq 0.01$, *** $P \leq 0.001$, **** $P \leq$

Comparing tissue area changes upon sorbitol treatment indicates that the marginal influence upon whole root area (which is significantly smaller only when grown on 300 mM sorbitol) is largely down to a decrease in cortex area, as the stele and external tissue layers show no significant change (Figure 3.9). It is curious to note that despite significant reduction in central metaxylem area when grown with sorbitol, peripheral metaxylem area shows no significant change. Collectively these results indicate that the major change observed when grown with sorbitol is a dramatic slowing of root growth. It was expected that the peripheral metaxylem area would decrease in order to improve water use efficiency by increasing resistance through development of narrower vessels. This, however, is not the case and instead there is a reduction in central metaxylem area only.

It is important to consider that this experiment was only done in young plants on plates and only a single root type, and a single cultivar, was considered. It may be the case that other root types would respond in different ways to osmotic stress, and that plants have more sophisticated mechanisms to perceive and respond to drought. While this experiment imposed drought stress upon plants from germination, it would be useful to understand how plants would respond when grown under normal conditions and then drought stressed. In this case, a fixed root anatomy would already be in place, so any anatomical changes would only occur in new growth. This would also enable an understanding of the timeframe between drought perception, the immediate cellular responses, and the slower anatomical changes. It seems likely that the

degree of plasticity a plant is able to exhibit is something that is very different between different cultivars.

3.5 Root anatomical responses to cytokinin and auxin

In *Arabidopsis*, elevated cytokinin levels lead to loss of root protoxylem. This can be seen in the *ahp6* mutants, which show breaks in protoxylem, or by growing plants on media with BA. When rice is treated with cytokinin, a similar phenotype is seen. However, in some cases the loss of protoxylem appears to be accompanied by loss of peripheral metaxylem (or at least abnormal secondary cell wall thickening of the peripheral metaxylem) (Figure 3.10). Growth on media with 100 nM BA results in the stele surrounding the central metaxylem vessel resembling a mass of undifferentiated cells, with only phloem poles easily distinguishable (Figure 3.10). This is quite variable, and while the images shown in Figure 3.10 are representative sections, there were also some which looked similar to wild type. In order to quantify the response to BA treatment and the variation in stele anatomy seen, multiple plants were grown on media with a range of BA concentrations, radial sections taken from seedlings seven days after germination 1 cm from the root tip, and resulting images analysed using the PHIV-RootCell toolkit. As observed when plants were grown with osmotic stress through the presence of sorbitol in the media, low concentrations of BA have more severe effects on root growth than anatomical

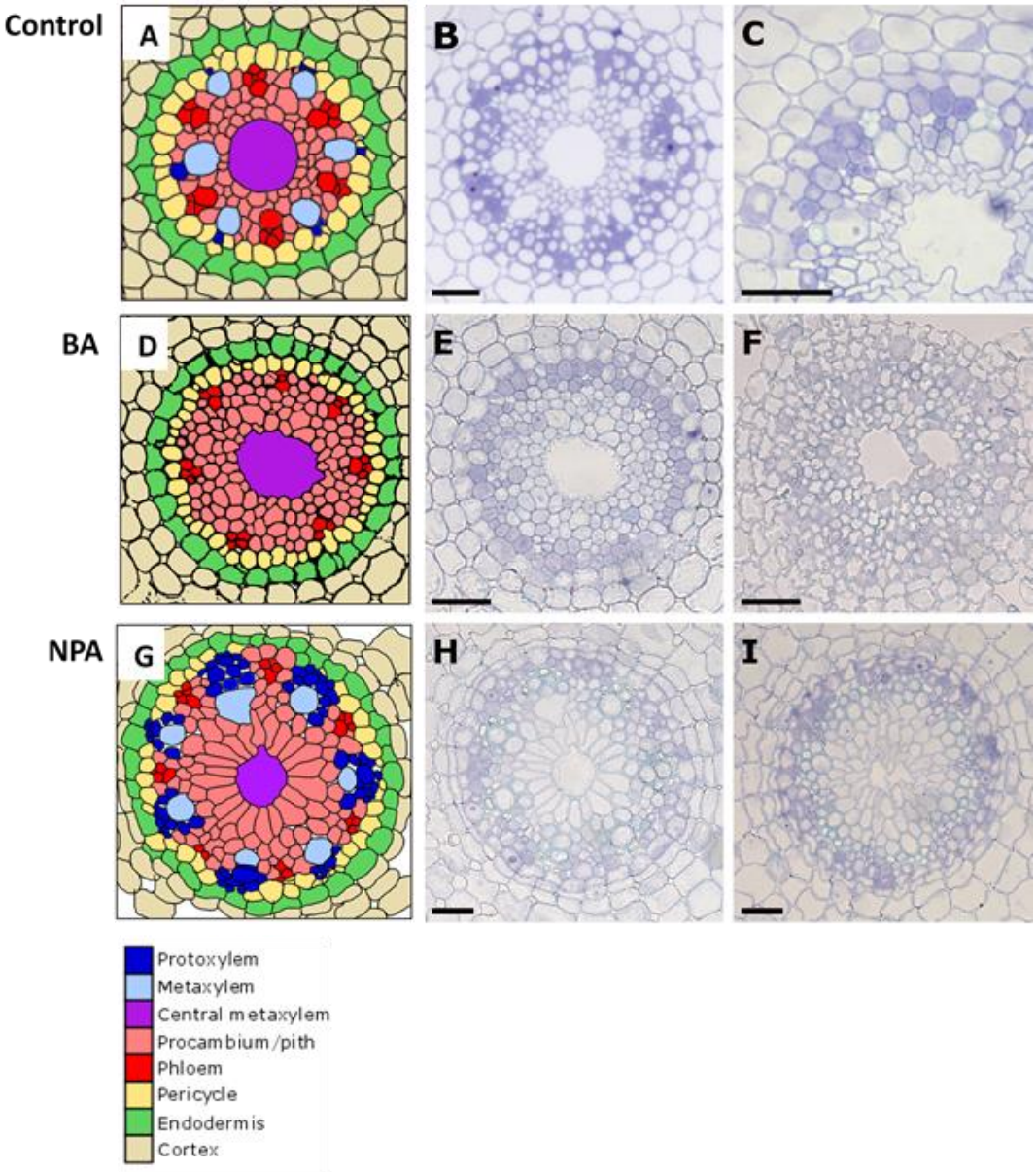


Figure 3.10. Treatment with BA and NPA lead to changes in vascular anatomy. Schematic diagrams show anatomic phenotypes of wild-type (A), BA treated (D) and NPA treated (G) roots. Images are representative of (B) and (C) untreated Kitaake, (E) 100 nM BA, (F) 10 uM BA, (H) 100 nM NPA, (I) 10 uM NPA. Sections were stained with toludine blue to enable identification of lignified tissues (in lighter blue). For details of protocol see materials and methods. Scale bars are 20 µm.

development, with the lowest concentration tested (10 nM) significantly reducing root length (Figure 3.11). Growth with 100 or 300 nM BA leads to a reduction of the peripheral metaxylem vessel area, with no significant effect on the area of the central metaxylem vessel. When comparing the anatomical effects of BA on *Arabidopsis* with those of rice, it is important to consider the possible differences in the ability to perceive and respond to different types of cytokinin. The aromatic cytokinins (such as BA and kinetin) are frequently used in research due to their affordability and stability as compared to the less stable, more expensive isoprenoid cytokinins (such as zeatin) (Mik et al. 2011). However, it has previously been shown that different cytokinin types show differential activity, and this is often dependent on the plant species studied. For example, it was previously thought cZ was an inactive isomer of tZ due to lower apparent activity in classical cytokinin bioassays, but recent studies have implicated cZ in a number of physiological processes (Kudo et al. 2012). To understand the effect of different cytokinins on vascular development of rice roots, radial anatomy after growth with kinetin or zeatin was compared in seven day old seedlings from sections taken 1 cm from the root tip. While an equal mix of cis and trans-zeatin slightly increases central metaxylem area, growth with kinetin shows no effect. In peripheral metaxylem, differential responses are seen in a dose dependent manner with both kinetin and zeatin increasing area at 1 µM but decreasing area at 1 mM (Figure 3.11). This indicates plants do show slightly differing responses to different cytokinins in terms of root xylem anatomy, with the response changing depending on concentration.

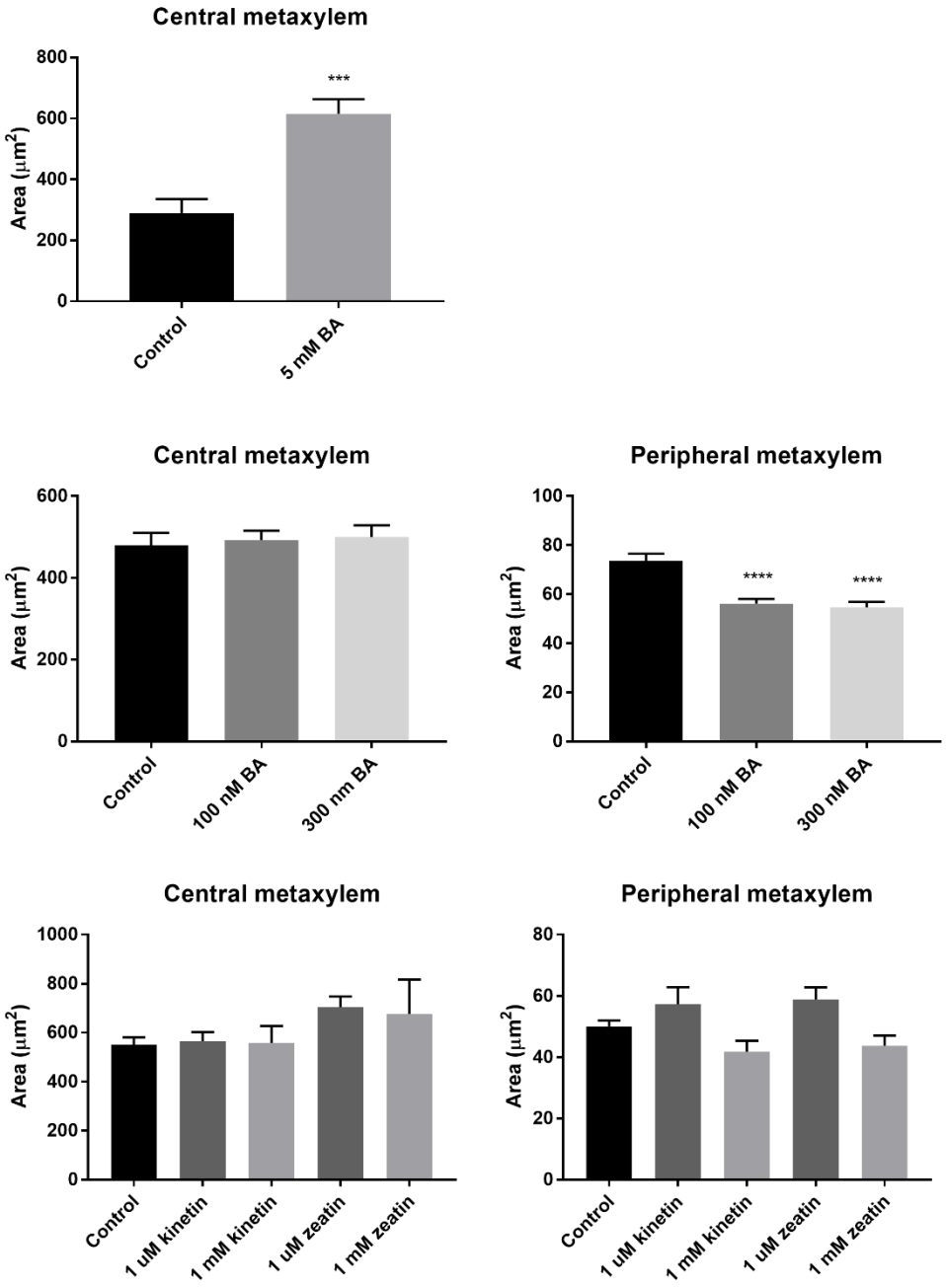


Figure 3.11. Treatment with BA significantly reduces root length and peripheral metaxylem areas. Treatment with different cytokinins show differing effects. Compare changes in central metaxylem with changes in peripheral metaxylem with different concentrations of different CKs. One-way ANOVA and Tukey tests were performed to test for significant differences as compared to the control. Asterisks indicate significance (* $P \leq 0.05$, ** $P \leq 0.01$, *** $P \leq 0.001$, **** $P \leq 0.0001$).

When *Arabidopsis* is grown on plates with NPA (an inhibitor of auxin transport) plants initially lose root protoxylem, but after longer growth times multiple aberrant xylem poles develop throughout the stele (Bishopp et al. 2011). When rice is grown on plates with NPA plants develop a much smaller central metaxylem vessel, elongated cells surrounding the central metaxylem vessel and deposition of lignin in cell walls throughout the entire stele (Figure 3.10). In these plants, over proliferation of protoxylem seems to make differentiating between surrounding tissue types difficult. This phenotype is much more reproducible than when rice is treated with BA. Since NPA inhibits auxin transport, these phenotypes are associated with accumulation of auxin in particular domains. In *Arabidopsis*, auxin has been shown to accumulate in the root apex upon NPA treatment due to inhibition of basipetal auxin transport (Casimiro et al. 2001). In rice much less is known about the dynamics of auxin movement within the root. It is likely the case that the phenotypes seen with NPA treatment in rice are a result of differences in auxin accumulation in specific tissues.

While resources to determine differences in hormone accumulation in rice remain far behind those of *Arabidopsis*, some useful reporters have been developed. The DR5-GFP reporter in rice (developed by Jing Yang, Shanghai Jiao Tong University) can be used to identify auxin response maxima. While the visualisation of fluorescent proteins in rice is hampered by the thick nature of the tissues being observed, taking thin sections of living tissue overcomes this problem. In the rice root tip, auxin response can be seen to be localised in the central metaxylem vessel, surrounding vascular poles and in the epidermis or

outer cell layers (Figure 3.12 A to C). This is seen very close to the root tip where these tissues are not yet lignified and consequently patterns of auxin response can be seen before observable differentiation of these tissues. In more mature zones of the root GFP signal is no longer present in the central metaxylem vessel but can be seen in phloem. Combining sectioning of live tissues with confocal microscopy in the DR5-GFP reporter also allows visualisation of auxin maxima in tissues which are more difficult to image. Spots of GFP signal can be seen in the central region of the shoot section (Figure 3.13). While it is difficult to say exactly the areas showing signal from this image, further study of this line may prove useful. In order to confirm the auxin response in the DR5-GFP line, it would be beneficial to compare expression patterns with known auxin response genes in rice. Analyses of this kind was done by Yang et al. (2017) using DII-VENUS and DR5-VENUS fluorescent reporter lines in combination with expression patterns of PIN1 homologues and OsAux1. Overlapping expression patterns validated the auxin response reporters, and these lines were then used to analyse auxin response dynamics in many tissues (Yang et al. 2017). Further analyses using these lines may enable a better understanding of patterns of auxin accumulation upon BA and NPA treatment, and consequently may help explain why NPA treatment (initially) phenocopies BA treatment in *Arabidopsis,* whereas they differ greatly in rice.

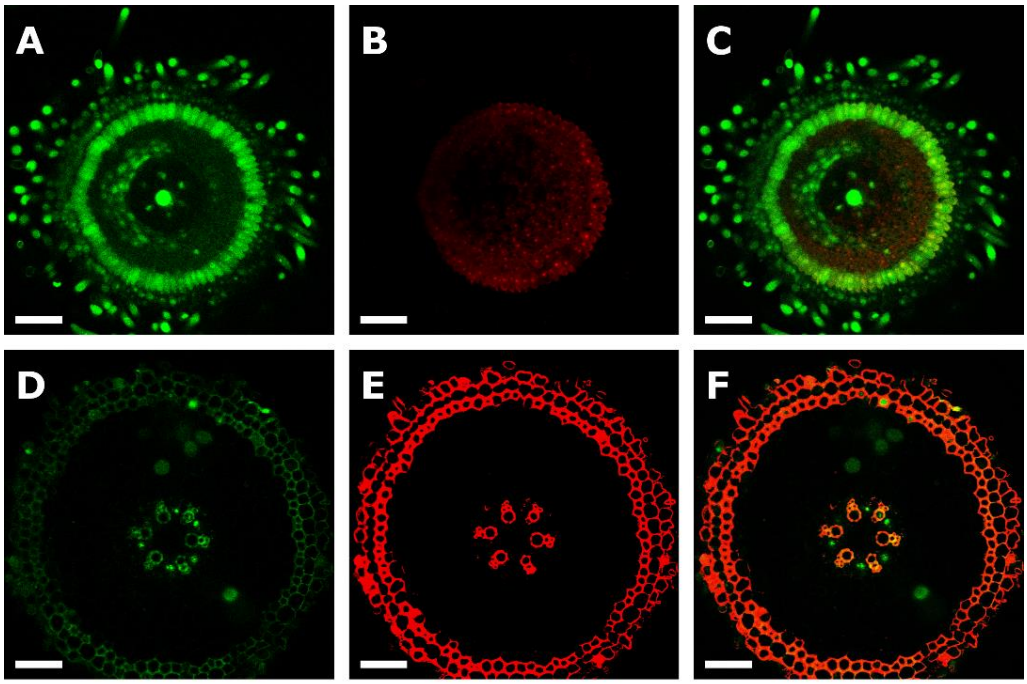


Figure 3.12. Primary roots of the rice DR5-GFP reporter can be sectioned to show auxin maxima in vascular poles and epidermis very close to the root tip (A,B and C) and in phloem in more mature sections of root (D, E and F). Pictures show GFP signal (A and D), autofluorescence (B and E) and an overlay of both signals (C and F). Scale bars are 50 µm.

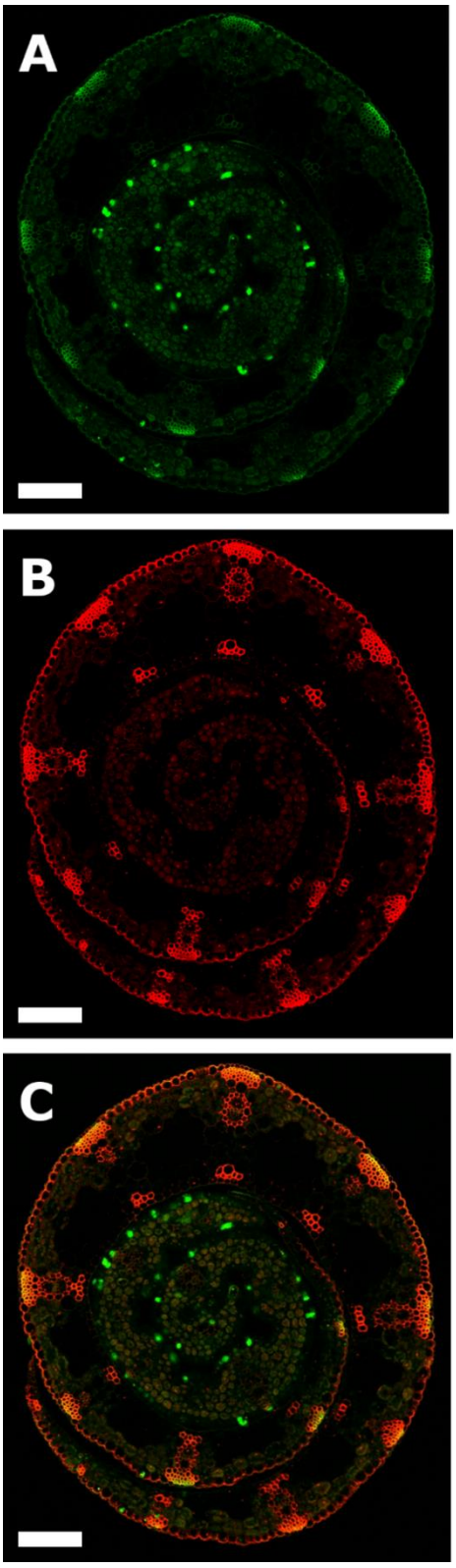


Figure 3.13. Shoots of the rice DR5-GFP reporter can be sectioned to show spots of auxin maxima within the shoot. Pictures show GFP signal (A and D), autofluorescence (B and E) and an overlay of both signals (C and F). Scale bars are 100 µm.

3.6 Discussion

This chapter has explored the great diversity in rice root anatomy across different cultivars, root types and within a single root type in response to different environmental stresses. The importance in understanding this diversity, and the signalling mechanisms governing these aspects of development is clear. Particular phenotypes may be better suited to particular environments, and understanding these relationships will be key to breeding superior cultivars which are able to maintain yield in changing environmental conditions. Many studies have been conducted which point to various morphological and anatomical traits which are heavily involved in rice response to drought, and QTL mapping has been used to determine the molecular regulation of some of these traits (reviewed by Gowda et al. 2011; Comas et al. 2013). Recent technological advances, such as the development of high-throughput sequencing, has enabled a more detailed understanding of these responses. For example, miRNA profiling of rice leaves grown under well-watered or drought conditions has shown miRNAs regulate various aspects of drought adaptation, with miRNAs which regulate hormones such as auxin, cytokinin, abscisic acid and jasmonic acid showing clear differential expression between growth conditions (Fard et al. 2017). Since auxin and cytokinin are both heavily involved in many aspects of radial anatomy development in *Arabidopsis*, including vascular patterning, it is likely the case that they are also involved in rice root vascular development.

From screening seedling root anatomy and physiological measurements, it is difficult to determine whether these are directly related. However, the fact that Nerica 7 shows the largest metaxylem area, the highest photosynthesis rates, and also the largest drop in photosynthesis rate when grown under droughted conditions suggests these characteristics are linked. In this cultivar, the output of photosynthesis may therefore be directly related to root vascular anatomy. This provides motivation for studying root xylem anatomy as a means to influence the drought response. While growing Kitaake on media with sorbitol to impose osmotic stress does not result in changes in peripheral metaxylem, it does decrease central metaxylem vessel area pointing to the plasticity of the vascular tissues. Anatomical plasticity is likely to vary between cultivars, and consequently study of diverse cultivars may yield an understanding of the patterning networks which govern these adaptive changes.

Given the important roles of auxin and cytokinin in root vascular patterning in *Arabidopsis*, it was hypothesised that they would also play roles in rice root vascular patterning. The loss of peripheral protoxylem and metaxylem upon BA treatment, and the unusual vascular phenotype seen in NPA treated rice roots, suggest that this is the case. However, these treatments also reveal differences in how auxin and cytokinin may interact in rice as compared to *Arabidopsis*. Whereas treatment with cytokinin and NPA show similar root vascular phenotypes in *Arabidopsis* (loss of protoxylem), they show very different phenotypes in rice (loss of protoxylem with cytokinin and proliferation of protoxylem with NPA). Since NPA functions by inhibiting auxin transport, any phenotypes observed must occur due to changes in domains of auxin

accumulation. The loss of protoxylem phenotype seen in *Arabidopsis* roots upon NPA treatment therefore occurs due to a lack of auxin signalling in the protoxylem domain. Treatment with cytokinin results in the same phenotype for the same reason, but via a different mechanism. Cytokinin influences auxin signalling by inhibiting expression (and possibly activity, stability and polar localisation) of PIN auxin efflux transporters, thereby regulating auxin accumulation. Cytokinin treatment therefore leads to a lack of auxin signalling and encroachment of cytokinin signalling at the protoxylem domain (as indicated by expression of AHP6 retreating from and ARR5 encroaching into the protoxylem domain). In rice, the differing effects of cytokinin and NPA on root vascular anatomy may result from differences in the action of cytokinin on PINs. In the next chapter, I examine the cytokinin signalling pathway of rice in detail with the aim of determining whether any genes may function in an AHP6-like role to specify vascular pattern in rice roots.

3.7 Summary

- Differences in root radial anatomy are highly dependent on genotype, and some genotypes show positive correlation between root xylem area and physiological measurements, indicating a possible direct relationship between root anatomy and photosynthesis.

- Vascular anatomy is dependent upon the spatial constraints of the tissue. This is seen both in different root types, and also within a single root as the stele narrows towards the root tip. The smaller the stele, the fewer vascular poles are seen.

- The major root anatomical response to drought in Kitaake seedlings is a decrease in central metaxylem vessel area. This may be highly dependent on genotype.

- In rice, cytokinin treatment leads to loss of protoxylem (and sometimes metaxylem) and NPA treatment leads to over-proliferation of protoxylem and development of elongated cells surrounding the central metaxylem. This is in contrast to *Arabidopsis*, in which both cytokinin and NPA treatment leads to loss of protoxylem.

Chapter 4: OsRR1, OsRR6 and OsRR7 are auxin inducible in the root tip

4.1 Introduction

As discussed in Chapter 1, it is clear cytokinin is a critical component in regulating the organisation of root vascular development in *Arabidopsis*, rice and various other species (Mähönen, Higuchi, et al. 2006; Bishopp, Lehesranta, et al. 2011; Nieminen et al. 2008). Given the complex nature of this multi-step signalling pathway, it is important that there are negative regulators at each step of the pathway, enabling precise control of the overall response to cytokinin. The intermediate component of the cytokinin signalling system is the HPT, which functions to relay the phosphate group from the activated receptor to cytokinin responsive transcription factors (or inhibitors) in the nucleus. It is at this level of the signalling pathway that the HPTs may encounter competition for binding both cytokinin receptors and transcription factors, from the PHPs. In *Arabidopsis*, the only protein currently known to be responsible for inhibition of the cytokinin signalling pathway at this level is AHP6, although it is quite possible there are others yet to be discovered. AHP6 shares sequence similarity with the HPTs, so presumably competes with the HPTs to bind both the receptors and RRs (possibly favouring binding to particular receptors or RRs) but has a substitution at the conserved histidine phosphoaccepting domain of the HPTs, so cannot accept a phosphate group. In this way AHP6 has been shown to inhibit cytokinin signalling at both the level of receptor to HPT, and from HPT to RR (Mähönen, Bishopp, et al. 2006).

The role of cytokinin in development of the vascular tissues can be clearly demonstrated by study of the *Arabidopsis ahp6* mutants, which show varying levels of absence of protoxylem in the root. As discovered by Mähönen et al., 2006, this mutant phenotype is caused by increased cytokinin response in the domain normally occupied by protoxylem. AHP6 occupies a crucial position in the vascular patterning mechanism, in that is acts as a node through crosstalk between auxin and cytokinin occurs. Crucial to this is the fact that AHP6 is directly regulated by auxin and that it acts specifically to inhibit cytokinin signalling. As an inhibitor of cytokinin signalling, AHP6 is a critical component involved in setting up and maintaining the spatial boundary between cytokinin in the procambium and auxin in the protoxylem. Activity of these hormones is required for development and maintenance of these different tissue types.

Given the importance of the vascular tissues, it might be expected that the molecular mechanisms and individual components governing its precise development would be evolutionarily conserved. Whereas *Arabidopsis* has 5 HPTs and a single PHP (AHP6), the rice genome encodes 2 HPTs and 3 PHPs (Tsai et al. 2012). It is possible that there is a degree of functional redundancy amongst the three OsPHPs, but it also seems likely that they will have evolved a number of their own independent roles. Given AHP6 has roles in phyllotaxy, lateral root organogenesis and gynoecium development as well as root vascular patterning (Mähönen, Bishopp, et al. 2006; Bishopp, Help, et al. 2011; S Moreira et al. 2013; Sofia Moreira et al. 2013; Besnard et al. 2014; Reyes-Olalde et al. 2017), it is plausible that the OsPHPs may have subfunctionalised so that individual members regulate specific processes. Rice encodes 5 cytokinin

receptors and given the proposed mechanism of action of AHP6 (as a competitive inhibitor) it is plausible that the OsPHPs have evolved specificity for particular receptors and RRs. This would enable a much finer degree of control of the outputs of cytokinin signalling both in terms of regulations of specific subsets of cytokinin responsive genes, and potentially also through spatial regulation of cytokinin responsive genes.

This chapter is divided into two sections. In the first, phylogenetic analyses of cytokinin signalling elements are displayed, which enable a deeper understanding of how hormonal signalling pathways can adapt functionally to fulfil diverse roles. In the second, a number of candidate genes are screened to find any which may potentially act in an AHP6-like manner (i.e. auxin inducible inhibition of cytokinin signalling) in rice roots.

4.2 Phylogeny of the HPTs and PHPs

Previous work identified phylogenetic relationships between cytokinin signalling components of *Arabidopsis* and rice. This kind of analysis revealed complex relationships enabling identification of genes which arose via speciation or gene duplication (Tsai et al. 2012). The alignment of amino acid sequence of HPTs and PHPs of *Arabidopsis* and rice reveal regions of high sequence conservation (Figure 4.1 A). Within one of these regions is the phosphoaccepting histidine residue of the HPTs (Figure 4.1 B), which accepts the phosphate group donated by the cytokinin receptors, and passes it on to an aspartic acid residue of the response regulators, which then go on to regulate

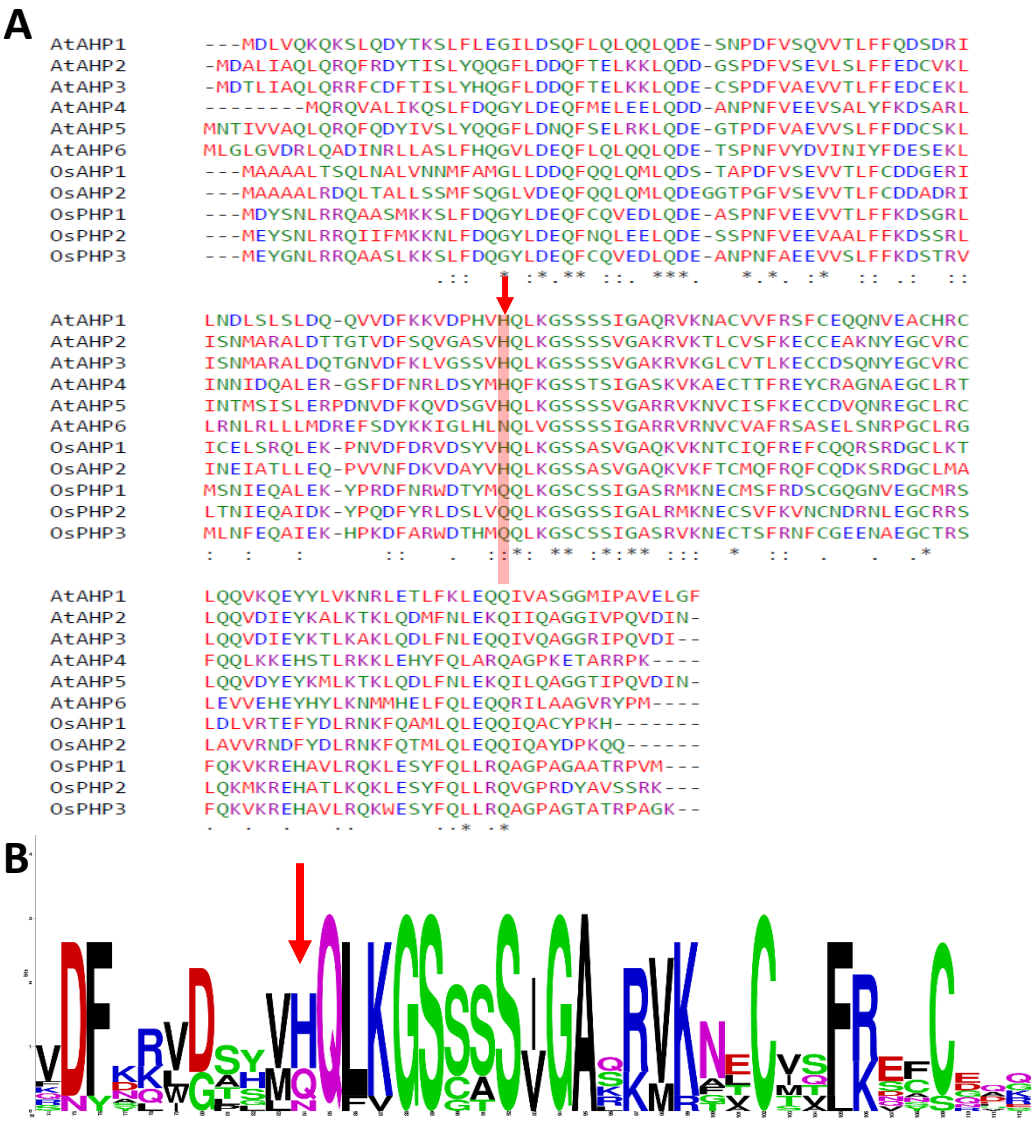


Figure 4.1. An alignment of the HPTs and PHPs of *Arabidopsis* and rice showing the conserved phosphoaccepting histidine residue of the HPTs and substitutions of this residue in the PHPs (A). The phosphoaccepting histidine domain is highlighted and indicated with a red arrow demonstrating AHP6 has an asparagine residue whereas the PHPs of rice have a glutamine residue substituted at this domain. The alignment was generated using Clustal Omega. Symbols under alignment with an asterisk, a colon and a period indicate fully conserved residues, conservation between groups of strongly similar, and weakly similar properties respectively. Amino acid residues are coloured according to their physiochemical properties (small amino acids in red; acidic in blue; basic in magenta; hydroxyl, sulfhydryl and amine in green). Amino acid sequence conservation of the HPTs and PHPs of *Arabidopsis* and rice (B). The conserved phosphoaccepting histidine domain is indicated by a red arrow, showing the three amino acids present at this domain are histidine, aspartic acid and glutamine. The sequence logo was generated using WebLogo.

cytokinin responsive genes. The PHPs lack the phosphoaccepting histidine residue and have a substitution at this domain. In AHP6 there is an asparagine (N) residue at this domain whereas the PHPs of rice have a glutamine (Q) residue (Figure 4.1 A).

From a more detailed phylogenetic analysis (consisting of HPTs and PHPs from 38 species), conducted by creating an unrooted neighbour-joining tree, it is clear that the substitution of the phosphoaccepting histidine domain of the HPTs to N in *Arabidopsis* and Q in the rice PHPs extends to form a more general difference between the PHPs of the dicots and those of the monocots. It seems there are two major PHP clades, one comprising proteins from dicots with an H to N substitution, and the other proteins from monocots with an H to Q substitution (Figure 4.2 and 4.3). The phylogenetic tree places all monocot HPTs and PHPs into monophyletic clades, and places AHP6 in a separate clade with likely orthologues from other dicot species. Most of these monophyletic clades are fairly well supported in terms of confidence derived from bootstrapping. Out of 100 bootstrap trials the monocot HPT clade is supported in 56, the monocot PHP clade (which includes the three rice PHPs) in 61 and the dicot PHP clade in 99 (Figure 4.3). Whereas the dicot PHPs form a distinct monophyletic clade, the dicot HPTs are spread across the phylogenetic tree. According to this phylogeny, the rice PHPs and AHP6 are not true orthologues, as the most parsimonious solutions show they share a common ancestor which probably predates the split of HPTs and PHPs. This indicates a likely independent evolutionary origin of the PHPs of rice (and the monocots as a whole). The major PHP clade of the eudicots forms a single monophyletic group, with every

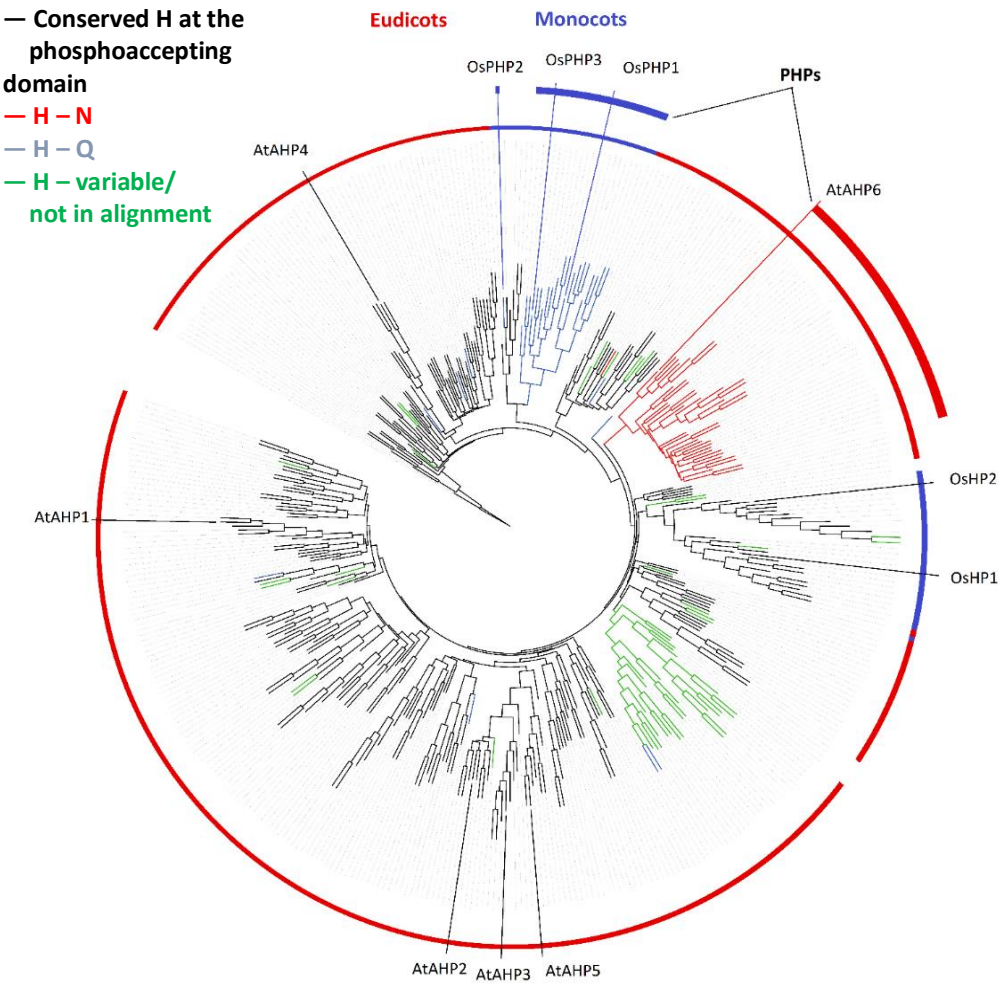


Figure 4.2. Phylogenetic relationships between the HPTs and PHPs of 38 different species; six monocots, thirty eudicots, *Selaginella moellendorffii* and *Physcomitrella patens* (see appendix for list of species included). The coloured circle surrounding the tree represents eudicot clades (in red) and monocot clades (in blue) and the location of the large PHP clades within the phylogeny are indicated by outer colour blocks. The location of *Arabidopsis* and rice HPTs and PHPs within the phylogeny are indicated by labels. The colour of individual lines within the phylogeny represent substitutions at the conserved phosphoaccepting histidine domain of the HPTs (in black) to an asparagine residue (red), a glutamine residue (blue) or variable other amino acids or loss of alignment (green). The HPTs retain the histidine domain whereas PHPs of the eudicots have a substitution at this domain to an aspartic acid residue, and those of the monocots have a substitution to a glutamine residue. The phylogeny is based on 100 bootstrap replicates. For simplicity, bootstrap values are not shown but the fully annotated tree is available at http://bit.ly/2y4LFse.

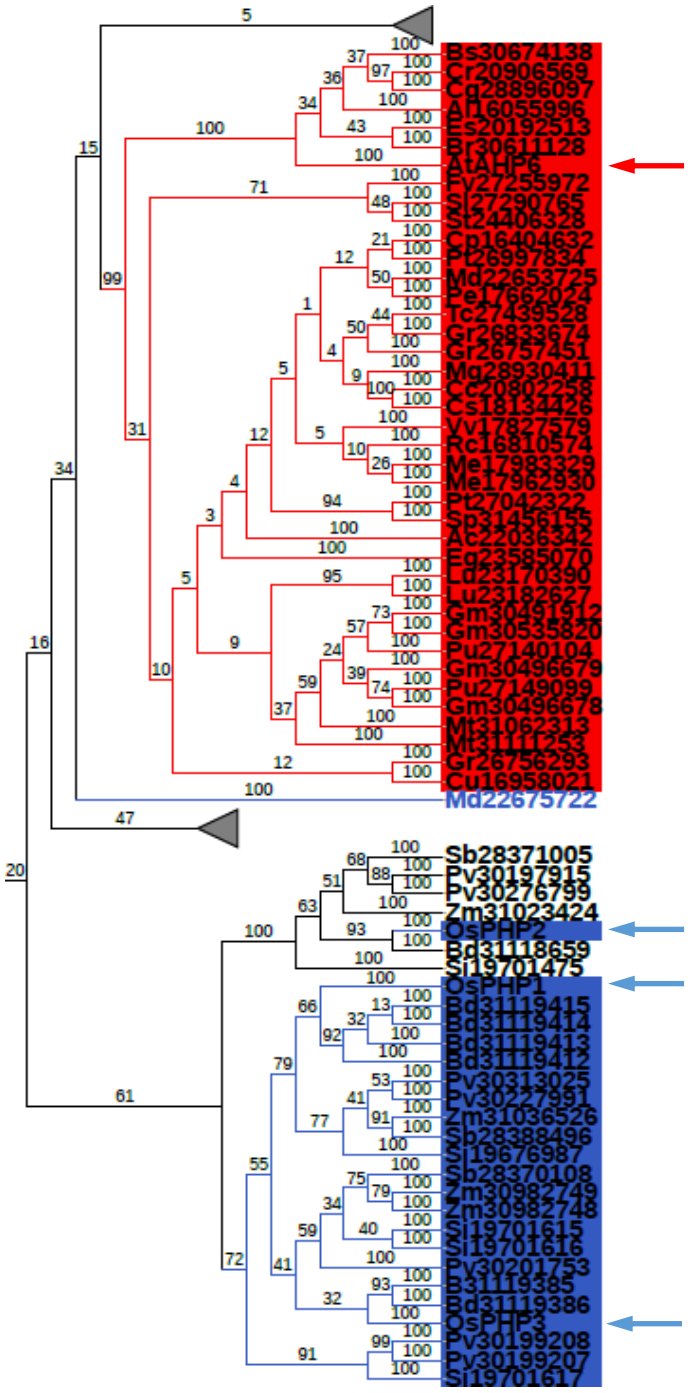


Figure 4.3. Details of phylogenetic relationships between the two core PHP clades of the eudicots (gene names highlighted in red) and the monocots (gene names highlighted in blue). The colour of individual lines within the phylogeny represent substitutions at the conserved phosphoaccepting histidine domain of the HPTs (in black) to an aspartic acid residue (red) or a glutamine residue (blue). Coloured arrows indicate positions of AHP6 (red) and the three rice PHPs (blue). Clades with grey triangles have been collapsed for easier viewing of the tree. The phylogeny is based on 100 bootstrap replicates. Gene identifiers are listed in Appendix Figure 6.

protein displaying the H-N substitution at the HPT phosphoaccepting histidine domain. However, the monocot PHPs form two distinct clades. One clade contains the rice PHPs OsPHP1 and OsPHP3 amongst PHPs from other monocot species, while the other clade contains OsPHP2 alongside HPTs from other species. The monophyletic clade of monocot PHPs, which excludes the clade with OsPHP2, is well supported by 72 out of 100 bootstrap trials. This indicates that there may have been multiple origins of the PHPs in monocots, with convergent evolution selecting for the H-Q substitution independently. An alternative solution is that this clade has the same evolutionary origin as the other monocot PHPs, but the proteins other than OsPHP2 (of other monocot species) have reverted back to HPTs via substitution to restore the phosphoaccepting histidine domain. However, according to this phylogeny the number of Q-H substitutions that would have had to take place throughout evolutionary history for this to be true is three, as opposed to the single H-Q substitution required for OsPHP2 to arise independently from an HPT lineage. Given the relatively high confidence in these clades as calculated from bootstrapping (Figure 4.3), the most parsimonious explanation is that OsPHP2 evolved independently of the other PHPs. However, as the genome sequence of more monocot species become available this claim may be re-tested with greater confidence. This phylogeny indicates that OsPHP1, OsPHP2 and OsPHP3 are more closely related to AtAHP4 (sharing 62.76, 55.86 and 60.69 % amino acid sequence similarity respectively) than to AHP6 (with which they share 36.67, 36 and 36 % sequence similarity respectively). AtAHP4 shares greater amino acid sequence similarity with the rice HPTs and PHPs than any of the

other *Arabidopsis* HPTs or AHP6 (Figure 4.4). This, along with the phylogenetic analysis, indicates AtAHP4 is distinct from the other *Arabidopsis* HPTs and consequently may be functionally distinct. Overall this phylogeny provides strong support for the two core PHP clades of the eudicots and monocots evolving independently of each other.

It is worth noting that there is another large dicot clade with a high degree of variation (with some missing this region) at the conserved phosphoaccepting H region; based on sequence data alone it is not possible to speculate whether these proteins function in cytokinin signalling, represent residual pseudogenes or have evolved other roles. Alternatively, they may have a genuine function in cytokinin signalling, but since these proteins are absent in *Arabidopsis* or rice, they are beyond the scope of this study. There are also a small number of other proteins from both dicots and monocots with amino acid substitutions other than N or Q at this conserved domain. Some of these proteins may have low amino acid similarity with true PHPs, suggesting they may not be functional components of cytokinin signalling. However, a Phytozome BLAST search with higher stringency of E -15 (the default being E -1) excludes the entire large variable clade mentioned above (and indeed several probably genuine HPTs) but still returns four of these proteins with variable amino acids at the phosphoaccepting H domain. These include one protein from *Mimulas guttatas* with a proline, one from *Frageria vesca* with a tyrosine and two proteins from *Glycine max* with arginine substituted at the phosphoaccepting H domain. Given the major structural differences between these amino acids it seems probable that the protein structure would be vastly different than that of the

	AtAHP1	*AtAHP2*	*AtAHP3*	*AtAHP4*	*AtAHP5*	*AtAHP6*	*OsAHP1*	*OsAHP2*	*OsPHP1*	*OsPHP2*	*OsPHP3*
AtAHP1	100	48.37	52.63	39.31	52.94	44.67	46.26	45.95	43.71	41.72	40.79
AtAHP2	48.37	100	81.29	43.45	70.51	37.91	41.5	40.54	41.72	41.06	38.16
AtAHP3	52.63	81.29	100	42.76	70.32	39.87	42.86	39.19	41.72	41.06	36.84
AtAHP4	39.31	43.45	42.76	100	44.14	35.86	39.44	37.76	62.76	55.86	60.69
AtAHP5	52.94	70.51	70.32	44.14	100	40.91	46.26	43.24	42.38	41.06	40.13
AtAHP6	44.67	37.91	39.87	35.86	40.91	100	35.37	35.14	36.67	36	36
OsAHP1	46.26	41.5	42.86	39.44	46.26	35.37	100	72.11	38.78	36.73	37.41
OsAHP2	45.95	40.54	39.19	37.76	43.24	35.14	72.11	100	38.51	35.14	36.49
OsPHP1	43.71	41.72	41.72	62.76	42.38	36.67	38.78	38.51	100	68.87	82.12
OsPHP2	41.72	41.06	41.06	55.86	41.06	36	36.73	35.14	68.87	100	64.24
OsPHP3	40.79	38.16	36.84	60.69	40.13	36	37.41	36.49	82.12	64.24	100

Figure 4.4. An amino acid identity matrix for the *Arabidopsis* and rice HPTs and PHPs. Amino acid sequence similarity was calculated using Clustal2.1.

other PHPs, but this doesn't necessarily exclude them from having a role in cytokinin signalling. It is possible these proteins act as true PHPs (or indeed HPTs) but study of individual proteins would have to be performed to provide any conclusive evidence. Indeed, it may be the case that the PHPs of monocots can be phosphorylated at another histidine residue and still function in phosphotransfer (although this is unlikely as any other histidine residue would lack the associated amino acids required to form the core phosphor-accepting motif). The same cannot be said of AHP6, as in-vitro phosphotransfer assays have proven it is able to inhibit cytokinin signalling, indicating it cannot accept a phosphate group from the receptor unless the N residue is substituted to an H (Mähönen, Bishopp, et al. 2006). Alternatively, it may be the case that the substitution to a different amino acid at the phosphoaccepting domain would change the intensity of inhibition of cytokinin signalling. The independent evolution of the dicot and monocot major PHP clades therefore raise two major questions. Firstly, do the PHPs of the monocots function as inhibitors of cytokinin signalling, and secondly, if so does the substitution influence intensity of inhibition? In addition, given the expansion of the PHP proteins, it seems likely that there will be differences in specificity of protein binding, providing another level of control of the pathway.

To answer these questions requires direct biochemical studies on these particular proteins, but it is also worth considering detailed analyses carried out in similar proteins. Some structural studies have been carried out in *Arabidopsis* proteins which provide an understanding of the details of binding of cytokinin signalling elements. Early work made use of single crystallised proteins to study

the role of co-factors or protein phosphorylation status in proposed mechanisms of binding (Pekárová et al. 2011; Hothorn et al. 2011). More recently, crystal structures of protein dimers have been obtained, which enable direct identification of critical domains and calculation of binding affinity. A study of AtAHK5 and AtAHP1 (Bauer et al. 2013) revealed, from the crystal structure of the bound protein complex, that the architecture of the AHK5-AHP1 interface is substantially different from that of characterised receptor and histidine phosphotransfer proteins from other species. By comparing conserved structures amongst the other *Arabidopsis* HPT proteins, the authors suggest that AHK5 would be able to bind the other HPTs in a similar manner, and also AHP6 (albeit with a weaker affinity). There are also a few examples of structural studies of cytokinin signalling components in other plant species, including in *Medicago* and maize, but none which successfully characterise protein complexes (Sugawara et al. 2005; Ruszkowski et al. 2013).

Given the transient nature of protein binding in cytokinin signalling, obtaining a crystal structure of a protein complex is not trivial and explains in part why so few two-component signalling protein complexes have been crystallised. There have however been many structural studies of two-component signalling proteins in bacteria and yeast, including many focussing on various substitutions identified from mutants. The two-component signalling system of *Saccharomyces cerevisiae* is composed of only four proteins; the hybrid histidine kinase Sln1, the histidine phosphotransfer protein Ypd1, the cytoplasm localised response regulator Ssk1 and the nuclear localised response regulator Skn7 (Posas et al., 1996). The simplicity of the two-component

signalling system of yeast has enabled detailed study of each component in a manner unfeasible for most eukaryotes. Multiple mutants have been made for every component which has enabled a detailed understanding of the role of particular residues in protein structure and consequent function in phosphorelay. In Ypd1 H64 is the phosphoaccepting histidine domain required for phosphorylation. Mutations of amino acids close to this domain (such as the K67A substitution) have been shown to cause loss of phosphotransfer (Fassler & West 2010; Janiak-Spens et al. 2000). This particular domain is well conserved amongst HPTs and is present in all *Arabidopsis* and rice HPTs and PHPs except AHP6, where it is substituted for a valine (Figure 4.1A). The G68Q substitution (another residue highly conserved and present in all *Arabidopsis* and rice HPTs and PHPs) also abolishes phosphotransfer, due to disrupting access of H64 for the receiver domain of the RR (Janiak-Spens et al. 2000; Fassler & West 2010; Porter & West 2005). Many mutations have been characterised which decrease or eliminate phosphotransfer altogether, but some mutations have also been found to increase phosphotransfer. For example, the G74C mutation in Ypd1 has been shown to enhance phosphotransfer, although the exact mechanism by which this occurs remains unknown (Hiramoto et al. 2003; Fassler & West 2013). This residue has been associated with maintaining structural integrity of the protein and is highly conserved amongst HPTs, including those of *Arabidopsis* and rice. Studies of this kind have been useful in understanding the details of protein-protein interactions in the particular system studied. However, data of this nature cannot be assumed to apply to every homologous

signalling cascade so it is important that the particular proteins of interest are studied in detail.

4.3 The OsPHPs as candidates for AHP6 function proteins

In order to dissect the roles of cytokinin and auxin in development of the vasculature of rice roots, it is useful to know if homologous genes of *Arabidopsis* may function in a similar manner. Given the central role of AHP6 in protoxylem development by enabling crosstalk between auxin and cytokinin, looking for a functional homologue in rice is a good place to start. As AHP6 is a cytokinin signalling inhibitor whose expression is inducible by auxin, screening known rice cytokinin signalling inhibitors for auxin inducibility may help pick out rice genes which function in an AHP6 like manner. The only components of cytokinin signalling which are known to function as inhibitors of cytokinin signalling via the TCS pathway are the PHPs (homologues of AHP6) and the type-A RRs.

Previous studies on cytokinin related gene expression after hormonal treatments revealed a number of cytokinin signalling inhibitors upregulated by auxin (Tsai et al. 2012), and the microarray database RiceXPro confirm these findings (Sato et al. 2013). Tsai et al. (2012) show that in whole root samples none of the three OsPHPs are significantly upregulated by auxin, whereas OsRR6 and OsRR7 show greater than 2-fold induction with IAA treatment. Interestingly this dataset also indicates OsRR3 expression in the root is inhibited by IAA treatment. The RiceXPro database also shows OsRR1, OsRR4 and OsRR11 to be auxin inducible in the root (Figure 4.5). For most of these genes expression

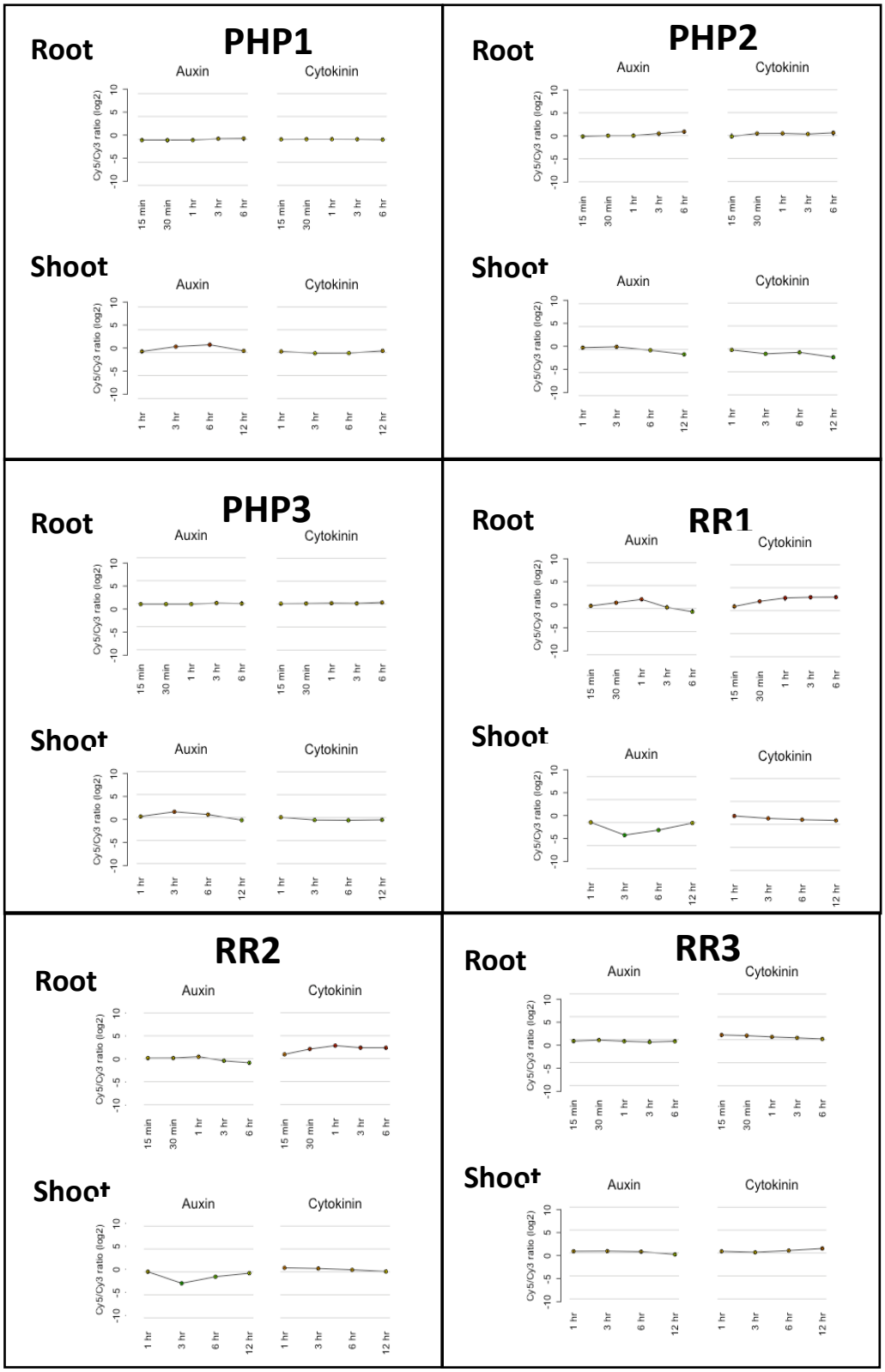


Figure 4.5. Expression data reveals OsPHPs are not responsive to cytokinin or auxin in roots whereas some type-A RRs show much greater response. Plants were treated with auxin (10 uM IAA) and cytokinin (1uM tras-zeatin) after time points indicated. Data was obtained from the RiceXPro database.

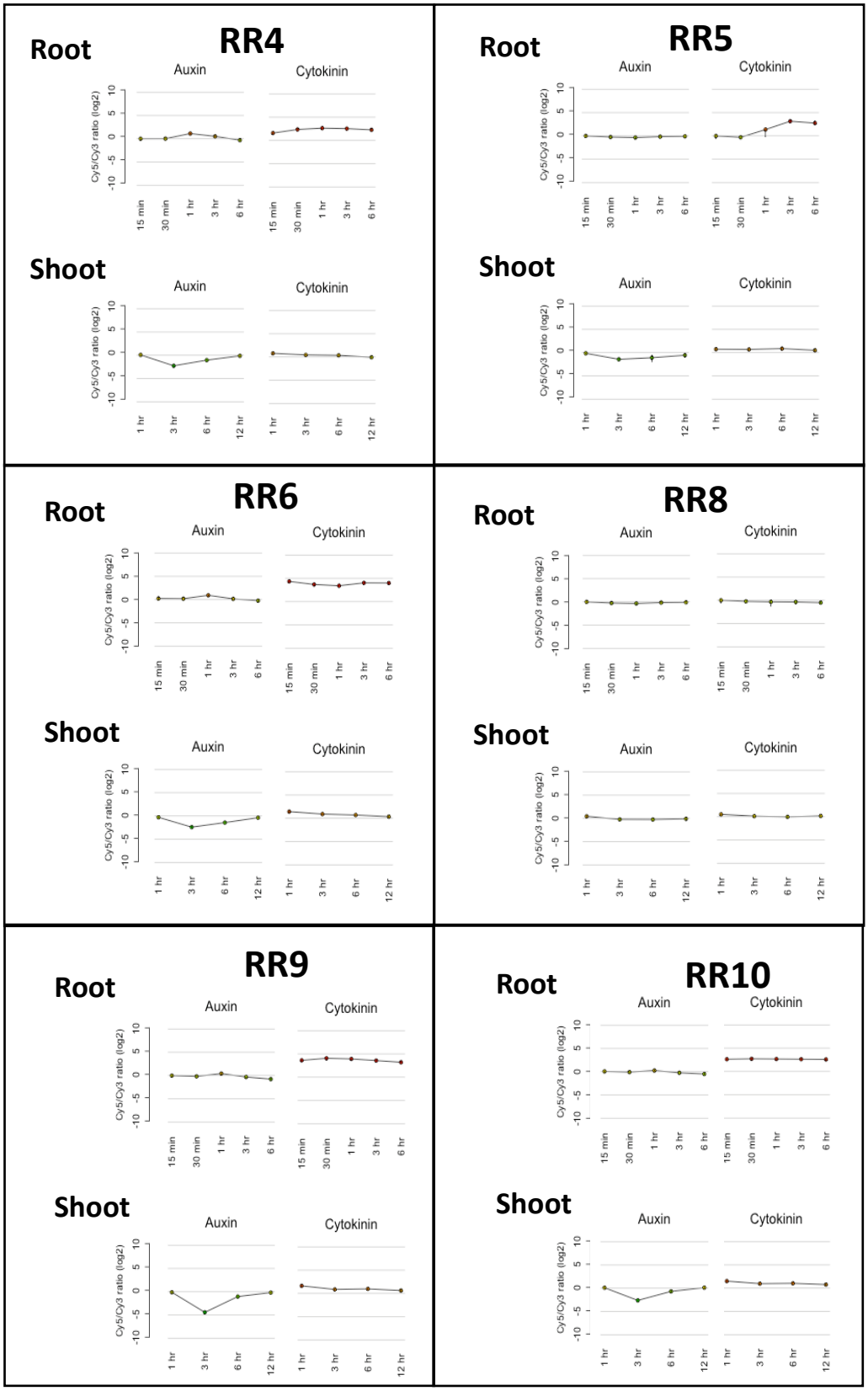


Figure 4.5 continued

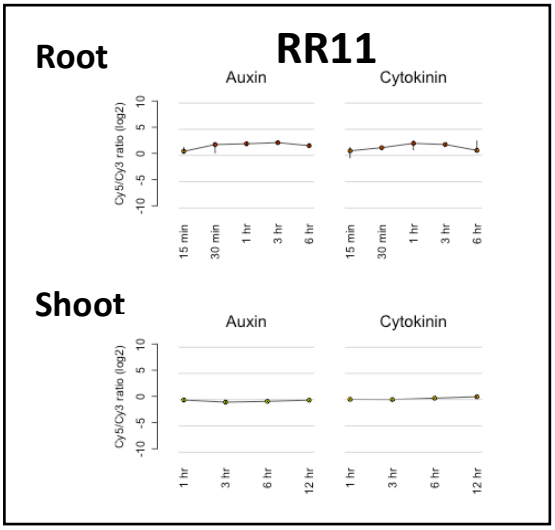


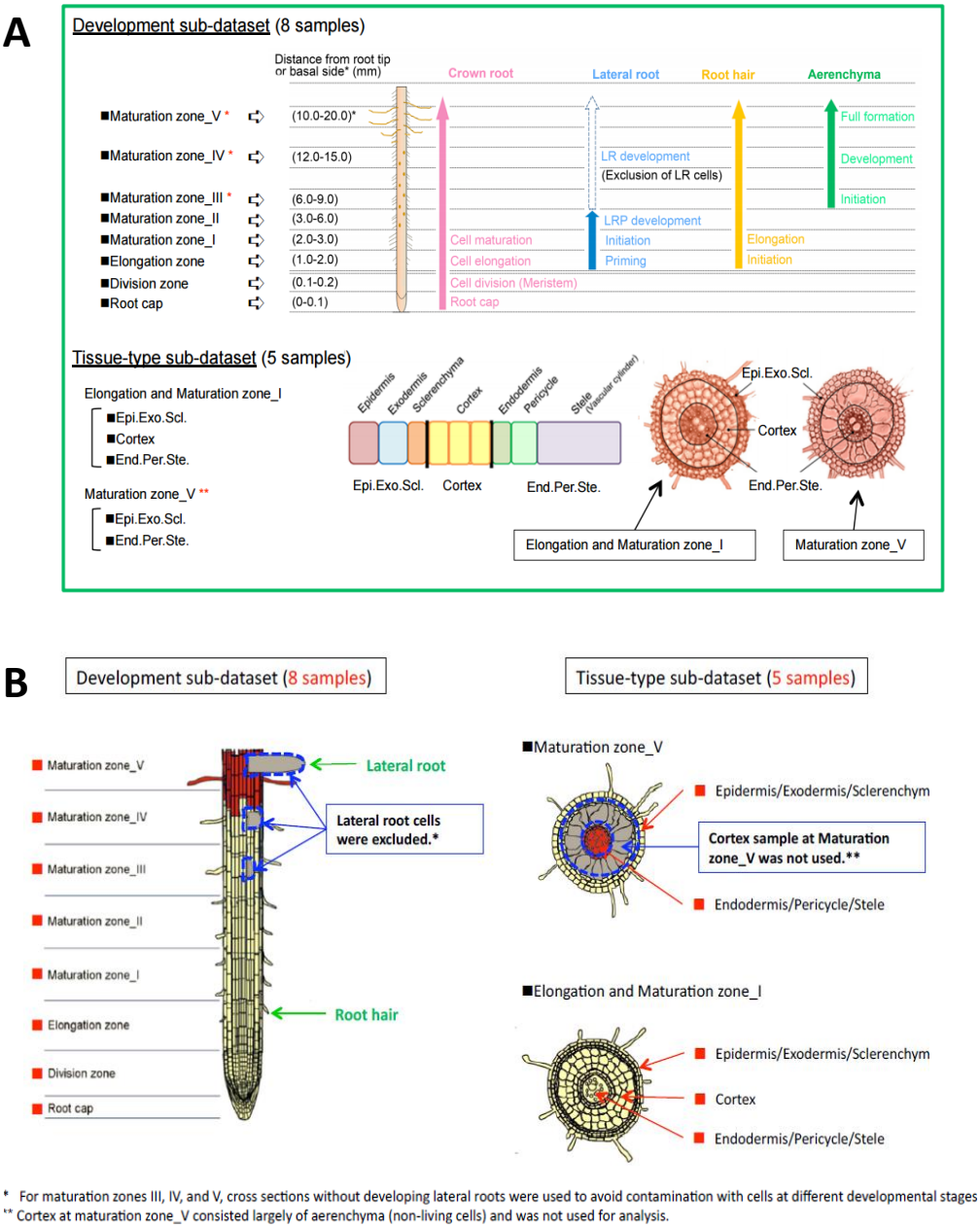
Figure 4.5 continued

levels peak after 1 hour with IAA, after which they decrease back to normal levels. The exception is OsRR11 which maintains a higher expression level even after being treated with IAA for as many as 6 hours. Unfortunately, there is no data available in the RiceXPro database for OsRR7, OsRR12 and OsRR13. Whilst this hormonal treatment data is useful it is limited by only being carried out in whole roots. In *Arabidopsis* AHP6 is only expressed in protoxylem and adjacent pericycle cells relatively close to the root tip (Mähönen, Bishopp, et al. 2006). Therefore, taking whole root data for auxin inducibility may be masking changes in gene expression closer to the root tip.

In order to get a more detailed analysis of expression changes at the root tip, the 3 OsPHPs and all 13 OsARRs in rice were screened by qRT-PCR after auxin treatment in dissected segments of root. Due to difficulty of accurately dissecting different developmental zones by hand, sections from the primary root tip of 0-1, 1-3 and 3-6 mm were taken. As shown in Figure 4.6 A, this roughly equates to the first section including root cap and meristem, the second section including elongation zone and maturation zone I, and the third section including maturation zone II. The PHPs and many of the type-A RRs did not amplify well in these sections, most likely due to low expression levels in these tissues. Microarray data describing expression domains confirms some of these genes as having low expression levels in the root (Sato et al. 2013). However, other genes which could be amplified also appear to have low expression in the roots (such as OsRR6). OsPHP1 and OsPHP2 did not amplify well with resulting qRT-PCR being difficult to interpret, and OsPHP3 could not be amplified at all. Expression data from the RiceXPro database indicate that

the three OsPHPs do have low expression levels in all tissues, including roots (Appendix Figure 7). This was confirmed by showing greater transcript abundance in whole shoots as compared to whole roots for all three OsPHPs (not shown here). Data from the RiceXPro microarray database indicate the other type-A RRs which could not be amplified by qRT-PCR (OsRR2, 4, 5, and 8-13) show low expression levels in the root as a whole, with the exception of OsRR2 and OsRR10 which showed moderate expression levels. As well as organ level expression, the RiceXPro database also collates data harnessed by laser microdissection of root samples by developmental stage and tissue type (Figure 4.6). This data shows that the type-A RRs mentioned above are not expressed or are expressed at very low levels in all root tissues (Appendix Figure 8). Whereas the OsPHPs have low expression levels in all root tissues (Figure 4.7), OsRR1, OsRR3 and (to a lesser extent), OsRR6, are most highly expressed in the root cap and root apical meristem (Figure 4.7).

Caution is needed when interpreting the results of the qRT-PCRs discussed in the following section. Because of the technical difficulty of dissecting small sections of root by hand, there was variability in resulting relative expression changes between the three biological replicates used. While the general trends were replicated (Appendix Figure 10), there are many instances where the difference in relative expression change between biological replicates was too large to give any significant results (when using 2 way ANOVA and Dunnett tests). This reflects error in technical details of the experiment, rather than having true biological relevance. This means that, even though no significant differences can be claimed between particular time points or sections, the



* For maturation zones III, IV, and V, cross sections without developing lateral roots were used to avoid contamination with cells at different developmental stages
** Cortex at maturation zone_V consisted largely of aerenchyma (non-living cells) and was not used for analysis.

Figure 4.6. Experimental outline and output from RiceXPro microarray database. (A) Microarray analysis was conducted both on sections of root as a whole and a sub set of tissue types. (B) The normalised output from the RiceXPro database displayed as a heatmap. Images are taken from RiceXPro manual.

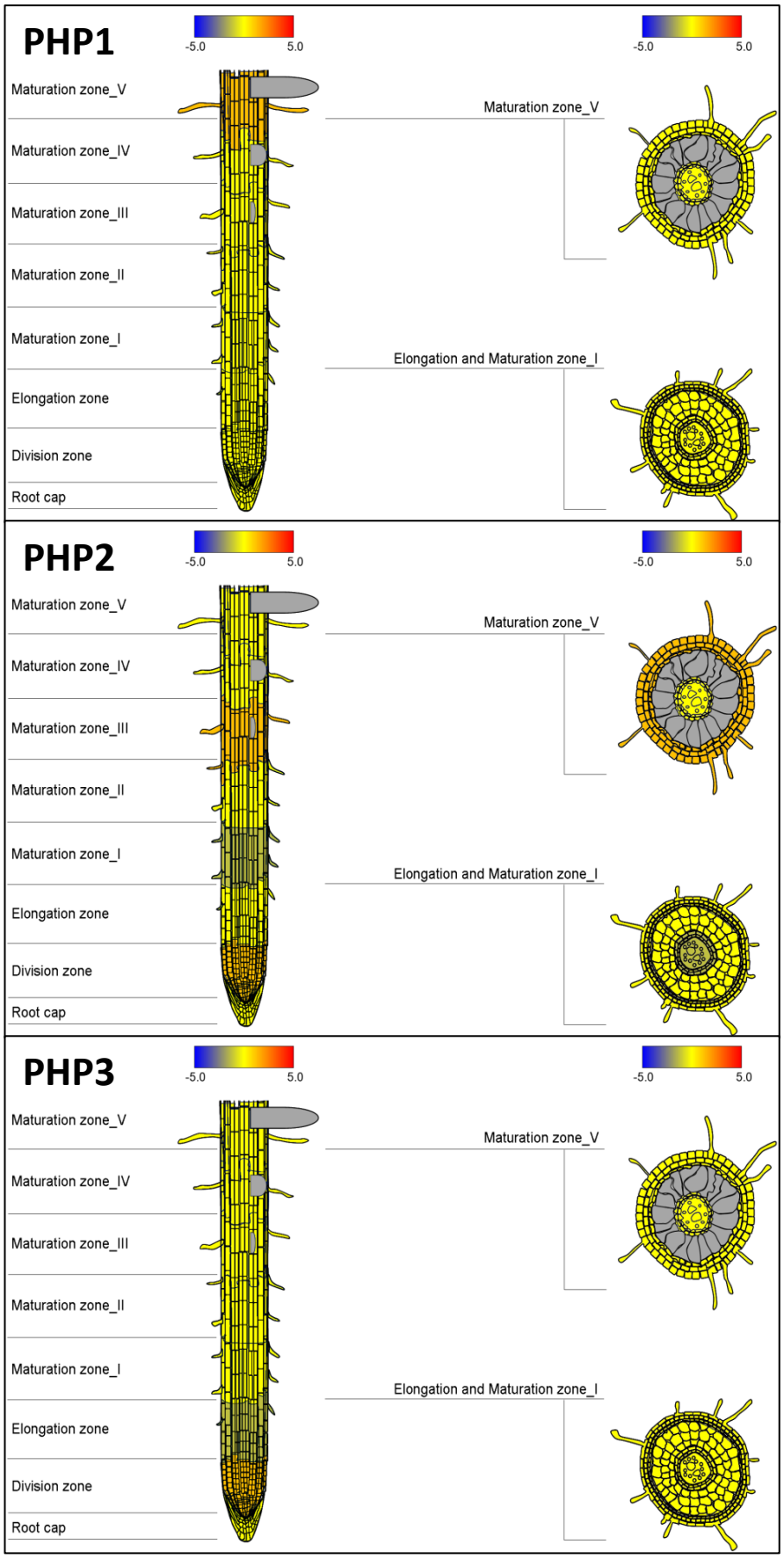


Figure 4.7. Expression domains of the OsPHPs and a sub set of the type-A RRs suggest OsRR1 and OsRR3 are expressed with highest abundance in the root tip. Taken from the RiceXPro database.

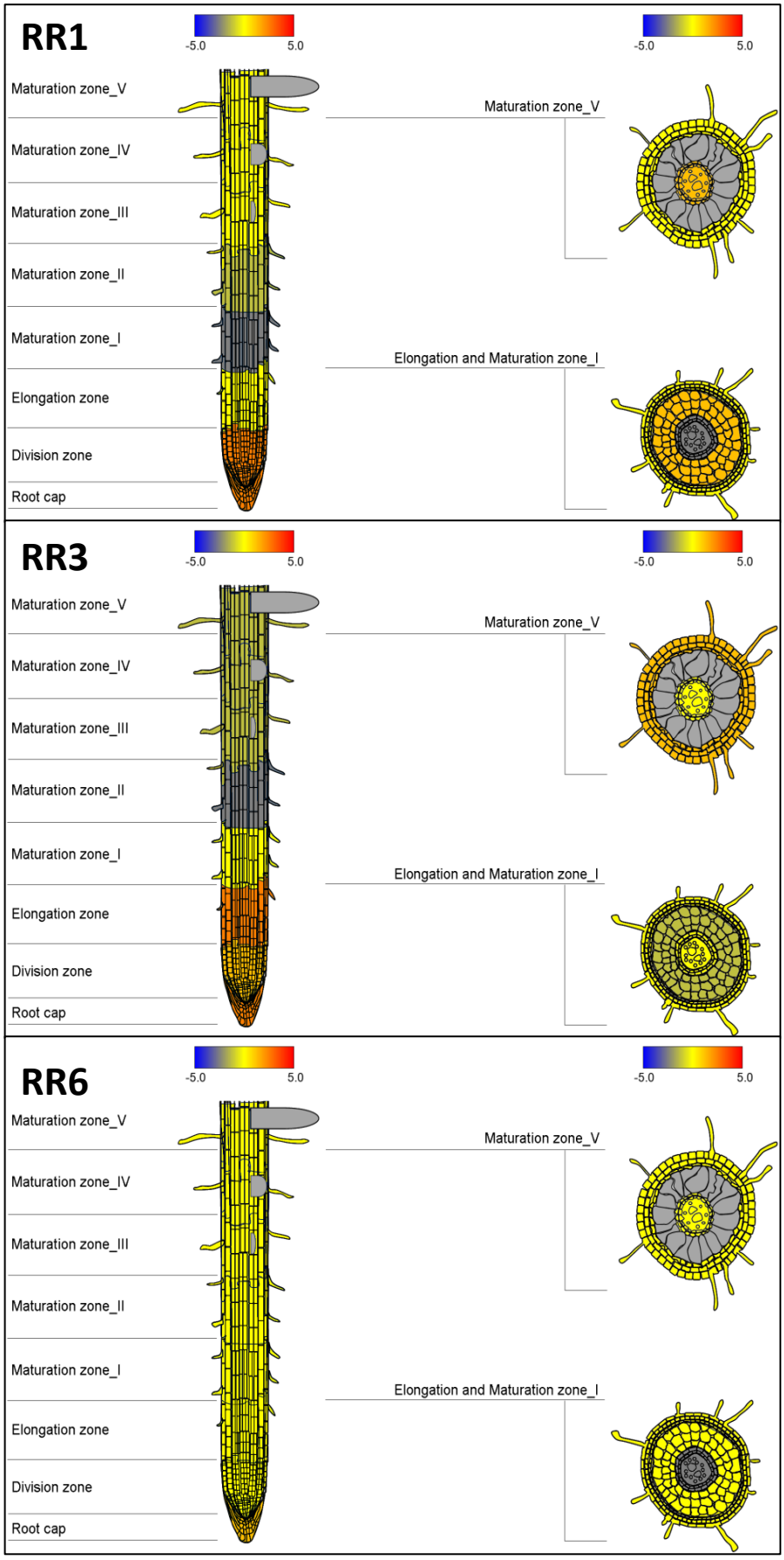


Figure 4.7 continued

trends displayed most likely do indicate real relationships. Two internal control genes (UBQ and 40S) were used in every experiment and although the fold changes differ slightly when calculated using the two different controls, the general trends remain the same. This provides further support for the validity of the overall experiment.

4.4 Candidate genes response to auxin

Given that the PHPs generally were difficult to amplify and showed high error even between technical replicates (likely due to low transcript abundance) it is difficult to interpret the results for these. Of the genes that were amplified well by qRT-PCR, OsRR1, OsRR6 and OsRR7 are consistently the most highly induced by auxin treatment at the root tip, in agreement with whole root studies. At 2 µM IAA, OsRR1 shows increases in expression in sections 0-1 and 1-3 after 1.5 hours, which then decrease with time (Figure 4.8). However, these changes were not significantly different across the three biological replicates. OsRR6 is induced in all three sections, with highest expression levels seen in section 3-6 at 2.5 hours, after which expression decreases. OsRR7 is induced particularly strongly in sections 0-1 and 1-3, with expression peaking after 2.5 hours. OsRR6 is still induced (at even higher levels) after 1.5 hours in section 3-6, whereas OsRR1 and OsRR7 showed less change this far up the root. This suggests the expression of OsRR1 and OsRR7 is restricted to the root tip only while OsRR6 is expressed more widely. This is in agreement with data for OsRR1 from the RiceXPro database (Figure 4.7), but no data on tissue expression levels for

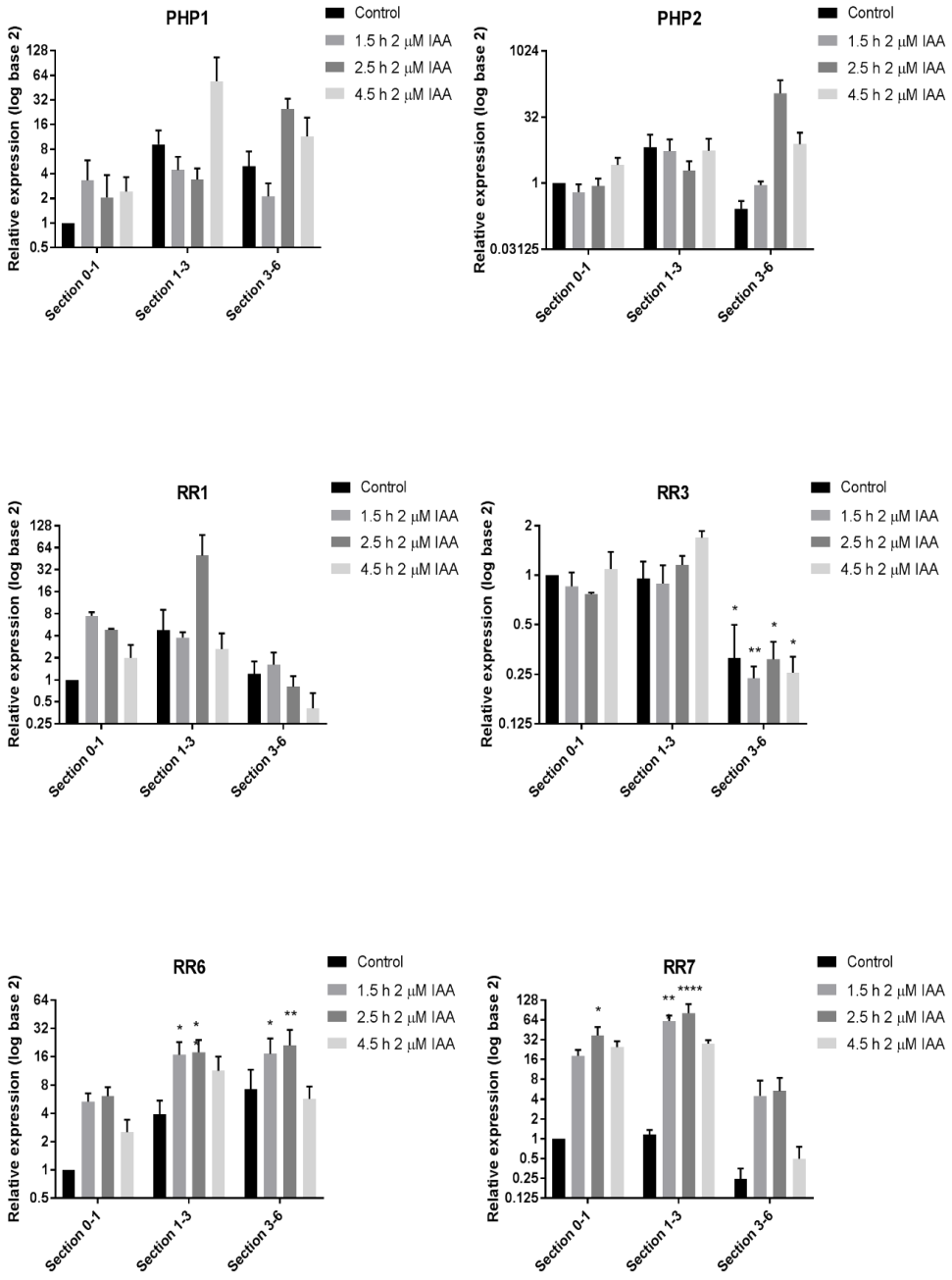


Figure 4.8. OsRR1, OsRR6 and OsRR7 are induced by 2 µM IAA in the root tip. Relative fold change (log base 2) in expression of OsPHP1, PHP2, OsRR1, OsRR3, OsRR6 and OsRR7 was detected after 1.5, 2.5 and 4.5 hours of treatment with 2 µM IAA and DMSO control in dissected segments of Kitaake root tip. All qRT-PCRs using rice tissue were performed with three biological replicates, four technical replicates and using UBQ (shown here) and 40S (see supplementary figures) as internal controls. Two-way ANOVA and Dunnett tests were performed and asterisks indicate significance (* $P \leq 0.05$, ** $P \leq 0.01$, *** $P \leq 0.001$, **** $P \leq 0.0001$)

OsRR7 have been published, so it is unclear whether the same is true of OsRR7. When treated with 10 µM IAA, induction of OsRR6 could not be detected with significance, whereas induction of OsRR7 was detected in section 0-1 and 1-3 after 1.5 hours (Figure 4.9). This may be because OsRR6 responds faster to auxin treatment and is able to bring expression levels down to normal levels after 1.5 hours due to the higher concentration treatment. Amongst the less dramatically reacting genes, OsRR1 was slightly induced by auxin in the root tip (but at much lower levels), and OsRR3 seemed slightly down regulated by auxin treatment (although this cannot be seen when averaging expression changes across the three biological replicates).

4.5 Candidate genes response to cytokinin

Given that the rice OsPHPs and OsRRs have not been well characterised, it is also useful to understand the effect of cytokinin on expression levels of these genes. Within the general scheme of cytokinin signalling it would be expected that type-A RRs, as inhibitors of cytokinin signalling, would be upregulated by cytokinin (Hwang et al. 2012; Tsai et al. 2012). Indeed, many type-B RRs act as transcription factors to up regulate expression of type-A RRs, forming a negative feedback loop which maintains cytokinin homeostasis. This does seem to be the case for some of the rice type-A RRs tested here, with OsRR6 and OsRR7 responding most strongly to 1 µM BA treatment and a similar pattern seen with 5 µM BA treatment (possibly due to having the highest expression levels in the root tip Figure 4.10 and 4.11). OsRR1 is significantly upregulated

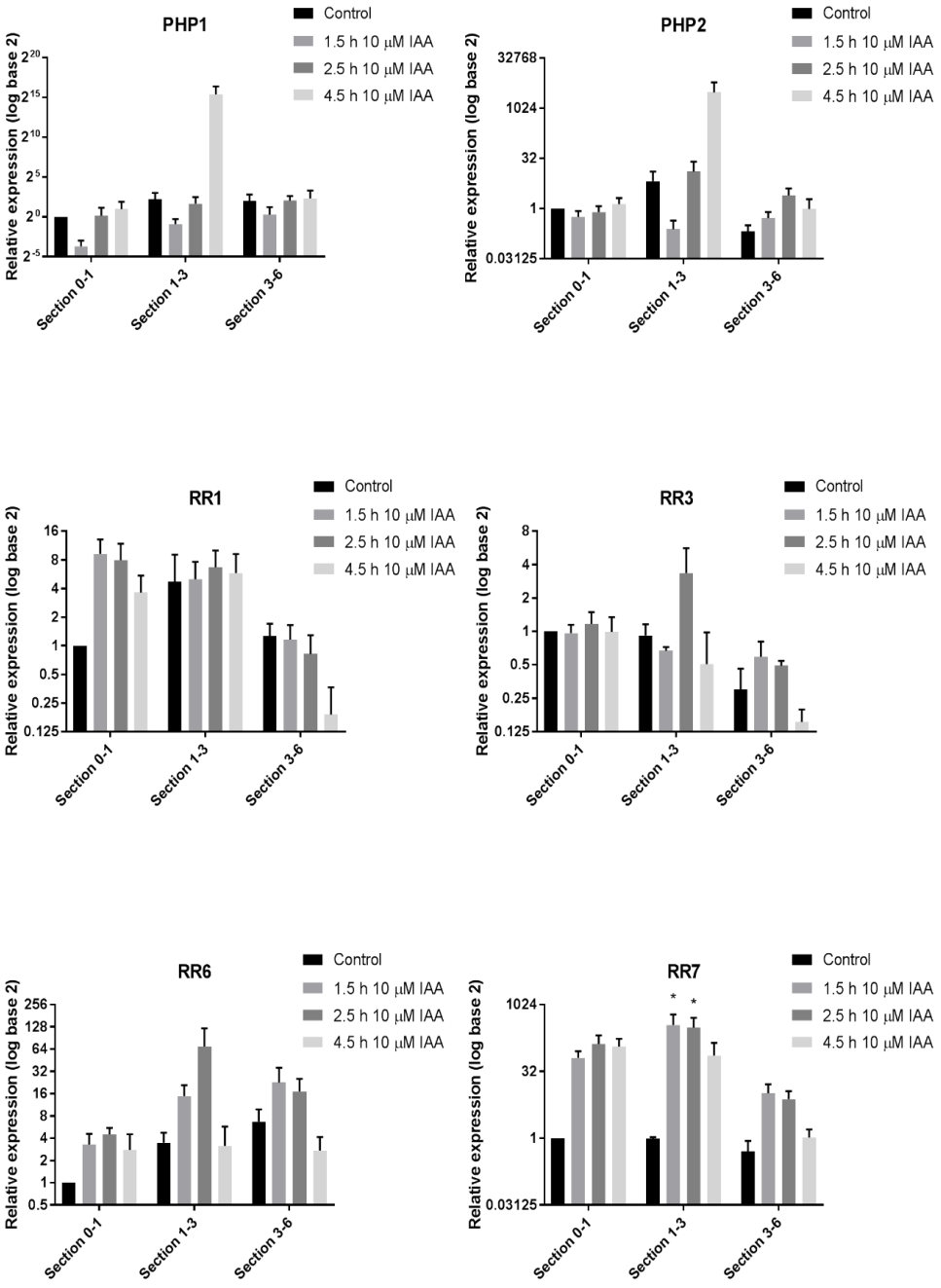


Figure 4.9. OsRR1, OsRR6 and OsRR7 are induced by 10 µM IAA in the root tip. Relative fold change (log base 2) in expression of OsPHP1, PHP2, OsRR1, OsRR3, OsRR6 and OsRR7 was detected after 1.5, 2.5 and 4.5 hours of treatment with 10 µM IAA and DMSO control in dissected segments of Kitaake root tip. All qRT-PCRs using rice tissue were performed with three biological replicates, four technical replicates and using UBQ (shown here) and 40S (see supplementary figures) as internal controls. Two-way ANOVA and Dunnett tests were performed and asterisks indicate significance (* $P \leq 0.05$, ** $P \leq 0.01$, *** $P \leq 0.001$, **** $P \leq 0.0001$)

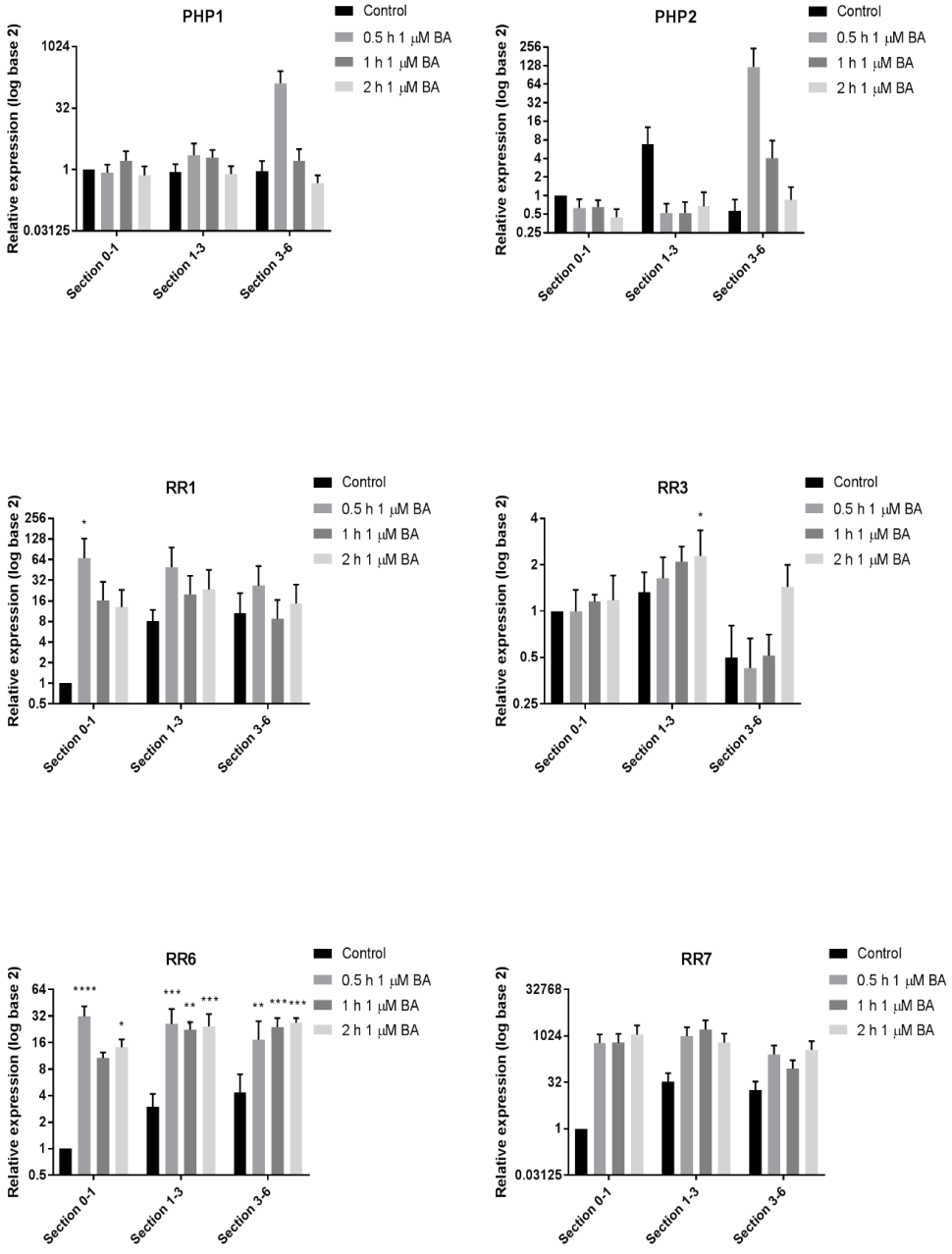


Figure 4.10. OsRR1, OsRR6 and OsRR7 are induced by 1 µM BA in the root tip. Relative fold change (log base 2) in expression of OsPHP1, PHP2, OsRR1, OsRR3, OsRR6 and OsRR7 was detected after 30 minutes, 1 hour and 2 hours of treatment with 1 µM BA and DMSO control in dissected segments of Kitaake root tip. All qRT-PCRs using rice tissue were performed with three biological replicates, four technical replicates and using UBQ (shown here) and 40S (see supplementary figures) as internal controls. Two-way ANOVA and Dunnett tests were performed and asterisks indicate significance (* $P \leq 0.05$, ** $P \leq 0.01$, *** $P \leq 0.001$, **** $P \leq 0.0001$)

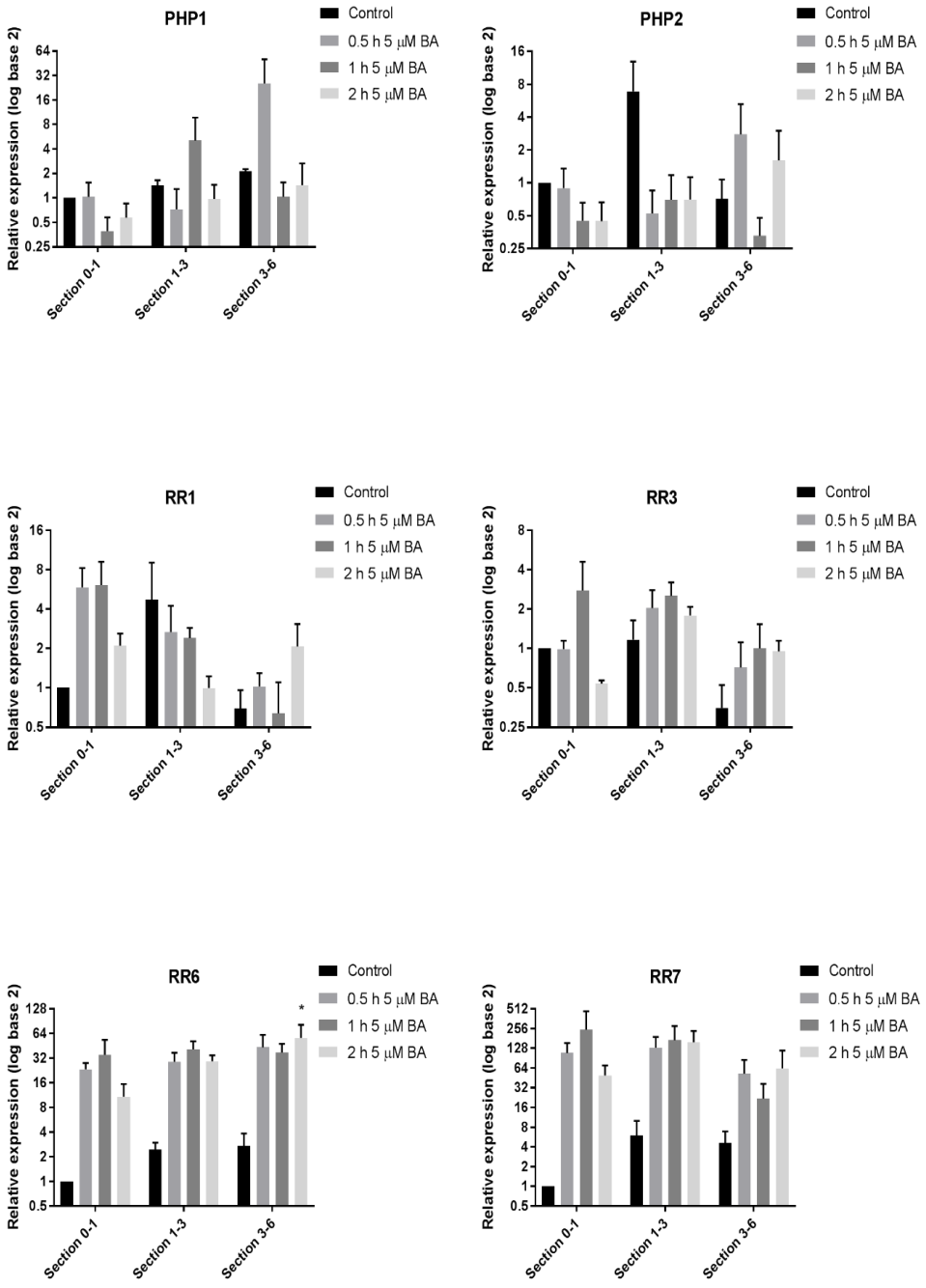


Figure 4.11. OsRR1, OsRR6 and OsRR7 are induced by 5 µM BA in the root tip. Relative fold change (log base 2) in expression of OsPHP1, PHP2, OsRR1, OsRR3, OsRR6 and OsRR7 was detected after 30 minutes, 1 hour and 2 hours of treatment with 5 µM BA and DMSO control in dissected segments of Kitaake root tip. All qRT-PCRs using rice tissue were performed with three biological replicates, four technical replicates and using UBQ (shown here) and 40S (see supplementary figures) as internal controls. Two-way ANOVA and Dunnett tests were performed and asterisks indicate significance (* $P \leq 0.05$, ** $P \leq 0.01$, *** $P \leq 0.001$, **** $P \leq 0.0001$)

after 30 minutes treatment with 1 µM BA in section 0-1, and OsRR3 appear to be unaffected by cytokinin treatment (Figure 4.10). The effect of cytokinin treatment on the OsPHPs however is a little more questionable. However, the combination of low expression and technical difficulty of this experiment make it very difficult to draw any conclusions about the effect of cytokinin on the expression of OsPHP1 and OsPHP2 in roots. It may be the case that the down regulation of PHP2 seen in section 1-3 after 30 minutes is real but the error is too great to make this claim. The three OsPHPs however, do seem to be slightly down regulated by cytokinin treatment in shoots (as seen in data from RiceXPro microarray database, and Tsai et al. 2012).

Given that the OsPHPs appear not to be responsive to auxin treatment in the root tip and their overall low expression level in these tissues, it is unlikely that they play an AHP6-like role in rice root vascular patterning. This raises two new questions:

1. What is the function of the OsPHPs? Could they have developmental roles other than root vascular patterning, such as some of the other processes that AHP6 is also involved in mediating?
2. Have the type-A RRs of rice been recruited to regulate root vascular patterning in rice? Could OsRR1, OsRR6 and OsRR7 function (possibly redundantly) in this process?

4.6 Discussion

Given the low expression levels and lack of an effect of auxin on expression of the OsPHPs in the root tip, it seems unlikely that these proteins would play any role in allowing crosstalk of auxin and cytokinin signalling to enable proper development of pattern in protoxylem of rice roots. However, OsRR1, OsRR6 and OsRR7 are all highly induced by auxin specifically at the root tip. Since these proteins are all known to be inhibitors of cytokinin signalling it may be the case that they function in an AHP6-like manner in this context, and possibly in a functionally redundant manner. If this is the case, it provides a system to study how the cytokinin signalling pathway has evolved to extend its developmental functions. In the context of root vascular patterning, expression of AHP6 is inhibited by cytokinin, whereas expression of most type-A RRs is induced by cytokinin (Mähönen, Bishopp, et al. 2006; Jain et al. 2006). However, although AHP6 expression is down-regulated by cytokinin, this is not a direct effect and AHP6 is not a primary cytokinin responsive gene. Therefore, the effect of cytokinin on AHP6 expression is not clear and may well be dependent on changes in auxin signalling. AHP6 has been shown to respond rapidly to auxin (with clear induction after a 2 hour treatment), whereas inhibition upon cytokinin treatment is delayed (seen after a 6 hour treatment), supporting this notion (Bishopp, Help, et al. 2011; Mähönen, Bishopp, et al. 2006). In addition, co-treatment of BA and NPA indicates PIN activity is required for inhibition of AHP6 expression by BA, suggesting regulation by auxin (Bishopp, Help, et al. 2011).

Hormonal regulation of the rice type-A RRs is also likely to be dependent on developmental context. Many studies have shown opposing effects of auxin on gene expression in roots and shoots. For example, auxin has been shown to inhibit expression of the *Arabidopsis* type-A response regulators ARR7 and ARR15 in the SAM, but directly induce expression of these genes in the basal cell in early embryogenesis which forms the RAM (Zhao et al. 2010; Müller & Sheen 2008). However, in both of these contexts, ARR7 and ARR15 are both induced by cytokinin signalling. This suggests that whereas auxin and cytokinin act antagonistically in the RAM, they may function in synergy in the SAM. Consequently, if the type-A RRs of rice have been recruited to fill an AHP6-like role in root vascular patterning, the context of cytokinin and auxin signalling must have been adapted to enable this.

The most likely mechanism by which AHP6 inhibits cytokinin signalling is by competitively interacting with cytokinin receptors and RRs, to prevent binding of HPTs which would otherwise function in phosphotransfer. Interaction of these proteins has yet to be directly confirmed, but in-vitro phosphotransfer assays indicate this is the most probable mechanism of action (Mähönen, Higuchi, et al. 2006). I hypothesize that the OsPHPs function in a similar manner, although this is yet to be directly shown. The mechanism of action of the type-A RRs, on the other hand, remains unclear. Previous work indicated that *Arabidopsis* type-A RRs may inhibit cytokinin signalling simply by sequestering phosphate groups, thereby preventing them from being passed onto, and consequently activating, type-B RRs (To et al. 2004). This has been seen in some bacterial two component system (Li et al. 1995; Sourjik & Schmitt

1998). Indeed, this may be the sole mechanism of action for some of the type-A RRs. However, To et al. (2004) also suggest that the type-A RRs may function by indirectly reducing expression levels of the type-B RRs, to dampen cytokinin response. More recently, To et al. (2007) suggested type-A RRs most likely inhibit cytokinin signalling via protein-protein interactions which are dependent on their phosphorylation status. They elegantly demonstrated this by showing that a non-phosphorylatable partially activated mutant of *Arabidopsis* ARR5 ($ARR5^{D87E}$) is able to partially rescue the phenotype of multiple ARR5 mutants. As the authors indicate, this does not rule out the possibility that ARR5 functions by sequestering phosphate groups, but does indicate ARR5 is able to function as a cytokinin signalling inhibitor independently of its ability to compete for phosphoryl groups with type-B RRs. In addition to this, for a subset of the type-A RRs phosphorylation increases stability of these proteins, and this may demonstrate a mechanistic basis for functional specificity amongst the type-A RRs (To et al. 2007).

As indicated from results in Chapter 3, auxin and cytokinin signalling are clearly involved in rice root vascular patterning. It seems likely that the interaction between these two hormones in establishing discrete domains of hormonal signalling, which consequently pattern the root vasculature, is conserved between *Arabidopsis* and rice. However, it appears the rice homologues of AHP6 (the three OsPHPs) are not involved in this process, and the type-A RRs OsRR1, OsRR6 and OsRR7 may have been recruited for this function. This suggests that while the basic mechanisms of vascular patterning may be conserved between *Arabidopsis* and rice, the wiring of the molecular networks

which achieve this may be very different. In the next chapter I examine whether this may be the case by describing the activity of the OsPHPs, OsRR1, OsRR6 and OsRR7 in planta.

4.7 Summary

- The PHPs of dicots and monocots evolved independently of each other, and have different substitutions (to asparagine in dicots and glutamine in monocots) at the residue corresponding to the conserved phosphoaccepting histidine domain of the HPTs.

- The OsPHPs are not auxin or cytokinin responsive in the root tip, and appear to be expressed at low levels in the root.

- The type-A RRs OsRR1, OsRR6 and OsRR7 are highly induced by auxin in the root tip, suggesting they may fulfil an AHP6-like function.

Chapter 5. OsRR1, OsRR6 and OsRR7 can rescue *Arabidopsis ahp6* mutants

5.1 Introduction

The earlier qRT-PCR results suggest that OsRR1, OsRR6 and OsRR7 may be good candidates for genes performing an AHP6 like function in rice (i.e. auxin inducible inhibitors of cytokinin signalling expressed in the root tip). It is interesting to consider whether this may be down to molecular characteristics in terms of mechanism of action of the proteins, or simply that these inhibitors of cytokinin are able to function if expressed in a particular domain. Assuming that the basic mechanism of auxin and cytokinin crosstalk is conserved within angiosperms, auxin inducibility would be a requirement of a cytokinin inhibitor to fulfil an AHP6-like role. However, it may be the case that any auxin inducible cytokinin signalling inhibitor would be able to function in an AHP6-like manner if expressed in the domain of expression of AHP6. If it is the case that one (or several) of the type-A OsRRs are able to restrict cytokinin signalling at the protoxylem position, new issues are raised concerning hormonal regulation of these genes at the root tip. Whereas AHP6 is rapidly induced by auxin and down-regulated by cytokinin over a much longer timescale, the type-A OsRRs (OsRR1, OsRR6 and OsRR7) are rapidly induced by both hormones. In terms of what is known about how type-A RRs function in cytokinin signalling this makes sense, as type-A RRs are widely thought to be primary response genes whose expression is induced by type-B RRs (reviewed by Hwang et al. 2012). While it may make sense conceptually that one of the responses to cytokinin would also

be to express inhibitors of cytokinin signalling, to dampen the response and bring about homeostasis, it is unclear how such a system would bring about a steady state, and exactly what that state would be. In rice there are 13 type-A RRs and 13 type-B RRs, and expression patterns of these genes are largely unknown. In addition, it is not clear exactly how the type-A RRs function as inhibitors of cytokinin signalling. It may be the case that some type-A RRs genuinely do function only by sequestering phosphate groups, while others may interact with a range of specific proteins to moderate responses (To et al. 2007). This may also be dependent on expression patterns of the interacting proteins, leading to greater complexity but more precise control of the diverse responses.

The function and mechanism of action of AHP6 has been studied in several publications (Mähönen et al. 2006; Bishopp et al. 2011; Moreira et al. 2013; Besnard, Rozier, et al. 2014; Besnard, Refahi, et al. 2014), while the OsPHPs of rice are uncharacterised. Whilst the OsRR family has not been systematically investigated in roots, some members have seen attention. OsRR6 for example, has been shown to be induced by various abiotic stresses (such as drought, salt and cold stress), with some other type-A RRs (such as OsRR3) showing responsiveness to cold stress (Hirose et al. 2006; Jain et al. 2006; Yang et al. 2015). However, overall very little about the type-A RRs of rice (both in terms of function as well as mechanism of action) is known as compared to those of *Arabidopsis*. Given the identification of candidate genes which may function in an AHP6-like manner in rice root meristems (identified simply as inhibitors of cytokinin signalling which are inducible by auxin) it is useful to understand

whether these genes are able to function as cytokinin signalling inhibitors in vivo. In addition to this, it is also useful to take more direct approaches and understand the ability of these proteins to inhibit cytokinin signalling in in vitro assays. In this chapter I demonstrate that some of these candidate genes are able to function as inhibitors of cytokinin signalling, by showing they are able to rescue the phenotype of the *Arabidopsis ahp6* mutants, and also provide more detailed in vitro analyses demonstrating the mechanism of action of the OsPHPs.

5.2 In planta analysis of candidate gene function: Complementation of *ahp6* mutants

Previous work on the *ahp6* mutants have shown the importance of this protein in regulating a number of developmental processes. As well as modulating crosstalk between cytokinin and auxin signalling to enable proper development of root protoxylem, AHP6 has also been shown to play a role in proper development of the shoot apical meristem, and consequently has impacts on phyllotaxy (Mähönen et al. 2006; Bishopp et al. 2011; Besnard, Rozier, et al. 2014; Besnard, Refahi, et al. 2014). However, in these assays I focus only on root vascular patterning.

In this section, two major questions are discussed. Firstly, are the OsPHPs able to confer inhibition of cytokinin signalling in a similar manner to AHP6? Secondly, can other negative regulators of cytokinin signalling function in place of AHP6 if expression is driven by the AHP6 promoter? In order to answer these

questions, the coding sequence (CDS) of the three OsPHPs and the subset of type-A RRs which were shown to be upregulated by auxin in the rice root tip (OsRR1, OsRR6, OsRR7), and OsRR3 which appears to inhibited by auxin, were expressed under the AHP6 promoter in two independent *ahp6* mutant alleles, and root protoxylem phenotypes of resulting progeny analysed. In addition to these, expressing the CDS of AHP6 under its own promoter was included as a control, and site directed mutagenesis was used to construct a version of AHP6 with a substitution from the N to a Q residue at the conserved phosphoaccepting H residue of the HPTs (as is seen in the rice PHPs). Whereas restoring the H at this residue has been shown to enable AHP6 to act as a positive regulator of cytokinin signalling in in-vitro assays (Mähönen et al. 2006), the AHP6N83Q mutant will show whether the substitution which occurred in the rice PHPs can confer inhibition of cytokinin signalling. Finally, expressing the *Arabidopsis* type-A RR AtARR5 was included, to determine whether a type-A RR of *Arabidopsis* would show any differences to those of rice. AtARR5 has previously been shown to be induced by cytokinin as a primary response gene, but down-regulated by auxin, and is expressed in the procambium (Bishopp et al. 2011; Lee et al. 2009; D'Agostino et al. 2000). In analysis of trans-complementation, multiple independent transgenic lines were used for each construct. There was a degree of heterogeneity in protoxylem defects in the independent transgenic lines for each construct. However, the data represented here were selected from multiple independent transgenic lines per construct, whose protoxylem defect phenotypes are considered representative. Data from independent transgenic lines expressing AHP6 are

shown in Appendix Figure 11 and the spread of protoxylem defects can be seen. In order to determine whether levels of protein expression could be the reason for heterogeneity amongst independent transgenic lines, determining expression levels of AHP6 in the mutant backgrounds was attempted by qRT-PCR. This was unsuccessful due to difficulty of differentiating between wild type and mutant cDNA. qRT-PCRs were also conducted to determine expression levels of the rice PHPs and type-A RRs in the various independent transgenic lines, but were unable to correlate expression levels with phenotypic differences (possibly due to the small domain of expression of AHP6 masking differences in expression levels). In absence of expression data from qRT-PCR, proteins could be tagged with GFP to directly visualise localisation of protein and whether any obvious differences in expression levels are seen. In the rest of this chapter only the representative lines (as displayed in Figures 5.5 and 5.6) are considered unless specifically mentioned.

In roots of wild-type Col-0 plants there are always two continuous protoxylem poles on either side of the metaxylem (Figure 5.1, Figure 5.4 A). *ahp6* mutants are characterised by loss of protoxylem with abrupt breaks where it has aborted development (Figure 5.2, Figure 5.4 B and C), but the exact degree of loss varies greatly between individuals as the phenotype is not fully penetrant (Mähönen et al. 2006). For example, individual plants may show loss of protoxylem at both poles, but there are also many plants with loss at only one pole. In addition, a small number of *ahp6* mutant plants have two continuous protoxylem poles like wild-type plants. To quantify the degree of loss of protoxylem, a scoring system was used to rank the severity of the protoxylem

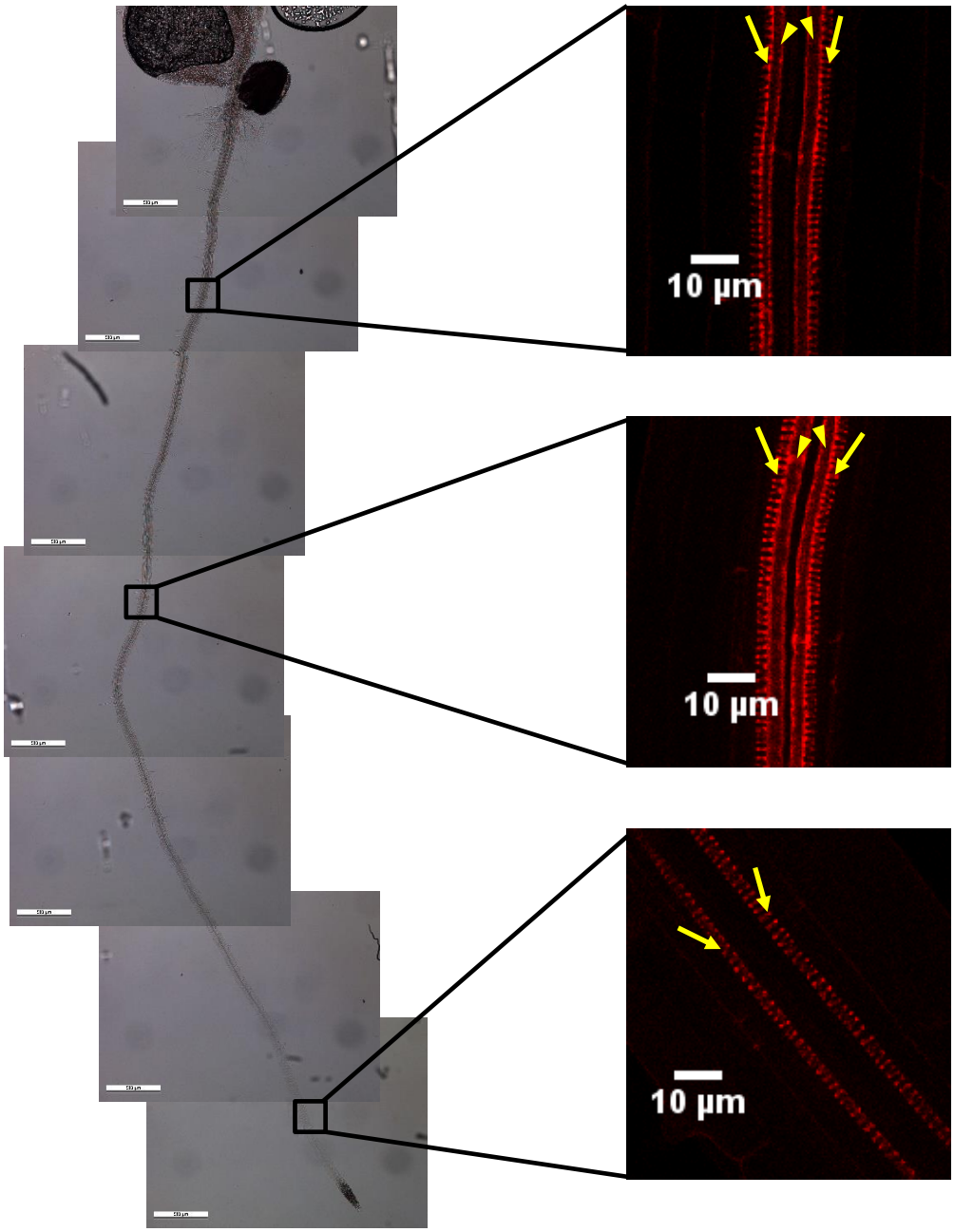


Figure 5.1. Fuchsin stained Col-0 showing the presence of two continuous protoxylem poles. Yellow arrowheads indicate metaxylem, yellow arrows indicate protoxylem. Scale bars in whole root image are 500 µm and in side panels 10 µm.

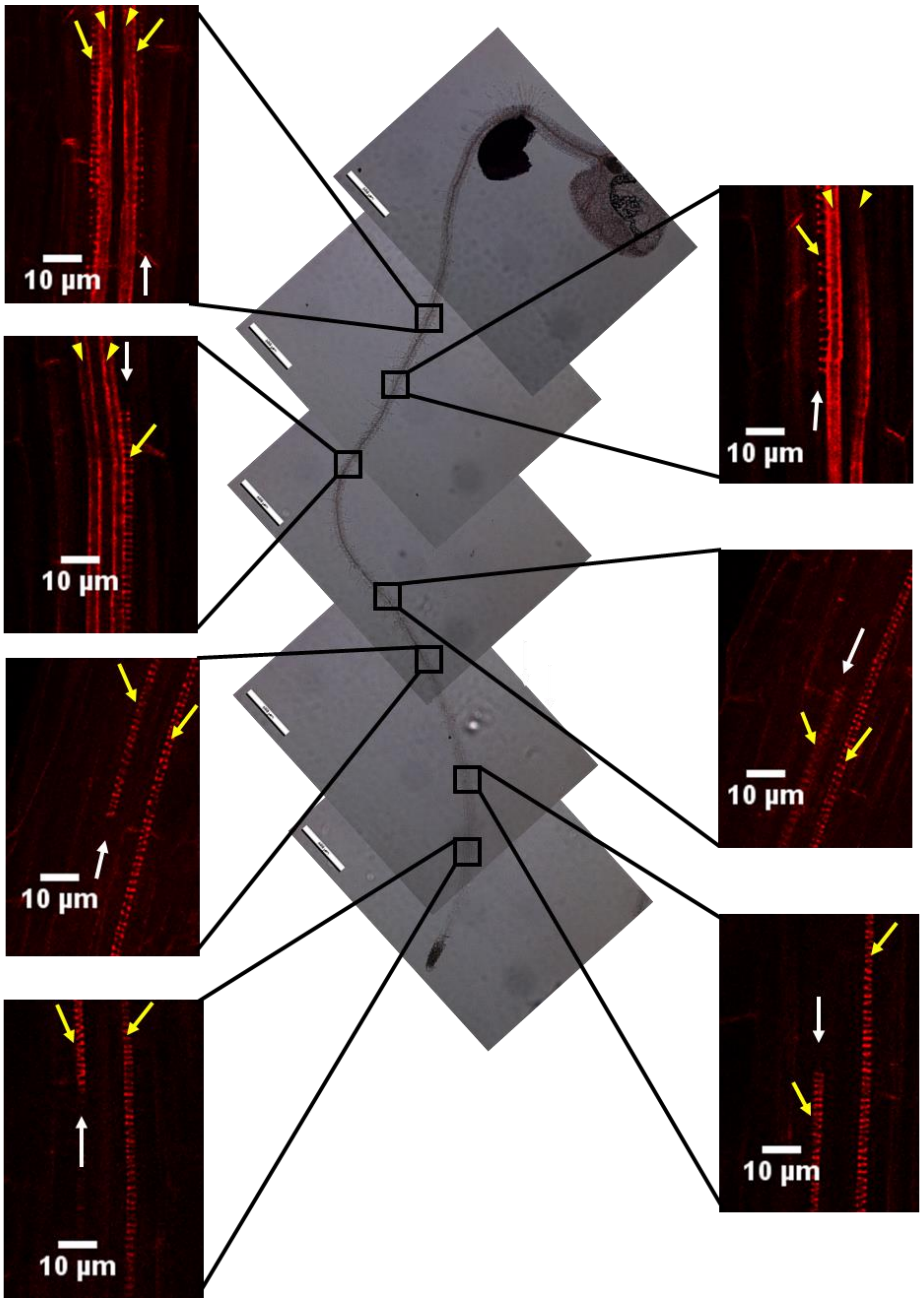


Figure 5.2. Fuchsin stained *ahp6-1* showing protoxylem developmental defects. Blown up images in panels indicate locations of breaks in protoxylem. Yellow arrowheads indicate metaxylem, yellow arrows indicate protoxylem and white arrows indicate breaks in protoxylem. Scale bars in whole root image are 500 µm and in side panels 10 µm.

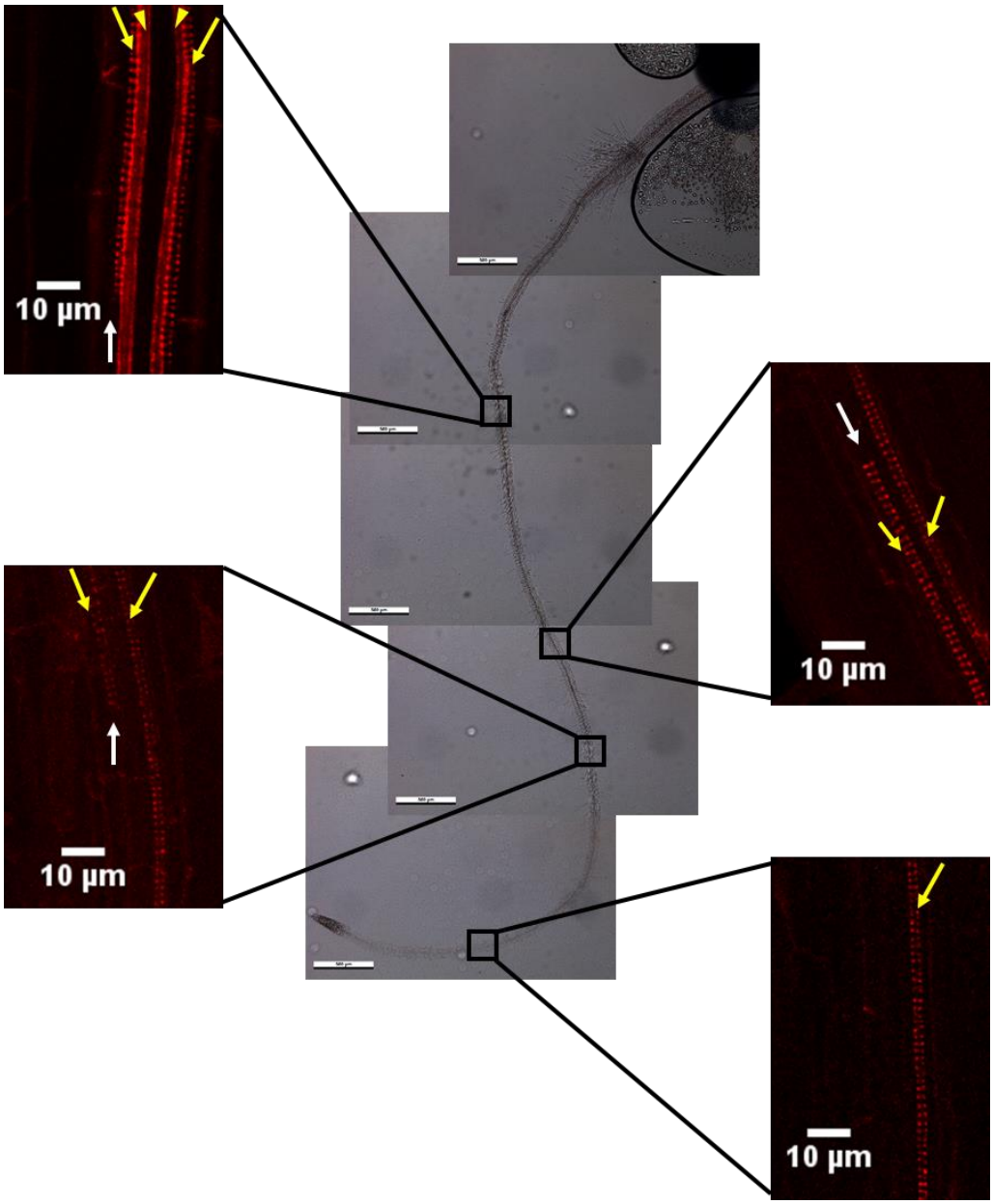


Figure 5.3. Fuchsin stained *ahp6-2* showing protoxylem developmental defects. Blown up images in panels indicate locations of breaks in protoxylem. Yellow arrowheads indicate metaxylem, yellow arrows indicate protoxylem and white arrows indicate breaks in protoxylem. Scale bars in whole root image are 500 µm and in side panels 10 µm.

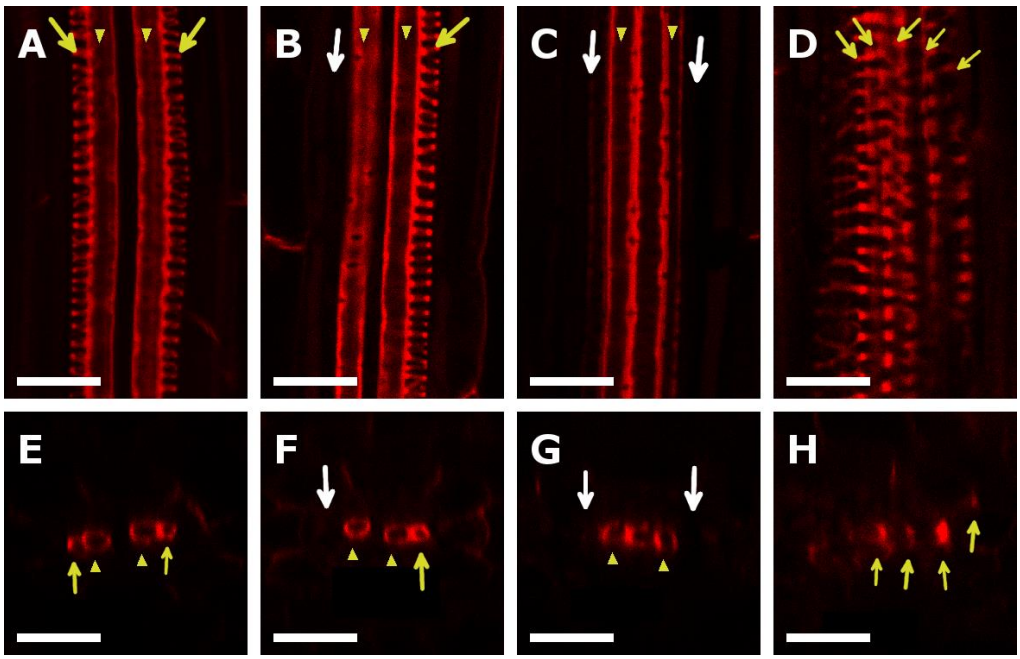


Figure 5.4. Longitudinal (A-D) and corresponding radial (E-H) confocal images of fuchsin stained roots, showing details of variations in protoxylem defects studied in mutant and complementation lines. Wild-type Col-0 (A and E) has two continuous protoxylem poles, *ahp6-1* mutants show breaks in protoxylem at one (B and F) or both (C and G) poles, and a small number plants of some complementation lines such as pAHP6::OsPHP3 (D and H) show areas with extra proliferation of protoxylem. The white dotted line in longitudinal images indicated location of radial imaging, yellow arrowheads indicate metaxylem, yellow arrows indicate protoxylem and white arrows where protoxylem would normally develop.

defects seen. Around 50 plants per independent transgenic line were analysed and scored based on the protoxylem phenotype as follows: 1 – two continuous protoxylem poles as is seen in wild-type plants; 2 – breaks in protoxylem at one pole; 3 – breaks in protoxylem at both poles; 4 – complete absence of protoxylem; 5 – extra proliferation of protoxylem. In this experiment, two independent *ahp6* mutant alleles were used; *ahp6-1* and *ahp6-2*. As these alleles phenocopy a T-DNA insert (*ahp6-3*), it is assumed that they represent null alleles. The *ahp6-1* mutant encodes a premature stop codon in the first exon, whereas the *ahp6-2* mutant has a substitution in the first intron, causing one of two splice variants to be expressed (Mähönen et al. 2006). Although the exact role of the different splice variants is not known, it has been shown that *ahp6-2* encodes a weaker allele, intermediate to wild-type and the strong *ahp6-1* and *ahp6-3* alleles. The *ahp6-2* mutant appears to be less severe than the *ahp6-1* mutant in terms of protoxylem phenotype (Figure 5.3). Whilst over half of individuals of *ahp6-1* have loss of protoxylem at both poles, in the *ahp6-2* mutant this number is reduced to 28 %, and a greater percentage of plants look wild-type or have loss of protoxylem in one pole in *ahp6-2* as compared to *ahp6-1* (Figure 5.5 and 5.6). Given the slightly weaker phenotype of *ahp6-2* plants, it seems this smaller protein is still functional, albeit less so than the other transcript.

All complementation lines were generated to express the coding sequence of proteins rather than the full genomic sequence, because the different genomic context of rice as compared to *Arabidopsis* may lead to improper expression and splicing of transcripts. By using the coding sequence, we can be sure that

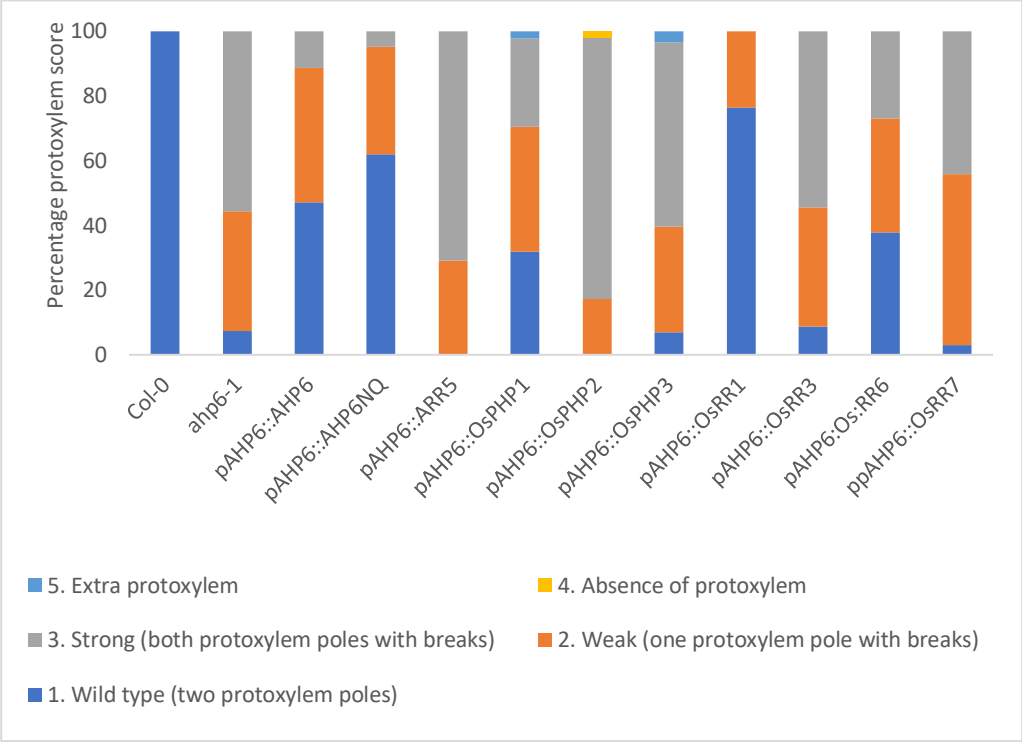


Figure 5.5. Expressing rice candidate genes under the AHP6 promoter in the *ahp6-1* mutant reveals only OsRR1 and OsRR6 partially rescue. Severity of protoxylem defects in trans-complementation lines was scored by screening whole roots and classifying them as indicated in the key. Expressing AHP6NQ partially rescues at similar levels as the pAHP6::AHP6 control, ARR5 increases severity of vascular defects, the OsPHPs do not rescue and possibly increase severity of vascular defects, and OsRR1 and OsRR6 partially rescue the *ahp6-1* phenotype.

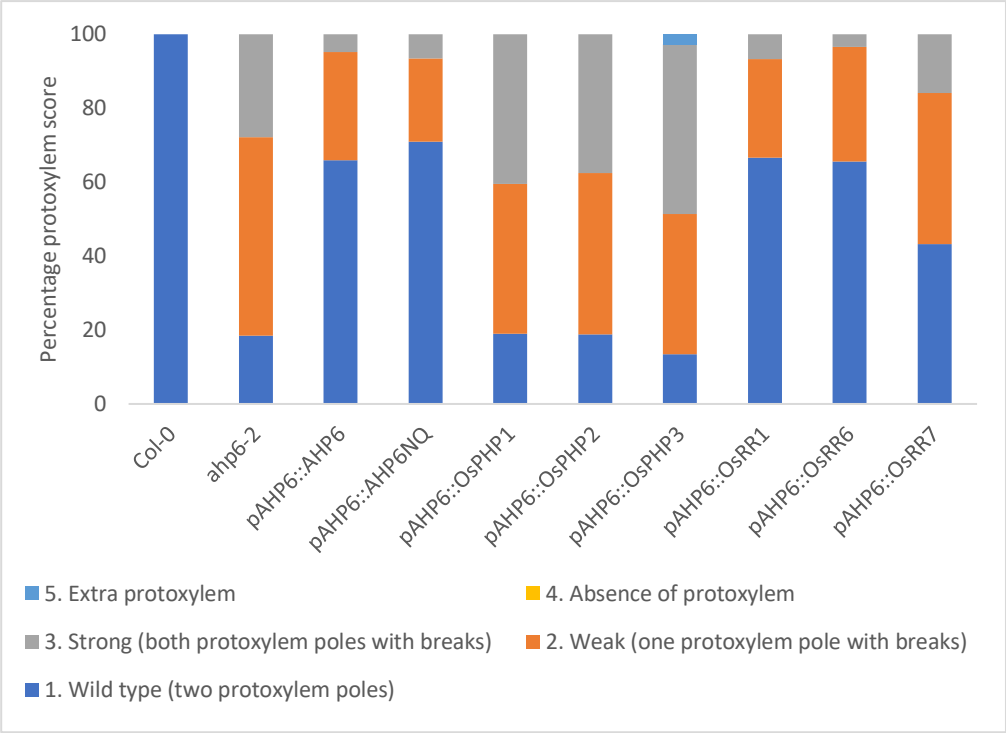


Figure 5.6. Expressing rice candidate genes under the AHP6 promoter in the *ahp6-2* mutant reveals OsRR1, OsRR6 and OsRR7 partially rescue. Severity of protoxylem defects in trans-complementation lines was scored by screening whole roots and classifying them as indicated in the key. Expressing AHP6NQ partially rescues at similar levels as the pAHP6::AHP6 control, the OsPHPs do not rescue, and OsRR1, OsRR6 and OsRR6 partially rescue the *ahp6-2* phenotype.

only the full protein should be expressed. The control of AHP6 CDS being driven under its native promoter was unable to fully complement the mutant protoxylem phenotype in either mutant allele, but multiple independent transgenic lines showed partial complementation. This is most likely because the coding sequence was used for complementation, as the genomic sequence has been previously shown to fully rescue the mutant phenotype (Mähönen et al. 2006). It may be the case that the introns contain crucial enhancer sequences which may influence expression levels, and a lack of these could be responsible for the failure of AHP6 to fully rescue.

Although expressing the coding sequence of AHP6 under its native promoter in the mutants does not fully rescue, there is clear partial rescue of the phenotype. In the *ahp6-1* mutant the percentage of plants with a wild type protoxylem phenotype increases from around 8 % to 47 % when AHP6 is expressed under its own promoter, and a similar trend is seen in the *ahp6-2* mutant (Figure 5.5 and 5.6). This indicates that the protein is functional and sets a baseline against which trans-complementation of other proteins can be compared. The mutant version of AHP6 with N83Q (which mimics the substitution seen at the HPT phosphoaccepting histidine domain of the OsPHPs and the other monocot PHPs) is also able to partially rescue the *ahp6* mutants at about the same levels as wild type AHP6 itself. This indicates the substitution still allows AHP6NQ to function as an inhibitor of cytokinin signalling with no apparent loss or gain of functionality. At the protein level, this means the substitution probably has little effect, if any, on the interaction of AHP6NQ with the cytokinin receptors and response regulators and consequently it seems

likely that AHP6NQ has a very similar conformation to wild type AHP6. Given the similarity of amino acid structure between asparagine and glutamine it may not be surprising that a substitution from one to the other would have little effect on protein conformation in this case. Whilst the partial complementation of AHP6NQ in both *ahp6* mutant backgrounds suggests the OsPHPs (which carry the same substitution) may also function in inhibition of cytokinin signalling, this does not answer whether they are able to function in place of AHP6 in the *Arabidopsis ahp6* mutants. To test this, I next looked at trans-complementation of the OsPHPs.

The trans-complementation results from the OsPHPs differ in the two different *ahp6* mutants and between the three OsPHPs. Expression of any of the three OsPHPs in the *ahp6-2* mutant doesn't seem to have much of an effect – the protoxylem defect scores are almost the same as that of the mutant, except that the percentage of plants with breaks in both poles as compared to one increases slightly. In the *ahp6-1* mutant however, there are a few more obvious differences. Although an admittedly small effect, it seems OsPHP1 may partially rescue the *ahp6-1* phenotype, and OsPHP2 appears to increase severity of the defect (including having few individuals with extra protoxylem on one pole) in a manner consistent across all independent transgenic lines (of which there were six). OsPHP3 on the other hand appears to make no difference whatsoever to the *ahp6-1* mutant phenotype. The reason expressing OsPHP1 and OsPHP2 in the *ahp6-2* mutant background makes little difference to the mutant phenotype, while bigger differences are seen in the *ahp6-1* allele, may be in part due to the *ahp6-2* mutant still expressing the shorter of two splice

variants of AHP6. It may be the case that this shorter version of AHP6 is still able to function and thereby prevent the more extreme phenotypes seen when OsPHP2 is expressed in the *ahp6-1* background. If the smaller splice variant of AHP6 being expressed in the *ahp6-2* mutant can act to dampen the effect of OsPHP2, this still does not explain why expressing OsPHP1 in the *ahp6-1* mutant appears to partially rescue (albeit negligibly), while in *ahp6-2* it does not. It may be the case that the three OsPHPs and AHP6 have different preferences for binding particular cytokinin receptors and particular RRs. In the *ahp6-2* mutant, perhaps the smaller variant of AHP6 which is expressed is able to overcome the effect of OsPHP1 by inhibiting transfer of the phosphate group to different response regulators than OsPHP1 alone. Similarly, this may also be the reason the opposite effect is observed with OsPHP2 (with a more severe phenotype in the *ahp6-1* mutant). In any case, what can be seen with certainty from these results is that AHP6N83Q complements better than any of the OsPHPs, in both *ahp6-1* and *ahp6-2* mutant backgrounds. This indicates that while substitution to a Q at the conserved phosphoaccepting H residue is enough to confer inhibition of cytokinin signalling, other mechanisms are required for functionality and specificity of these proteins in planta. These mechanisms likely involve differing specificities of protein-protein interactions between the OsPHPs and the *Arabidopsis* cytokinin receptors and RRs.

Whereas AHP6 and the OsPHPs function as competitive inhibitors, the type-A RRs may function by sequestering phosphate groups, by downstream protein-protein interactions which are dependent on phosphorylation status, or both. Consequently, this may influence their ability to rescue the *ahp6* mutants when

expression is driven by the AHP6 promoter. In order to test whether the type-A RRs of rice are functional if substituted in place of AHP6, OsRR1, OsRR3, OsRR6 and OsRR7 were screened for trans-complementation. Whereas there were great phenotypic differences seen in trans-complementation of the OsPHPs between the two *ahp6* mutant alleles, the type-A OsRRs showed more phenotypic uniformity in this respect. In the *ahp6-1* background OsRR3 and OsRR7 have no or negligible effect on protoxylem phenotype (with phenotypic variability amongst independent transgenic lines for OsRR7 in particular complicating analysis). OsRR6 partially complements and OsRR1 complements the *ahp6-1* mutant very well (with percentage of plants with a wild type phenotype increasing from around 8% in the mutant to around 76% with OsRR1). In the *ahp6-2* mutant background, OsRR7 partially complements, and OsRR1 and OsRR6 both complement well and at about the same level (with percentage of plants with a wild type phenotype increasing from around 19% in the *ahp6-2* mutant to around 66% with OsRR1 or OsRR6). This indicates that different types of cytokinin signalling inhibitors, with different mechanisms of action, can fulfil the function of AHP6. This also suggests OsRR1, OsRR6 and OsRR7 may, possibly redundantly, function in rice root vascular patterning via inhibition of cytokinin signalling. However, whereas some of the rice type-A RRs rescue the mutant phenotype, expressing *Arabidopsis* ARR5 increases severity of the protoxylem defect in *ahp6-1* mutants. While details of the mechanism of action of ARR5 are not fully understood, it has been shown that its function is dependent on protein-protein interactions associated with its phosphorylation

state (To et al. 2007). Understanding these details may be key to understand how the severe loss of protoxylem phenotype results.

From these complementation assays as a whole it seems clear that simply expressing any inhibitor of cytokinin signalling is not enough to rescue the mutant phenotype, although different types of inhibitor can bring about the same effect. However, the mechanism of action of the cytokinin signalling inhibitors needs to be considered to draw any reasonable conclusions about this assay. The PHPs (or at least AHP6) have been shown to function as inhibitors of cytokinin signalling through competitive inhibition, thereby preventing binding of HPTs to cytokinin receptors and response regulators. Type-A RRs on the other hand, have been shown to function via two different mechanisms. Given their similarity to type-B RRs but the lack of a DNA-binding domain, for many years it was assumed they functioned only by scavenging phosphate groups. However, they also function (at least in part) via downstream protein-protein interactions which are dependent on their phosphorylation status (and consequent conformation) (To et al. 2007). Given the large family of type-A RRs (10 in *Arabidopsis* and 13 in rice) it may be the case that not all of them function in this manner. Indeed, they may not all even be inhibitors of cytokinin signalling (the rice A-RRs in particular have not been well studied). This complicates interpretation of results of complementation. It cannot be assumed that the rice A-RRs will not bind other *Arabidopsis* proteins (outside of HPTs which will transfer a phosphate group to them). Even if this seems unlikely, given the different systems, we cannot know for sure until more detailed studies are done on each A-RR. The different context they are

expressed in in these assays may mean the genes from rice are not functioning as they would in rice. With this in mind, it might be the case (although this may be unlikely) that results of complementation of the *Arabidopsis ahp6* mutants could be misleading. However, taken together with other data (such as their auxin inducibility in the rice root tip) it seems clear that OsRR1, OsRR6 and OsRR7 are good candidate genes which may well function (possibly with a degree of redundancy) in an AHP6-like manner to specify protoxylem development in rice roots.

5.3 In vitro analysis of OsPHP function: Phosphotransfer assays

As well as getting insight into candidate gene function using in planta complementation assays, it is also useful to look at in-vitro interactions. In particular, this will be useful to directly determine whether the OsPHPs do inhibit cytokinin signalling and also allow us to draw conclusions about their mechanism of action (since no other proteins are present, if they do inhibit transfer of the phosphate group we can be sure that it is via competitive inhibition – although this does not suggest this will be their only mechanism of action). If they are shown to inhibit cytokinin signalling, these assays can be used to show if cytokinin signalling capability is restored upon restoring the phosphoaccepting H of the OsPHPs, as has been demonstrated in AHP6 (Mähönen et al. 2006). This will show whether changing this single amino acid residue is enough to enable changing the OsPHPs from a negative to a positive regulator of cytokinin signalling. The potential for a single substitution of the

conserved phosphoaccepting H residue of the HPTs to change a protein from a positive to a negative regulator of cytokinin signalling can also be demonstrated by making substitutions in the OsAHPs. In addition, these assays will be useful to determine the effect of having an N or a Q substitution at this residue. It may be the case that the presence of either an N or a Q residue at the conserved phosphoaccepting H could influence intensity of inhibition of cytokinin signalling, although from the trans-complementation assays this appears not to be the case for AHP6 in planta. This could be nicely demonstrated by creating mutant versions of OsAHPs with the phosphoaccepting H substituted for N or Q, and looking at how these can inhibit phosphate transfer through the cytokinin signalling circuitry.

These assays require purification of many different proteins; cytokinin receptors, the OsPHPs, OsHPTs and the various mutant versions of each, and a response regulator as a final receiver of the phosphate group. To achieve this, various expression and purifications systems were used, with proteins being tagged with either GST or MBP and being expressed in bacterial or insect cells. The reason different systems were used was because previous work had indicated expression and purification conditions were more favourable for different proteins in different systems (Mähönen et al. 2006). In these assays, the yeast cytokinin receptor SLN1 was used as a phosphate group donor in place of *Arabidopsis* or rice cytokinin receptors, due to plant cytokinin receptors being difficult to express and purify (Professor Tatsuo Kakimoto, Osaka University, personal communications). Exact details of cloning, expression and purification procedures used are listed in Materials and

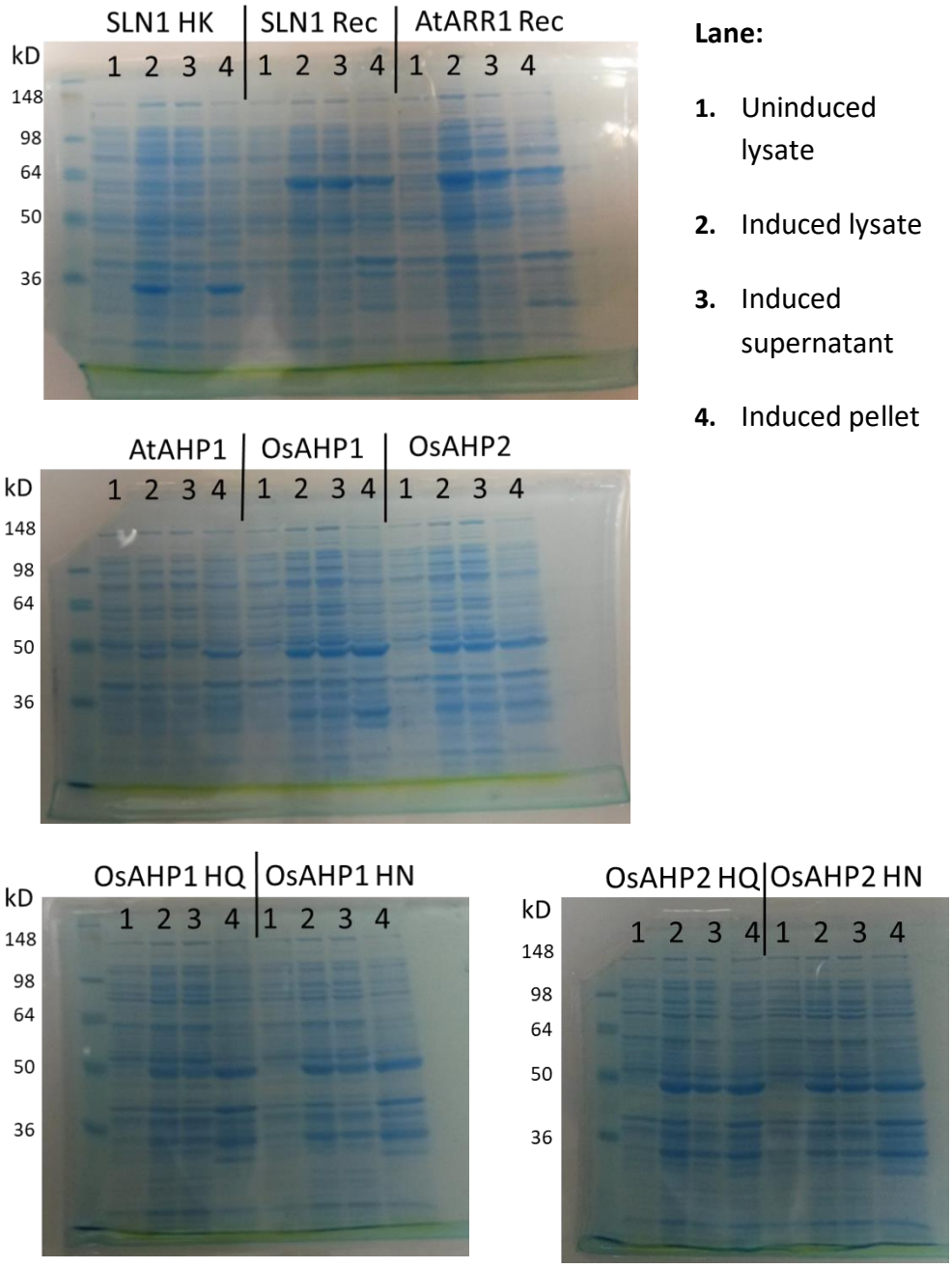
Methods. The following sections describe the basic principles of expressing and purifying proteins in the different systems, and any optimisations which were required and troubleshooting which was carried out.

5.4 Bacterial protein expression and purification

Expression of protein in bacteria is a relatively simple process consisting of transforming bacteria with the cloned expression vector, growing transformed bacteria in liquid culture, and inducing expression with IPTG. Once plasmids were transformed into the bacterial strain used for expression and purification (Origami 2(DE3)pLysS), preliminary experiments were conducted to check for successful induction of protein expression and appropriate localisation of protein in the soluble fraction. This was done for each construct by growing 5 ml cultures, inducing expression and after growth for a further 2 hours harvesting cells. For each culture, 0.5 ml of cells before induction were taken as a control. Once induced cells were harvested, they were lysed by sonication and centrifuged to separate supernatant from the cell pellet. At each stage, a small volume was taken and kept to end up with separate fractions from uninduced lysate as a control (which was lysed by sonication separately), induced lysate, induced supernatant and induced pellet. After performing a protein assay on each of these fractions to determine protein concentration, an equal mass of each fraction was run on an SDS PAGE gel, which was then stained for protein using Instant Blue.

For most constructs good induction of expression could be observed (Figure 5.7). By comparing band intensities from supernatant and pellet it was estimated that for most constructs about 50 % of protein is in the soluble fraction as compared to the insoluble cell pellet (with considerably less in the soluble fraction in AtAHP1). To improve this ratio, the experiment was repeated with cells being grown at 23 ˚C rather than 37 ˚C (not shown). This improved the ratio of protein seen in the soluble fraction as compared to the insoluble fraction, and consequently when cultures were scaled up for purification all cultures were grown at 23 ˚C. For SLN1-HK, induced protein was seen in the induced lysate and pellet, but this protein was under 36 kD. The SLN1-HK protein with the MBP tag used should be 89.3 kD, and no induction of a protein this weight could be seen. After sequencing the plasmid to double check the construct was correct, it was discovered that induced expression of this 34 kD protein was due to a stop codon within the MBP tag sequence. SLN1-HK was consequently amplified and cloned into another vector which would enable its correct expression as an MBP fusion.

For purification, cultures were scaled up to 500 ml, grown at 23 ˚C and purified following protocols described in materials and methods. With the exception of SLN1-HK and AtAHP1, all proteins were isolated with appropriate purity and concentration (Figure 5.8). For SLN1-HK a band at the correct weight is seen but is very dilute. Although dilute, it was expected that this protein would still be functional in the assays. However, this proved not to be the case, and



Lane:

1. Uninduced lysate
2. Induced lysate
3. Induced supernatant
4. Induced pellet

Figure 5.7. Preliminary expression experiments showed successful expression of all proteins, with the exception of SLN1-HK. Fractions were taken to determine protein localisation in induced lysate (lane 2), induced supernatant (lane 3), and induced pellet (lane 4) as compared to the uninduced lysate control (lane 1). All expressed proteins were present in good abundance in the soluble fraction, with the exception of AtAHP1 which was only present in the insoluble fractions. Protein gels were stained with InstantBlue protein stain (Expedeon Protein Solutions).

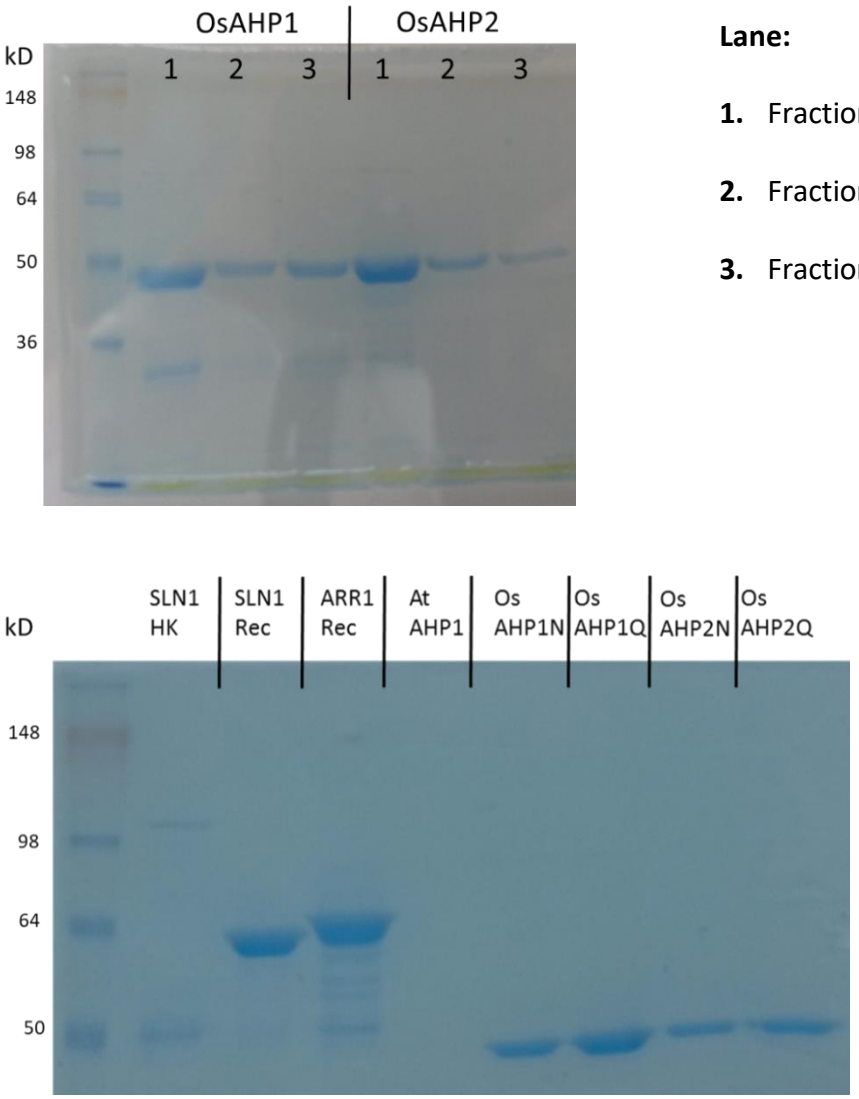


Figure 5.8. Purification of proteins expressed in bacteria showed suitable concentrations, with the exception of the corrected version of SLN1-HK which was very dilute, and AtAHP1 which was too dilute to be seen on the protein gel. OsAHP1 and OsAHP2 were initially purified in three separate fractions to determine how many washes would be suitable to elute most protein from beads, and subsequent purifications were carried out using three washes. Protein gels were stained with InstantBlue protein stain (Expedeon Protein Solutions).

troubleshooting of this is described in the section troubleshooting SLN1-HK (pg 175). For AtAHP1, no protein is seen and this is possibly due to accumulation of this protein in the insoluble fraction. Because this protein was required as an *Arabidopsis* control, it is not essential for assays and due to difficulty in purification it was not pursued.

5.5 Insect cell protein expression and purification

Expression of protein in insect cells is a slightly more complicated process, as it makes use of a recombinant baculovirus to infect cells and promote protein production. To generate these recombinant baculoviruses, pFastBac plasmids containing the CDS of the protein to be expressed are transformed into the *E. coli* strain DH10Bac. This strain contains a helper plasmid which enables transposition of the pFastBac expression construct into a baculovirus shuttle vector (or bacmid) which, after confirmation of correct transposition, can then be isolated. Isolated recombinant bacmid can then be used to infect insect cells, which consequently produce recombinant baculovirus (P1) which can be used to infect other stocks of insect cells for protein expression. This is done in duplicate for each construct to ensure at least one is successful. Recombinant baculovirus can be amplified to produce a high-titer stock (P2 or P3) which may be preferable for expression, through successive infection and isolation of baculovirus from insect cell culture. Alternatively, stocks of baculovirus infected insect cells (BIIC stocks) can be prepared and used directly to infect new insect

cell cultures for expression and purification and this is what was done in this case.

It is important to check for correct expression of protein in insect cells at the earliest availability. This can be done in cells infected with recombinant bacmid, from which the initial P1 baculovirus is isolated (provided appropriate timing of harvesting cells before they lyse due to baculovirus production). Because recombinant baculovirus is released into the media while insect cells adhere to the bottom of the container, the P1 baculovirus is easily collected by removing media without disturbing insect cells. The insect cells can be resuspended, lysed, and lysate run by PAGE and a Western blot performed to check for expression of the correct protein. Good levels of expression were seen (both by Western as well as being visible from a PAGE gel stained with Instant Blue) for all OsPHPs and mutants from these initial bacmid infected cells (Figure 5.9). When scaling up cultures for infection with BIIC stocks, initial experiments to determine the time of optimal protein expression were carried out. Cultures were infected with appropriate BIIC stock, and at time points of 0, 26, 44, 52 and 77 hours after infection aliquots of cells were taken. From these samples PAGE gels and Western blots were run. This showed a suitable amount of protein (visible even in the PAGE gel stained with Instant Blue) after 77 hours and consequently this was the time point of harvesting cells in scaled up cultures for purification. For AHP6 and the two mutant versions (AHP6Q and AHP6H), time course experiments were only carried out 0 and 72 hours after infection with BIIC stock infection, with induction of protein expression visible clearly in the PAGE gel (Figure 5.9 D). For this reason, a Western blot from a

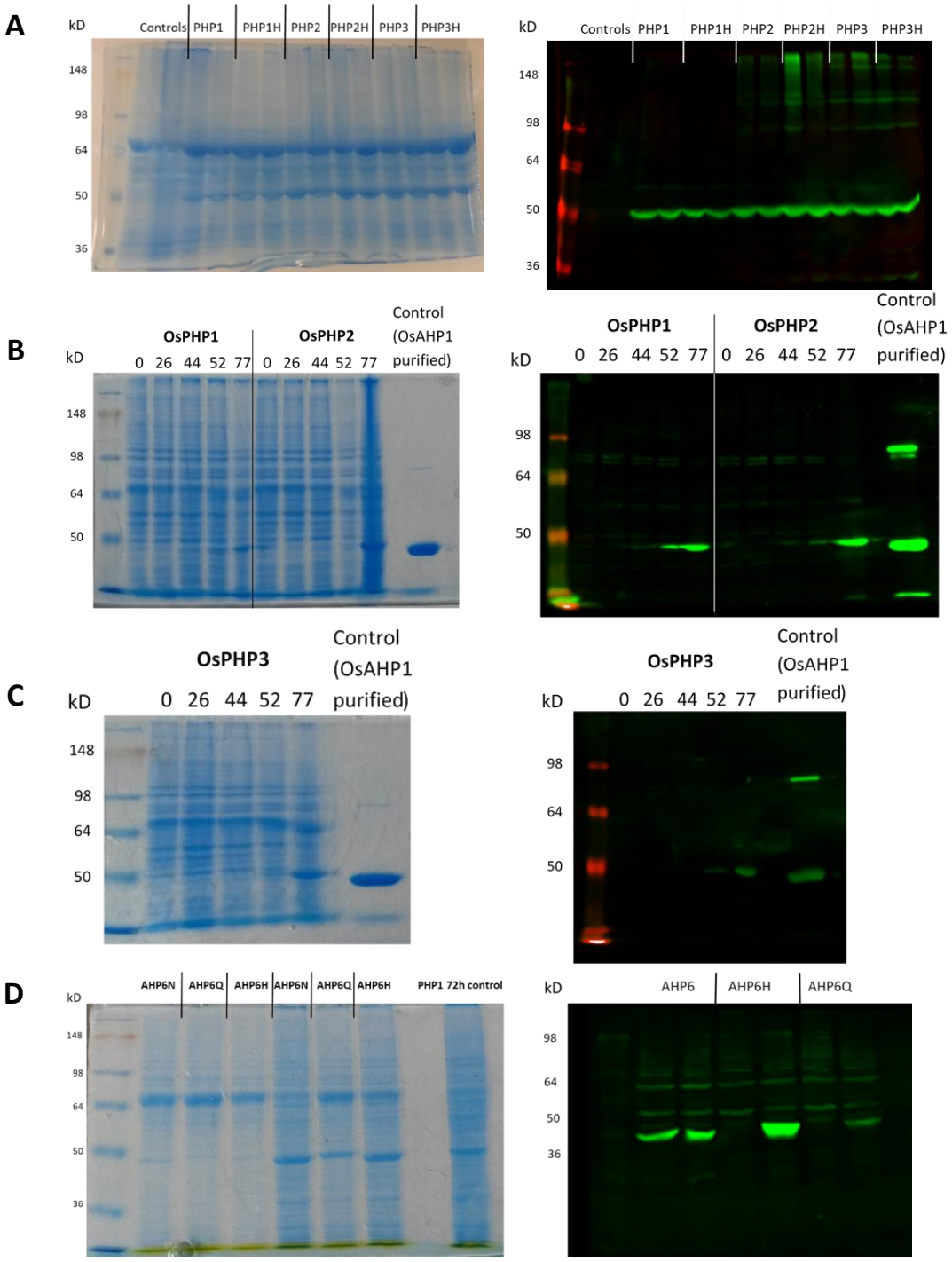


Figure 5.9. Protein gels and corresponding Western blots showing expression of OsPHPs, AHP6 and mutant versions of these proteins indicate suitable expression levels for purification. Initially protein gels and Western blots were run using cell lysate from which P1 virus was harvested, for the OsPHP and mutants (A) and AHP6 and mutants (D). Once BIIC stocks were prepared, to determine the optimal time point of highest protein production after BIIC infection, aliquots were taken at time points of 0, 26, 44, 52 and 72 hours after infections and protein gels and Westen blotting performed for the OsPHPs and mutants (B and C).

time course was not required to be carried out. Details of purification protocols after BIIC stock infected insect cell cultures were harvested are shown in the Materials and Methods section.

5.6 SLN1 kinase domain troubleshooting

As previously mentioned, the initial SLN1-HK plasmid was found to have a stop codon in the MBP tag, seen in the protein gels as induction of a small ~34 kD protein. Once this was corrected, SLN1-HK could be successfully purified, but only with very low concentrations. When initial phosphotransfer labelling experiments were carried out, no signal was seen in any reaction including the control of SLN1-HK as a single protein incubated with ^{32}P ATP. Because phosphorylation and consequent signal would be expected to be seen, even if the protein was dilute, it was determined that the SLN1-HK protein is not functional. Initially it was assumed this may be due to inappropriate reaction conditions but after trying a number of different protocols with no success, it was determined there was something wrong with the protein itself. In order to overcome this, SLN1-HK-Rec and SLN1-HK plasmids in a different expression vector and with a different tag (GST rather than MBP) were obtained from the lab of Ann West (the University of Oklahoma). A similar purification protocol was used (but without eluting protein), which yielded good protein concentrations, and protein identity was confirmed by Western blot (Figure 5.10 A). One major difference which effected experimental design of the

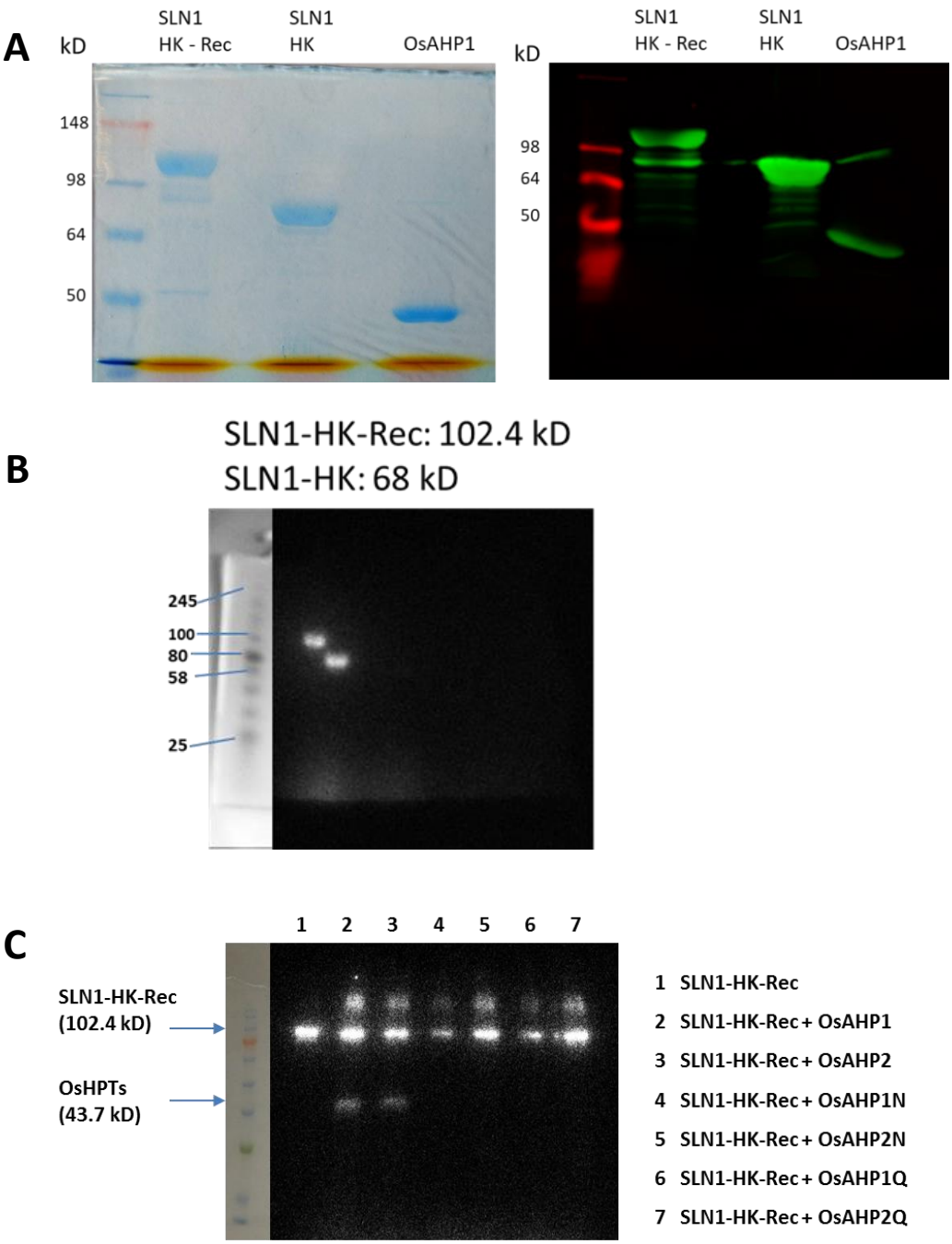


Figure 5.10. Glutathione sepharose bead-bound SLN1-HK and SLN1-HK-Rec is functional in preliminary phosphotransfer assays. Purification of bead bound SLN1-HK and SLN1-HK-Rec was confirmed by running protein gels and performing Western blotting (A). Initial phosphotransfer experiments indicated the bead-bound receptors are able to autophosphorylate (B) and pass the phosphate group onto OsAHP1 and OsAHP2 but not mutant versions of these proteins which lack the conserved phosphoaccepting H domain (C).

following phosphotransfer assays was that these kinase proteins remain bound to the glutathione sepharose 4B beads which were used to purify them.

5.7 Preliminary results of phosphotransfer experiments

Due to time constraints and initial difficulty in producing repeatable results for some reactions, few of the intended reactions were carried out. Initial preliminary labelling experiments of SLN1-HK-Rec and SLN1-HK (obtained from Ann West) with ^{32}-P shows they are able to accept the phosphate group (Figure 5.10 B), and consequently they were successfully used in phosphotransfer reactions. Initially the SLN1-HK-Rec full protein was tested to determine if it could pass on the phosphate group to the two OsHPTs and mutant versions of these proteins (with substitutions of the phosphoaccepting histidine residue to a Q or an N residue). This showed OsAHP1 and OsAHP2 are able to accept the phosphate group, whereas when the phosphoaccepting histidine residue of these two proteins is substituted for either an asparagine or a glutamine residue, they can no longer accept the phosphate group (Figure 5.10 C). Whilst these preliminary results do not directly show inhibition of cytokinin signalling by the mutant version of the OsHPTs, it seems likely that this will be the case.

Furthermore, through the results reported within this chapter, I have optimised protocols for purifying yeast, *Arabidopsis* and rice TCS components, enabling such assays to be completed in the future.

5.8 Discussion

The data presented in this chapter gives an idea of the functionality of the genes identified in Chapter 4. Data from the trans-complementation assays indicate that expressing different types of cytokinin signalling inhibitor (with different mechanisms of action) are able to function and consequently rescue the mutant phenotype. However, not every inhibitor of cytokinin signalling is capable of this. Whilst the AHP6NQ substitution appears not to affect protein function at all, the OsPHPs are not functional as inhibitors of cytokinin signalling in this context. As discussed, it may be the case that this is due to differing specificity of AHP6 as compared to the OsPHPs for binding the *Arabidopsis* cytokinin receptors and RRs. Specificity between OsPHPs and the *Arabidopsis* cytokinin signalling components may be important, but it would be expected that specificity of the type-A OsRRs for binding AtHPTs would also be important. For the type-A OsRRs to function as inhibitors in this context, they must be able to bind and accept a phosphate group from the AtHPTs. The trans-complementation assays indicate that OsRR1, OsRR6 and OsRR7 are able to function as cytokinin signalling inhibitors in this context. The mechanism of action of these proteins remains unknown (they may simply sequester phosphate groups but the possibility remains that they bring about their response due to downstream protein-protein interactions dependent on their phosphorylation state). However, the fact that these proteins, as cytokinin signalling inhibitors which are inducible by auxin in the root tip, can function in this manner, indicates that they may play a role in rice root vascular patterning. This assay cannot imply that the OsPHPs do not function in vascular patterning

in the rice root, because they are being expressed in a very different context. However, together with data from Chapter 4, it seems this may be the case. These assays also make the assumption that the OsPHPs function in cytokinin signalling, yet this has never been directly shown. Data from the phosphotransfer assays implies this is the case, but more work needs to be done using this system to confirm this. In the next chapter I describe characterisation of these genes in rice through the use of reporters and mutants.

5.9 Summary

- OsPHPs are unable to rescue the *Arabidopsis ahp6* mutant loss of protoxylem phenotype, but the type-A RRs OsRR1, OsRR6 and OsRR7 are able to (at least partially) rescue.

- Protein expression and purification was optimised using bacterial and insect cell expression systems.

- Preliminary results from phosphotransfer assays indicate that the wild-type OsHPTs are able to accept phosphate groups from SLN1-HK-Rec, whereas mutant versions of these proteins (with the conserved phosphoaccepting histidine substituted to an asparagine or glutamine residue) are unable to accept phosphate groups.

Chapter 6. Reporters and CRISPR constructs

6.1 Introduction

In order to gain a detailed understanding of how candidate genes function, looking at expression patterns and mutant phenotypes is key. One of the major reasons *Arabidopsis* makes a good model organism is the ease with which it can be transformed, through use of the floral dip method. In rice, the most common transformation method proceeds through *Agrobacterium* infection of callus in tissue culture, which is a more challenging and time consuming process. However, the huge popularity of rice in research (primarily driven by its importance as a major food crop) has enabled great improvements in transformation efficiency and consequently many more resources for molecular studies. More recently, the development of CRISPR as a targeted genome editing tool has enabled the production of mutants in single genes in a number of plant species, with many examples in rice.

Previous gene editing technology (such as T-DNA inserts, EMS mutagenesis and screening, ZFN and TALENs) has successfully been used in research for many years, but these methods are time consuming and difficult to implement. Insertion of Transfer-DNA (T-DNA) into the genome can interrupt gene sequences and cause mutation (Sessions et al. 2002; Alonso et al. 2003). However, since this is a random process it may not be possible to easily mutate genes of interest. In addition, T-DNA inserts may affect function of neighbouring genes, further complicating mutant analysis. Treatment of seeds

with the chemical mutagen ethyl methanesulfonate (EMS) leads to the creation of point mutations throughout the genome (Qu & Qin 2014; Kim et al. 2006). Target genes can be screened to identify these mutations (for example by detection of heteroduplex DNA in PCR product, which forms as a result of mis-matching DNA). However, this process is time consuming and leads to the creation of many mutations in the genome, not specifically in the target gene. The Zinc Finger Nucleases (ZFNs) were the first engineered nucleases which allow specific binding to target sites (reviewed by Petolino 2015). These proteins consist of DNA binding domains (the Zinc Fingers) and the FokI endonuclease, which creates double strand breaks in the DNA, which are frequently incorrectly repaired by DNA repair mechanisms creating mutations. FokI is only functional as a dimer, and consequently ZFNs must be designed to bring two FokI monomers together in the correct orientation. While this system greatly improved specificity of mutation, it also proved very difficult to design ZFNs to recognise new target sequences. The TALE nucleases (TALENs), however, are much more easily engineered to recognise new target sequences. This group of engineered nuclease also uses FokI to create double strand breaks in DNA, but instead of using Zinc Fingers, target specificity is brought about by use of the recognition repeats of Transcription Activator-Like effectors (TALEs) (Forner et al. 2015). These are proteins secreted by *Xanthomonas* which are able to manipulate host plant gene expression to aid bacterial infection. DNA binding specificity is brought about by repeat units of around 34 amino acids, within which only two amino acid residues bind one DNA base. These two

amino acids in the various repeats can be engineered to recognise almost any DNA sequence.

CRISPR enables much easier targeting of specific genes without the need for complicated protein design. There is now a huge body of resources available to aid design of CRISPR constructs, predict off-target effects, and optimise all stages of the experimental design to the particular organism being studied. Combined with traditional molecular biology experimental techniques (such as the use of GUS staining for determining expression patterns), newer techniques such as CRISPR and improved transformation techniques enable a deeper understanding of the function of particular genes in rice.

In this chapter I examine the expression patterns of the genes previously discussed, the process used to design and construct CRISPR plasmids and details of the resulting mutants. This data adds to our understanding of the function of these genes in rice root vascular development and also indicates developmental processes they may be involved in in other tissues.

6.2 Expression patterns of candidate genes

In order to fully understand the function of the candidate genes, knowing their domains of expression is important. As an inhibitor of cytokinin signalling, AHP6 is expressed specifically in protoxylem poles very close to the root tip. This has been shown both through the use of reporters, and more directly by RNA in-situ hybridisation (Mähönen et al. 2006). Expression of AHP6 specifically in this region is essential for its developmental role in protoxylem specification,

through inhibition of cytokinin signalling. The trans-complementation assays discussed in Chapter 5 show that some of the candidate type-A RRs of rice are able to rescue the *Arabidopsis ahp6-1* and *ahp6-2* mutant phenotype when driven by the AHP6 promoter. This indicates that they are able to act as inhibitors of cytokinin signalling even in this very different context. It may be the case that some, or many, of the rice type-A RRs function in an AHP6-like manner in rice roots, and if they are expressed in rice root protoxylem this lends evidence to this theory. It is also of value to consider the expression patterns of the three OsPHPs. Although qRT-PCR data suggest that they are not expressed (or are expressed at very low levels) in the root tip, it may well be the case that they play roles in other developmental contexts, as does AHP6 itself. Indeed, the same is true of the type-A RRs of rice, and consequently it is of value to look at expression patterns in tissues other than only roots.

In addition to studying expression patterns of candidate genes in a number of tissues, reporters can also be used to confirm results obtained by qRT-PCR. Although perhaps less precise than qRT-PCR (which is dependent on detection of RNA abundance and therefore is easily quantifiable) the use of reporters can not only indicate up or down regulation of genes of interest upon certain treatments, but also whether these changes occur in certain tissues only. So long as appropriate controls are used, up or down regulation of gene expression can be easily visualised. While fluorescent reporters have successfully been used in rice when combined with sectioning and confocal microscopy (for example the DR5-GFP reporter discussed in Chapter 3), for the purposes of looking at gene expression in whole tissues other methods are favourable. For

this reason, all reporter constructs were designed as promoter-GUS fusions. In this system, GUS protein expression is driven by the promoter of the gene of interest, and can be visualised by supplying the substrate X-gluc which GUS converts to a blue coloured compound (chloro-bromo indigo). One issue with this method is that the GUS protein itself, which functions as a tetramer, takes a long time to fold (Matsuura et al. 2011). This is not a problem for looking at native expression, but for looking at induction or repression of gene expression upon certain treatments it means that the treatments themselves need to be long enough to allow the protein to fold. For this reason, all hormone treatments discussed were carried out for four hours. This means that the small time sensitive changes indicated by qRT-PCRs are not observable when using the GUS reporter system. However, taken together, data from reporters and qRT-PCR make a powerful tool to understand the details of candidate gene expression.

In these sections, the expression patterns of candidate genes is discussed in detail. Due to limited transgenic seed and time, hormonal treatment of some reporter roots (OsPHP2 and OsPHP3) was conducted only on crown roots and without an untreated control. Ideally these analyses will be repeated to confirm the results. Initially, primary roots of plants grown on plates were GUS stained, and the same plants were then transferred to hydroponics where they eventually developed crown roots which were tested for induction by hormones. As well as changing root types the method of growth was also changed, both of which may affect expression patterns seen. This means that the expression patterns from primary roots and crown roots with auxin or

cytokinin treatment are not directly comparable, despite performing staining for the same amount of time. However, individually the data from the reporters is still useful, and expression patterns in crown roots treated with auxin or cytokinin can be compared. These experiments should be repeated to validate whether the patterns seen in crown roots upon hormonal treatment is also true in primary roots. In addition, only one concentration of BA (5 µm) and IAA (10 µm) was used for the treatments. These correspond to the higher concentrations used in the qRT-PCRs carried out (Chapter 4). However, in future it may be useful to check a range of concentrations. Expression patterns in lateral roots were only checked upon hormonal treatments because these were emerging from the crown roots tested.

6.3 OsPHP1 expression patterns

Data from qRT-PCRs suggest low levels of expression of all three OsPHPs in the root tip, with OsPHP3 in particular being so difficult to amplify from root cDNA that it was left out. OsPHP1 and OsPHP2 also show a great deal of variability between the biological replicates such that no significant differences in expression, either between different sections of root tip or between different treatments, can be seen. This is in agreement with data obtained from the RiceXPro microarray database and what is published in the literature. However, the reporters indicate that there is expression of the OsPHPs in the root.

In whole mounts of primary roots, OsPHP1 expression is seen starting around 600 µm from the root tip and extends up the entire root (Figure 6.1 A and B).

OsPHP1

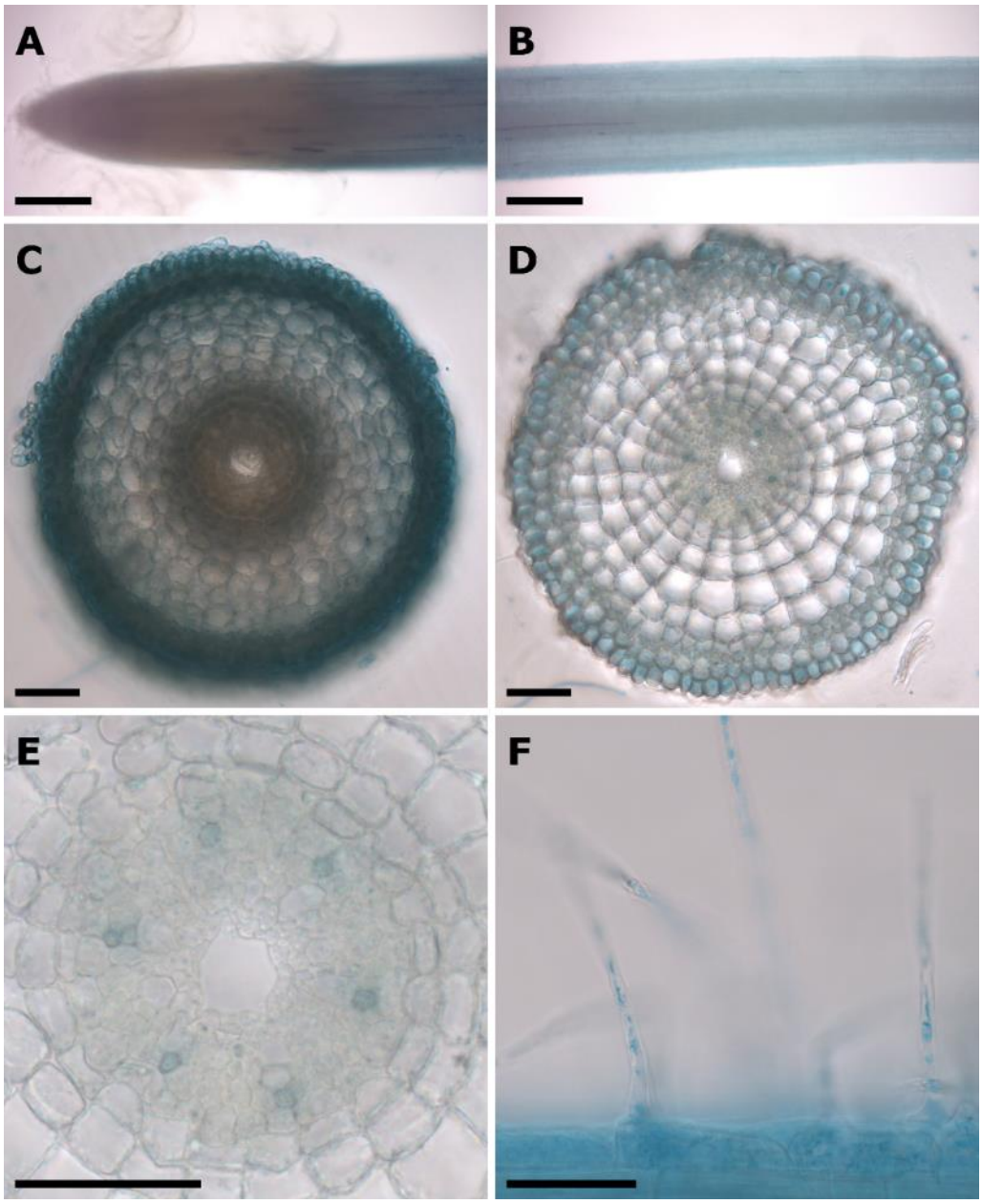


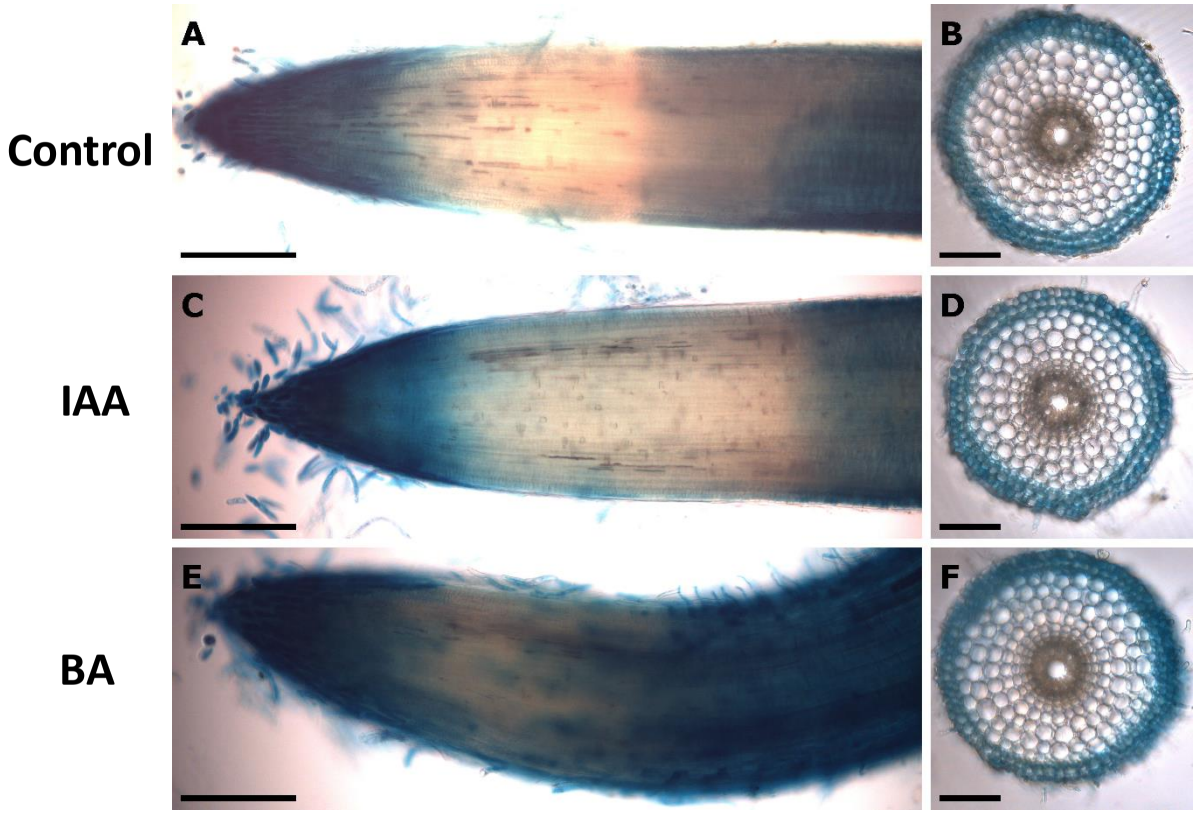
Figure 6.1. Histochemical localisation of GUS activity driven by the OsPHP1 promoter. Whole mounts show longitudinal expression patterns at the primary root tip (A) and further up the root (B). Radial sections were taken near the root tip (C) and further up the root (D) with greater magnification indicating protoxylem expression (E). GUS activity was also observed in epidermal cells and root hairs (F). Scale bars in A and B are 200 µm, C to F are 50 µm.

Taking radial sections of stained primary roots revealed that close to the root tip expression is confined to the 'outer tissues' of the sclerenchyma, exodermis and epidermis (Figure 6.1 C). In more mature sections further from the root tip, expression is strongest in the epidermis and is also seen in protoxylem poles (Figure 6.1 D and E). From looking at details of epidermal cells it can be seen that GUS activity extends into root hairs (Figure 6.1 F). While it is surprising that there is expression of OsPHP1 in the root whereas qRT-PCRs were inconclusive in this respect, it may be the case that the domain of expression was missed by focussing on the root tip. Alternatively, it may be the case that there are low levels of expression in the root, and expression indicated from reporters is due to overstaining of tissues (although this seems unlikely given the speed with which staining was observed).

Repeats of GUS staining in primary roots revealed that upon hormonal treatments, expression is seen in very similar patterns with no obvious expression changes. However, expression patterns differed slightly from initial staining, with clear expression in the root tip (Figure 6.2).

These results – expression of OsPHP1 in the root tip – contradict what was shown from the qRT-PCRs. There are a number of reasons this may be the case. The contradiction of these results could be explained by problems in either the qRT-PCRs or in the reporter. In order to understand whether there is a problem with the reporter, OsPHP1::GUS plants crown root tips were harvested after auxin, cytokinin, or a control treatment for 2 hours and qRT-PCR performed to detect expression of OsPHP1 and GUS (Figure 6.3). If these reporters are

Figure 6.2. GUS activity showing OsPHP1 expression in primary root tips (A, C and E) and in radial sections (B, D and F). Roots were treated with 5 µm BA (E and F) or 10 µm IAA (C and D) alongside the DMSO treated control (A and B) for 4 hours prior to staining. Scale bars are 200 µm.



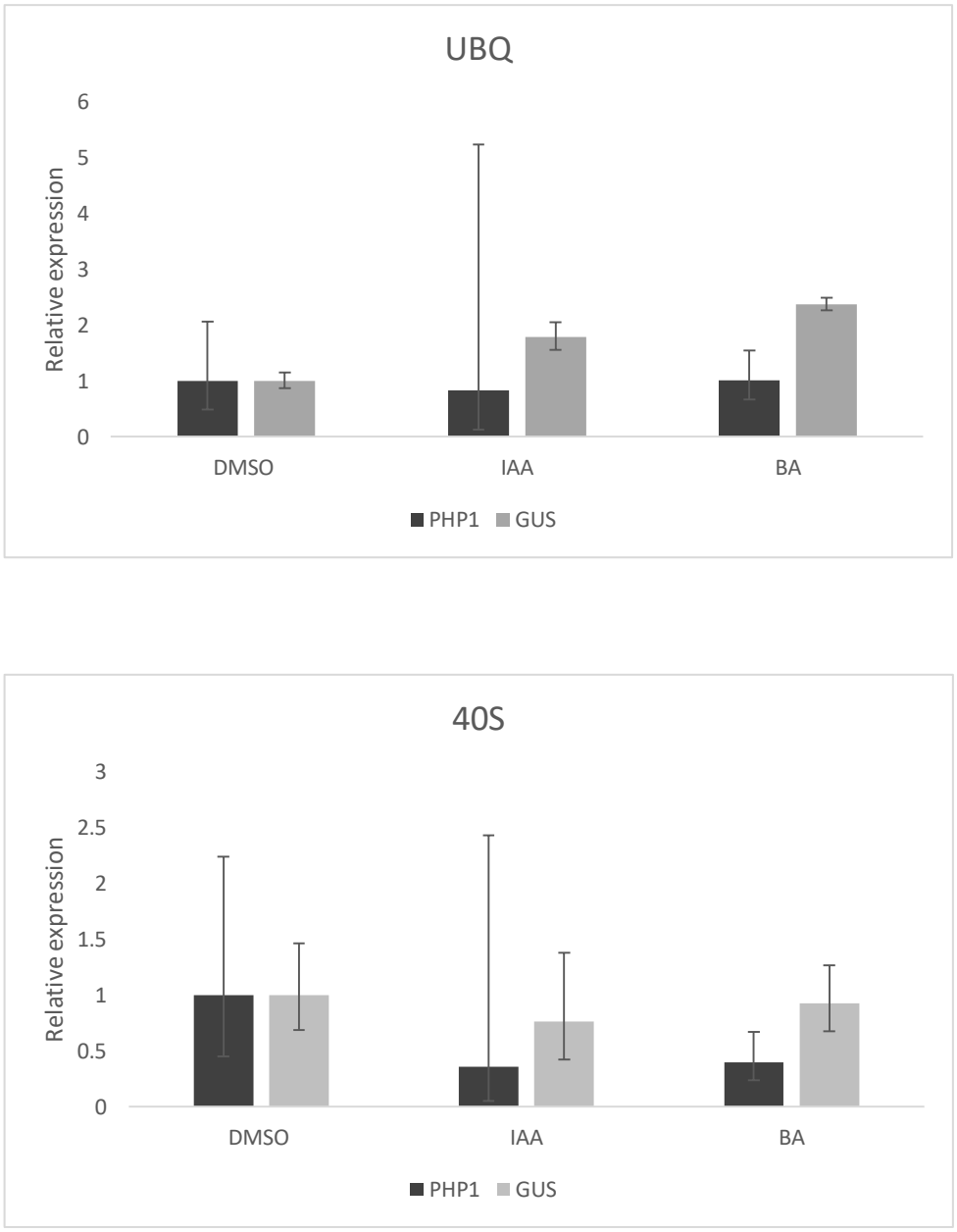


Figure 6.3. qRT-PCRs to determine expression of PHP1 and GUS in the roots of the PHP1 reporter upon treatment with 10 µM IAA or 5 µM BA. Error bars show standard error from four technical replicates.

correct, it would be expected that as GUS expression increases upon auxin treatment (assuming auxin inducibility of OsPHP1), OsPHP1 expression would increase by a similar amount also. While qRT-PCRs suggest expression of GUS may increase slightly more than expression of OsPHP1 upon auxin and cytokinin treatment, the differences are not significant due to large error within OsPHP1 relative expression. This suggests that the OsPHP1 primers perform less well than the GUS primers. Therefore, the expression data displayed in Chapter 4 for OsPHPs upon auxin and cytokinin treatment should be repeated using new primers.

In leaves, OsPHP1 expression appears to be quite patchy, although it appears to be most highly expressed in the region surrounding the central vein (Figure 6.4).

6.4 OsPHP2 expression patterns

The expression patterns for OsPHP2 seem to be similar to those of OsPHP1, except that OsPHP2 is much more strongly expressed throughout the whole root, including the root tip (Figure 6.5 A and B). Close to the root tip expression is confined to the epidermis (Figure 6.5 C) whereas in more mature radial sections expression is seen in many tissues, with greatest intensity in epidermis, endodermis, pericycle and possibly in protoxylem poles (Figure 6.5 D and E). It may be the case that the radial sections displayed are slightly overstained, leading to difficulty in interpreting which exact tissue type highest levels of

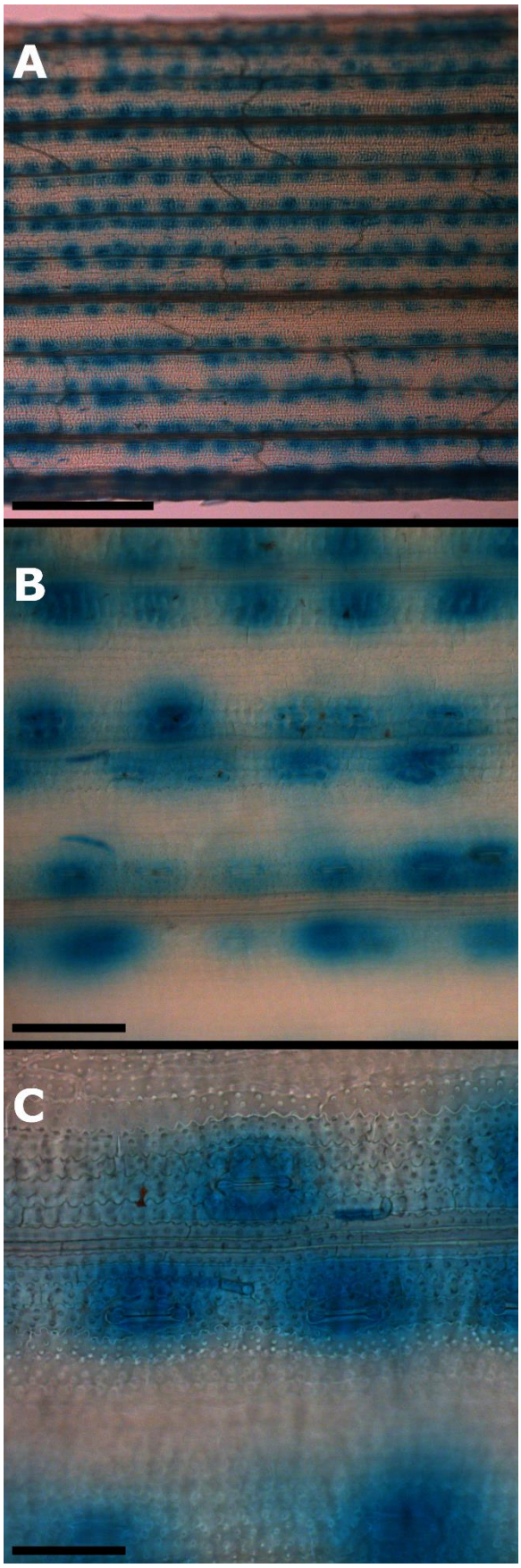


Figure 6.4. GUS activity showing OsPHP1 expression in leaves. Scale bars are 500 µm in A, 100 µm in B and 50 µm in C.

OsPHP2

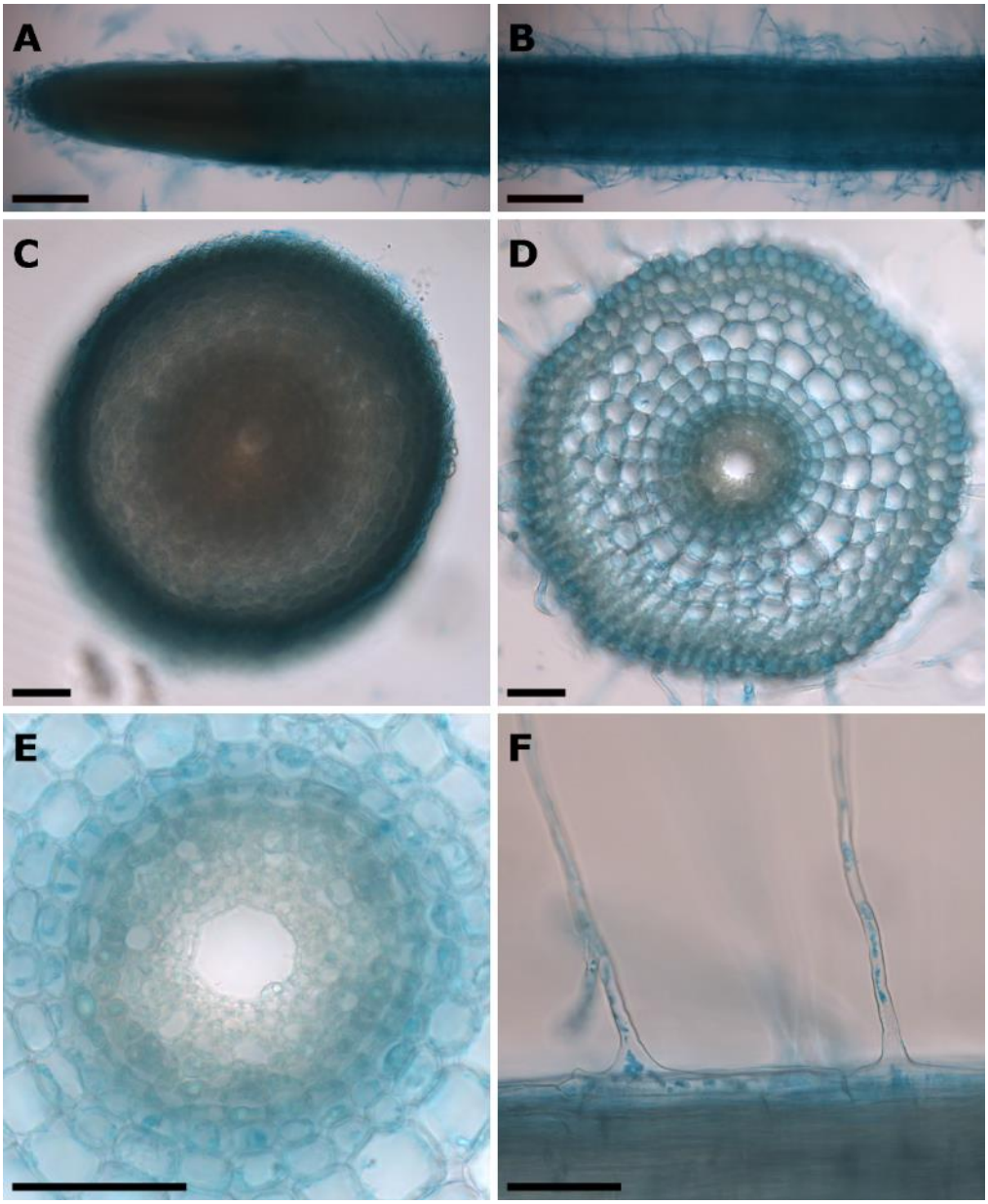


Figure 6.5. Histochemical localisation of GUS activity driven by the OsPHP2 promoter. Whole mounts show expression at the primary root tip (A) and further up the root (B). Radial sections were taken near the root tip (C) and further up the root (D) with greater magnification (E). GUS activity was also observed in epidermal cells and root hairs (F). Scale bars in A and B are 200 µm and C to F are 50 µm.

expression are. As seen in OsPHP1, details of the epidermis show GUS activity in root hairs (Figure 6.5 F).

With both BA and IAA treatment expression in whole crown roots is very strong, particularly in the root tip but also extending to more mature sections of root (Figure 6.6). There appear to be no real observable difference between untreated primary root and crown roots after auxin or cytokinin treatment. It is therefore difficult to make any claims about induction by hormones in this instance.

In leaves OsPHP2 shows spots of expression localised to leaf edge trichomes, trichomes and stomata (Figure 6.7).

6.5 OsPHP3 expression patterns

OsPHP3 seems to be expressed in similar patterns as OsPHP2, but is perhaps more highly expressed in the epidermis (Figure 6.8). Unfortunately, only very poor quality root radial sections were obtained for the OsPHP3 reporters so these are not displayed. However, from the whole mounts, it seems expression is highest in the outer tissues. This is easiest to see in the more mature sections of root (Figure 6.8 B). As observed with the other two OsPHPs, expression of OsPHP3 is seen in epidermal cells and signal extends into root hairs (Figure 6.8 C). In lateral roots expression is seen with greatest intensity in the columella and root cap (Figure 6.8 D). Although no experiments with hormonal treatment were performed with OsPHP3 (due to few seed initially harvested) the results of native expression contradict the results obtained by qRT-PCR.

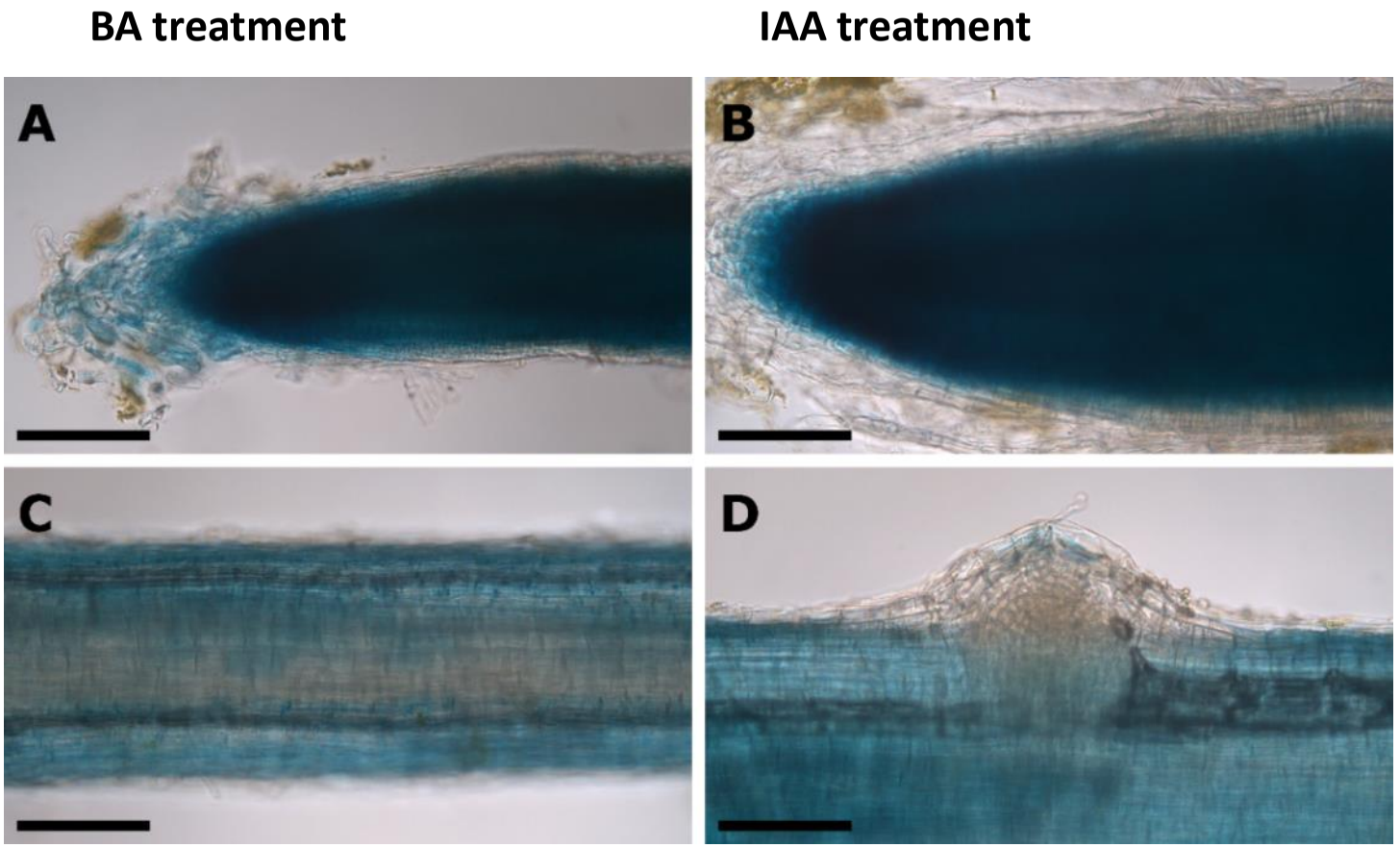
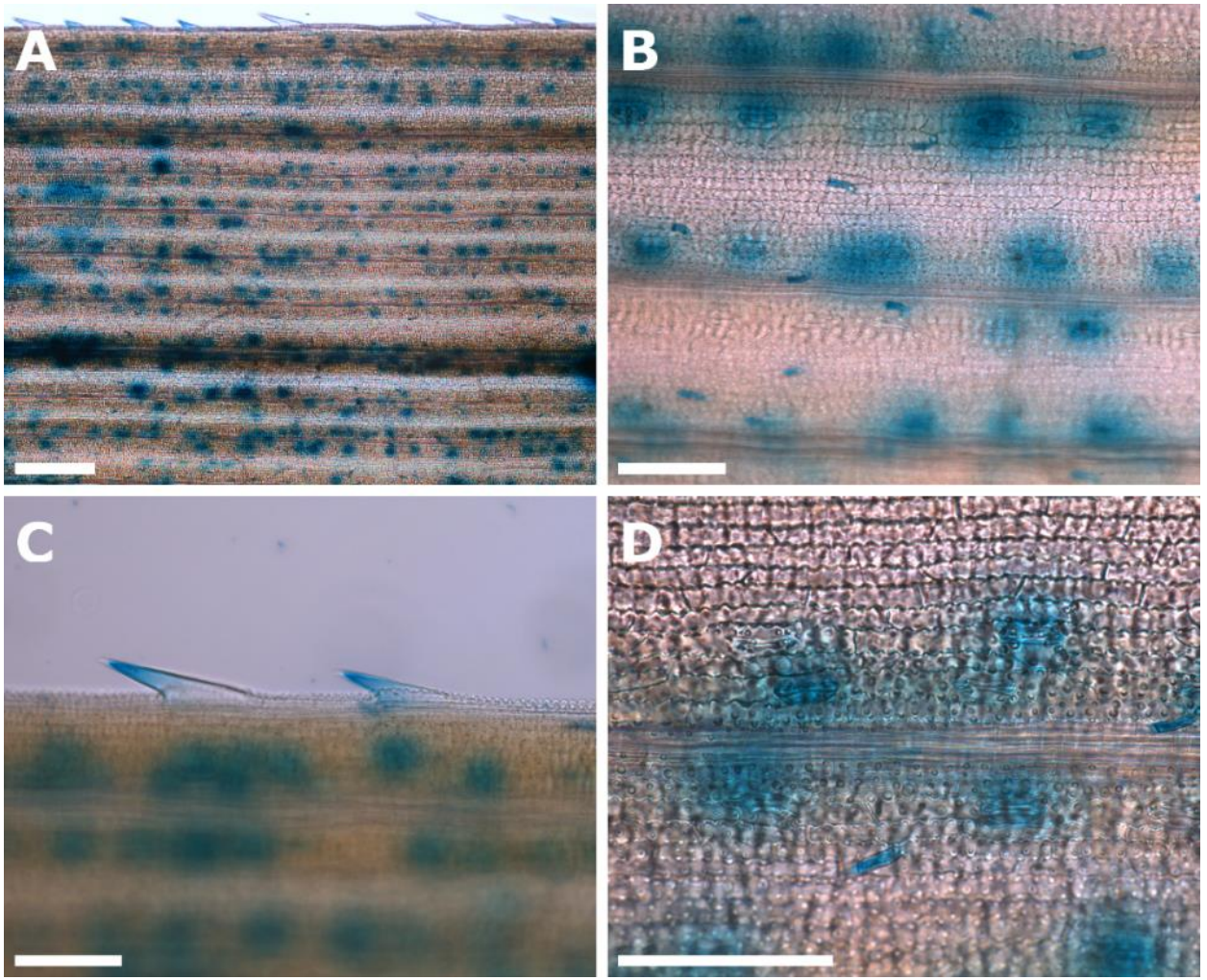


Figure 6.6. GUS activity showing OsPHP2 expression in crown root tips (A and B) and mature zones of crown roots (C and D). Roots were treated with either 5 µm BA (A and C) or 10 µm IAA (B and D) for 4 hours prior to staining. Scale bars are 100 µm.

Figure 6.7. GUS activity showing OsPHP2 expression in leaves. Scale bars in A is 300 µm and B to D is 100 µm.



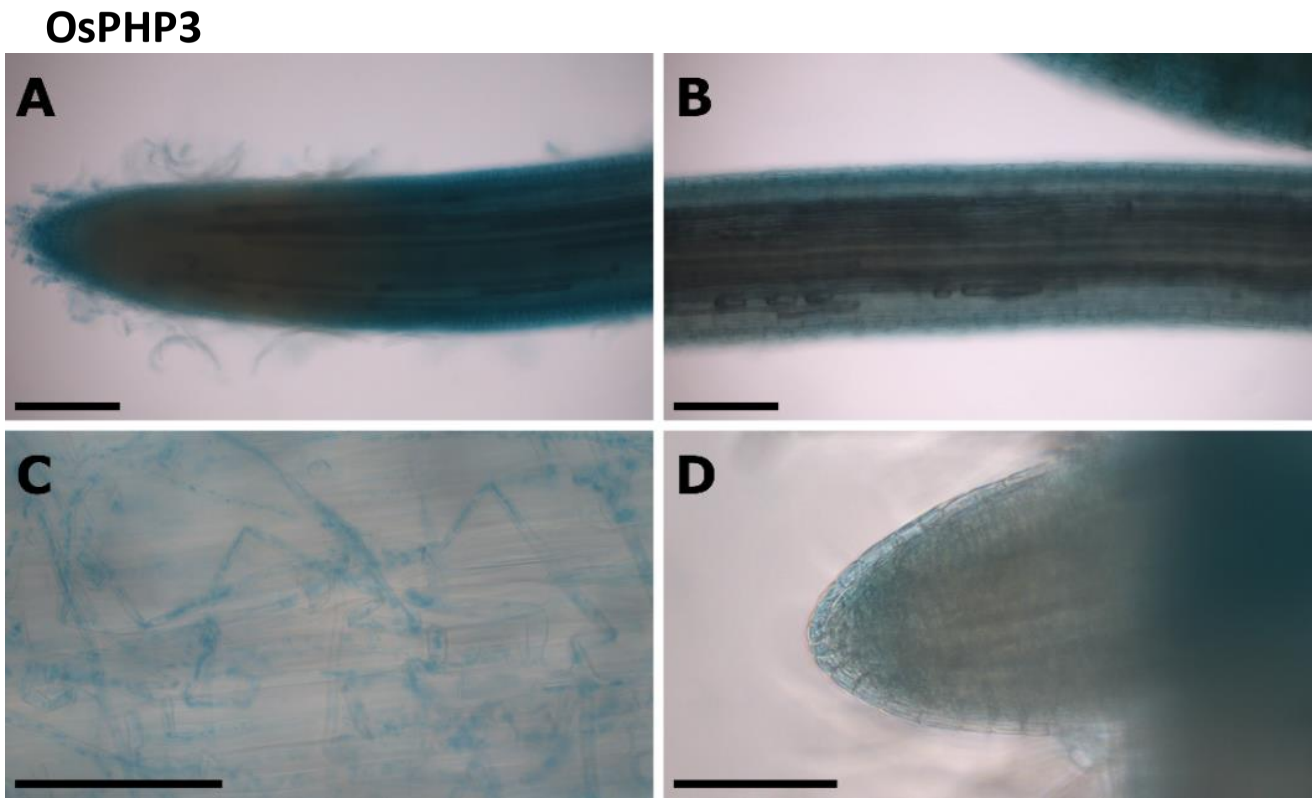


Figure 6.8. Histochemical localisation of GUS activity driven by the OsPHP3 promoter. Whole mounts show longitudinal expression patterns at the primary root tip (A) and further up the root (B). GUS activity was seen in root hairs (C) and lateral roots (D). Scale bars are in A and B are 200 µm and C and D are 100 µm.

In leaves, expression patterns are similar to those of OsPHP2, with GUS activity shown in trichomes and stomata (Figure 6.9). However, this appears to be much less uniform as some trichomes and some stomata are not stained at all, whereas in OsPHP2 every one is stained. In addition, there are high levels of GUS activity in the central vessel, but not in the other smaller vessels. Expression in the central vessel also does not extend throughout the whole leaf but is seen in a reducing gradient towards the leaf tip (not seen in the figure).

6.6 OsRR1 expression patterns

In primary roots, native expression of OsRR1 is seen throughout the whole root with highest expression levels at the root tip and further up the root (Figure 6.10). Further up the root there is a patchy expression pattern associated with root hair epidermal cells. Radial sections reveal the expression is at greatest intensity in epidermis, exodermis and sclerenchyma, although staining is seen throughout the whole radial section.

Upon treatment with BA or IAA slightly different patterns of expression are seen. With BA treatment, expression is seen in a pattern very similar to the control (in the root tip and further up the root but is absent between) (Figure 6.10 D and E). With IAA treatment the zone lacking expression narrows slightly (Figure 6.10 B and C).

In the leaf the expression pattern of OsRR1 is very similar to that of OsPHP3, except that it is absent from trichomes. Expression is seen in some, but not all, stomata, and in areas of the main leaf vein (Figure 6.11).

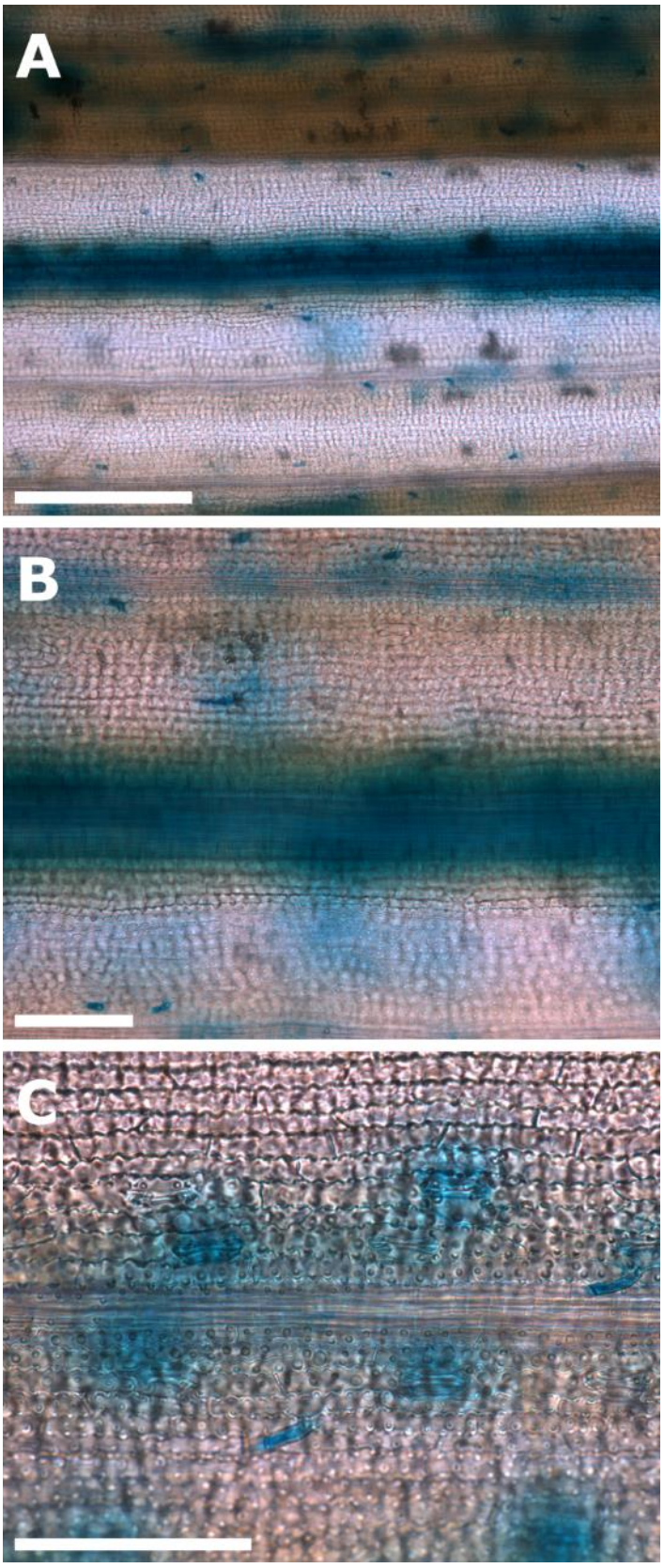
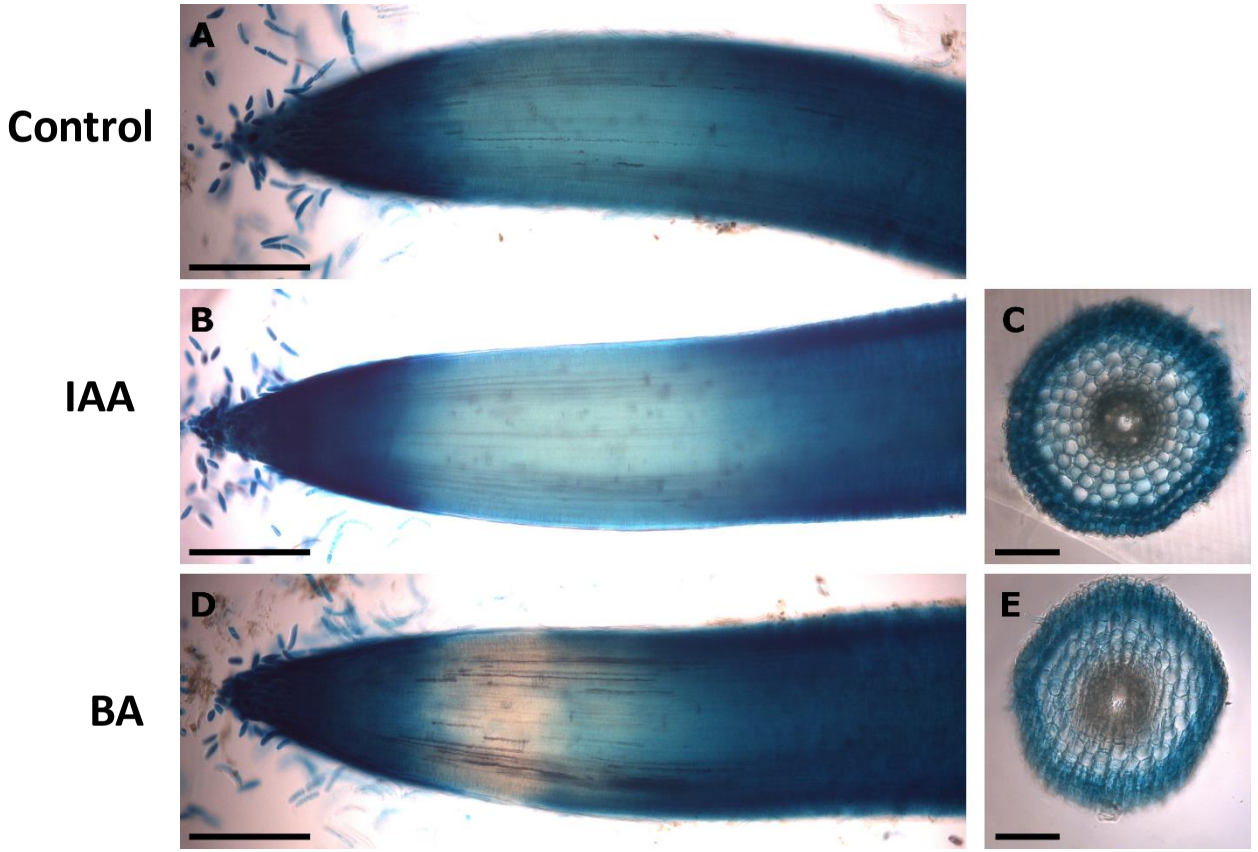


Figure 6.9. GUS activity showing OsPHP3 expression leaves. Scale bar in A is 300 µm and B and C are 100 µm.

Figure 6.10. GUS activity showing OsRR1 expression in primary root tips (A, B and D) and in radial sections (C and E). Roots were treated with 5 µm BA (D and E) or 10 µm IAA (B and C) alongside the DMSO treated control (A) for 4 hours prior to staining. Scale bars are 200 µm.



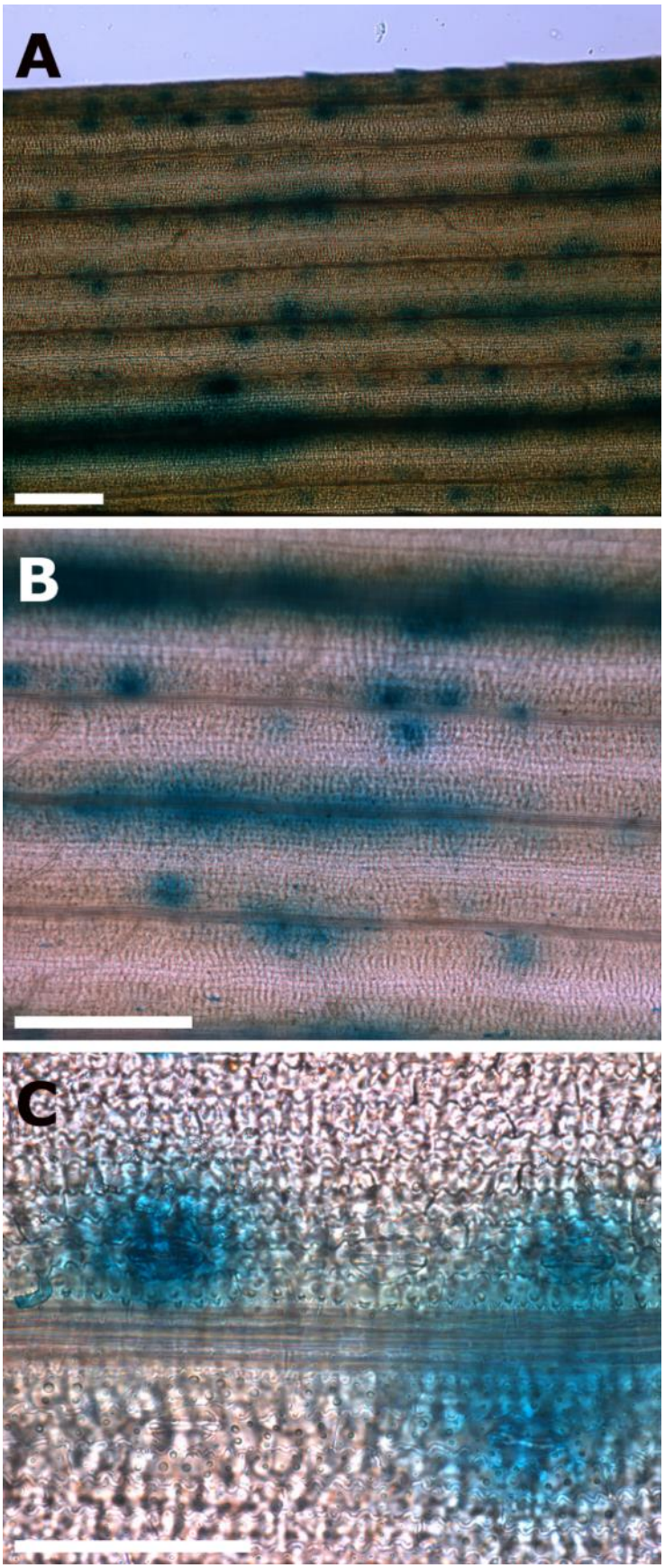


Figure 6.11. GUS activity showing OsRR1 expression in leaves. Scale bars are 200 μm.

6.7 OsRR3 expression patterns

In primary roots OsRR3 expression is seen at low levels in the root cap, is absent in the differentiation zone and is at greatest intensity beginning after this in more mature areas of root (Figure 6.12 A and B). Radial sections through these areas reveal greatest expression is seen in epidermal cells including root hairs (not exodermis or sclerenchyma) and in protoxylem poles (Figure 6.12 C and D).

Upon BA treatment of crown roots, expression of OsRR3 is seen in the columella and QC area, with some patchy expression in epidermal cells close to the root tip, in a similar pattern to native expression in untreated roots (Figure 6.13 E and F). In more mature areas of these roots expression is seen in the epidermis. Upon IAA treatment the expression patterns look similar to untreated roots, but with a clear lack of expression in the root tip, suggesting expression of OsRR3 is inhibited by auxin (Figure 6.13 C and D). This is in agreement with data obtained from qRT-PCRs (Chapter 4).

In leaves expression of OsRR3 is clearly associated with the vascular bundles within the leaf veins. GUS activity was strong surrounding the central vein, but was also seen in all parallel veins (Figure 6.14).

6.8 OsRR7 expression patterns

In primary roots, native expression of OsRR7 appears to be very similar to that of OsRR3. GUS activity is seen in the root tip, is absent in the differentiation

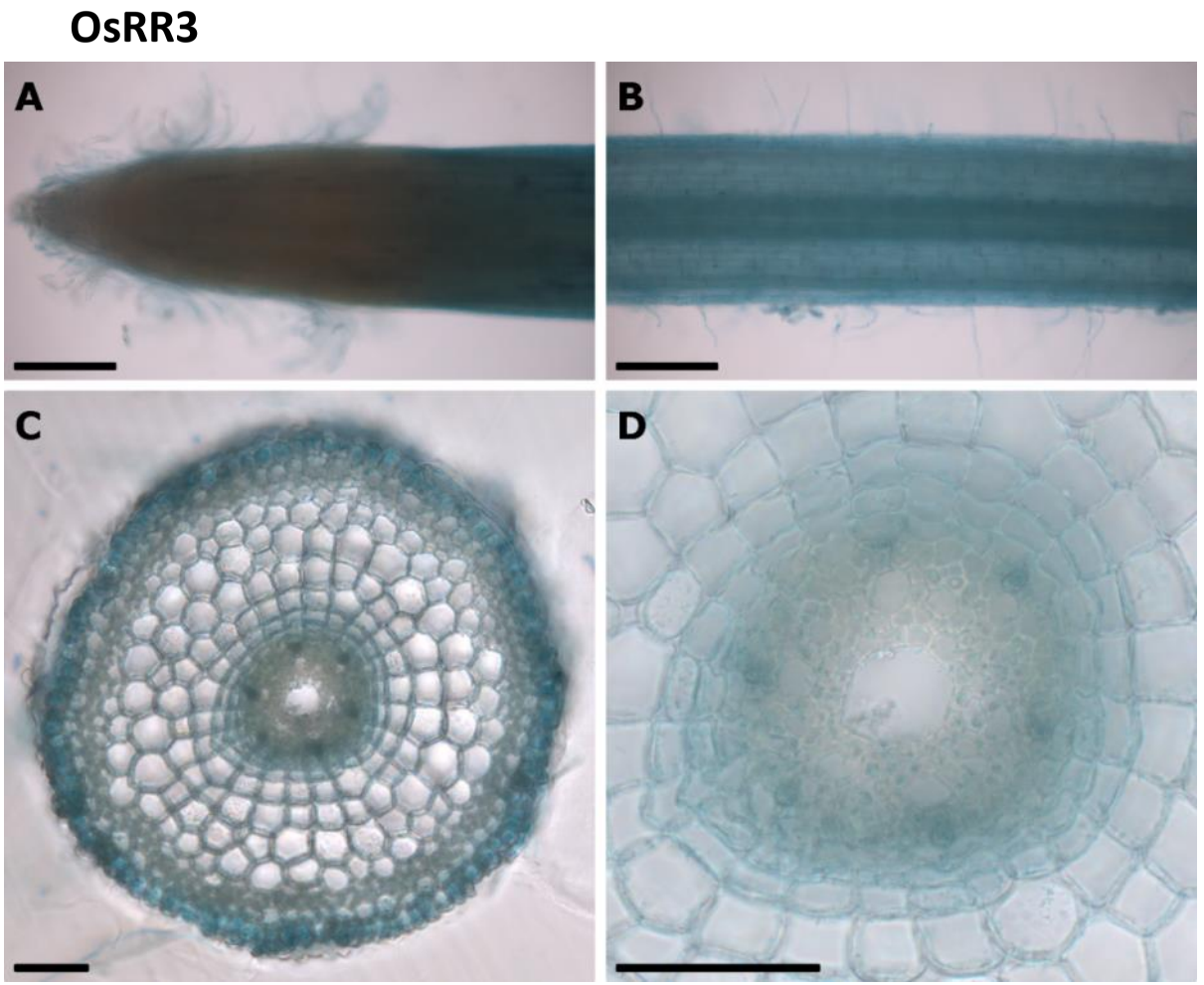
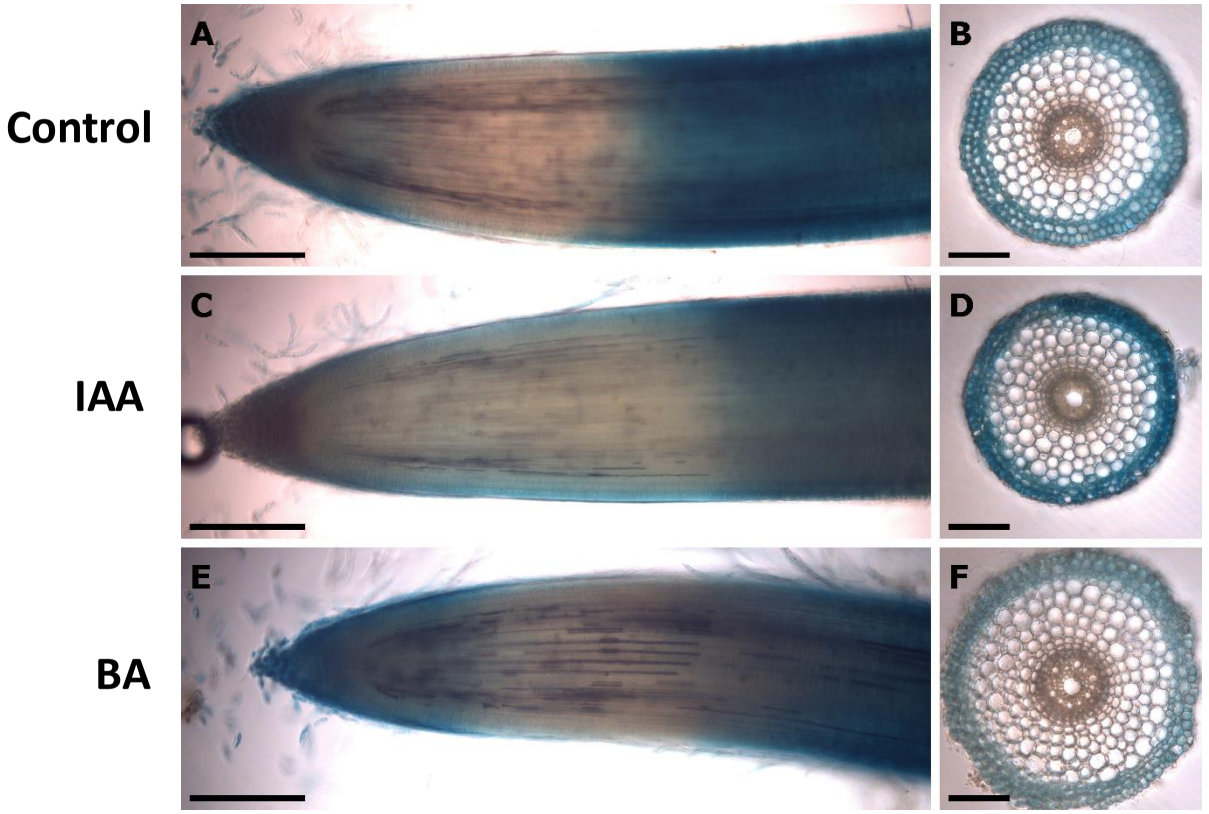


Figure 6.12. Histochemical localisation of GUS activity driven by the OsRR3 promoter. Whole mounts show longitudinal expression patterns at the primary root tip (A) and further up the root (B). Radial sections at lower (C) and higher magnification (D) show GUS activity in epidermis and protoxylem. Scale bars in (A) and (B) are 200 µm and in (C) and (D) are 50 µm.

Figure 6.13. GUS activity showing OsRR3 expression in primary root tips (A, C and E) and in radial sections (B, D and F). Roots were treated with 5 µm BA (E and F) or 10 µm IAA (C and D) alongside the DMSO treated control (A and B) for 4 hours prior to staining. Scale bars are 200 µm.



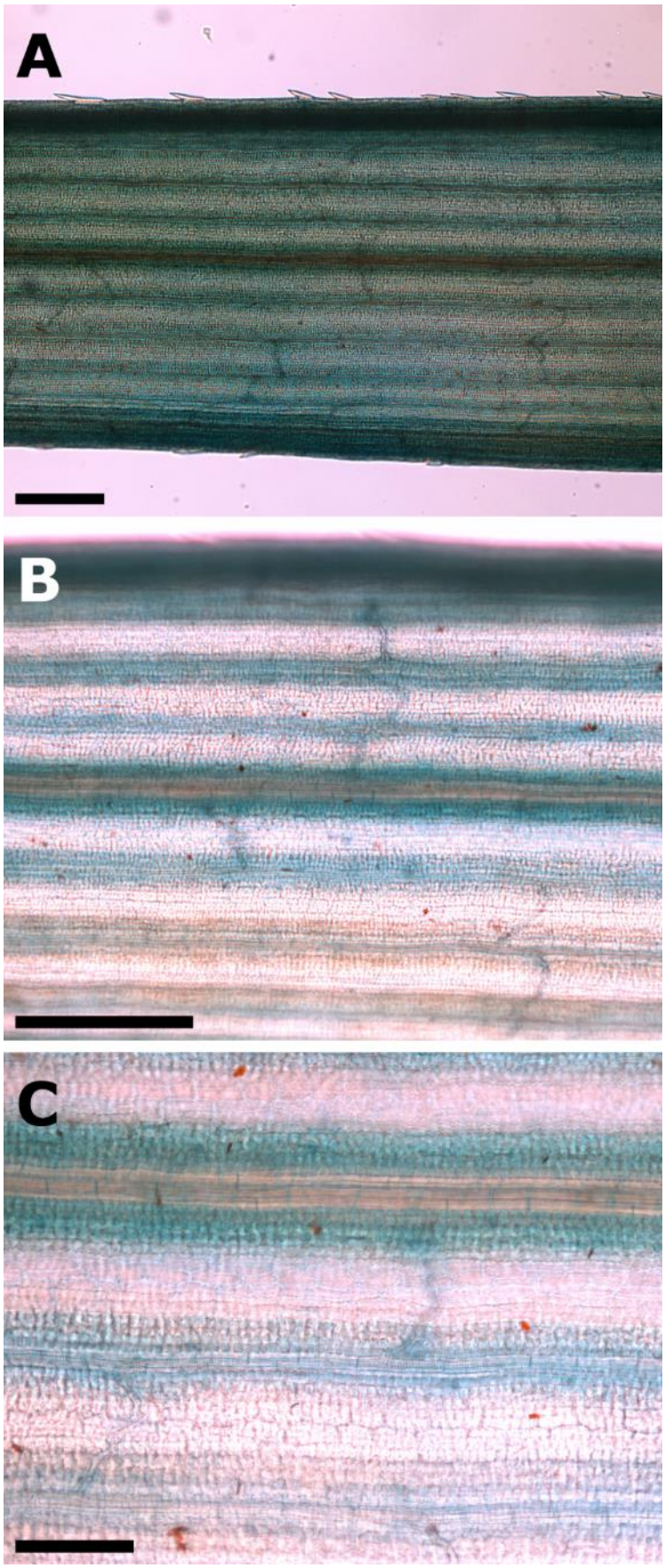


Figure 6.14. GUS activity showing OsRR3 expression in leaves. Scale bars in A and B are 200 µm and in C 100 µm.

zone and becomes stronger further up the root (Figure 6.15 A and B). Radial sections of mature primary root segments show expression is strongest in the epidermis (but absent in exodermis and sclerenchyma as in OsRR3) and is particularly strong in protoxylem poles (Figure 6.15 C and D). As seen in many of the other reporters, expression in epidermal cells includes root hair cells (Figure 6.16 E).

When treated with BA, expression of OsRR7 is seen in patterns reminiscent of untreated roots (Figure 6.16 E and F). However, when treated with IAA, expression is seen at great intensity throughout the whole root tip (Figure 6.16 C and D).

In leaves expression of OsRR7 is seen very specifically only at the distal ends of transverse veins, where they join the parallel main veins (Figure 6.17).

6.9 CRISPR construct design

CRISPR as a genome editing tool is based on the adaptive immune mechanism present in many bacteria and Archaea (reviewed by Doudna & Charpentier 2014; Wang et al. 2016). In this system, DNA fragments from invading viruses or foreign plasmids are recognised and incorporated into what is referred to as the Clustered Regularly Interspaced Short Palindromic Repeats (CRISPR) locus. These fragments of foreign DNA are referred to as protospacers, and are incorporated between repetitive DNA sequences. This CRISPR locus is then transcribed to pre-CRISPR RNA (pre-crRNA) which is processed to mature crRNA. The mature crRNA contains the protospacer, which recognises and

OsRR7

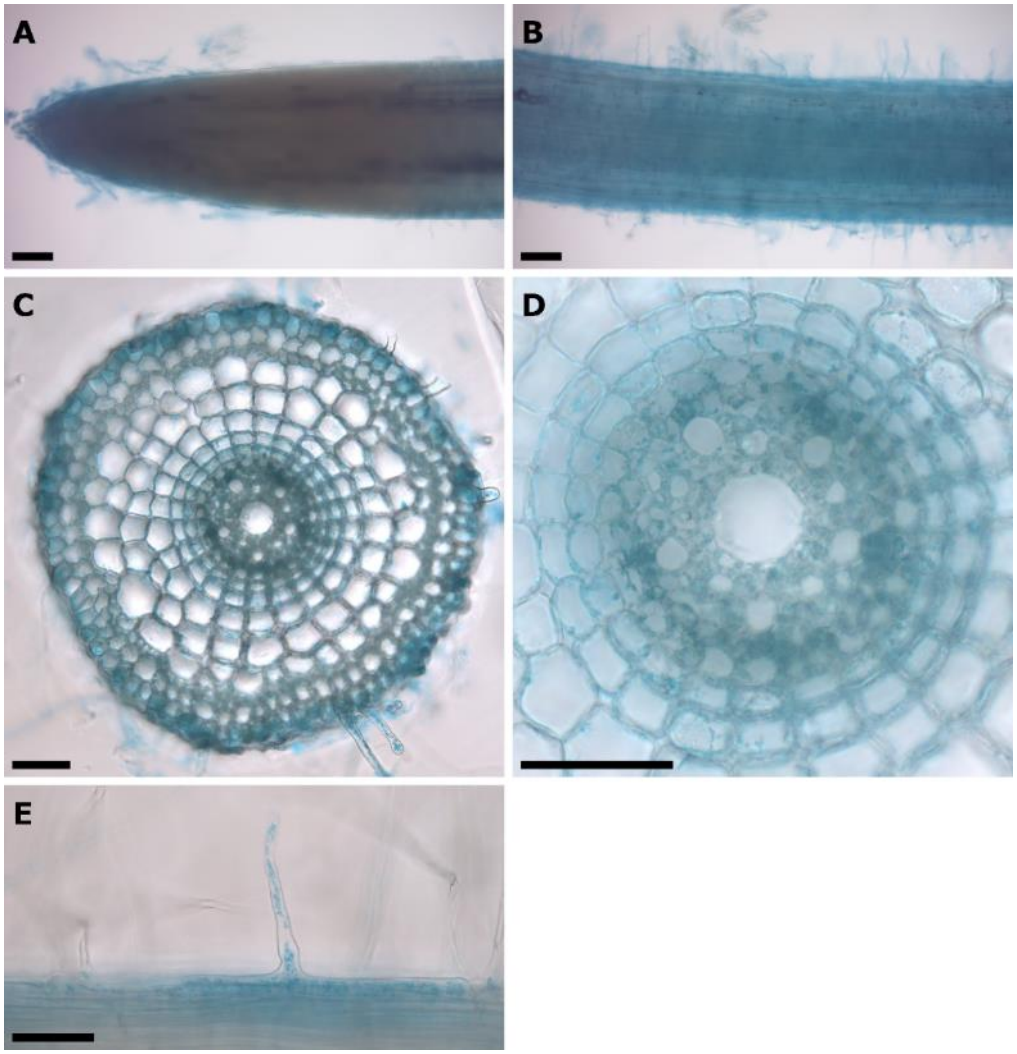
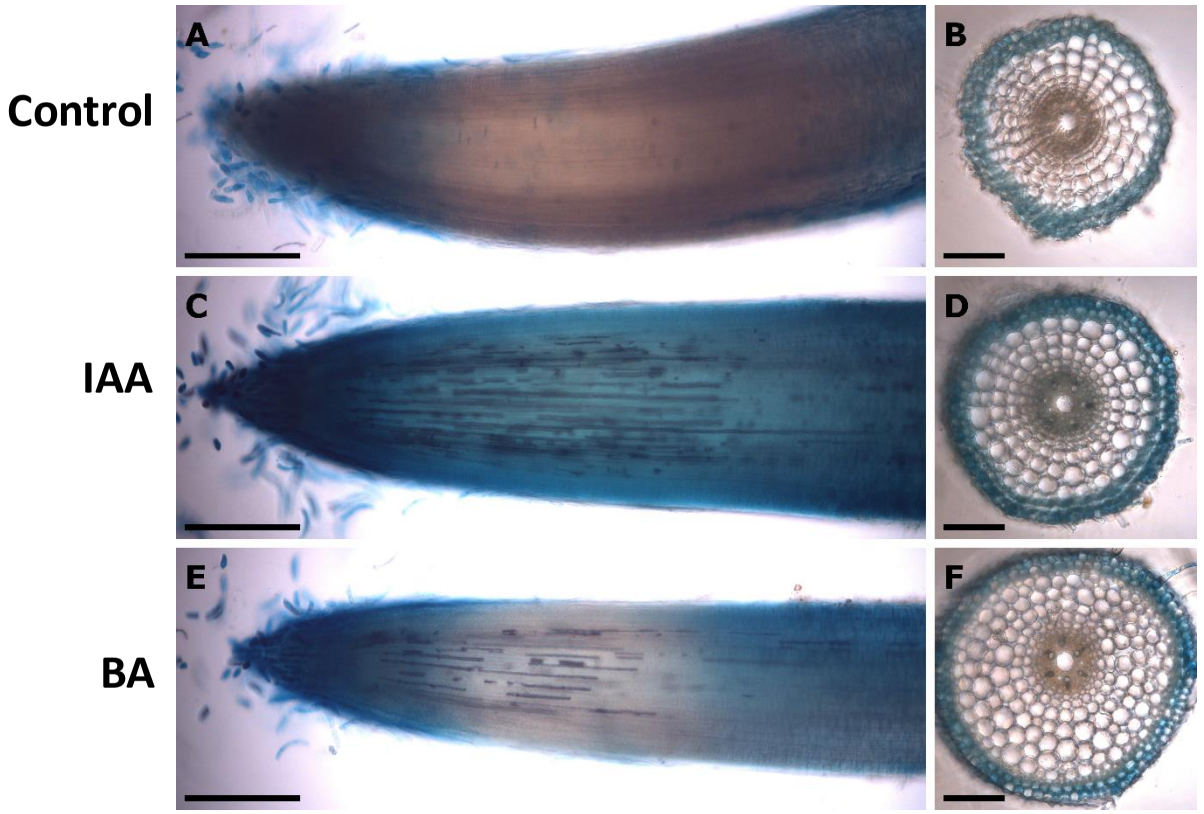


Figure 6.15. Histochemical localisation of GUS activity driven by the OsRR7 promoter. Whole mounts show longitudinal expression patterns at the primary root tip (A) and further up the root (B). Radial sections at lower (C) and higher magnification (D) show GUS activity in epidermis and protoxylem. GUS activity was also detected in epidermal cells and root hairs (E). Scale bars in (A) and (B) and (E) are 100 µm and in (C) and (D) are 50 µm.

Figure 6.16. GUS activity showing OsRR7 expression in primary root tips (A, C and E) and in radial sections (B, D and F). Roots were treated with 5 µm BA (E and F) or 10 µm IAA (C and D) alongside the DMSO treated control (A and B) for 4 hours prior to staining. Scale bars are 200 µm.



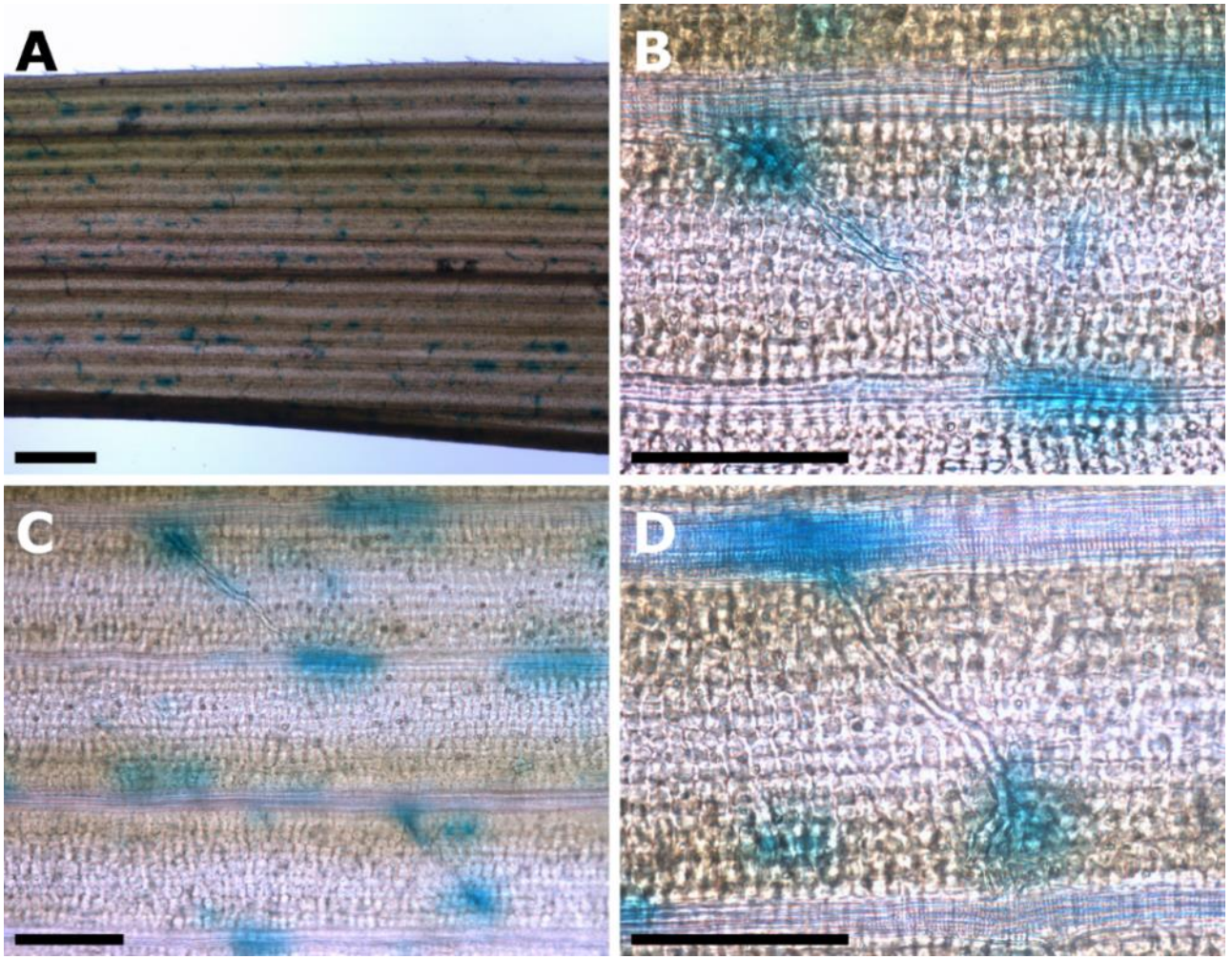
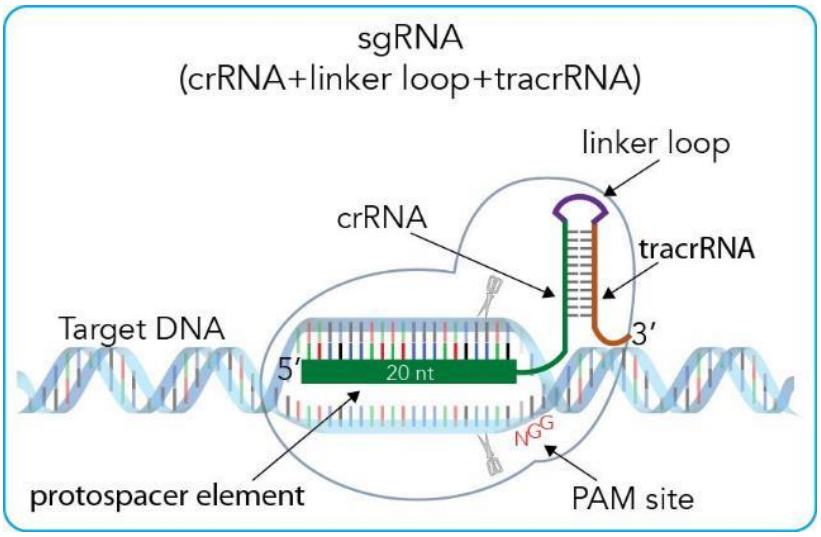


Figure 6.17. GUS activity showing OsRR7 expression in leaves. Scale bar in A is 500 µm, and in B to D are 100 µm

targets the invading DNA, and the crRNA repeat sequence which recruits other RNA components along with the Cas9 nuclease which causes double strand breaks in target DNA. In bacteria, 2 major classes consisting of 6 different types of CRISPR systems have been described, based on differences in components and mechanism of action. Whereas the class 1 system requires multiple proteins for cleavage, the class 2 systems make use of a single protein, such as the Cas9 nuclease from the type II CRISPR system. Because expressing this single RNA guided nuclease is considerably easier than the multiple components seen in other systems, the class 2 type II CRISPR system has been the major system exploited in biotechnology. In this system another non-coding RNA, the trans-activating CRISPR RNA (tracrRNA) interacts with crRNA, and is required for its processing and in recruiting Cas9. In addition, for the CRISPR system to function a specific sequence is required adjacent to the crRNA target site in the invading DNA, referred to as the protospacer adjacent motif (PAM). This is absent in the in the CRISPR locus in the host genome and consequently only invading DNA, and not host genomic DNA, is cleaved. For Cas9, the PAM sequence is NGG (with N being any nucleotide).

In 2012, crRNA and tracrRNA was combined in a single guide RNA (sgRNA) consisting of the protospacer (which binds the target site), the crRNA, the tracrRNA, and a linker loop connecting crRNA and tracrRNA in a double stranded structure, which recruits Cas9 (Jinek et al. 2012) (Figure 6.18 A). This made targeting specific genes much easier, as all that needed to be expressed was the sgRNA (with the appropriate protospacer) and Cas9. Since then, recognition of the importance and multiple potential uses of CRISPR technology

A



B

	Protospacer Non-seed Seed PAM	CasOT software (Xiao 2014)	OryGenes DB (CIRAD)
PHP1 sgRNA_283f	AGATGAGCAATTTTGTCAGGTGG	9 with 4 mismatches	2 with 3 mismatches
PHP1 sgRNA_319f	TGAAGCTAGTCCTAATTTTGTGG	1 with 3	2 with 7
PHP2 sgRNA_55f	GATGAACAGTTTAATCAGCTGG	2 with 3	2 with 6
PHP2 sgRNA_79r	CGCAACTTCCTCAACAAAATTGG	3 with 4	4 with 5
PHP3 sgRNA1_530f	TGAGCAATTTTGTCAGGTTGAGG	8 with 4	2 with 4
PHP3 sgRNA2_576r	GGTTGAATCCTTAAAAAACAAGG	1 with 3	1 with 5
RR1 sgRNA 52f	GCTGCTGGTGGACGACTCGCCGG	1 with 1	1 with 1
RR1 sgRNA 182r	GTCGGTGAGCACCATGTCGATGG	5 with 3	1 with 4
RR6 sgRNA 115f	GAAGGTGGTGCCGGTTGTGGTGG	40 with 3	4 with 3
RR6 sgRNA 160f	GCAGAGCGAGATGCACGTGCTGG	1 with 3	3 with 5
RR7 sgRNA1_137f	ATGAAGAGTGTCGTCGTCAAGGG	2 with 4	1 with 8
RR7 sgRNA2_163r	GCCGATGCGTTGTCGTGCAGCGG	8 with 4	1 with 7

Figure 6.18. The CRISPR-Cas9 sgRNA contains crRNA (with appropriate protospacer element), tracrRNA, and a linker loop connecting them (A). The cartoon is taken from the IDT website. Sequences of protospacer elements within sgRNA designed for target regions, displayed with predictions for off target effects (B). Off target effects were predicted using CasOT software (Xiao et al. 2014) and OryGenes DB (CIRAD).

has led to a massive increase in the number of research groups working on CRISPR. Consequently, there are many variants on the original system. The Cas9 nuclease itself has been modified in various ways. Cas9 was engineered to cut only one DNA strand (referred to as a nickase), so that two separate Cas9 proteins targeted to adjacent sites will cause a double strand break. This increases specificity and reduces that chance of off-target cutting. In addition, Cas9 can be inactivated while still retaining DNA binding activity, and this has been adopted for several applications. These include transcriptional activation or repression of specific target genes, direct imaging of genomic dynamics, and studying DNA-protein interactions at specific loci.

In this section, the use of CRISPR in creating mutant plants is discussed. The first step in experimental design of a CRISPR experiment is locating appropriate regions within genes of interest to target, and predicting any off-target effects which may occur if these regions are targeted. Within the CRISPR construct, it is the protospacer element which binds the target genomic DNA and consequently only this 20 bp region which lends specificity to where cuts will take place throughout the whole genome. The only caveat concerning which regions of genomic DNA can be targeted is that the correct PAM (in the case of Cas9, NGG) must be present in the genomic DNA, immediately after the protospacer specific sequence. In the system used in this project, Cas9 nuclease should create a double strand break. Consequently, it does not matter which strand the protospacer is designed to bind to, and it also does not matter in which direction (5’ – 3’ or 3’ – 5’). Therefore, within even small genes there are a huge number of potential target sites.

There are a few major considerations to take when choosing which area of the genomic DNA of the gene of interest to target. Given that the only requirement for gDNA regions that can be targeted is the PAM sequence being NGG, there are a huge number of potential sites that could be targeted in any gene. Firstly, for the purposes of producing loss of function mutants, it is easiest to target regions early on in the CDS. This ensures disruption of the gene, whereas targeting introns may not. Targeting the CDS closer to the stop codon may result in a truncated protein which may still be at least partially functional. Another major point to consider when deciding which site to target is any off-target effects which may occur. Because the protospacer (the region which recognises target DNA) is only 20 bp, there is the possibility that it may recognise other identical or similar 20 bp sequences elsewhere in the genome. For this reason, it is important to predict off-target effects for each potential target region before deciding which to use.

Recently many groups have developed software to recognise potential target sites and test the predicted frequency of off-target recognition events for these target sites (Haeussler et al. 2016). This kind of software is similar to many of the alignment tools already available, but is designed for more exhaustive searching for short nucleotide sequences (such as the 20 bp protospacer) and takes into account the different types of PAM which may be recognised. In most cases, this kind of software can display frequency of off-target effects with different levels of mis-matching of the protospacer, as well as displaying exactly where these are expected to occur in the genome. This allows identification of suitable protospacer elements with the lowest chance of off-target mutation,

and also gives a list of the most likely locations for these off-target mutations. If need be, these off-target locations can later be checked for mutations by sequencing.

In the experiments described, CasOT software was used to identify suitable target regions and predict off target cutting (Figure 6.18 B). This was used in conjunction with the OryGenes DB online tool to check off-target events. Because these tools work in different ways they usually give slightly different results, but together can be used to validate which target site would give the lowest chance of off-target cutting. In addition, the CasOT software takes into account that the chance of an off-target cutting event due to a mis-match between protospacer and gDNA is highly dependent on where the mis-match in the gDNA is located. Mis-matches in the 12 nt adjacent to the PAM (referred to as the seed region) are more likely to cause reduced activity of Cas9 nuclease, whereas mis-matches in the non-seed region are less likely to influence cutting. As well as displaying total mis-matches in potential off-target regions, the CasOT software categorises them based on whether they occur in seed or non-seed regions of the protospacer. This gives extra detail and aids choosing appropriate protospacer elements to use.

6.10 Genotyping CRISPR transformants

Because CRISPR relies on mistakes in DNA repair mechanisms, it is possible to have positive transformants which have correctly repaired the cut made in the gDNA and consequently display no change. This means confirming mutations

must be done by amplifying the target region and sequencing the PCR product. Other methods, such as digestion of PCR product with T7E1 or High-Resolution Melt analysis, can be performed before sequencing. These methods rely on the formation of heteroduplex DNA which occurs upon base mis-matching, and consequently can only be used to detect heterozygous mutants unless wild type gDNA is provided. Sequencing PCR product also enables identification of zygosity of the mutant plants. This can be seen as homozygous plants will have a single trace in the electropherogram, whereas heterozygous plants will have double peaks due to equal abundance of wild type and mutant DNA being amplified.

Of many independent transgenic lines, only two homozygous mutants were identified, one in OsPHP3 and the other in OsRR7 (Figure 6.19 and 6.20). In the OsPHP3 mutant, a single nucleotide insertion towards the end of the protospacer target region causes a frame shift which results in a premature stop codon immediately after the mutation. In the OsRR7 mutant, there is also a single nucleotide addition towards the end of the protospacer target region causing a frame shift which results in replacement of H with 16 amino acids before a premature stop codon.

As well as these two homozygous mutants produced, many heterozygous mutants were identified (four for PHP3 and two for RR7, Figure 6.21 and 6.21). Heterozygosity can be clearly observed in the electropherogram where double peaks appear in the trace immediately after (or towards the end of) the protospacer target region. While it may be possible to pick apart the individual

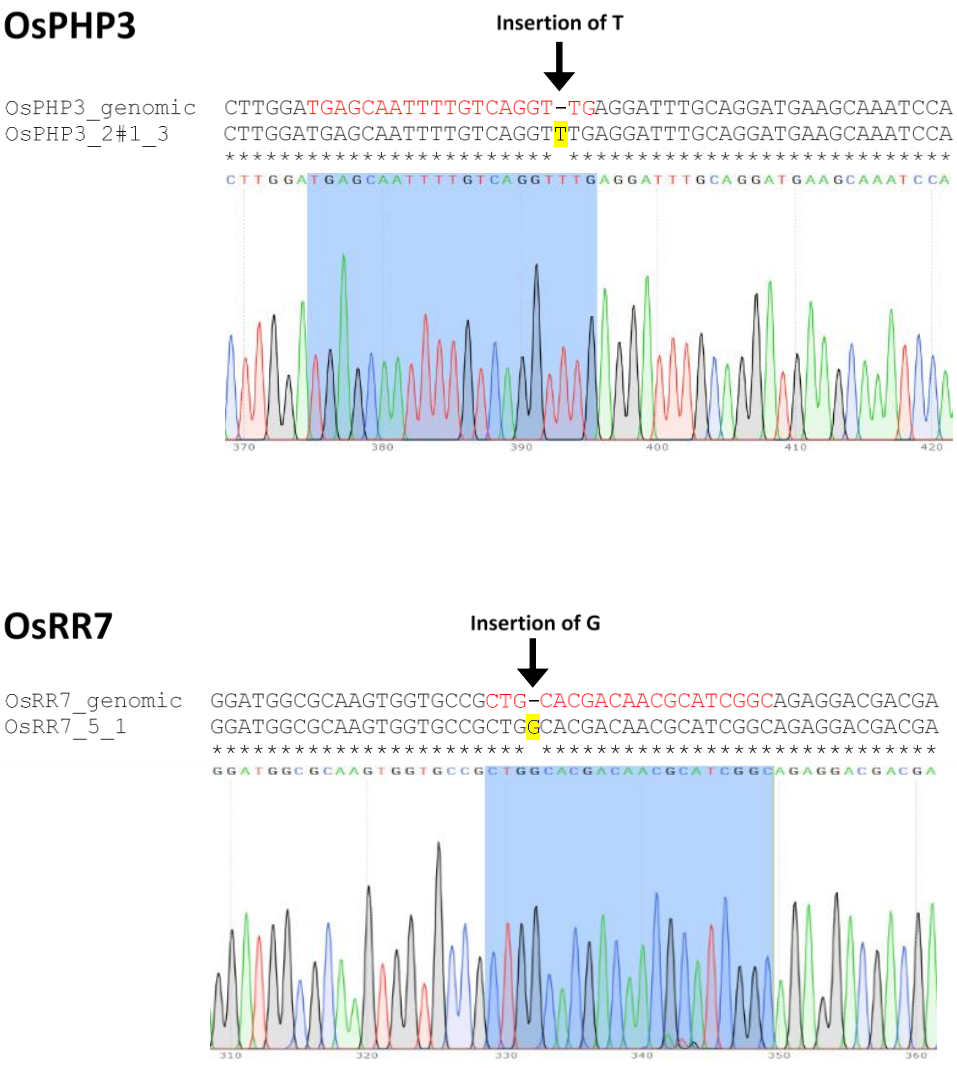


Figure 6.19. Details of sequencing of homozygous mutants in OsPHP3 and OsRR7. The target protospacer is in red font in the genomic sequences and highlighted blue in the electropherograms. Sites of mutation are indicated by arrows and inserted bases highlighted in yellow. The single clean trace in the electropherograms indicate homozygosity.

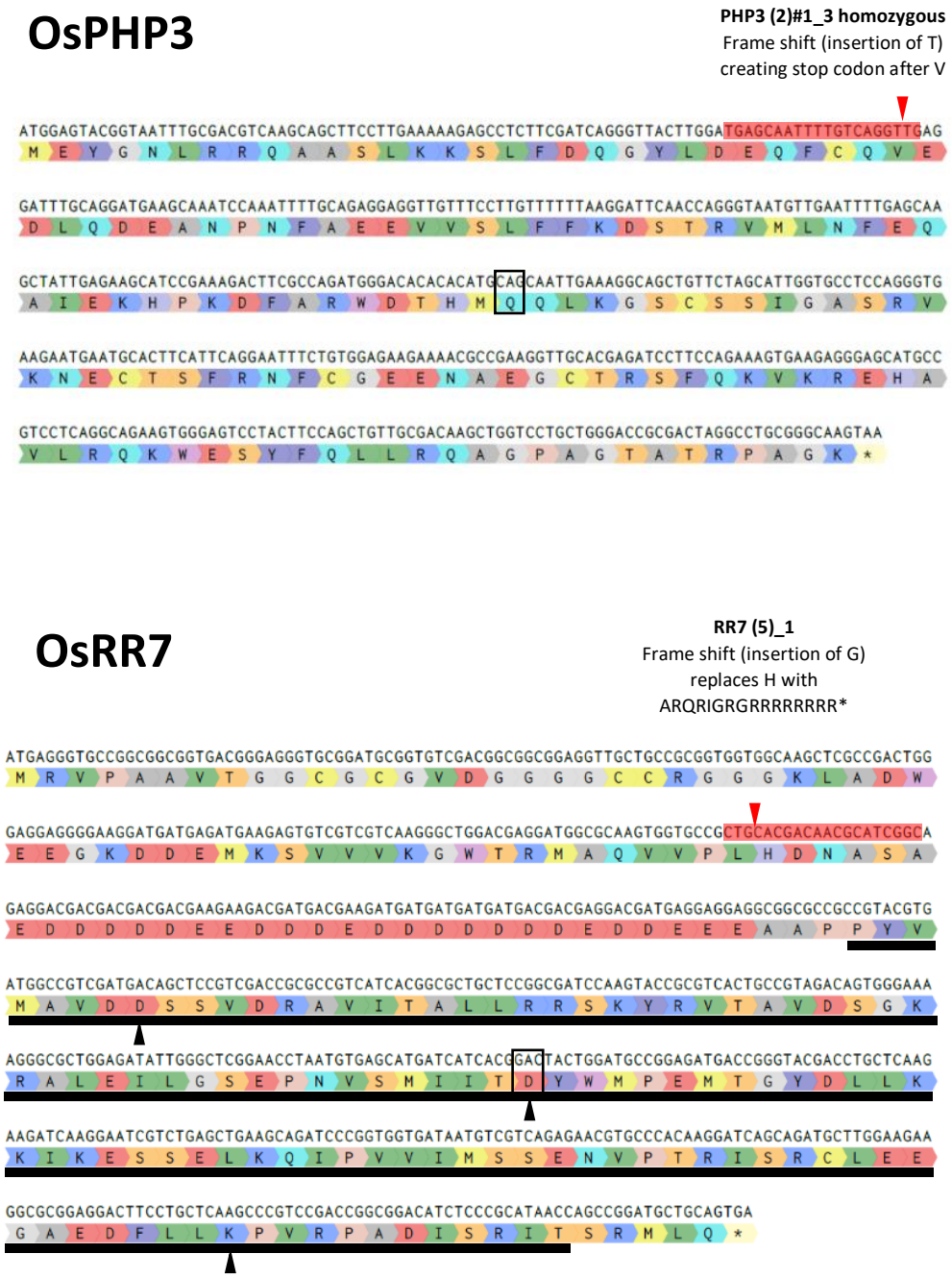
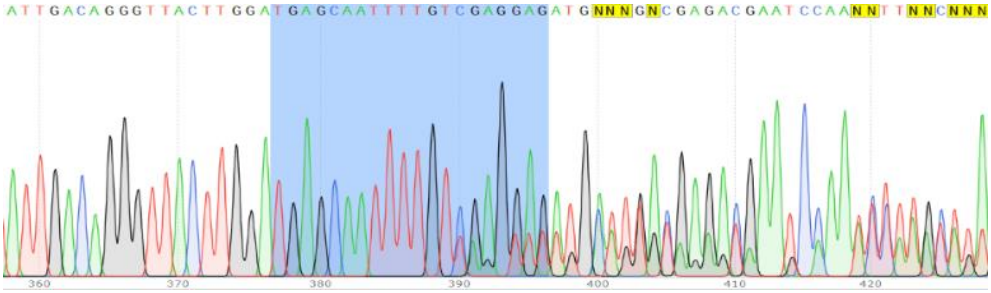
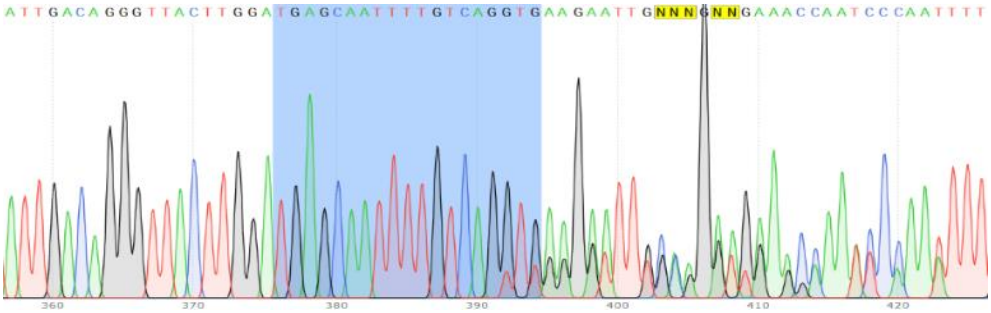


Figure 6.20. Details of the homozygous mutants generated through CRISPR. The full CDS of OsPHP3 and OsRR7 are displayed with both DNA and amino acid sequences shown. The 20 bp protospacer elements are highlighted in red in the DNA sequence, and red arrows indicate locations of resulting mutations. For OsPHP3 the Q at the conserved phosphoaccepting H of the OsHPTs is indicated by a black box. For OsRR7, the receiver domain is underlined, the conserved DDK residues characteristic of the receiver domain are indicated by black arrows and the phosphoaccepting D residue is indicated by a black box.

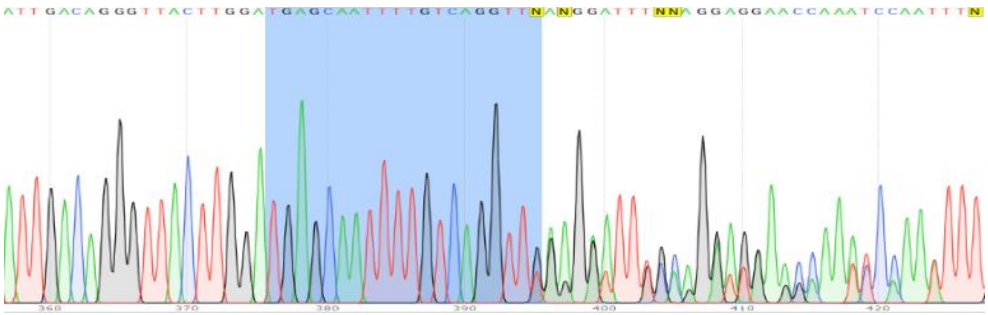
PHP3 (2)_1



PHP3 (3)_2



PHP3 (4)_2



PHP3 (6)_2

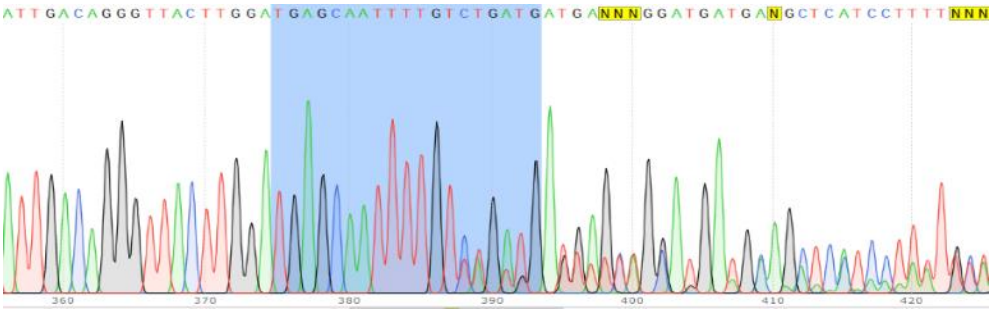
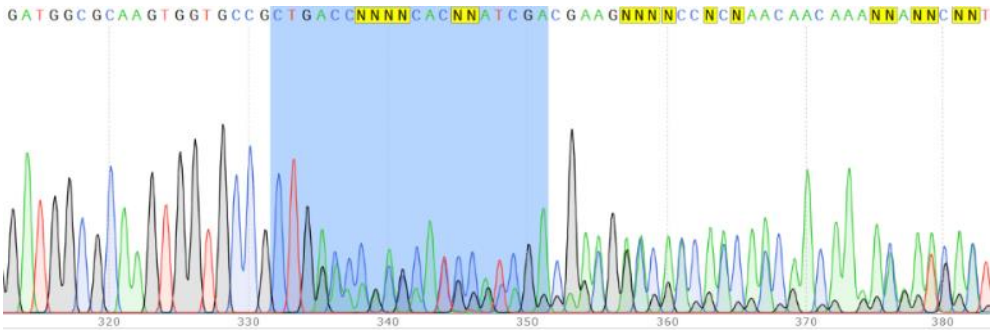


Figure 6.21. Electropherograms showing the four independent heterozygous mutants identified in OsPHP3. The protospacer is highlighted in blue.

RR7 (1)_2



RR7 (2)_1

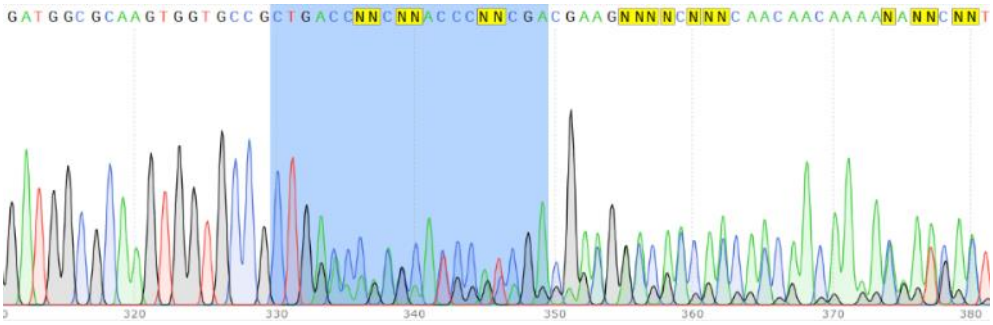


Figure 6.22. Electropherograms showing the two independent heterozygous mutants identified in OsRR7. The protospacer is highlighted in blue.

traces to understand what the resulting mutations are, this proves very difficult in practice. The easiest method to determine these mutations will be generate homozygous plants via self-pollination, and then sequence target regions.

6.11 CRISPR mutant phenotyping

Due to time constraints and low quantity of material available, only root radial anatomy of CRISPR mutants were conducted. This was done both by vibratome sectioning of live tissue and imaging sections by confocal microscopy (Figure 6.23), and embedding in plastic resin, sectioning on a microtome, staining for lignin using toluidine blue and imaging by light microscopy (Figure 6.24). Because genotyping was being taken place at the same time, some plants were analysed which it was later found are not mutants. In Figures 6.23 and 6.24, only OsRR7 are mutants. The other plants can therefore serve as wild-type controls. Overall, there were no observable differences seen in any of the mutants. However, as discussed in Chapter 3, root radial anatomy is highly diverse so given the small amount of material available it is possible that real biologically significant differences have been missed in this analysis. Once multiple independent homozygous mutants are confirmed for each gene targeted, it will be easier to perform more detailed experiments to understand genuine phenotypic differences. One aspect of this may be sectioning through the RAM to determine whether any subtle differences are seen in mutant plants.

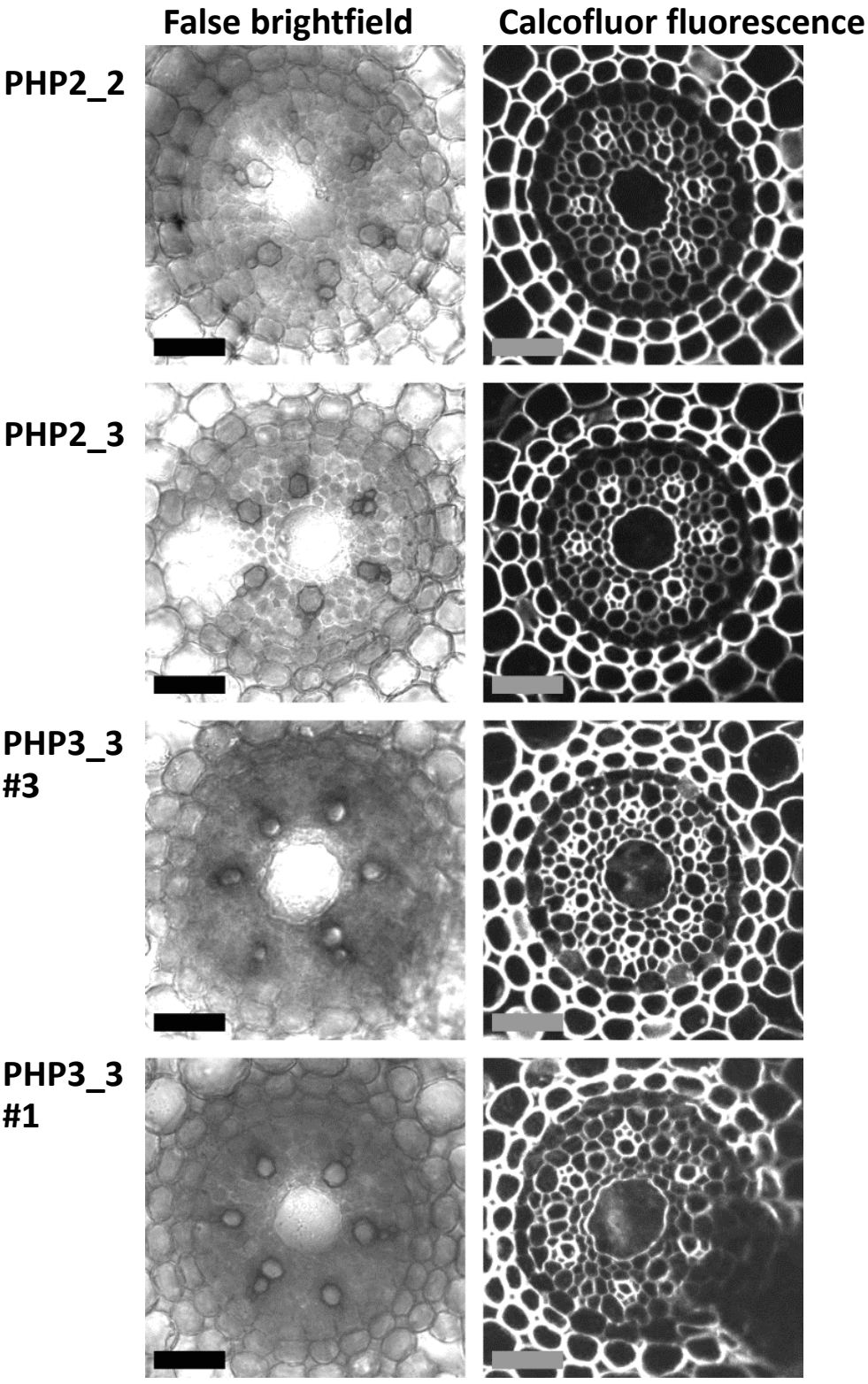


Figure 6.23. Radial sections of CRISPR mutants show no obvious differences in vascular anatomy. Representative images from two independent transgenic lines for each gene targeted are shown. Sections were stained with calcofluor and imaged using a confocal microscope to show false brightfield and calcofluor fluorescence. Scale bars are 25 µm.

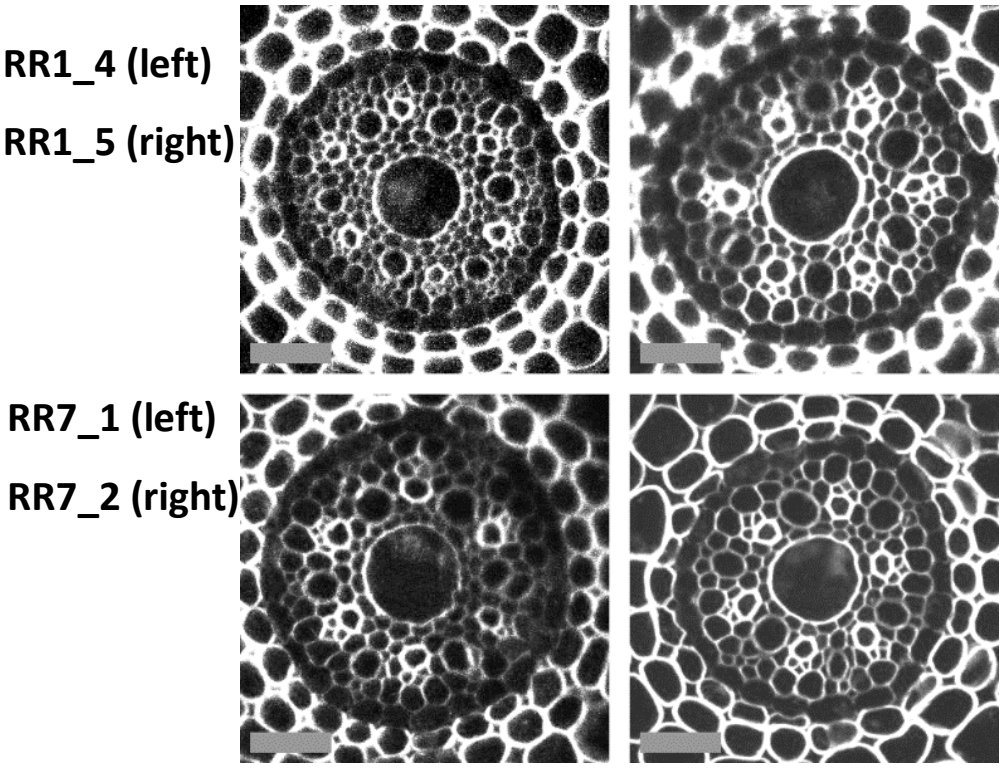


Figure 6.23 continued

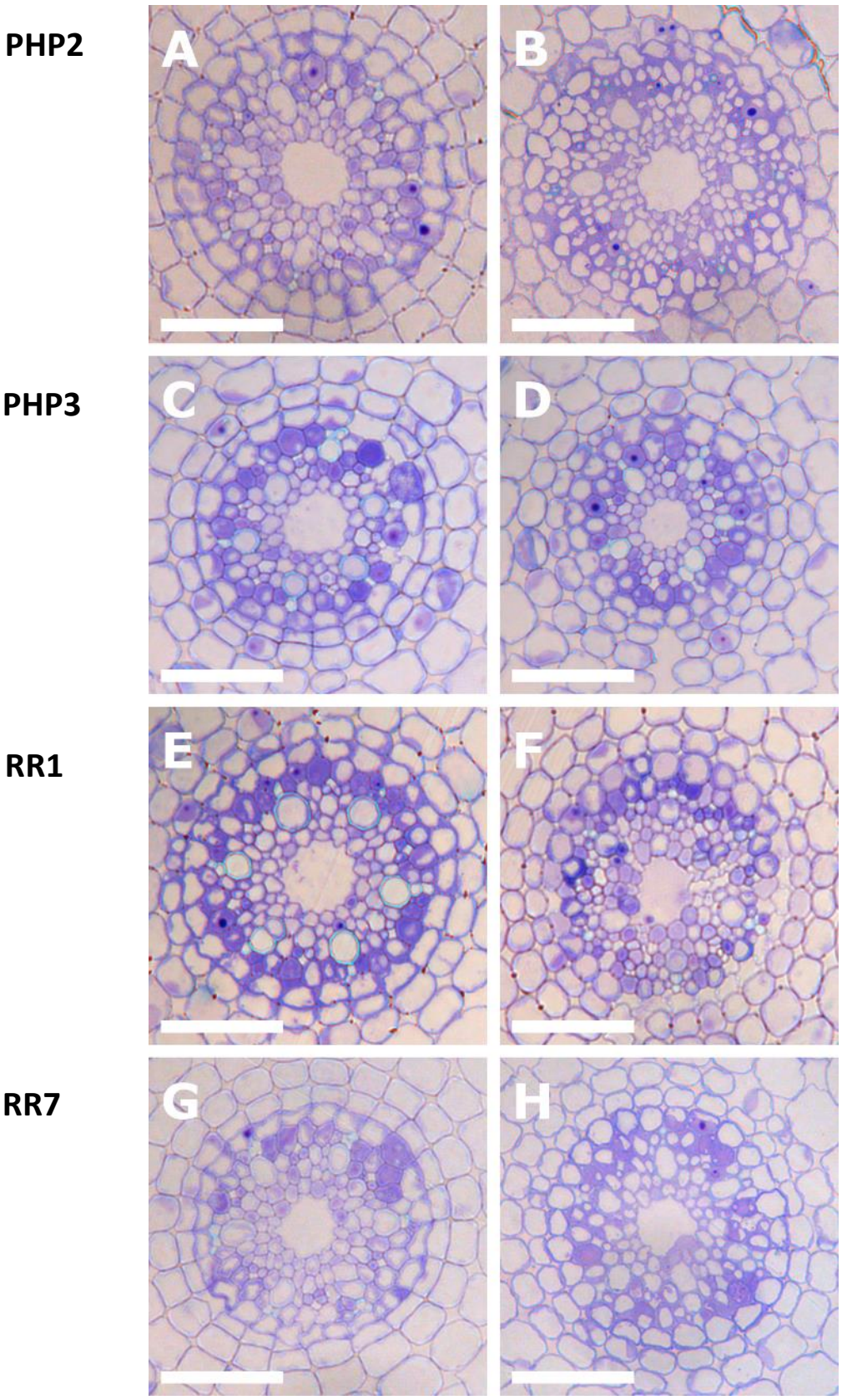


Figure 6.24. Plastic sectioning can show more detail than imaging live sections on the confocal, but no obvious differences were seen in any CRISPR mutants. Representative images from two independent transgenic lines for each CRISPR target are shown. Scale bars are 50 µm.

6.12 Discussion

In this chapter the expression patterns of candidate genes were analysed and mutants generated via CRISPR identified. Much of this work remains unfinished (reporter lines for OsRR6 were not yet prepared and mutants identified only in OsPHP3 and OsRR7), but the preliminary results give us a better idea of the potential function of candidate genes. For example, while the root longitudinal expression patterns for most candidate genes are fairly similar, radial sectioning revealed differential tissue expression patterns. This enabled identification of OsPHP1, OsRR3 and OsRR7 as being expressed in protoxylem. Expression of the OsPHPs in the root is surprising, since they were unable to be detected well using qRT-PCR. However, as revealed by qRT-PCR using OsPHP1 and GUS primers, it may be the case that the primers for the OsPHPs are not amplifying in a hugely reproducible way. This suggests qRT-PCRs detecting possible auxin and cytokinin induction of the OsPHPs should be repeated using new primers. Given expression of OsPHP1, OsRR3 and OsRR7 is seen in the protoxylem poles, it may be the case that these genes act redundantly in inhibition of cytokinin signalling to enable protoxylem specification. However, it may be the case that some zones of expression were missed. In *Arabidopsis*, AHP6 can clearly be seen to be expressed specifically in protoxylem close to the root tip. Because most of the OsPHPs and OsRRs studied here are also expressed in the epidermis (and possibly other outer tissues) which mask internal expression patterns, it is difficult to tell from longitudinal whole mounts how far up the root protoxylem expression is seen. Therefore, for those genes where no protoxylem expression is seen, it may simply be the case that

the domain of expression in the longitudinal plane was missed. For expression patterns in roots treated with auxin and cytokinin, interpretation of results is difficult but as a preliminary experiment they suggest that the results of the qRT-PCRs in Chapter 4 may not be entirely accurate. It would be beneficial to confirm the expression patterns and changes in expression upon hormonal treatment shown here using RNA in-situ hybridisations, which would give a more direct representation of expression.

While expression patterns in the root are more difficult to interpret, expression patterns in the leaves seemed to be more uniform and showed clear differences. In terms of genes which may function in leaf vascular patterning, OsRR3 and OsRR7 are of particular interest. OsRR3 shows clear expression in leaf vascular bundles, and OsRR7 at distal ends of tranverse vessels which connect the parallel vascular bundles. Previous mutants have been identified with incomplete or aberrant transverse vessel development, and these mutants are also associated with changes in cytokinin signalling (Scarpella et al. 2003).

CRISPR was successfully used to generate mutant plants, with both homozygous and heterozygous mutants for OsPHP3 and OsRR7 having been identified. Initial phenotypic analysis was conducted to determine whether there would be any obvious large-scale changes. This appears not to be the case, and further detailed analysis is required. This may be due to genetic redundancy between gene family members. To determine whether this is the case, multiple mutants should be made. In addition, it would be of value to determine cytokinin sensitivity of resulting mutants. This can be done using

various bioassays which have been well described, such as root growth, development of shoots in callus, and hypocotyl elongation (Higuchi et al. 2004; Riefler et al. 2006).

6.13 Summary

- OsPHPs and the type-A OsRRs studies show differential tissue specific expression patterns. In the roots, expression patterns for all genes are broadly similar (in the root tip, absent after 200 to 400 µm with expression seen further up the root, and in mature sections of root expression primarily seen in root hair epidermal cells). Hormonal induction or repression of expression was observed for some genes (IAA repression of OsRR3 and IAA induction of OsRR7).

- CRISPR was used to generate mutant plants, and genotyping revealed homozygous and heterozygous mutants for OsPHP3 and OsRR7.

- More detailed studies on reporters and mutants (including multiple mutants) will be beneficial to gain a detailed understanding of gene function.

7. Discussion

In this thesis, I have examined how auxin and cytokinin communicate to specify vascular pattern in rice roots. While many complex and converging signalling pathways are involved in vascular development, the focus of this project has been on finding a functionally equivalent signalling pathway in rice to the mutually inhibitory feedback loop determined by AHP6 in *Arabidopsis*. AHP6 plays a major role in specifying boundaries between protoxylem and procambium. In *Arabidopsis*, AHP6 (as an auxin inducible inhibitor of cytokinin signalling) mediates cross-talk between these two hormones, resulting in distinct boundaries of hormonal signalling and consequent specification of cell fate (Mähönen et al. 2006; Bishopp et al. 2011). This thesis examines whether rice also makes use of proteins with an AHP6-like function to allow communication between the auxin and cytokinin signalling pathways, to regulate vascular patterning.

7.1 Vascular anatomy is primarily dependent on cultivar rather than the environment

The importance of vascular anatomy for improving water use efficiency and consequent drought tolerance has been demonstrated multiple times, including in breeding studies where changes in xylem vessel size and number affected plant fitness. Richards & Passioura (1989), for example, showed breeding to reduce xylem vessel size in wheat roots improved drought tolerance, with no yield penalty when plants were grown in well-watered

conditions. Although this study took place in specific environmental conditions found in Eastern Australia where there is availability of deep groundwater but the topsoil is dry, this study indicated the potential for manipulating xylem anatomy for improved water use efficiency. Screenings of diverse cultivars of rice has also indicated drought tolerant varieties have fewer, smaller xylem vessels (Henry et al. 2012). The two major growing environments for rice are rainfed upland or irrigated (flooded) lowland areas and these two environments favour the use of different cultivars, largely due to the ability of these cultivars to adapt to the local environment (Parameswari et al. 2014). In upland areas where farmers are reliant on rainfall rather than irrigation, plants frequently experience water stress and consequently drought tolerant cultivars have been selected and are predominantly grown in these areas. In irrigated lowland areas, where plants are often grown in flooded paddy fields, such selection pressures are not present and consequently rice favoured in these environments may be more susceptible to drought. As such, the growing environment of particular cultivars can, to a certain extent, be used to infer drought tolerance.

The response to drought is complex and tolerance is governed by multiple traits, both physiological and anatomical (Henry et al. 2012). Previous work comparing upland and lowland cultivars identified root architectural and anatomical traits which are important in drought tolerance and show differences across cultivars (Uga et al. 2009). However, understanding the influence of anatomy on physiology has not been studied in such great detail. Since root xylem anatomy directly affects water availability to plants, I

hypothesised that differences in root xylem anatomy may be directly related to physiological measures such as rate of photosynthesis (for which water availability can be a limiting factor), and consequently root xylem anatomy would be a major factor in enabling drought tolerance. In order to test this, 4 lowland and 8 upland cultivars were chosen for anatomical and physiological analysis (with physiological analyses conducted by Umar Mohammed, the University of Nottingham). These included the African rice (*Oryza glaberrima*) accession CG14, the Asian rice (*Oryza sativa*) cultivars FARO52, IR64, and Kaybonnet, and a number of improved cultivars developed by crossing African and Asian rice cultivars (NERICA cultivars). While probable confounding factors may make linking root xylem anatomy to physiological measurements difficult, the more extreme root xylem phenotypes may be more easily correlated to physiological responses. For example, of the cultivars examined Nerica 7 (an upland cultivar) shows the largest central and peripheral metaxylem areas (Figure 3.3), and one of the highest rates of transpiration, stomatal conductance and photosynthesis (Figure 3.4). In terms of reducing photosynthesis rates, this cultivar also responds most severely to drought stress, possibly as a result of its root xylem phenotype (Figure 3.5). This is not what was expected from an upland cultivar which was assumed to show drought tolerance, although it may be the case that other adaptations make this cultivar more suitable for growth in upland environments. However, none of the analyses showed correlation of root anatomy or physiology between upland or lowland cultivars. This indicates differences in both root radial anatomy and physiological measures are more dependent on the particular

cultivar than on the environment, with no obvious common features shared between upland and lowland cultivars. Another factor to consider is the drought response strategy employed by different cultivars. While some cultivars may grow more slowly and minimise water use upon drought stress, other may attempt to complete their life cycle as quickly as possible. This could explain the differences in response seen here.

In addition, roots also show a degree of plasticity in response to various stresses. When grown with osmotic stress, Kitaake primary roots show a significant decrease in central, but not peripheral, metaxylem area (Figure 3.9). In addition to changing anatomy, a major response to osmotic stress is a decrease in root length. Different cultivars may show differences in plasticity of response to drought, meaning looking at root growth in diverse cultivars in response to drought would be valuable to determine how responsive they are to drought.

7.2 Vascular pattern is dependent on stele size

Whereas *Arabidopsis* roots show a consistent vascular anatomy, that of rice roots is considerably more variable, even when considering single genotypes. This is true both in terms of anatomical variation across different root types, and variation seen within a single root type. Different root types show differences in vascular anatomy based on stele size (Figure 3.6), with those displaying larger steles (such as crown roots) having more vascular poles than those with smaller steles (such as lateral roots). The number of vascular poles

within a single root is not constant but also changes depending on stele size. As the root narrows towards the tip, the number of vascular poles decreases (Figure 3.7). This raises questions about initial pattern formation in roots and the process of re-patterning throughout growth. Once an initial fixed pattern is specified it cannot be changed as the root grows, but this initial pattern can be adapted in younger immature sections of the same root which have different spatial constraints. Since the highest number of vascular poles is consistently seen towards the top of the root, regardless of root age, this indicates re-patterning takes place in the developing root primordia as the root grows. It is this re-patterning process which seems to be influenced by stele size, with loss of vascular poles as the root narrows.

In order to determine whether the molecular mechanisms which pattern the root vasculature of *Arabidopsis* are able to give rise to the diverse vascular patterns seen throughout flowering plants, Mellor et al (in review) developed a mathematical model to test this (see Appendix for manuscript). Previous modelling work has indicated an initial asymmetry is required between auxin and cytokinin, to develop the stable diarch vascular pattern seen (De Rybel et al. 2014; Muraro et al. 2014; el-Showk et al. 2015; Mellor et al. 2017). These studies have suggested that this asymmetry arises from differential accumulation of auxin, following transport from the two cotyledons during embryogenesis (De Rybel et al. 2014). In support of this, mutants with altered cotyledon number show corresponding changes in number of xylem poles in the hypocotyl (Help et al. 2011). While these studies can explain early pattern development in *Arabidopsis*, they cannot explain patterns seen in many other

species. Many eudicots show more than two root vascular poles early in development, and many monocots (such as rice) show over five (Esau 1977). This indicates the involvement of other mechanisms. The idea that the number of vascular poles is constrained by the size of the stele is not new. In 1884 de Bary et al. described the observation that as root thickness decreases, so does the number of vascular poles. Early work by Wardlaw (1929) and Bower (1930) indicated the number of vascular strands is almost directly proportional to stele diameter, and this work enabled a better understanding of morphology outside of plant science. By using a simple static model consisting of three components (auxin, cytokinin and PIN) in a ring of cells of fixed number, it was observed that poles of high auxin response (inferred as cells primed for xylem differentiation) are produced. Increasing the number of cells increases the likelihood of a higher number of xylem poles developing, in a similar manner seen in rice roots experimentally (Figure 3.7). In addition to this static model, a growing model was developed which showed organ growth is involved in stabilising the patterning process. Together, these models suggest that an initial asymmetry in auxin is not required for stable pattern formation, and instead the final pattern formed is dependent upon spatial constraints and growth. This indicates that the basic mechanisms (mutually inhibitory activity between auxin and cytokinin) governing root vascular patterning in *Arabidopsis* would in theory be sufficient to specify the alternative vascular pattern in rice, with different patterns arising primarily due to the different morphological context. As this is a simple model which does not explicitly model individual mechanistic components but rather describes the three major components (auxin, cytokinin

and PIN proteins), it is not possible to determine whether homologous genes would regulate this process in rice roots.

7.3 Auxin and cytokinin influence rice root vascular development

While modelling suggests the basic mechanisms governing root vascular patterning (involving communication between auxin and cytokinin signalling) may be conserved between *Arabidopsis* and rice, various experimental lines of evidence support this. Growing *Arabidopsis* and rice on media with cytokinin (BA) or the inhibitor of auxin transport NPA point to the crucial roles of these two hormones in proper development of the rice root vasculature. When *Arabidopsis* is grown with BA, plants show loss of protoxylem in a similar manner seen in the *ahp6* mutants (which also has elevated cytokinin levels). In rice grown with BA, loss of protoxylem and often metaxylem is seen (Figure 3.10). When grown with NPA, *Arabidopsis* initially shows loss of root protoxylem, but with time multiple aberrant xylem poles develop throughout the stele (Bishopp et al. 2011). When rice is grown with NPA plants show smaller central metaxylem vessels which are surrounded by abnormally elongated cells, over proliferation of peripheral protoxylem and lignin deposition in cell walls throughout the entire stele. NPA acts via inhibition of polar auxin transport suggesting that the observed phenotype results from aberrant accumulation of auxin.

Although the action of cytokinin on auxin signalling is complex and not fully understood, it has been shown to be largely dependent on activity of PIN

proteins. Previous studies have indicated cytokinin inhibits expression of PINs, as well as leading to their post-transcriptional degradation, in some cases in a manner dependent on their polar localisation (Dello Ioio et al., 2008; Zhang et al., 2011b; Marhavy et al., 2011; Marhavy et al., 2014). In *Arabidopsis*, cytokinin treatment (at least in the young seedling) phenocopies NPA treatment. In both cases, auxin flow is redirected leading to loss of auxin signalling at the protoxylem position, and consequent inhibition of protoxylem differentiation. In rice BA treatment results in loss of protoxylem (and sometimes metaxylem), whereas NPA treatment results in huge over-proliferation of protoxylem (amongst various other anatomical changes). The reasons for these differences are unknown and should be tested, firstly by looking at expression of auxin-responsive reporters upon cytokinin and NPA treatment. It may be the case that cytokinin has a different activity on rice PINs, in part due to the different spatial constraints of the rice vasculature.

A mutant identified from an EMS screen in barley (which shows a similar polyarch root vascular pattern to rice) displays a similar phenotype to NPA treated roots in rice (developed by the lab of Silvio Salvi, the University of Bologna). Compared to wild type barley roots, the mutant shows a smaller central metaxylem vessel, larger cells surrounding the central metaxylem vessel and proliferation of peripheral metaxylem (Cristovao De Jesus Vieira Teixeira, personal communication). Treatment of wild-type barley (cultivar Morex) with NPA phenocopies the mutant (Figure 7.1), implying deficient auxin transport in the mutant. This mutant has been identified as a *pin1* mutant, confirming the phenotype results from abnormal distribution of auxin in the root. While little

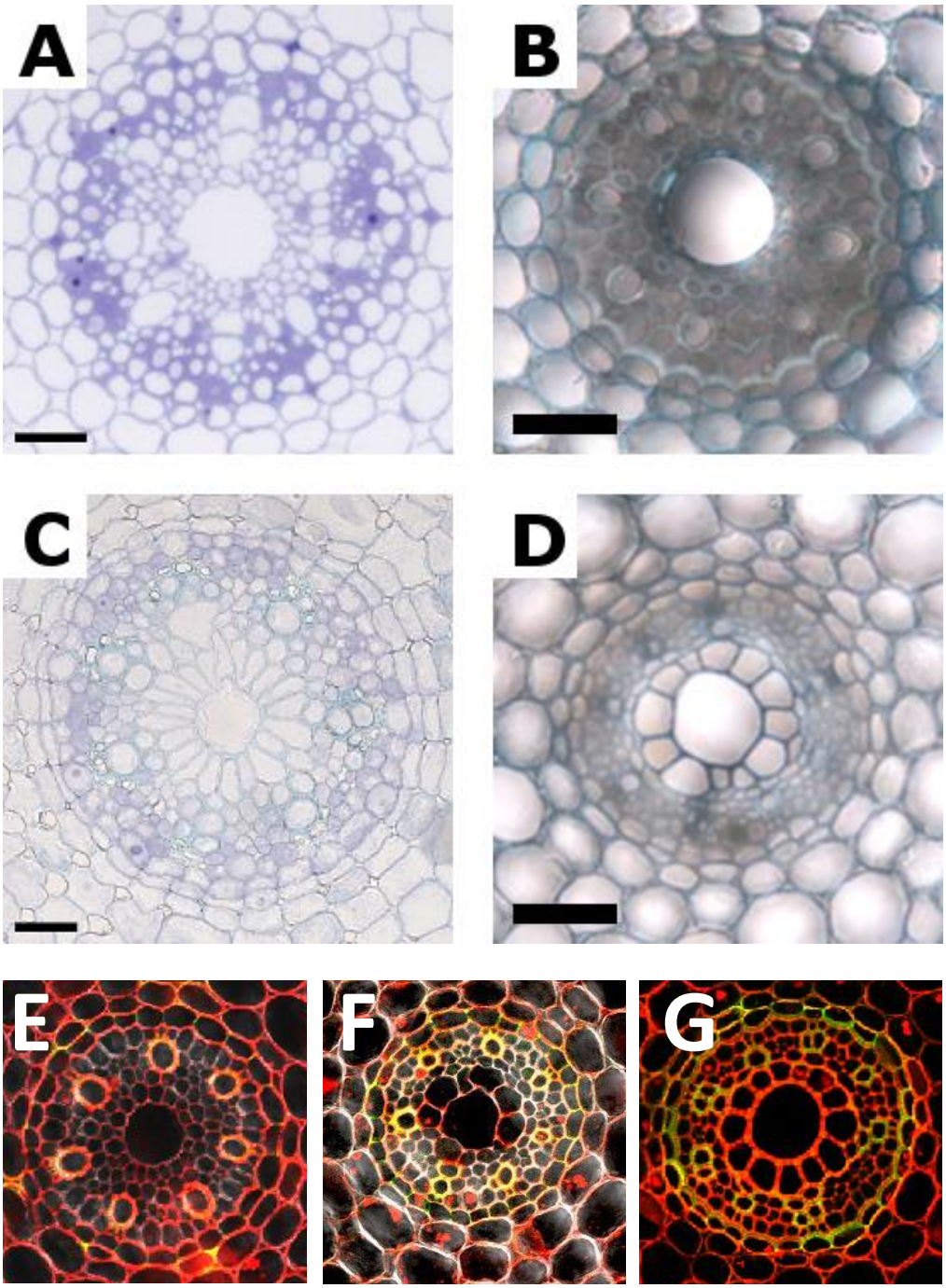


Figure 7.1. The barley *pin1* mutant phenocopies the NPA treatment phenotype seen in rice. Wild type rice (Kitaake) (A) and barley (Morex) (B) develops elongated cells surrounding the central metaxylem vessel, over-proliferation of peripheral metaxylem vessels and more lignin deposition throughout the stele upon NPA treatment (C) or mutation in *pin1* (D). Growth of wild-type barley (E) with NPA (F) phenocopies the mutant phenotype (G). A to D were stained with toluidine blue, E to F were stained with calcofluor and imaged to detect fluorescence. Scale bars in A and D are 20 µm and B and D are 50 µm. Barley images obtained by Cristovao De Jesus Vieira Teixeira.

is currently known about the PIN proteins in barley, studies have been conducted to characterise the PIN protein families of other monocots (reviewed by Balzan et al. 2014).

Monocots often have multiple copies of PIN proteins, resulting from whole genome duplications and retention of similar genes in these lineages. For example, in rice there are four copies of PIN1 (named OsPIN1a – d), all of which show differing tissue specific expression patterns (Wang et al. 2009). In *Brachypodium distachyon* there are two PIN1s (BdPIN1a and BdPIN1b), with BdPIN1b showing a wider expression pattern and BdPIN1a confined to narrow canals in the SAM. Modelling of the two copies of PIN1 along with Sister-of-PIN1 (SoPIN1) – a protein conserved in angiosperms but lost in the Brassicaceae - allowed authors to propose that these three proteins play distinct roles which together form the minimal set of functions required for patterning organ initiation and the vasculature at the SAM (O'Connor et al. 2014). More recently, *Brachypodium* mutants and heterologous expression analyses have been used to confirm this, with authors suggesting that the different functions performed by these proteins in *Brachypodium* are performed by one protein in *Arabidopsis* – AtPIN1 (O'Connor et al. 2016). The severe phenotype in the single barley *pin1* mutant suggests this protein may be the key PIN1 copy involved in transporting auxin into cells which consequently differentiate as xylem. No PIN1 mutants in rice have yet been identified, and consequently the *pin1* mutant in barley may provide insight into the functions of rice PINs. Creating mutants of barley PIN1 homologues in rice could be used to confirm whether a single PIN may play a similar role in rice. These results also support the hypothesis that the basic

mechanisms governing vascular patterning are highly conserved throughout flowering plants.

7.4 OsPHPs are unlikely to function in an AHP6-like manner in rice roots

If the OsPHPs are to function in rice root vascular patterning in an analogous manner to AHP6 in *Arabidopsis*, one requirement would be that they are inducible by auxin in the root tip. Publicly available microarray data, and more detailed qRT-PCR data presented here (Chapter 4), indicate this is not the case. In order to test whether OsPHPs are functional in planta, they were expressed under the AHP6 promoter in *Arabidopsis ahp6* mutants and analysed for trans-complementation of the mutant loss of protoxylem phenotype. A mutant version of AHP6 was prepared with the conserved N residue (which takes the place of the phosphoaccepting histidine residue of the HPTs) substituted for a Q residue, as is seen in the OsPHPs. This version of AHP6 is able to rescue the mutant phenotype at the same level as wild type AHP6, showing PHPs with this substitution can act as functional inhibitors of cytokinin signalling. However, none of the OsPHPs are able to rescue the *ahp6* mutant phenotypes. These results may point to differences in binding specificity between the OsPHPs and *Arabidopsis* cytokinin receptors and RRs. As the mechanism of action of the OsPHPs is assumed to be to compete with the HPTs by binding cytokinin receptors and RRs, it may be the case that rice OsPHPs show lower binding affinity for *Arabidopsis* proteins than AtHPTs, preventing OsPHPs complementing the *ahp6* mutant phenotype. This could be tested in a number

of ways. Biochemical assays could be conducted to determine binding affinities of proteins in vitro, to verify the likelihood of AtHPTs binding *Arabidopsis* cytokinin receptors and RRs over OsPHPs binding the same proteins. Alternatively, protein-protein interactions could be inferred in vivo through the use of yeast two-hybrid assays. In this system, proteins to be tested are expressed as fusions containing either an activation or a DNA-binding domain of a transcription factor, which upon interaction will induce expression of a reporter gene. The use of reporter genes, such as *lacZ* for colourimetric assays, are useful for quantitative determination of protein interactions (reviewed by Stephens & Banting 2000). These assays would be useful to understand the reason the OsPHPs are unable to rescue *Arabidopsis ahp6* mutants.

Differences in binding between AHP6 or the OsPHPs and the *Arabidopsis* cytokinin receptors or RRs may simply be a result of sequence divergence in the different species. Calculation of amino acid sequence similarities show that while sequence similarity between AtAHP6 and OsPHPs is low (between 36 and 36.67 %), sequence similarity between the OsPHPs and the AtHPTs is higher (between 38.16 and 62.76 %) than that between AHP6 and AtHPTs (between 39.87 and 44.67) (Figure 4.4). However, the AtHPT with highest similarity to the OsPHPs by far is AtAHP4 (with 62.76, 55.86 and 60.69 % similarity to OsPHP1, OsPHP2 and OsPHP3 respectively), whereas similarity of most other AtHPTs is around the level of 40 % - close to that between AHP6 and AtHPTs. These calculations support the phylogeny placing AtAHP4 as arising independently of the other AtHPTs. This does however raise questions about the function of AtAHP4, and whether the OsPHPs could be playing similar roles. The role of

AtAHP4 in phosphorelay is not clear, and it has been suggested it may function as an inhibitor of cytokinin signalling in some contexts (albeit via unknown mechanisms) (Hutchison et al. 2006). While no expression is seen in roots, stems or leaves, AtAHP4 has been shown to play a role in anther endothecium development where it negatively regulated secondary cell wall thickening (Jung et al. 2007). While the exact mechanism of action remains unknown, AtAHP4 has been proposed to function (at least in part) via indirectly inhibiting expression of the type-B RR AtARR22 (Jung et al. 2007). In this way AtAHP4, although an HPT, may act to inhibit cytokinin signalling upon activation by accepting a phosphate group. Expressing AtAHP4 in the AHP6 domain of the *ahp6* mutants could be used to test whether it inhibits cytokinin signalling, although this may be complicated by the requirement for expression of other proteins in the same domain (such as AtARR22) to function in inhibition (Jung et al. 2007). It is possible that the OsPHPs, given their similarity to AtAHP4, may regulate cytokinin signalling via similar downstream mechanisms, which could explain their inability to complement if these proteins are not present in this domain.

AHP6 has been shown to function in many developmental contexts which require cross-talk between auxin and cytokinin, such as in lateral root development (Moreira et al. 2013), SAM regulation of organ initiation and phyllotaxy (Besnard et al. 2013; Besnard, Rozier, et al. 2014), and development of the gynoecium (Reyes-Olalde et al. 2017). In other species, AHP6 homologues have also been suggested to function in other developmental processes such as root nodule development in *Medicago* (Sofia Moreira et al.

2013). While this study showed activity of the *Arabidopsis* AHP6 promoter in lateral roots and root nodules, the *Medicago* homologues of AHP6 have not been tested so may not share expression patterns described. In order to better describe the functions of the OsPHPs, I generated reporter lines and identified mutants generated using CRISPR. Whilst these studies are in the early stages, I have shown OsPHPs have differences in expression patterns, but all three show expression in the root tip. While all three OsPHPs show expression in the root tip only OsPHP1 was seen in protoxylem poles. OsPHPs also show specific and differing expression patterns in leaves, with OsPHP2 strikingly localised to stomata, and OsPHP3 being present in the central vein. Recently, cytokinin has been implicated in regulating stomatal density in tomato (Farber et al. 2016). The same may be true in rice, and the strong expression of OsPHP2 in stomata suggests it may be involved in regulating cytokinin signalling to control stomatal density.

Results obtained by qRT-PCR suggest low levels of expression of OsPHPs in root tips (Figure 4.8 to 4.11), yet reporters show clear root tip expression (Figure 6.1, 6.5, 6.8). To understand this discrepancy, qRT-PCR was performed to detect expression of OsPHP1 and GUS in the reporter, upon IAA and BA treatment. Cp values obtained for OsPHP1 were considerably more variable than those for GUS, and no significant differences are seen upon treatment with either hormone, for both OsPHP1 and GUS. This suggests that OsPHP1 is not induced by auxin or cytokinin (or at least not strongly induced) in the root tip, and that the primers used to detect OsPHP1 expression by qRT-PCR were sub optimal. The same may be true for those of all OsPHPs, and consequently hormonal

induction in the root tip for these genes should be repeated using different primers.

However, there are a number of other possibilities which could explain this discrepancy. For reporters, around 3 to 4 kb of promoter sequence immediately upstream of the start codon was used. While these are large sequences, there is the potential that there are important regulatory elements outside of this (possibly in the exon) which were missed. Alternatively, there may be regulatory elements in introns which could influence expression levels. Although experimental detection is required to confirm auxin inducibility of genes, this may be predicted by the presence of Auxin Response Elements (AuxREs) in the promoter. AuxREs are binding sites for Auxin Response Factors (ARFs), transcription factors which regulate auxin response. There are various AuxRE sequences which ARFs are able to bind to, with the most common being TGTCTC. However, only the first four nucleotides are crucial for ARF binding, with variation in sequence requirement observed for the other two (Ulmasov et al. 1999). In AHP6, the 1.6 kb promoter has 1 TGTCTC site and has 8 putative AuxREs with the sequence TGTC (Bishopp et al. 2011). The promoters of the OsPHPs also have similar numbers of AuxREs for the size of their promoter, indicating they may be regulated by auxin (Figure 7.2). It could be the case that while what is seen from the reporters is accurate, the qRT-PCRs were giving misleading results due to degradation of OsPHP mRNA. This discrepancy could be resolved by performing RNA in-situ hybridisations to directly visualise localisation of mRNA. The same approach could be used to determine whether OsPHPs are induced by auxin or cytokinin. In addition, making translational

Promoter	AuxRE sequences	
	TGTC	TGTCTC
AHP6 1.6 kb	8	1
OsPHP1 4 kb	21	1
OsPHP2 4 kb	25	2
OsPHP3 4 kb	22	0
OsRR1 4kb	22	2
OsRR3 4kb	19	1
OsRR6 4kb	30	2
OsRR7 4kb	24	0

Figure 7.2. The number of AuxRE sequences in the promoters of AHP6 and the OsPHPs and type-A OsRRs studied.

fusions could be used to prove induction of expression without direct visualisation of mRNA. If protein is seen in greater abundance upon hormonal treatment in translational fusions, while no changes are seen in RNA in-situ hybridisations, this would suggest that mRNA is quickly degraded after translation, or the protein is stabilised upon hormonal treatment. Additionally, the effect of auxin on the OsPHPs could be determined by treating the transcriptional reporters with NPA and observing resulting changes in expression patterns. If conducted alongside NPA treatment in the DR5 reporter this would show whether OsPHP expression patterns match auxin accumulation.

7.5 OsRR1, OsRR6 and OsRR7 may function in an AHP6-like manner in rice roots

The data so far suggests the OsPHPs do not function in an AHP6-like role in vascular patterning of rice roots. I hypothesised that the type-A OsRRs (as known inhibitors of cytokinin signalling), may function in this role. Multiple lines of evidence suggest that the type-A RRs OsRR1, OsRR6 and OsRR7 may function in rice root vascular patterning. These three genes are highly induced by auxin in the root tip (Figure 4.8 and 4.9) and are able to rescue the *Arabidopsis ahp6* mutants when expressed under the AHP6 promoter (Figure 5.5 and 5.6). Their ability to function in place of AHP6 in *Arabidopsis* suggests these genes may also be functional in rice roots to mediate cytokinin signalling in an auxin dependent manner, for proper vascular pattern development. However, these

genes are also primary response genes upregulated by cytokinin, whereas AHP6 is down-regulated by cytokinin after a longer (6 hours) time period. This indicates that if these genes function in an AHP6-like manner in rice roots, the signalling context they are placed in must be adapted to accommodate this.

The ability of OsRR1, OsRR6 and OsRR7 to complement the *Arabidopsis ahp6* mutants (while the OsPHPs do not) may be more related to the mechanism of action of the type-A OsRRs. While it is assumed the PHPs competitively inhibit binding of the HPTs to cytokinin receptors and RRs, the type-A RRs inhibit cytokinin signalling via sequestering phosphate groups and/or via unknown downstream protein-protein interactions dependent on their phosphorylation status. In terms of protein-proteins interactions involved, it may be easier for the rice type-A RRs to accept phosphate groups from *Arabidopsis* HPTs, than it is for OsPHPs to bind *Arabidopsis* cytokinin receptors and RRs. To answer this question, it would be valuable to determine whether AHP6 is able to rescue mutants of the OsPHPs and OsRR1, OsRR6 and OsRR7 in rice. Before this can take place the rice mutants identified will have to be phenotyped in detail, with the possibility that multiple mutants will need to be generated before visible phenotypes result. Alternatively, this discrepancy may be explained by the OsPHPs having to bind two classes of protein (receptors and RRs) whereas type-A OsRRs only have to bind one (HPT), to bring about their response. Again, this may come down to sequence divergence in the different species. Percentage amino acid sequence similarities between OsPHPs and AtHPTs are close to those of AHP6 and AtHPTs (with the exception of AtAHP4, which shows much greater similarity to the OsPHPs as previously discussed). This suggests

(indirectly) that the OsPHPs will be able to bind the same cytokinin receptors and RRs which the other HPTs and AHP6 bind (although there may be a preference for interaction with the proteins AtAHP4 binds with). Sequence similarities between the type-A RRs of *Arabidopsis* and rice range from 37.75 to 62.88 %, which is not far from the range seen within the type-A RRs from *Arabidopsis* themselves (44.68 to 80.87 %) (Appendix Figure 12). This suggests many type-A OsRRs would be able to accept phosphate groups from AtHPTs, and therefore inhibit cytokinin signalling through phosphate group sequestration. This is supported by phylogenetic analysis, with the spread of type-A RRs of monocots and dicots mixed throughout the tree indicative of similarity between these proteins in the two groups (Figure 7.3). The ability of these proteins to bring about inhibition of cytokinin signalling via downstream protein-protein interactions dependent on their phosphorylation status is unclear.

While OsRR1, OsRR6 and OsRR7 do complement the *ahp6* mutant phenotypes, not every type-A RR does. OsRR3 has little effect, whereas AtARR5 leads to an increase in severity of the protoxylem defect of *ahp6-1* (Figure 5.5 and 5.6). Given that amino acid sequence similarity of these two type-A RRs is similar to those of the OsRRs which rescue the *ahp6* mutants, this suggests these proteins are still likely to bind AtHPTs. However, sequence similarity between proteins does not guarantee interaction, and it is unclear what downstream protein-protein interactions the type-A RRs make use of to regulate cytokinin signalling. ARR5, as a primary cytokinin responsive gene, has been used as a marker of cytokinin response. In the *Arabidopsis* vasculature, AtARR5 is expressed in the

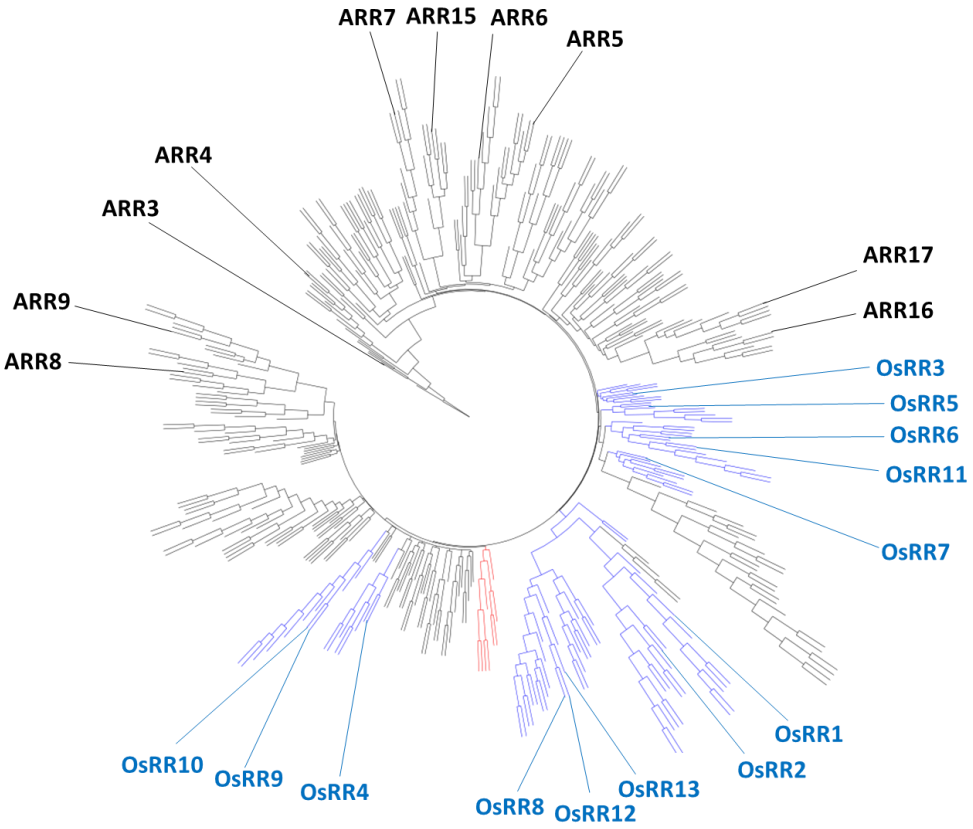


Figure 7.3. Phylogenetic relationships between the type-A RRs of 38 different species; six monocots, thirty eudicots, *Selaginella moellendorffii* and *Physcomitrella patens* (see appendix for list of species included). Coloured clades indicate proteins from eudicots (black), monocots (blue) or those from *Selaginella* and *Physcomitrella*. The *Arabidopsis* and rice type-A RRs are labelled. The phylogeny is based on 100 bootstrap replicates. For simplicity, bootstrap values are not shown but the fully annotated tree is available at http://bit.ly/2y9Rh3B.

procambium, and extends into the protoxylem domain when cytokinin signalling inhibition is abolished as a result of a mutation in *ahp6* (Bishopp et al. 2011). AtARR5 expression is directly induced by cytokinin signalling and down-regulated by auxin, unlike AHP6 which is directly induced by auxin and down-regulated by cytokinin (possibly as a secondary response dependent on auxin signalling) (D'Agostino et al. 2000; Lee et al. 2009). However, when driven by the AHP6 promoter it is assumed this activity of AtARR5 will be abolished and it will be inducible by auxin, not cytokinin. Although the mechanism of action is still unclear, AtARR5 has been shown to inhibit cytokinin signalling via downstream protein-protein interactions which are dependent on phosphorylation status, rather than via phosphate scavenging alone. The targets of AtARR5 are still unknown, but may explain why the severe loss of protoxylem phenotype is seen when AtARR5 is expressed in the AHP6 domain of the *ahp6-1* mutant in the complementation assays. This could be studied by using protein pull-down assays, which would reveal protein targets of AtARR5 and potentially reveal a mechanism of cytokinin signalling inhibition. Another factor worth considering is the stability of the type-A RRs (Ren et al. 2009; To et al. 2007). A subset of the type-A RRs are stabilised in response to cytokinin signalling, which may affect their activity in the protoxylem domain where there is a lack of cytokinin signalling.

In order to better characterise the type-A OsRRs studied, I generated reporters and identified mutants generated by CRISPR for these genes. As with those of the OsPHPs, these lines are in the early stages of analysis but expression data for reporters does give some interesting hints about the different

developmental roles of these genes. While OsRR1 shows patchy expression in the root mainly localised to the epidermis, OsRR3 and OsRR7 shows strong expression throughout the root tip with expression in radial sections seen in protoxylem. In leaves, OsRR1 shows expression in some (but not all) stomata, and OsRR7 shows expression specifically at distal ends of transverse vessels which connect the parallel vascular bundles. Auxin and cytokinin have been implicated in development of these transverse vessels with the rice *ral1* mutant, which shows insensitivity to auxin and hypersensitivity to cytokinin, displaying (amongst various other changes) defective development of these transverse vessels (Scarpella et al. 2003). OsRR7 may play a role in development of these vessels. Expression patterns of OsRR6 are yet to be analysed.

A plausible model for rice root xylem patterning may be OsRR1, OsRR6 and OsRR7 (possibly with input from OsRR3 which is expressed in the protoxylem), acting together with OsPHP1 (which is expressed in the protoxylem but whose auxin response remains unclear) and possibly the other OsPHPs, as the node governing crosstalk between auxin and cytokinin in this process. In this way, these genes may act redundantly in the patterning process. To date, no *Arabidopsis* type-A RR has been shown to be auxin inducible in the root tip. However, searching the gene expression database in eFP Browser (Winter et al. 2007) reveals the only type-A RR of *Arabidopsis* which is up-regulated by auxin is AtARR17 (Figure 7.4). AtARR17, like the type-A OsRRs examined, is up-regulated by cytokinin as well as auxin, although response to both hormones is slower than that of the OsRRs with changes only seen after an hour treatment. From looking at differential tissue expression data from the same database it is

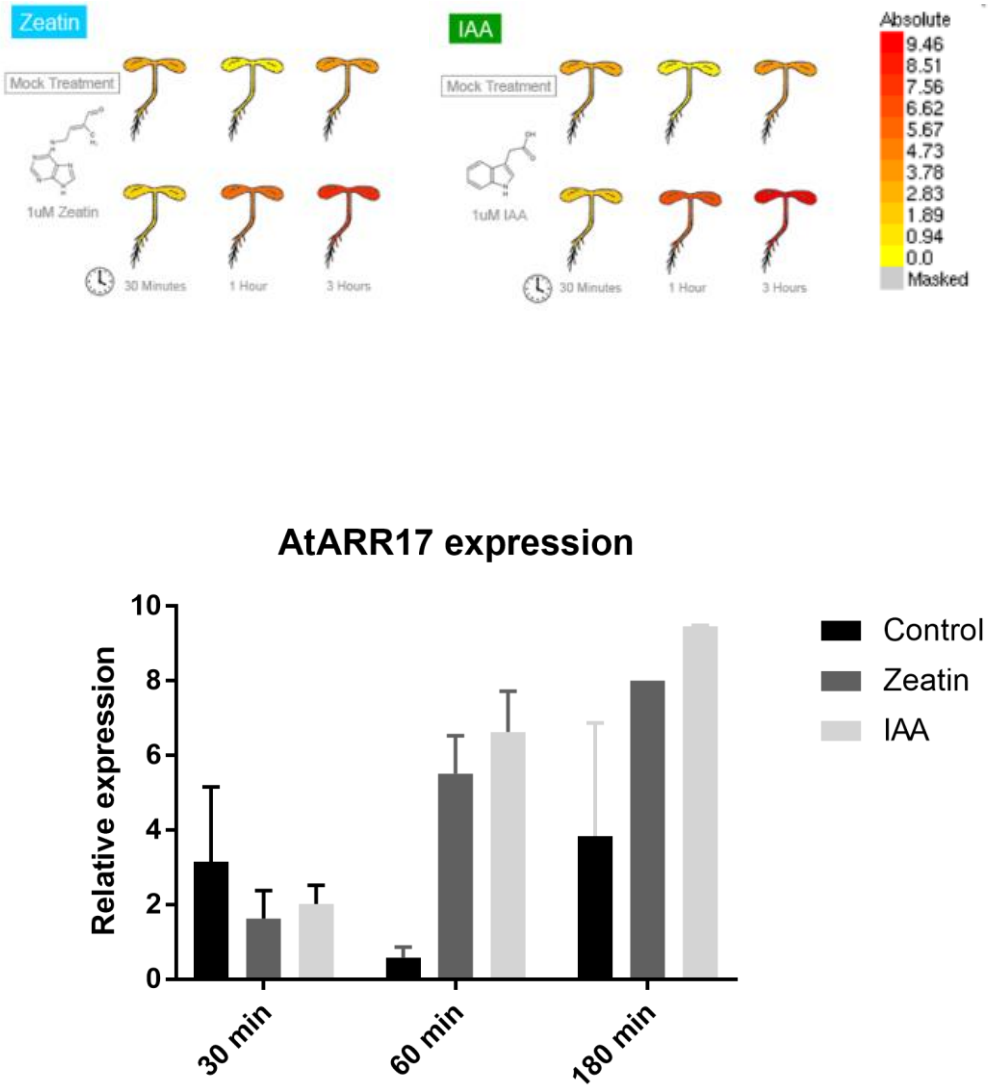


Figure 7.4. The type-A RR AtARR17 is induced by auxin and cytokinin treatment. The same data is represented by heat map and chart. Data was taken from the *Arabidopsis* eFP Browser (Winter et al. 2007).

unclear if AtARR17 shows expression in the root, and more detailed study is required to confirm this. However, as an inhibitor of cytokinin signalling which is auxin inducible, AtARR17, or another candidate, may act together with AHP6 to regulate hormonal crosstalk in xylem specification. This could explain why the *ahp6* mutant phenotypes are not fully penetrant. To determine whether this is the case AtARR17 should be studied in detail, using reporters to determine expression patterns and creating mutants to see if resulting phenotypes share similarity to those of *ahp6* mutants. Generating an *ahp6 arr17* double mutant could be used to confirm whether these genes act in consort to inhibit cytokinin signalling in the protoxylem domain. An increase in severity of the protoxylem defect in the double mutants as compared to the single mutants would suggest this is the case. In addition, it would be useful to determine whether AtARR17 is able to rescue the *ahp6* mutant phenotype (and possibly vice versa if obvious phenotypes result from the *arr17* mutant).

Taken together, this work has suggested that rice may have adopted a subset of the type-A RRs to fulfil the role AHP6 plays in *Arabidopsis*. While OsRR1 and OsRR7 show differing expression patterns, they overlap in root tips upon hormonal treatment. Although OsRR6 expression patterns have not yet been analysed, it may show similar patterns. In this case OsRR1, OsRR6 and OsRR7 may function redundantly. In addition, although possibly not directly induced by auxin, OsPHP1 does show expression in root protoxylem, indicating it may function as a constitutive inhibitor of cytokinin signalling in this domain.

7.6 Future work

This work suggests that the OsPHPs are unlikely to function in a similar mutually inhibitory feedback loop between auxin and cytokinin signalling which specifies protoxylem domain. However, reporters have indicated expression of these genes in roots and other tissues. It has been assumed that the OsPHPs would function in inhibition of cytokinin signalling in a similar manner to AHP6, but the inability of OsPHPs to rescue the *Arabidopsis ahp6* mutant shows this cannot be confirmed in planta. Instead, more direct approaches are required to definitively show the inhibition of cytokinin signalling by the OsPHPs. To this end, in vitro phosphotransfer assays were carried out, to directly follow transfer of radio-labelled phosphate through the cytokinin signalling system. These approaches allow determination of any functional differences which may occur between the different substituted residues seen in the dicot vs the monocot PHPs. So far these assays have shown that the wild type OsHPTs are able to accept the phosphate group, while versions of these proteins with the phosphoaccepting histidine residue substituted to an asparagine (as in dicot PHPs) or a glutamine residue (as in monocot PHPs) are unable to accept the phosphate group. While it is likely these mutant versions of the OsHPTs are able to function as inhibitors of cytokinin signalling, this has not yet been directly shown in these assays. The function of the OsPHPs as inhibitors of cytokinin signalling, and mutant versions of the OsPHPs with the phosphoaccepting histidine domain restored as positive regulators of cytokinin signalling, is yet to be shown. As well as directly showing whether the OsPHPs inhibit cytokinin signalling, these assays will also determine whether substitution of a single

amino acid to restore the phosphoaccepting histidine residue is enough to turn an inhibitor to a positive regulator of cytokinin signalling, as was already shown with AHP6 in *Arabidopsis* (Mähönen et al. 2006). In addition, as mutant versions of the same proteins have been made with this conserved residue showing an asparagine or a glutamine residue, these assays will show whether these different substitutions result in any functional differences in terms of intensity of inhibition of cytokinin signalling. In addition, the purified OsPHPs and mutant versions with the phosphoaccepting histidine restored may also be tested to determine whether the substitutions effect protein binding affinity. It may be the case that the PHPs show higher binding affinity to particular cytokinin receptors and RRs than the HPTs, allowing them to out compete and more efficiently block cytokinin signalling. Other assays may be used in future to help answer these questions.

While these in vitro assays are valuable in understanding the details of cytokinin signalling, to understand the role of the OsPHPs and type-A RRs identified reporters and mutant plants are required. While analysis of reporters has indicated potential functions, these analyses are incomplete. Of particular importance is understanding expression patterns of OsRR6, as this was one of the genes identified as highly auxin inducible in the root tip. In addition, responses of reporters to hormonal treatments do not correlate with what was observed from qRT-PCRs for the type-A OsRRs. Because reporter analysis was conducted with the little material which was available at the time, this could be an artefact of changes in root type or growth conditions. Consequently, these analyses should be repeated. In addition, it will be useful to look for expression

patterns in other tissues which were not included here, such as flowers. AHP6 plays important roles in crosstalk between cytokinin and auxin in the SAM and developing gynoecium (Besnard, Rozier, et al. 2014; Besnard, Refahi, et al. 2014; Reyes-Olalde et al. 2017), and it is likely some of the cytokinin signalling inhibitors of rice studied here may play similar roles.

While CRISPR mutants were generated and identified, preliminary phenotyping has not shown any differences in mutant phenotypes from wild type plants. However, this may be in part due to redundancy between gene family members. To determine whether this is the case, multiple mutants should be generated and analysed. It is also worth noting that resulting mutants should be analysed for multiple phenotypes (guided in part by expression patterns seen from reporters). For example, while OsRR7 mutants may show defective root vascular development, they are also likely to affect development of transverse vessels in leaves.

Given the great variation and plasticity of rice root vasculature, a feature not seen in *Arabidopsis*, it is of interest to consider how the underlying molecular mechanisms governing vascular development may be adapted to allow development of diverse phenotypes. In the long term, research in this direction may enable manipulation of root xylem anatomical traits and this may have impacts for future breeding. Many studies have shown that root vascular anatomy (amongst many other traits such as root architecture and more physiological responses) are important factors in adaptation to drought (Richards & Passioura 1989; Henry et al. 2012; Gowda et al. 2011; Torres &

Henry 2016). Therefore, understanding the details of vascular patterning may prove important in the effort to produce crops better suited to increasingly challenging environmental conditions. This is especially important in rice, which is often grown in flooded conditions and consequently many cultivars have not been selected for tolerance to drought. Modelling studies have shown development of a specific vascular pattern is dependent on spatial constraints placed by the size of the stele (Mellor et al. in review). Therefore, manipulating the size of the stele should allow manipulation of vascular anatomy. This may be considerably easier to achieve than manipulating specifically xylem anatomy, which is tightly regulated by complex and inter-connected networks.

In *Arabidopsis*, the bHLH transcription factors TMO5 and LHW function as dimers to regulate periclinal cell divisions of the vasculature, thereby regulating width (De Rybel et al. 2013). Whereas mutation of TMO5 and LHW family members leads to reduction, over-expression of these proteins leads to a striking increase in vascular cell file (De Rybel et al. 2013). Although these plants contain the same number of xylem poles, there is the potential that manipulating stele size could lead to changes in xylem number. More recently, cytokinin has been found to regulate auxin levels in the RAM by controlling both auxin transport and degradation (Di Mambro et al. 2017), and a role for gibberellin has also been revealed in regulating meristem size (Moubayidin et al. 2016). As the complex hormonal interactions governing meristem maintenance and vascular patterning become clearer, it will be beneficial to translate knowledge into other species. This will facilitate development of crops better able to tolerate increasingly unfavourable environmental conditions.

References

Alonso, J.M., Stepanova, A.N., Leisse, T.J., Kim, C.J., Chen, H., Shinn, P., et al. (2003) Genome-Wide Insertional Mutagenesis of Arabidopsis thaliana. *Science*, **301**, 653–657.

Ashikari, M., Sakakibara, H., Lin, S., Yamamoto, T., Takashi, T., Nishimura, A., et al. (2005) Cytokinin Oxidase Regulates Rice Grain Production. *Science*, **309**, 741–745.

Baima, S., Possenti, M., Matteucci, A., Wisman, E., Altamura, M.M., Ruberti, I., et al. (2001) The arabidopsis ATHB-8 HD-zip protein acts as a differentiation-promoting transcription factor of the vascular meristems. *Plant Physiol*, **126**, 643–655.

Balzan, S., Johal, G.S. and Carraro, N. (2014) The role of auxin transporters in monocots development. *Frontiers in Plant Science*, **5**, 393.

de Bary, A., Bower, F.O., Scott, D.H. and Scott, D.H. (1884) *Comparative Anatomy of the Vegetative Organs of the Phanerogams and Ferns,* Clarendon Press, Oxford.

Bauer, J., Reiss, K., Veerabagu, M., Heunemann, M., Harter, K. and Stehle, T. (2013) Structure-function analysis of arabidopsis thaliana histidine kinase AHK5 bound to its cognate phosphotransfer protein AHP1. *Molecular Plant*, **6**, 959–970.

Belda-Palazón, B., Almendáriz, C., Martí, E., Carbonell, J. and Ferrando, A. (2016) Relevance of the Axis Spermidine/eIF5A for Plant Growth and Development. *Frontiers in plant science*, **7**, 245.

Belda-Palazón, B., Nohales, M.A., Rambla, J.L., Aceña, J.L., Delgado, O., Fustero, S., et al. (2014) Biochemical quantitation of the eIF5A hypusination in Arabidopsis thaliana uncovers ABA-dependent regulation. *Frontiers in plant science*, **5**, 202.

Besnard, F., Refahi, Y., Morin, V., Marteaux, B., Brunoud, G., Chambrier, P., et al. (2014a) Cytokinin signalling inhibitory fields provide robustness to phyllotaxis. *Nature*, **505**, 417–21.

Besnard, F., Rozier, F. and Vernoux, T. (2014b) The AHP6 cytokinin signaling inhibitor mediates an auxin-cytokinin crosstalk that regulates the timing of organ initiation at the shoot apical meristem. *Plant signaling & behavior*, **9,** e28788-1–e28788-4.

Bishopp, A., Help, H., El-Showk, S., Weijers, D., Scheres, B., Friml, J., et al. (2011a) A mutually inhibitory interaction between auxin and cytokinin specifies vascular pattern in roots. *Current biology*, **21**, 917–26.

Bishopp, A., Lehesranta, S., Vatén, A., Help, H., El-Showk, S., Scheres, B., et al. (2011b) Phloem-transported cytokinin regulates polar auxin transport and maintains vascular pattern in the root meristem. *Current biology*, **21**, 927–32.

Bower, F.O. (1930) Size and Form in Plants. *Science*, **72**, 227–233.

Bürkle, L., Cedzich, A., Döpke, C., Stransky, H., Okumoto, S., Gillissen, B., et al. (2003) Transport of cytokinins mediated by purine transporters of the PUP family expressed in phloem, hydathodes, and pollen of Arabidopsis. *The Plant journal : for cell and molecular biology*, **34**, 13–26.

Capra, E.J. and Laub, M.T. (2012) Evolution of two-component signal transduction systems. *Annual review of microbiology*, **66**, 325–47.

Carlsbecker, A., Lee, J.-Y.Y., Roberts, C.J., Dettmer, J., Lehesranta, S., Zhou, J., et al. (2010) Cell signalling by microRNA165/6 directs gene dose-dependent root cell fate. *Nature*, **465**, 316–321.

Casimiro, I., Marchant, A., Bhalerao, R.P., Beeckman, T., Dhooge, S., Swarup, R., et al. (2001) Auxin transport promotes Arabidopsis lateral root initiation. *The Plant cell*, **13**, 843–52.

Chatterjee, J., Dionora, J., Elmido-Mabilangan, A., Wanchana, S., Thakur, V., Bandyopadhyay, A., et al. (2016) The Evolutionary Basis of Naturally Diverse Rice Leaves Anatomy. *PLOS ONE*, **11**, e0164532.

Comas, L.H., Becker, S.R., Cruz, V.M. V, Byrne, P.F. and Dierig, D.A. (2013) Root traits contributing to plant productivity under drought. *Frontiers in plant science*, **4**, 442.

Cucinotta, M., Manrique, S., Guazzotti, A., Quadrelli, N.E., Mendes, M.A., Benkova, E., et al. (2016) Cytokinin response factors integrate auxin and

cytokinin pathways for female reproductive organ development. *Development*, **143,** 4419-4424.

Cui, H., Levesque, M.P., Vernoux, T., Jung, J.W., Paquette, A.J., Gallagher, K.L., et al. (2007) An Evolutionarily Conserved Mechanism Delimiting SHR Movement Defines a Single Layer of Endodermis in Plants. *Science*, **316**, 421–425.

D'Agostino, I.B., Deruère, J. and Kieber, J.J. (2000) Characterization of the response of the Arabidopsis response regulator gene family to cytokinin. *Plant physiology*, **124**, 1706–17.

Datta, K. and Datta, S.K. (2006) Indica Rice (Oryza sativa, BR29 and IR64). *Agrobacterium Protocols* pp. 201–212. Humana Press, New Jersey.

Dello, I. R., Nakamura, K., Moubayidin, L., Perilli, S., Taniguchi, M., Morita, M. T., et al. (2008) A genetic framework for the control of cell division and differentiation in the root meristem. *Science*, **322**, 1380-1384.

Ding, W., Tong, H., Zheng, W., Ye, J., Pan, Z., Zhang, B., et al. (2017) Isolation, Characterization and Transcriptome Analysis of a Cytokinin Receptor Mutant Osckt1 in Rice. *Frontiers in plant science*, **8**, 88.

Doudna, J.A. and Charpentier, E. (2014) The new frontier of genome engineering with CRISPR-Cas9. *Science*, **346**, 1258096–1258096.

Du, Q. and Wang, H. (2015) The role of HD-ZIP III transcription factors and *miR165/166* in vascular development and secondary cell wall formation. *Plant Signaling & Behavior*, **10**, e1078955.

Eichinger, L., Pachebat, J.A., Glöckner, G., Rajandream, M.-A., Sucgang, R., Berriman, M., et al. (2005) The genome of the social amoeba Dictyostelium discoideum. *Nature*, **435**, 43–57.

el-Showk, S., Help-Rinta-Rahko, H., Blomster, T., Siligato, R., Marée, A.F.M., Mähönen, A.P., et al. (2015) Parsimonious Model of Vascular Patterning Links Transverse Hormone Fluxes to Lateral Root Initiation: Auxin Leads the Way, while Cytokinin Levels Out. *PLoS Computational Biology*, **11**, 1–40.

Enders, T.A. and Strader, L.C. (2015) Auxin activity: Past, present, and future. *American journal of botany*, **102**, 180–96.

Endo, H., Yamaguchi, M., Tamura, T., Nakano, Y., Nishikubo, N., Yoneda, A., et al. (2015) Multiple Classes of Transcription Factors Regulate the Expression of VASCULAR-RELATED NAC-DOMAIN7, a Master Switch of Xylem Vessel Differentiation. *Plant and Cell Physiology*, **56**, 242–254.

Esau, K. (1977) *Anatomy of Seed Plants*. Wiley, New York.

Farber, M., Attia, Z. and Weiss, D. (2016) Cytokinin activity increases stomatal density and transpiration rate in tomato. *Journal of experimental botany*, **67**, 6351–6362.

Fard, E.M., Bakhshi, B., Farsi, M., Kakhki, A.M., Nikpay, N., Ebrahimi, M.A., et al. (2017) MicroRNAs regulate the main events in rice drought stress response by manipulating the water supply to shoots. *Molecular bioSystems*.

Fassler, J.S. and West, A.H. (2010) Genetic and biochemical analysis of the SLN1 pathway in Saccharomyces cerevisiae. *Methods in enzymology*, **471**, 291–317.

Fassler, J.S. and West, A.H. (2013) Histidine phosphotransfer proteins in fungal two-component signal transduction pathways. *Eukaryotic cell*, **12**, 1052–1060.

Forner, J., Pfeiffer, A., Langenecker, T., Manavella, P.A., Manavella, P. and Lohmann, J.U. (2015) Germline-transmitted genome editing in Arabidopsis thaliana Using TAL-effector-nucleases. *PloS one*, **10**, e0121056.

Fukuta, Y., Konisho, K., Senoo-Namai, S., Yanagihara, S., Tsunematsu, H., Fukuo, A., et al. (2012) Genetic characterization of rainfed upland New Rice for Africa (NERICA) varieties. *Breeding science*, **62**, 27–37.

Fusco, G. and Minelli, A. (2010) Phenotypic plasticity in development and evolution: facts and concepts. Introduction. *Philosophical transactions of the Royal Society of London. Series B, Biological sciences*, **365**, 547–56.

Gajdošová, S., Spíchal, L., Kamínek, M., Hoyerová, K., Novák, O., Dobrev, P.I., et al. (2011) Distribution, biological activities, metabolism, and the conceivable function of cis-zeatin-type cytokinins in plants. *Journal of Experimental Botany*, **62**, 2827–2840.

Gallagher, K. L. & Benfey, P. N. (2009) Both the conserved GRAS domain and nuclear localisation are required for SHORT-ROOT movement. *The Plant Journal: for Cell and Molecular Biology*, **5**, 785–797.

Gillissen, B., Bürkle, L., André, B., Kühn, C., Rentsch, D., Brandl, B., et al. (2000) A New Family of High-Affinity Transporters for Adenine, Cytosine, and Purine Derivatives in Arabidopsis. *The Plant Cell Online*, **12**, 291-300.

Gowda, V.R.P., Henry, A., Yamauchi, A., Shashidhar, H.E. and Serraj, R. (2011) Root biology and genetic improvement for drought avoidance in rice. *Field Crops Research*, **122**, 1–13.

Gray, S.B. and Brady, S.M. (2016) Plant developmental responses to climate change. *Developmental Biology*, **419**, 64–77.

Grienenberger, E. and Douglas, C.J. (2014) Arabidopsis VASCULAR-RELATED UNKNOWN PROTEIN1 regulates xylem development and growth by a conserved mechanism that modulates hormone signaling. *Plant physiology*, **164**, 1991–2010.

Großkinsky, D.K., Edelsbrunner, K., Pfeifhofer, H., van der Graaff, E. and Roitsch, T. (2013) Cis- and trans-zeatin differentially modulate plant immunity. *Plant signaling & behavior*, **8**, e24798.

von Guttenberg, H. (1968) Der primäre Bau der Angiospermenwurzel. *Handbuch der Pflanzenanatomie*, **8**, 141–159.

Haeussler, M., Schönig, K., Eckert, H., Eschstruth, A., Mianné, J., Renaud, J.-B., et al. (2016) Evaluation of off-target and on-target scoring algorithms and integration into the guide RNA selection tool CRISPOR. *Genome Biology*, **17**, 148.

Hamim, H., Banon, S. and Dorly, D. (2016) Comparison of physiological and anatomical changes of C3 (*Oryza sativa* [L.]) and C4 (*Echinochloa crusgalli* [L.]) leaves in response to drought stress. *IOP Conference Series: Earth and Environmental Science*, **31**, 12040.

Hanzawa, Y., Takahashi, T. and Komeda, Y. (1997) ACL5: an Arabidopsis gene required for internodal elongation after flowering. *The Plant journal : for cell and molecular biology*, **12**, 863–74.

He, W., Adachi, S., Sage, R.F., Ookawa, T. and Hirasawa, T. (2017) Leaf photosynthetic rate and mesophyll cell anatomy changes during ontogenesis in backcrossed indica x japonica rice inbred lines. *Photosynthesis Research*. Epub ahead of print.

Heimsch, C. and Seago, J.L. (2008) Organization of the root apical meristem in angiosperms. *American journal of botany*, **95**, 1–21.

Help, H., Mähönen, A.P., Helariutta, Y. and Bishopp, A. (2011) Bisymmetry in the embryonic root is dependent on cotyledon number and position. *Plant Signaling & Behavior*, **6**, 1837–40.

Henry, A., Cal, A.J., Batoto, T.C., Torres, R.O., Serraj, R., DT, L., et al. (2012) Root attributes affecting water uptake of rice (Oryza sativa) under drought. *Journal of Experimental Botany*, **63**, 4751–4763.

Henry, S., Dievart, A., Divol, F., Pauluzzi, G., Meynard, D., Swarup, R., et al. (2017) SHR overexpression induces the formation of supernumerary cell layers with cortex cell identity in rice. *Developmental Biology*, **425**, 1–7.

Henry, S., Divol, F., Bettembourg, M., Bureau, C., Guiderdoni, E., Périn, C., et al. (2016) Immunoprofiling of Rice Root Cortex Reveals Two Cortical Subdomains. *Frontiers in Plant Science*, **6**, 1139.

Heo, J.-O., Roszak, P., Furuta, K.M. and Helariutta, Y. (2014) Phloem development: current knowledge and future perspectives. *American journal of botany*, **101**, 1393–402.

Hiei, Y. and Komari, T. (2008) Agrobacterium-mediated transformation of rice using immature embryos or calli induced from mature seed. *Nature Protocols*, **3**, 824–834.

Higuchi, M., Pischke, M.S., Mähönen, A.P., Miyawaki, K., Hashimoto, Y., Seki, M., et al. (2004) In planta functions of the Arabidopsis cytokinin receptor family. *Proceedings of the National Academy of Sciences of the United States of America*, **101**, 8821–6.

Hiramoto, F., Nomura, N., Furumai, T., Igarashi, Y. and Oki, T. (2003) Pradimicin-resistance of yeast is caused by a point mutation of the histidine-

containing phosphotransfer protein Ypd1. *The Journal of antibiotics*, **56**, 1053–7.

Hirose, N., Makita, N., Yamaya, T. and Sakakibara, H. (2005) Functional characterization and expression analysis of a gene, OsENT2, encoding an equilibrative nucleoside transporter in rice suggest a function in cytokinin transport. *Plant physiology*, **138**, 196–206.

Hirose, N., Takei, K., Kuroha, T., Kamada-Nobusada, T., Hayashi, H. and Sakakibara, H. (2008) Regulation of cytokinin biosynthesis, compartmentalization and translocation. *Journal of experimental botany*, **59**, 75–83.

Horgan, R., Hewett, E.W., Horgan, J.M., Purse, J. and Wareing, P.F. (1975) A new cytokinin from Populus x robusta. *Phytochemistry*, **14**, 1005–1008.

Hothorn, M., Dabi, T. and Chory, J. (2011) Structural basis for cytokinin recognition by Arabidopsis thaliana histidine kinase 4. *Nature Chemical Biology*, **7**, 766–768.

Hutchison, C.E., Li, J., Argueso, C., Gonzalez, M., Lee, E., Lewis, M.W., et al. (2006) The Arabidopsis histidine phosphotransfer proteins are redundant positive regulators of cytokinin signaling. *Plant Cell*, **18**, 3073–3087.

Hwang, I., Chen, H.C., Sheen, J. and Hwang, D. (2002) Two-component signal transduction pathways in Arabidopsis. *Plant Physiology*, **129**, 500–515.

Hwang, I. and Sheen, J. (2001) Two-component circuitry in Arabidopsis cytokinin signal transduction. *Nature*, **413**, 383–389.

Hwang, I., Sheen, J. and Mueller, B. (2012) Cytokinin Signaling Networks. *Annual Review of Plant Biology, Vol 63*, **63**, 353–380.

Imai, A., Hanzawa, Y., Komura, M., Yamamoto, K.T., Komeda, Y. and Takahashi, T. (2006) The dwarf phenotype of the Arabidopsis acl5 mutant is suppressed by a mutation in an upstream ORF of a bHLH gene. *Development*, **133**.

International Rice Genome Sequencing Project (2005) The map-based sequence of the rice genome. *Nature*, **436**, 793–800.

Jain, M., Tyagi, A.K. and Khurana, J.P. (2006) Molecular characterization and differential expression of cytokinin-responsive type-A response regulators in rice (Oryza sativa). *BMC plant biology*, **6**, 1.

Janiak-Spens, F., Sparling, D.P. and West, A.H. (2000) Novel role for an HPt domain in stabilizing the phosphorylated state of a response regulator domain. *Journal of bacteriology*, **182**, 6673–8.

Jinek, M., Chylinski, K., Fonfara, I., Hauer, M., Doudna, J.A. and Charpentier, E. (2012) A Programmable Dual-RNA–Guided DNA Endonuclease in Adaptive Bacterial Immunity. *Science*, **337**.

Jung, K.W., Oh, S.-I., Kim, Y.Y., Yoo, K.S. and Shin, M.H.C. and J.S. (2007) Arabidopsis Histidine-containing Phosphotransfer Factor 4 (AHP4) Negatively

Regulates Secondary Wall Thickening of the Anther Endothecium during Flowering. *Molecules and Cells*, **25**, 294–300.

Kadam, N.N., Yin, X., Bindraban, P.S., Struik, P.C. and Jagadish, K.S. V. (2015) Does morphological and anatomical plasticity during the vegetative stage make wheat more tolerant of water deficit stress than rice? *Plant physiology*, **167**, 1389–401.

Kang, J., Lee, Y., Sakakibara, H. and Martinoia, E. (2017) Cytokinin Transporters: GO and STOP in Signaling. *Trends in Plant Science*, **22**, 455–461.

Karimi, M., Depicker, A. and Hilson, P. (2007) Recombinational Cloning with Plant Gateway Vectors. *Plant Physiology*, **145**.

Katayama, H., Iwamoto, K., Kariya, Y., Asakawa, T., Kan, T., Fukuda, H., et al. (2015) A Negative Feedback Loop Controlling bHLH Complexes Is Involved in Vascular Cell Division and Differentiation in the Root Apical Meristem. *Current Biology*, **25**, 3144–3150.

Kim, Y., Schumaker, K.S. and Zhu, J.-K. (2006) EMS Mutagenesis of Arabidopsis; *Arabidopsis Protocols* pp. 101–104. Humana Press, New Jersey.

Knott, J.M., Römer, P. and Sumper, M. (2007) Putative spermine synthases from Thalassiosira pseudonana and Arabidopsis thaliana synthesize thermospermine rather than spermine. *FEBS letters*, **581**, 3081–6.

Ko, D., Kang, J., Kiba, T., Park, J., Kojima, M., Do, J., et al. (2014) Arabidopsis ABCG14 is essential for the root-to-shoot translocation of cytokinin.

Proceedings of the National Academy of Sciences of the United States of America, **111**, 7150–5.

Kono, Y. and Yamada, N. (1972) Studies on the developmental physiology of the relationship between the cortical disintegration and lateral root growth in rice seminal roots. *Proceedings of the Crop Science Society of Japan*, **41**, 256-266.

Kubo, M., Udagawa, M., Nishikubo, N., Horiguchi, G., Yamaguchi, M., Ito, J., et al. (2005) Transcription switches for protoxylem and metaxylem vessel formation. *Genes Dev*, **19**, 1855–1860.

Kudo, T., Makita, N., Kojima, M., Tokunaga, H. and Sakakibara, H. (2012) Cytokinin Activity of cis-Zeatin and Phenotypic Alterations Induced by Overexpression of Putative cis-Zeatin-O-glucosyltransferase in Rice. *Plant Physiology*, **160**, 319–331.

Kuroha, T., Tokunaga, H., Kojima, M., Ueda, N., Ishida, T., Nagawa, S., et al. (2009) Functional analyses of LONELY GUY cytokinin-activating enzymes reveal the importance of the direct activation pathway in Arabidopsis. *The Plant cell*, **21**, 3152–3169.

Lartaud, M., Perin, C., Courtois, B., Thomas, E., Henry, S., Bettembourg, M., et al. (2015) PHIV-RootCell: a supervised image analysis tool for rice root anatomical parameter quantification. *Frontiers in Plant Science*, **5**, 790.

Lee, D.J., Park, J.W., Lee, H.W. and Kim, J. (2009a) Genome-wide analysis of the auxin-responsive transcriptome downstream of iaa1 and its expression analysis reveal the diversity and complexity of auxin-regulated gene expression. *Journal of experimental botany*, **60**, 3935–57.

Letham, D.S. (1963) Zeatin, a factor inducing cell division isolated from Zea mays. *Life sciences*, **8**, 569–73.

Letham, D.S. and Palni, L.M.S. (1983) The Biosynthesis and Metabolism of Cytokinins. *Annual Review of Plant Physiology*, **34**, 163–197.

Li, J., Swanson, R. V, Simon, M.I. and Weis, R.M. (1995) The response regulators CheB and CheY exhibit competitive binding to the kinase CheA. *Biochemistry*, **34**, 14626–36.

de Lucas, M., Pu, L., Turco, G., Gaudinier, A., Morao, A.K., Harashima, H., et al. (2016) Transcriptional Regulation of Arabidopsis Polycomb Repressive Complex 2 Coordinates Cell-Type Proliferation and Differentiation. *The Plant Cell*, **28**, 2616–2631.

Müller, B. and Sheen, J. (2008) Cytokinin and auxin interaction in root stem-cell specification during early embryogenesis. *Nature*, **453**, 1094–1097.

Ma, Z., Bielenberg, D.G., Brown, K.M. and Lynch, J.P. (2001) Regulation of root hair density by phosphorus availability in Arabidopsis thaliana. *Plant, Cell and Environment*, **24**, 459–467.

Mähönen, A.P., Bishopp, A., Higuchi, M., Nieminen, K.M., Kinoshita, K., Törmäkangas, K., et al. (2006a) Cytokinin signaling and its inhibitor AHP6 regulate cell fate during vascular development. *Science,* **311**, 94–8.

Mähönen, A.P., Higuchi, M., Törmäkangas, K., Miyawaki, K., Pischke, M.S., Sussman, M.R., et al. (2006b) Cytokinins regulate a bidirectional phosphorelay network in Arabidopsis. *Current biology*, **16**, 1116–22.

Di Mambro, R., De Ruvo, M., Pacifici, E., Salvi, E., Sozzani, R., Benfey, P.N., et al. (2017) Auxin minimum triggers the developmental switch from cell division to cell differentiation in the Arabidopsis root. *Proceedings of the National Academy of Sciences of the United States of America*, **114**, E7641–E7649.

Matsuura, T., Hosoda, K., Ichihashi, N., Kazuta, Y. and Yomo, T. (2011) Kinetic Analysis of β-Galactosidase and β -Glucuronidase Tetramerization Coupled with Protein Translation. *The Journal of Biological Chemistry*, **286**, 22028–22034.

Mellor, N., Adibi, M., El-Showk, S., De Rybel, B., King, J., Mähönen, A.P., et al. (2017) Theoretical approaches to understanding root vascular patterning: a consensus between recent models. *Journal of Experimental Botany*, **68**, 5–16.

Meng, W.J., Cheng, Z.J., Sang, Y.L., Zhang, M.M., Rong, X.F., Wang, Z.W., et al. (2017) Type-B ARABIDOPSIS RESPONSE REGULATORs Specify the Shoot Stem Cell Niche by Dual Regulation of WUSCHEL. *The Plant cell*, **29**, 1357–1372.

Mik, V., Szucova, L., Spichal, L., Plihal, O., Nisler, J., Zahajska, L., et al. (2011) N9-Substituted N(6)-[(3-methylbut-2-en-1-yl)amino]purine derivatives and their biological activity in selected cytokinin bioassays. *Bioorg Med Chem*, **19**, 7244–7251.

Miller, C.O. (1961a) A kinetin like compound in maize. *Proceedings of the National Academy of Sciences of the United States of America*, **47**, 170–4.

Miller, C.O. (1961b) Kinetin and Related Compounds in Plant Growth. *Annual Review of Plant Physiology*, **12**, 395–408.

Miller, C.O., Skoog, F., Von Saltza, M.H. and Strong, F.M. (1955) Kinetin, a cell division factor from deoxyribonucleic acid [1]. *Journal of the American Chemical Society*, **77**, 1392–1392.

Moreira, S., Bishopp, A., Carvalho, H. and Campilho, A. (2013a) AHP6 Inhibits Cytokinin Signaling to Regulate the Orientation of Pericycle Cell Division during Lateral Root Initiation. *Plos One*, **8**, e56370.

Moreira, S., Braga, T., Carvalho, H. and Campilho, A. (2013b) The Arabidopsis HP6 gene is expressed in Medicago truncatula lateral roots and root nodule primordia. *Plant signaling & behavior*, **8**, e25262.

Moubayidin, L., Salvi, E., Giustini, L., Terpstra, I., Heidstra, R., Costantino, P., et al. (2016) A SCARECROW-based regulatory circuit controls Arabidopsis thaliana meristem size from the root endodermis. *Planta*, **243**, 1159–1168.

Müller, C.J., Valdés, A.E., Wang, G., Ramachandran, P., Beste, L., Uddenberg, D., et al. (2016) PHABULOSA Mediates an Auxin Signaling Loop to Regulate Vascular Patterning in Arabidopsis. *Plant physiology*, **170**, 956–70.

Muñiz, L., Minguet, E.G., Singh, S.K., Pesquet, E., Vera-Sirera, F., Moreau-Courtois, C.L., et al. (2008) ACAULIS5 controls Arabidopsis xylem specification through the prevention of premature cell death. *Development*, **135**, 2573–82.

Muraro, D., Mellor, N., Pound, M.P., Help, H., Lucas, M., Chopard, J., et al. (2014) Integration of hormonal signaling networks and mobile microRNAs is required for vascular patterning in Arabidopsis roots. *Proceedings of the National Academy of Sciences of the United States of America*, **111**, 857–862.

Nandi, S.K., Letham, D.S., Palni, L.M.S., Wong, O.C. and Summons, R.E. (1989) 6-benzylaminopurine and its glycosides as naturally occurring cytokinins. *Plant Science*, **61**, 189–196.

Nestler, J., Keyes, S.D. and Wissuwa, M. (2016) Root hair formation in rice (*Oryza sativa* L.) differs between root types and is altered in artificial growth conditions. *Journal of Experimental Botany*, **67**, 3699–3708.

Nieminen, K., Blomster, T., Helariutta, Y. and Mähönen, A.P. (2015) Vascular Cambium Development. *The Arabidopsis book*, **13**, e0177.

Nieminen, K., Immanen, J., Laxell, M., Kauppinen, L., Tarkowski, P., Dolezal, K., et al. (2008) Cytokinin signaling regulates cambial development in poplar.

Proceedings of the National Academy of Sciences of the United States of America, **105**, 20032–7.

Niones, J.M., Suralta, R.R., Inukai, Y. and Yamauchi, A. (2013) Roles of Root Aerenchyma Development and Its Associated QTL in Dry Matter Production under Transient Moisture Stress in Rice. *Plant Production Science*, **16**, 205–216.

O'Connor, D.L., Elton, S., Ticchiarelli, F., Hsia, M.M., Vogel, J. and Leyser, O. (2016) Cross-species functional diversity within the PIN auxin efflux protein family. *eLifeSciences.org*, 89854.

O'Connor, D.L., Runions, A., Sluis, A., Bragg, J., Vogel, J.P., Prusinkiewicz, P., et al. (2014) A Division in PIN-Mediated Auxin Patterning during Organ Initiation in Grasses. *PLoS Computational Biology*, **10**, e1003447.

Ohashi-Ito, K. and Bergmann, D.C. (2007) Regulation of the Arabidopsis root vascular initial population by LONESOME HIGHWAY. *Development*, **134**, 2959–2968.

Ohashi-Ito, K., Oguchi, M., Kojima, M., Sakakibara, H. and Fukuda, H. (2013) Auxin-associated initiation of vascular cell differentiation by LONESOME HIGHWAY. *Development*, **140**, 765–769.

Ohashi-Ito, K., Saegusa, M., Iwamoto, K., Oda, Y., Katayama, H., Kojima, M., et al. (2014) A bHLH Complex Activates Vascular Cell Division via Cytokinin Action in Root Apical Meristem. *Current Biology*, **24**, 2053–2058.

Van Overbeek, J., Conklin, M.E. And Blakeslee, A.F. (1941) Factors in Coconut Milk Essential for Growth and Development of Very Young Datura Embryos. *Science*, **94**, 350–351.

Parameswari, Y.S., Srinivas, A., Prakash, T.R. and Narendar, G. (2014) Effect of different crop establishment methods on rice (*Oryza sativa* L.) growth and yield – A review. *Agricultural Reviews*, **35**, 74.

Pekárová, B., Klumpler, T., Třísková, O., Horák, J., Jansen, S., Dopitová, R., et al. (2011) Structure and binding specificity of the receiver domain of sensor histidine kinase CKI1 from Arabidopsis thaliana. *The Plant journal : for cell and molecular biology*, **67**, 827–39.

Petolino, J.F. (2015) Genome editing in plants via designed zinc finger nucleases. *In vitro cellular & developmental biology. Plant : journal of the Tissue Culture Association*, **51**, 1–8.

Pils, B. and Heyl, A. (2009) Unraveling the Evolution of Cytokinin Signaling. *Plant Physiology*, **151**, 782–791.

Plíhalová, L., Vylíčilová, H., Doležal, K., Zahajská, L., Zatloukal, M. and Strnad, M. (2016) Synthesis of aromatic cytokinins for plant biotechnology. *New Biotechnology*, **33**, 614–624.

Porter, S.W. and West, A.H. (2005) A common docking site for response regulators on the yeast phosphorelay protein YPD1. *Biochimica et Biophysica Acta (BBA) - Proteins and Proteomics*, **1748**, 138–145.

Posas, F., Wurgler-Murphy, S. M., Maeda, T., Witten, E. A., Thai, T. C. and Saito, H. (1996) Yeast HOG1 MAP Kinase Cascade is Regulated by a Multistep Phosphorelay Mechanism in the SLN1-YPD-SSK1 "Two-Component" Osmosensor. *Cell*, **86**, 865–876.

Qi, Z. and Xiong, L. (2013) Characterization of a Purine Permease Family Gene *Os PUP 7* Involved in Growth and Development Control in Rice. *Journal of Integrative Plant Biology*, **55**, 1119–1135.

Qu, L.-J. and Qin, G. (2014) Generation and Identification of Arabidopsis EMS Mutants. *Methods in molecular biology (Clifton, New Jersey.)* pp. 225–239.

Raines, T., Shanks, C., Cheng, C.-Y., McPherson, D., Argueso, C.T., Kim, H.J., et al. (2016) The cytokinin response factors modulate root and shoot growth and promote leaf senescence in Arabidopsis. *The Plant Journal*, **85**, 134–147.

Rashotte, A.M. and Goertzen, L.R. (2010) The CRF domain defines cytokinin response factor proteins in plants. *BMC plant biology*, **10**, 74.

Rashotte, A.M., Mason, M.G., Hutchison, C.E., Ferreira, F.J., Schaller, G.E. and Kieber, J.J. (2006) A subset of Arabidopsis AP2 transcription factors mediates cytokinin responses in concert with a two-component pathway. *Proceedings of the National Academy of Sciences of the United States of America*, **103**, 11081–5.

Rebouillat, J., Dievart, A., Verdeil, J.L., Escoute, J., Giese, G., Breitler, J.C., et al. (2008) Molecular Genetics of Rice Root Development. *Rice*, **2**, 15–34.

Ren, B., Chen, Q., Hong, S., Zhao, W., Feng, J., Feng, H., et al. (2013) The Arabidopsis Eukaryotic Translation Initiation Factor eIF5A-2 Regulates Root Protoxylem Development by Modulating Cytokinin Signaling. *The Plant Cell*, **25**, 3841–3857.

Ren, B., Liang, Y., Deng, Y., Chen, Q., Zhang, J., Yang, X., et al. (2009) Genome-wide comparative analysis of type-A Arabidopsis response regulator genes by overexpression studies reveals their diverse roles and regulatory mechanisms in cytokinin signaling. *Cell research*, **19**, 1178–90.

Reyes-Olalde, J.I., Zúñiga-Mayo, V.M., Serwatowska, J., Chavez Montes, R.A., Lozano-Sotomayor, P., Herrera-Ubaldo, H., et al. (2017) The bHLH transcription factor SPATULA enables cytokinin signaling, and both activate auxin biosynthesis and transport genes at the medial domain of the gynoecium. *PLoS genetics*, **13**, e1006726.

Richards, R. and Passioura, J. (1989) A breeding program to reduce the diameter of the major xylem vessel in the seminal roots of wheat and its effect on grain yield in rain-fed environments. *Australian Journal of Agricultural Research*, **40**, 943.

Riefler, M., Novak, O., Strnad, M. and Schmülling, T. (2006) Arabidopsis Cytokinin Receptor Mutants Reveal Functions in Shoot Growth, Leaf Senescence, Seed Size, Germination, Root Development, and Cytokinin Metabolism. *The Plant Cell Online*, **18**, 40–54.

Rudall, P. (1991) Lateral meristems and stem thickening growth in monocotyledons. *The Botanical Review*, **57**, 150–163.

Ruszkowski, M., Brzezinski, K., Jedrzejczak, R., Dauter, M., Dauter, Z., Sikorski, M., et al. (2013) Medicago truncatula histidine-containing phosphotransfer protein: structural and biochemical insights into the cytokinin transduction pathway in plants. *The FEBS journal*, **280**, 3709–20.

Růžička, K., Zhang, M., Campilho, A., Bodi, Z., Kashif, M., Saleh, M., et al. (2017) Identification of factors required for m6A mRNA methylation in *Arabidopsis* reveals a role for the conserved E3 ubiquitin ligase HAKAI. *New Phytologist*.

De Rybel, B., Adibi, M., Breda, A.S., Wendrich, J.R., Smit, M.E., Novak, O., et al. (2014) Integration of growth and patterning during vascular tissue formation in Arabidopsis. *Science*, **345**, 1255215–1255215.

De Rybel, B., Moller, B., Yoshida, S., Grabowicz, I., Barbier de Reuille, P., Boeren, S., et al. (2013) A bHLH complex controls embryonic vascular tissue establishment and indeterminate growth in Arabidopsis. *Developmental cell*, **24**, 426–37.

Sandhu, N., Raman, K.A., Torres, R.O., Audebert, A., Dardou, A., Kumar, A., et al. (2016) Rice root architectural plasticity traits and genetic regions for adaptability to variable cultivation and stress conditions. *Plant Physiology*, **171**, 2562–2576.

Sato, Y., Takehisa, H., Kamatsuki, K., Minami, H., Namiki, N., Ikawa, H., et al. (2013) RiceXPro Version 3.0: Expanding the informatics resource for rice transcriptome. *Nucleic Acids Research*, **41**, 1206–1213.

Sato, A. and Yamamoto, K.T. (2008a) Overexpression of the non-canonical Aux/IAA genes causes auxin-related aberrant phenotypes in Arabidopsis. *Physiologia Plantarum*, **133**, 397–405.

Sato, A. and Yamamoto, K.T. (2008b) What's the physiological role of domain II-less Aux/IAA proteins? *Plant signaling & behavior*, **3**, 496–7.

Scarpella, E., Rueb, S. and Meijer, A.H. (2003) The RADICLELESS1 gene is required for vascular pattern formation in rice. *Development (Cambridge, England)*, **130**, 645–58.

Schäfer, M., Brütting, C., Meza-Canales, I.D., Großkinsky, D.K., Vankova, R., Baldwin, I.T., et al. (2015) The role of cis-zeatin-type cytokinins in plant growth regulation and mediating responses to environmental interactions. *Journal of experimental botany*, **66**, 4873–84.

Schaller, G.E., Shiu, S.-H. and Armitage, J.P. (2011) Two-component systems and their co-option for eukaryotic signal transduction. *Current biology*, **21**, 320–330.

Sena, G., Jung, J. W. & Benfey, P. N. (2004) A broad competence to respond to SHORT ROOT revealed by tissue-specific ectopic expression. *Development*, **12**, 2817–2826.

Sessions, A., Burke, E., Presting, G., Aux, G., McElver, J., Patton, D., et al. (2002) A High-Throughput Arabidopsis Reverse Genetics System. *The Plant Cell Online*, **14**, 2985–2994.

Šimášková, M., O'Brien, J.A., Khan, M., Van Noorden, G., Ötvös, K., Vieten, A., et al. (2015) Cytokinin response factors regulate PIN-FORMED auxin transporters. *Nature Communications*, **6**, 8717.

Singh, A., Roy, S., Singh, S., Das, S.S., Gautam, V., Yadav, S., et al. (2017) Phytohormonal crosstalk modulates the expression of miR166/165s, target Class III HD-ZIPs, and KANADI genes during root growth in Arabidopsis thaliana. *Scientific Reports*, **7**, 3408.

Sourjik, V. and Schmitt, R. (1998) Phosphotransfer between CheA, CheY1, and CheY2 in the Chemotaxis Signal Transduction Chain of *Rhizobium meliloti* †. *Biochemistry*, **37**, 2327–2335.

Spicer, R. and Groover, A. (2010) Evolution of development of vascular cambia and secondary growth. *New Phytologist*, **186**, 577–592.

Sridevi, V., Chellamuthu, V. and Jeyaraman, S. (2011) *System of Rice Intensification - A Review*. Agricultural Research Communication Centre.

Stephens, D.J. and Banting, G. (2000) The use of yeast two-hybrid screens in studies of protein:protein interactions involved in trafficking. *Traffic (Copenhagen, Denmark)*, **1**, 763–8.

Stiller, V., Lafitte, H.R. and Sperry, J.S. (2003) Hydraulic properties of rice and the response of gas exchange to water stress. *Plant physiology*, **132**, 1698–706.

Strnad, M. (1997) The aromatic cytokinins. *Physiologia Plantarum*, **101**, 674–688.

Strnad, M., Hanuš, J., Vaněk, T., Kamínek, M., Ballantine, J.A., Fussell, B., et al. (1997) Meta-topolin, a highly active aromatic cytokinin from poplar leaves (Populus × canadensis Moench., cv. Robusta). *Phytochemistry*, **45**, 213–218.

Strnad, M., Peters, W., Hanuš, J. and Beck, E. (1994) Ortho-topolin-9-glucoside, an aromatic cytokinin from Populus x canadensis cv Robusta leaves. *Phytochemistry*, **37**, 1059–1062.

Sugawara, H., Kawano, Y., Hatakeyama, T., Yamaya, T., Kamiya, N. and Sakakibara, H. (2005) Crystal structure of the histidine-containing phosphotransfer protein ZmHP2 from maize. *Protein science : a publication of the Protein Society*, **14**, 202–8.

Sun, J., Hirose, N., Wang, X., Wen, P., Xue, L., Sakakibara, H., et al. (2005) Arabidopsis SOI33/AtENT8 Gene Encodes a Putative Equilibrative Nucleoside Transporter That Is Involved in Cytokinin Transport In Planta. *Journal of Integrative Plant Biology*, **47**, 588–603.

Takano, A., Kakehi, J.-I. and Takahashi, T. (2012) Thermospermine is not a minor polyamine in the plant kingdom. *Plant & cell physiology*, **53**, 606–16.

Tarkowská, D., Dolezal, K., Tarkowski, P., Astot, C., Holub, J., Fuksová, K., et al. (2003) Identification of new aromatic cytokinins in Arabidopsis thaliana and Populus x canadensis leaves by LC-(+)ESI-MS and capillary liquid chromatography/frit-fast atom bombardment mass spectrometry. *Physiologia plantarum*, **117**, 579–590.

Taylor-Teeples, M., Lin, L., de Lucas, M., Turco, G., Toal, T.W., Gaudinier, A., et al. (2015) An Arabidopsis gene regulatory network for secondary cell wall synthesis. *Nature*, **517**, 571–5.

Thimann, K. V. And Koepfli, J.B. (1935) Identity of the Growth-Promoting and Root-Forming Substances ofPlants. *Nature*, **135**, 101–102.

Thimann, K.V., Went, F.W. and Thimann, K.V. (1937) Phytohormones. *The Macmillan Company*, New York.

To, J.P.C., Deruere, J., Maxwell, B.B., Morris, V.F., Hutchison, C.E., Ferreira, F.J., et al. (2007) Cytokinin Regulates Type-A Arabidopsis Response Regulator Activity and Protein Stability via Two-Component Phosphorelay. *The Plant Cell Online*, **19**, 3901–3914.

To, J.P.C., Haberer, G., Ferreira, F.J., Deruère, J., Mason, M.G., Schaller, G.E., et al. (2004) Type-A Arabidopsis response regulators are partially redundant negative regulators of cytokinin signaling. *The Plant cell*, **16**, 658–71.

Torres, R.O. and Henry, A. (2016) Yield stability of selected rice breeding lines and donors across conditions of mild to moderately severe drought stress. *Field Crops Research*.

Toungos, M.D. (2016) Introduction of Faro – 52 (WITA – 4) Rice Variety as A Measure of Solving Low Yield Problem among Farmers in Yola-North Local Government Area of Adamawa State, Nigeria. *International Journal of Innovative Agriculture & Biology Research*, **4**, 1–7.

Tsai, Y.-C.C., Weir, N.R., Hill, K., Zhang, W., Kim, H.J., Shiu, S.-H.H., et al. (2012) Characterization of genes involved in cytokinin signaling and metabolism from rice. *Plant Physiol*, **158**, 1666–1684.

Turner, S., Gallois, P. and Brown, D. (2007) Tracheary Element Differentiation. *Annual Review of Plant Biology*, **58**, 407–433.

Uga, Y., Ebana, K., Abe, J., Morita, S., Okuno, K. and Yano, M. (2009) Variation in root morphology and anatomy among accessions of cultivated rice (Oryza sativa L.) with different genetic backgrounds. *Breeding Science*, **59**, 87–93.

Uga, Y., Okuno, K. and Yano, M. (2008) QTLs underlying natural variation in stele and xylem structures of rice root. *Breeding Science*, **58**, 7–14.

Uga, Y., Okuno, K. and Yano, M. (2011) Dro1, a major QTL involved in deep rooting of rice under upland field conditions. *Journal of Experimental Botany*, **62**, 2485–2494.

Uga, Y., Sugimoto, K., Ogawa, S., Rane, J., Ishitani, M., Hara, N., et al. (2013) Control of root system architecture by DEEPER ROOTING 1 increases rice yield under drought conditions. *Nature genetics*, **45**, 1097–102.

Ulmasov, T., Hagen, G. and Guilfoyle, T.J. (1999) Dimerization and DNA binding of auxin response factors. *The Plant journal: for cell and molecular biology*, **19**, 309–19.

Ursache, R., Miyashima, S., Chen, Q., Vaten, A., Nakajima, K., Carlsbecker, A., et al. (2014) Tryptophan-dependent auxin biosynthesis is required for HD-ZIP III-mediated xylem patterning. *Development*, **141**, 1250–1259.

Vera-Sirera, F., De Rybel, B., Úrbez, C., Kouklas, E., Pesquera, M., Álvarez-Mahecha, J.C., et al. (2015) A bHLH-Based Feedback Loop Restricts Vascular Cell Proliferation in Plants. *Developmental Cell*, **35**, 432–443.

Wang, J.-R., Hu, H., Wang, G.-H., Li, J., Chen, J.-Y. and Wu, P. (2009) Expression of PIN genes in rice (Oryza sativa L.): tissue specificity and regulation by hormones. *Molecular plant*, **2**, 823–31.

Wang, H., La Russa, M. and Qi, L.S. (2016) CRISPR/Cas9 in Genome Editing and Beyond. *Annual Review of Biochemistry*, **85**, 227–264.

Wang, J., Tian, C., Zhang, C., Shi, B., Cao, X., Zhang, T.-Q., et al. (2017) Cytokinin Signaling Activates WUSCHEL Expression during Axillary Meristem Initiation. *The Plant cell*, **29**, 1373–1387.

Wang, M., Yu, Y., Haberer, G., Marri, P.R., Fan, C., Goicoechea, J.L., et al. (2014) The genome sequence of African rice (Oryza glaberrima) and evidence for independent domestication. *Nature Genetics*, **46**, 982–988.

Wardlaw, C.W. (1929) II.—Size in Relation to Internal Morphology. No. 3. The Vascular System of Roots. *Transactions of the Royal Society of Edinburgh*, **56**, 19–55.

Weiler, E.W. and Ziegler, H. (1981) Determination of phytohormones in phloem exudate from tree species by radioimmunoassay. *Planta*, **152**, 168–170.

Weller, B., Zourelidou, M., Frank, L., Barbosa, I.C.R., Fastner, A., Richter, S., et al. (2017) Dynamic PIN-FORMED auxin efflux carrier phosphorylation at the plasma membrane controls auxin efflux-dependent growth. *Proceedings of the National Academy of Sciences of the United States of America*, **114**, E887–E896.

Wells, B.R., Dilday, R.H., Rohman, P.C. and Blocker, M.M. (1995) Registration of "Kaybonnet" Rice. *Crop Science*, **35**, 587.

Went, F. (1928) Wuchsstoff und Wachstum. *Extrait du Recueil des Travaux Botaniques Neerlandais*, **25**, 1–116.

Winter, D., Vinegar, B., Nahal, H., Ammar, R., Wilson, G. V and Provart, N.J. (2007) An "Electronic Fluorescent Pictograph" browser for exploring and analyzing large-scale biological data sets. *PloS one*, **2**, e718.

Wu, S., Lee, C.-M., Hayashi, T., Price, S., Divol, F., Henry, S., et al. (2014) A plausible mechanism, based upon Short-Root movement, for regulating the number of cortex cell layers in roots. *Proceedings of the National Academy of Sciences of the United States of America*, **111**, 16184–9.

Wulfetange, K., Lomin, S.N., Romanov, G.A., Stolz, A., Heyl, A. and Schmulling, T. (2011) The Cytokinin Receptors of Arabidopsis Are Located Mainly to the Endoplasmic Reticulum. *Plant Physiology*, **156**, 1808–1818.

Xiao, A., Cheng, Z., Kong, L., Zhu, Z., Lin, S., Gao, G., et al. (2014) CasOT: a genome-wide Cas9/gRNA off-target searching tool. *Bioinformatics,* **30**, 1180-1182.

Yamamoto, M. and Takahashi, T. (2017) Thermospermine enhances translation of *SAC51* and *SACL1* in Arabidopsis. *Plant Signaling & Behavior*, **12**, e1276685.

Yamauchi, A., Kono, Y. And Tatsumi, J. (1987) Comparison of root system structures of 13 species of cereals. *Japanese journal of crop science*, **56**, 618–631.

Yambao, E.B., Ingram, K.T. And Real, J.G. (1992) Root Xylem Influence on the Water Relations and Drought Resistance of Rice. *Journal of Experimental Botany*, **43**, 925–932.

Yang, J., Yuan, Z., Meng, Q., Huang, G., Perin, C., Bureau, C., et al. (2017) Dynamic Regulation of Auxin Response during Rice Development Revealed by

Newly Established Hormone Biosensor Markers. *Frontiers in Plant Science*, **8**, 256.

Yang, Y.-W., Chen, H.-C., Jen, W.-F., Liu, L.-Y., Chang, M.-C. and Lu, W. (2015) Comparative Transcriptome Analysis of Shoots and Roots of TNG67 and TCN1 Rice Seedlings under Cold Stress and Following Subsequent Recovery: Insights into Metabolic Pathways, Phytohormones, and Transcription Factors. *PLOS ONE*, **10**, e0131391.

Yeh, S.-Y., Chen, H.-W., Ng, C.-Y., Lin, C.-Y., Tseng, T.-H., Li, W.-H., et al. (2015) Down-Regulation of Cytokinin Oxidase 2 Expression Increases Tiller Number and Improves Rice Yield. *Rice (New York)*, **8**, 36.

Yu, Q., Li, P., Liang, N., Wang, H., Xu, M. and Wu, S. (2017) Specifying cell fate in roots requires coordinative lineage instruction and positional reprogramming. *Plant physiology*, **175**, 816–827.

Zhang, T.-Q., Lian, H., Zhou, C.-M., Xu, L., Jiao, Y. and Wang, J.-W. (2017a) A Two-Step Model for de Novo Activation of WUSCHEL during Plant Shoot Regeneration. *The Plant cell*, **29**, 1073–1087.

Zhang, F., May, A. and Irish, V.F. (2017b) Type-B ARABIDOPSIS RESPONSE REGULATORs Directly Activate WUSCHEL. *Trends in plant science*, **22,** 815–817.

Zhang, J., Nodzynski, T., Pencík, A., Rolcík, J. and Friml, J. (2010) PIN phosphorylation is sufficient to mediate PIN polarity and direct auxin

transport. *Proceedings of the National Academy of Sciences of the United States of America*, **107**, 918–22.

Zhang, K., Novak, O., Wei, Z., Gou, M., Zhang, X., Yu, Y., et al. (2014) Arabidopsis ABCG14 protein controls the acropetal translocation of root-synthesized cytokinins. *Nature communications*, **5**, 3274.

Zhao, Z., Andersen, S.U., Ljung, K., Dolezal, K., Miotk, A., Schultheiss, S.J., et al. (2010) Hormonal control of the shoot stem-cell niche. *Nature*, **465**, 1089–1092.

Zhao, J., Liu, J.-S., Meng, F.-N., Zhang, Z.-Z., Long, H., Lin, W.-H., et al. (2016) ANAC005 is a membrane-associated transcription factor and regulates vascular development in Arabidopsis. *Journal of integrative plant biology*, **58**, 442–51.

Zhong, R. and Ye, Z.H. (1999) IFL1, a gene regulating interfascicular fiber differentiation in Arabidopsis, encodes a homeodomain-leucine zipper protein. *Plant Cell*, **11**, 2139–2152.

Zhong, R. and Ye, Z.-H. (2015) Secondary Cell Walls: Biosynthesis, Patterned Deposition and Transcriptional Regulation. *Plant and Cell Physiology*, **56**, 195–214.

Zhou, J., Wang, X. and Lee, J.Y. (2013) Cell-to-cell movement of two interacting AT-hook factors in Arabidopsis root vascular tissue patterning. *Plant Cell*, **25**, 187–201.

Zubo, Y.O., Blakley, I.C., Yamburenko, M. V, Worthen, J.M., Street, I.H., Franco-Zorrilla, J.M., et al. (2017) Cytokinin induces genome-wide binding of the type-B response regulator ARR10 to regulate growth and development in Arabidopsis. *Proceedings of the National Academy of Sciences of the United States of America*, **114**, E5995–E6004.

Zürcher, E., Liu, J., di Donato, M., Geisler, M. and Müller, B. (2016) Plant development regulated by cytokinin sinks. *Science*, **353**, 1027–1030.

Zwack, P.J., De Clercq, I., Howton, T.C., Hallmark, H.T., Hurny, A., Keshishian, E.A., et al. (2016) Cytokinin Response Factor 6 Represses Cytokinin-Associated Genes during Oxidative Stress. *Plant physiology*, **172**, 1249–1258.



Figure 1. Plasmid maps of pDONR_221 and pDONR_P4P1R_AHP6, which were used in MultiSite Gateway cloning. CDS of genes of interest were inserted into pDONR_221 using the BP reaction. pDONR_P4P1R_AHP6 contains the AHP6 promoter.

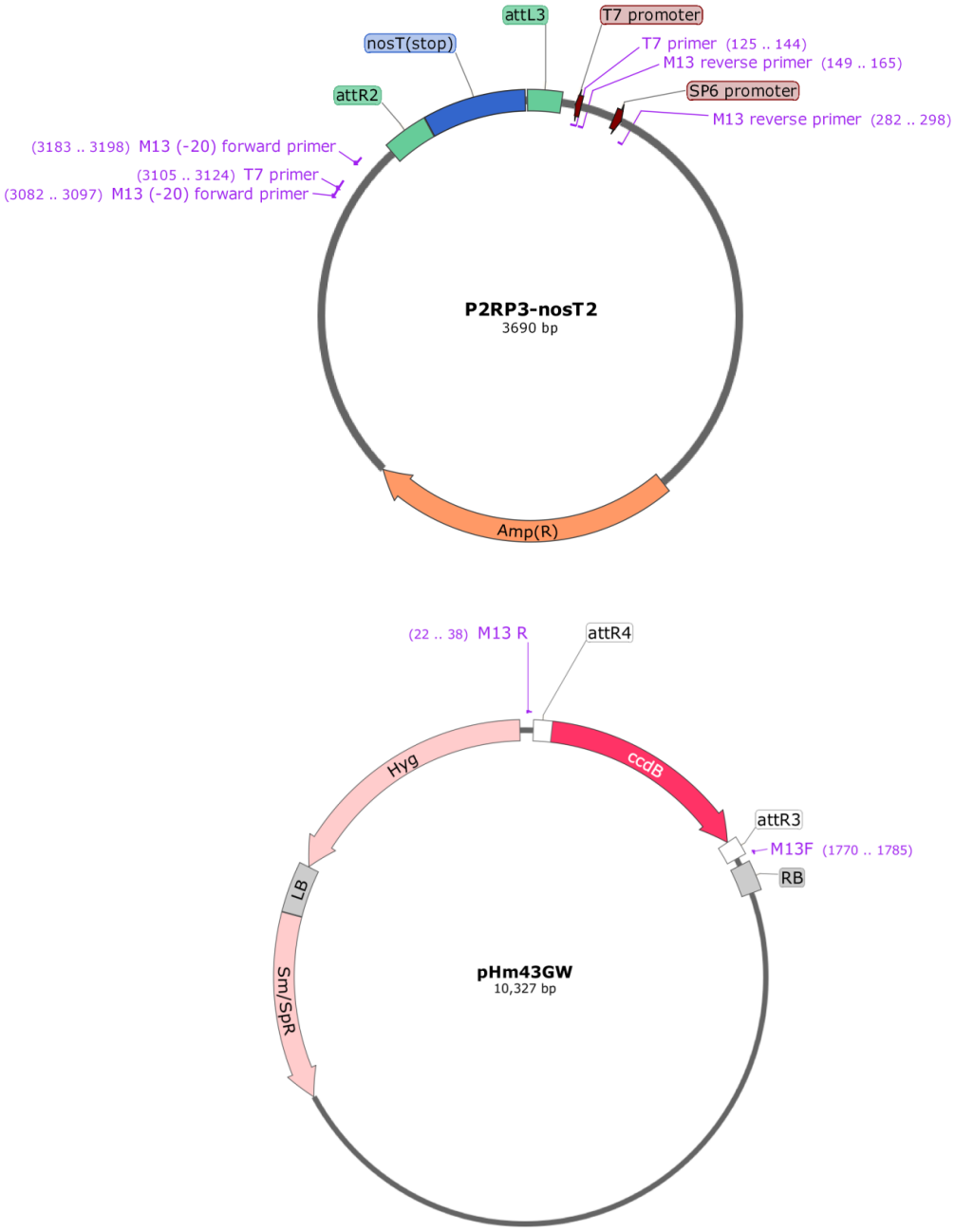


Figure 2. Plasmid maps of p2Rp3-nosT2 and pHm34GW, which were used in MultiSite Gateway cloning. P2RP3_nosT2 contains a terminator sequence, and pHm34GW forms the backbone of the recombined plasmid containing left and right border sequences necessary for Agrobacterium mediated transformation.

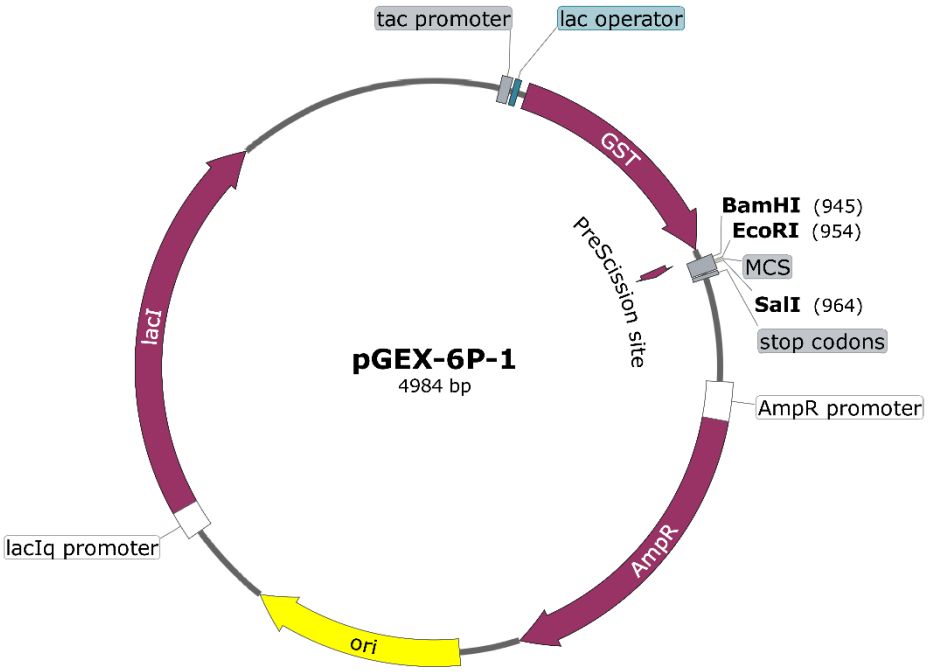


Figure 3. Plasmid map of pGEX-6p-1 which was used for bacterial expression of

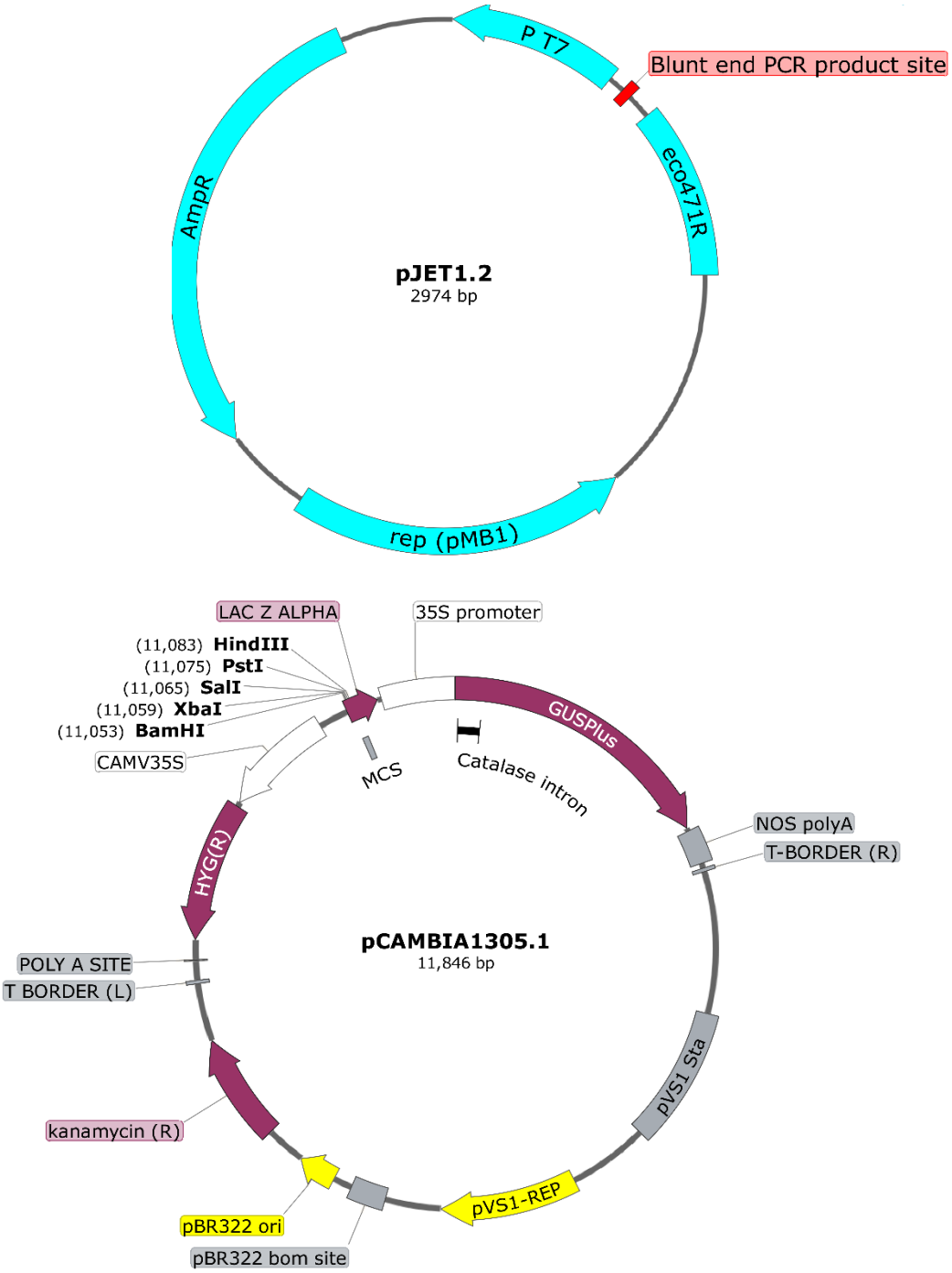


Figure 4. Plasmid maps of pJET1.2 and pCAMBIA1305.1, which were used to generate reporters.

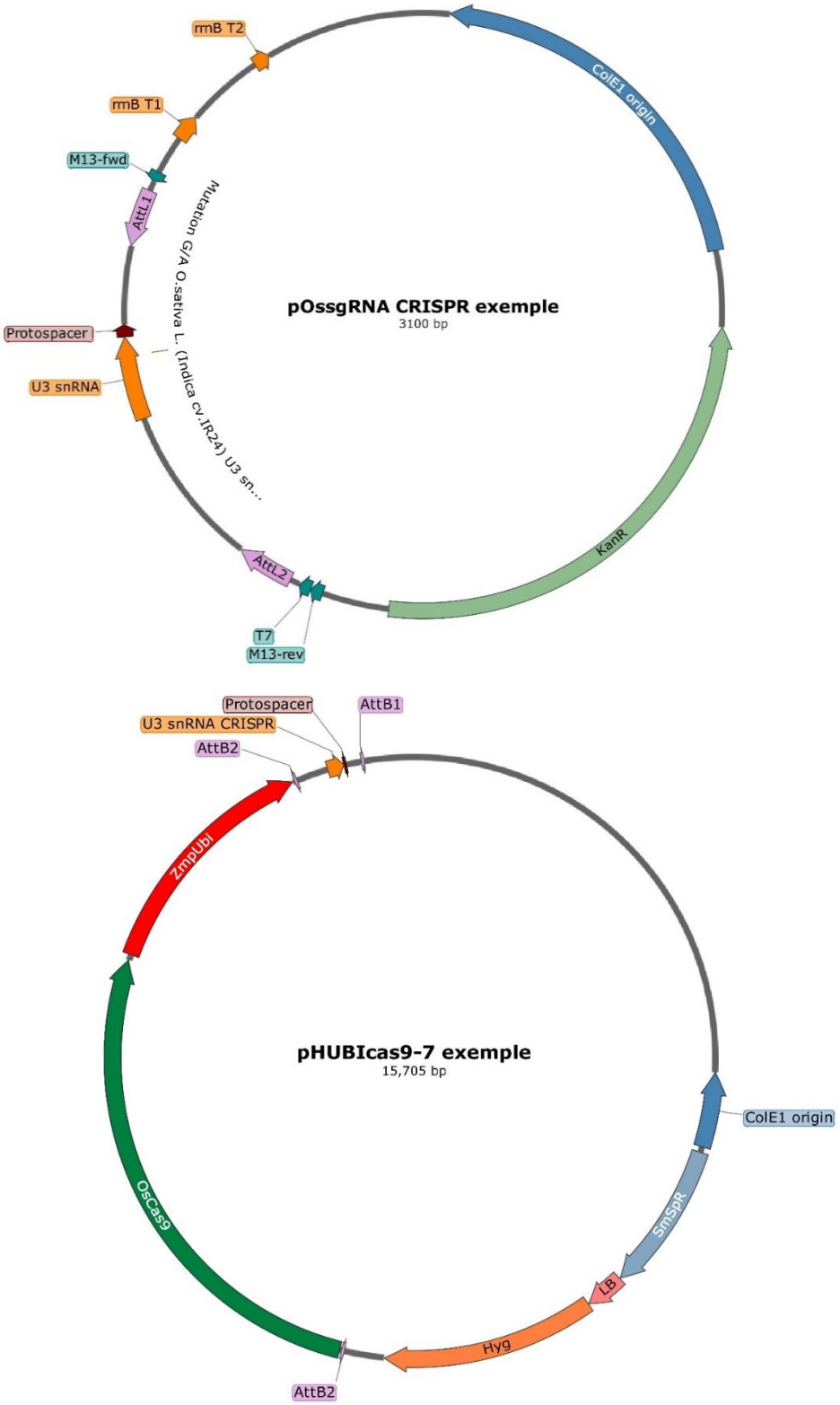


Figure 5. Plasmid maps of pOssgRNA and pHUBIcas9-7, which were used to generate CRISPR mutant plants.

Identifier	Species
Ac	*Aquilegia coerulea*
Al	*Arabidopsis lyrata*
At	*Arabidopsis thaliana*
Bd	*Brachypodium distachyon*
Br	*Brassica rapa*
Bs	*Boechera stricta*
Cc	*Citrus clementina*
Cg	*Capsella grandiflora*
Cp	*Carica papaya*
Cr	*Capsella rubella*
Cs	*Citrus sinensis*
Cu	*Cucumis sativus*
Eg	*Eucalyptus grandis*
Es	*Eutrema salsugineum*
Fv	*Fragaria vesca*
Gm	*Glycine max*
Gr	*Gossypium raimondii*
Lu	*Linum usitatissimum*
Md	*Malus domestica*
Me	*Manihot esculenta*
Mg	*Mimulus guttatus*
Mt	*Medicago truncatula*
Os	*Oryza sativa*
Pe	*Prunus persica*
Pp	*Physcomitrella patens*
Pt	*Populus trichocarpa*
Pu	*Phaseolus vulgaris*
Pv	*Panicum virgatum*
Rc	*Ricinus communis*
Sb	*Sorghum bicolor*
Si	*Setaria italica*
Sl	*Solanum lycopersicum*
Sm	*Selaginella moellendorffii*
Sp	*Salix purpurea*
St	*Solanum tuberosum*
Tc	*Theobroma cacao*
Vv	*Vitis vinifera*
Zm	*Zea mays*

Figure 6. The list of species used in the phylogenetic study, along with the corresponding two letter identifiers used. Species listed in black font are eudicots, in blue are monocots and red are the Bryophyte *Physcomitrella patens* and the Lycopod *Selaginella moellendorffii.*

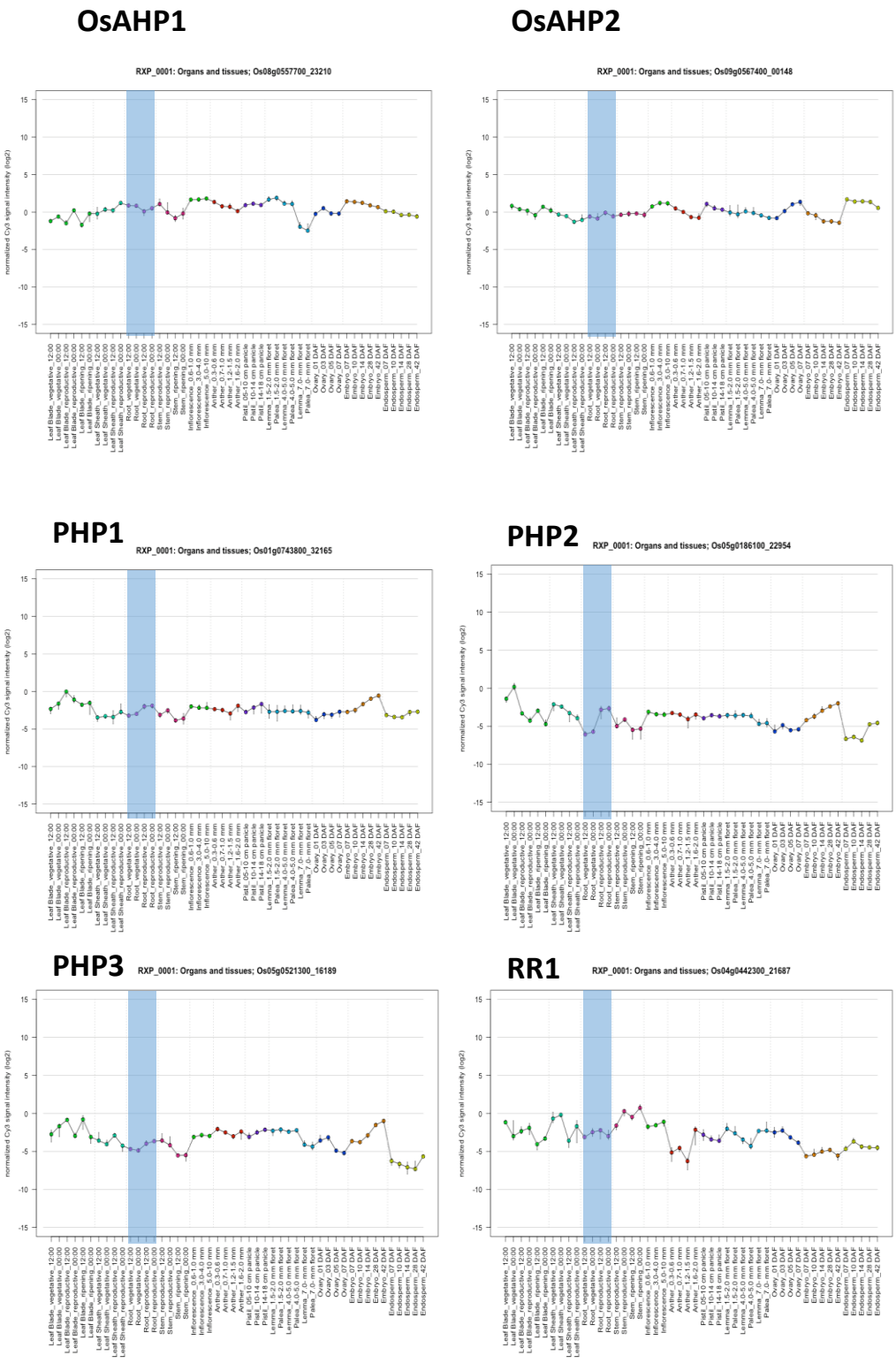
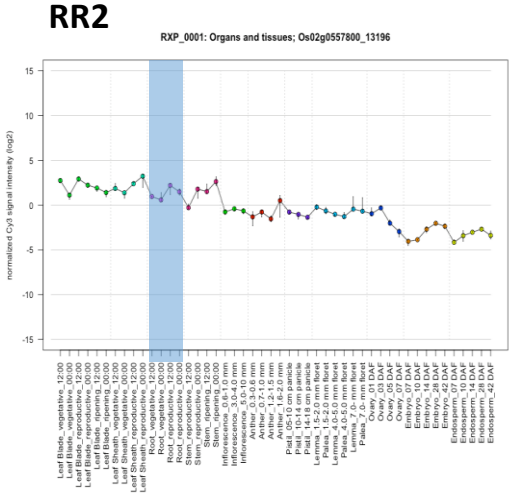
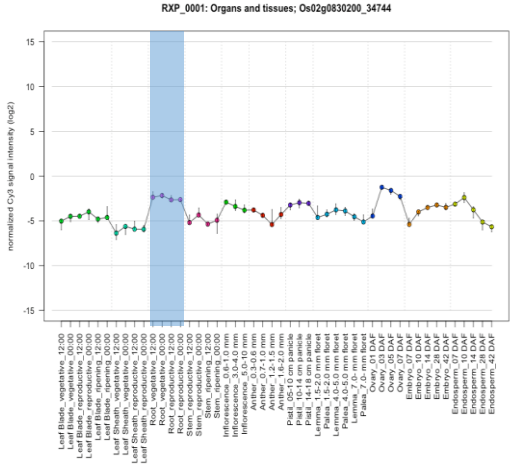


Figure 7. Tissue expression profile data for a subset of the rice PHPs and type-A RRs. Expression levels in root tissues are highlighted in blue bars. Data indicate expression in all three PHPs are fairly low, RR3 is quite high and RR6 is the highest. Graphs represent normalised data of median value in triplicate for different tissues at different times. Data was accessed from the RiceXPro database.

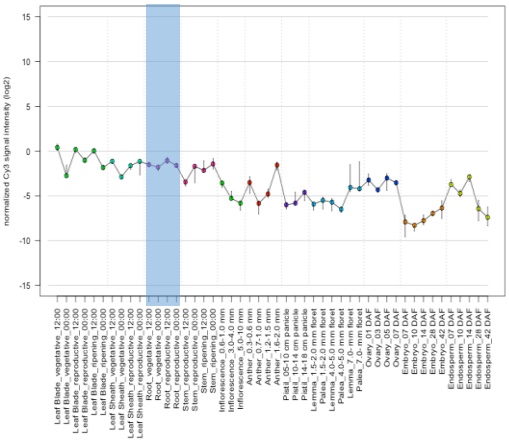
RR2



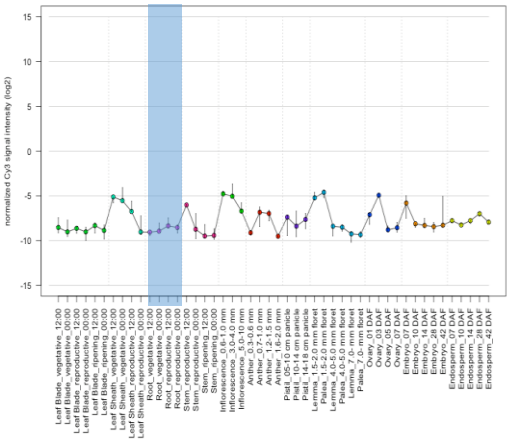
RR3



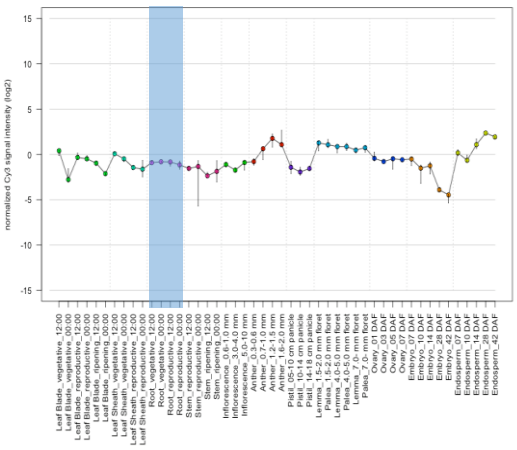
RR4



RR5



RR6



RR8

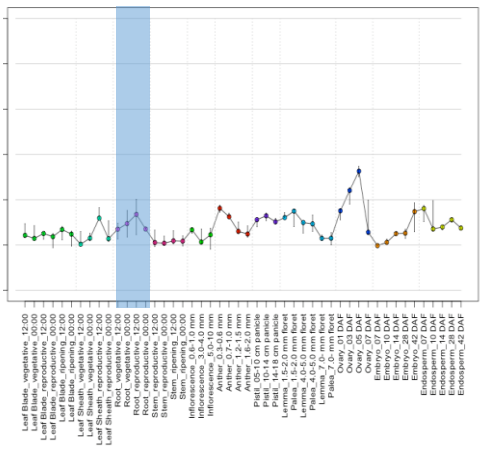
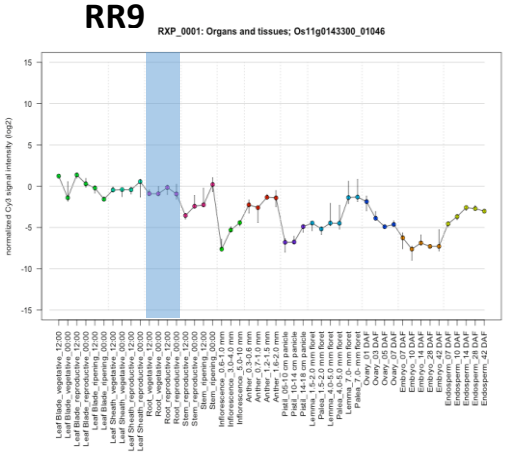
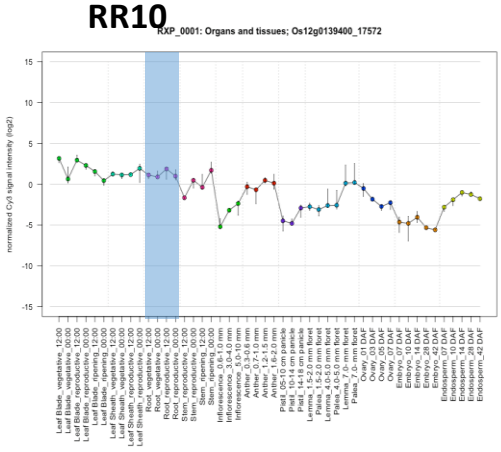


Figure 7 continued.

RR9



RR10



RR11

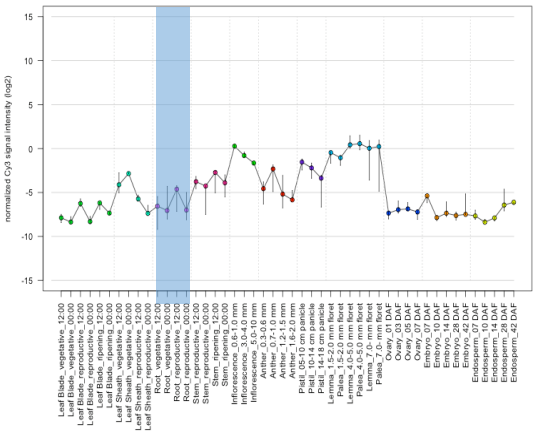


Figure 7 continued.

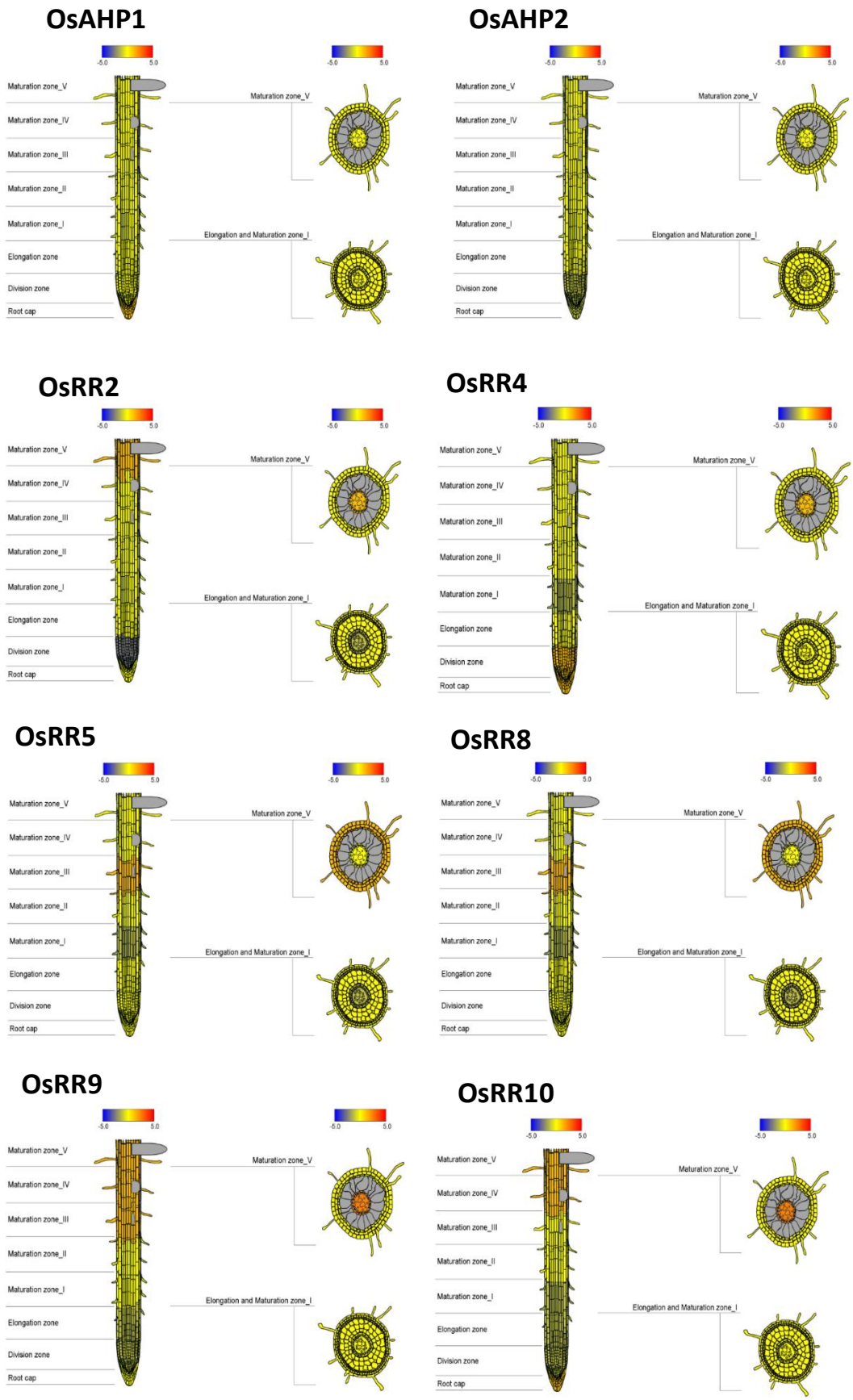


Figure 8. Tissue specific expression patterns of candidate genes in rice. Data taken from the RiceXPro microarray database.

OsRR11

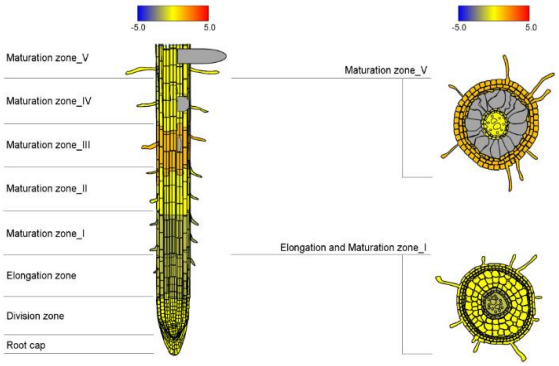


Figure 8 continued.

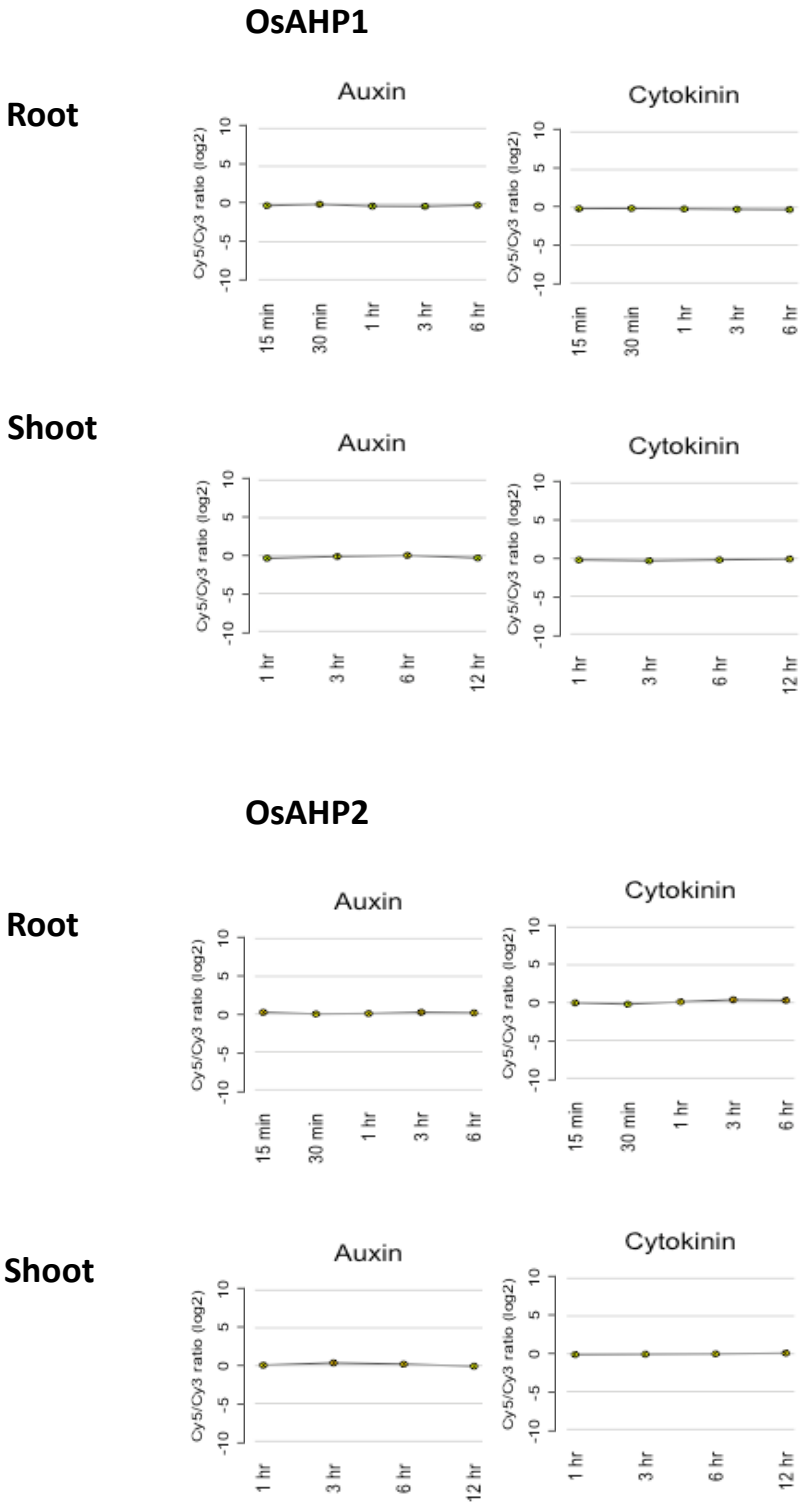


Figure 9. Expression of the OsAHPs in response to auxin or cytokinin treatment.

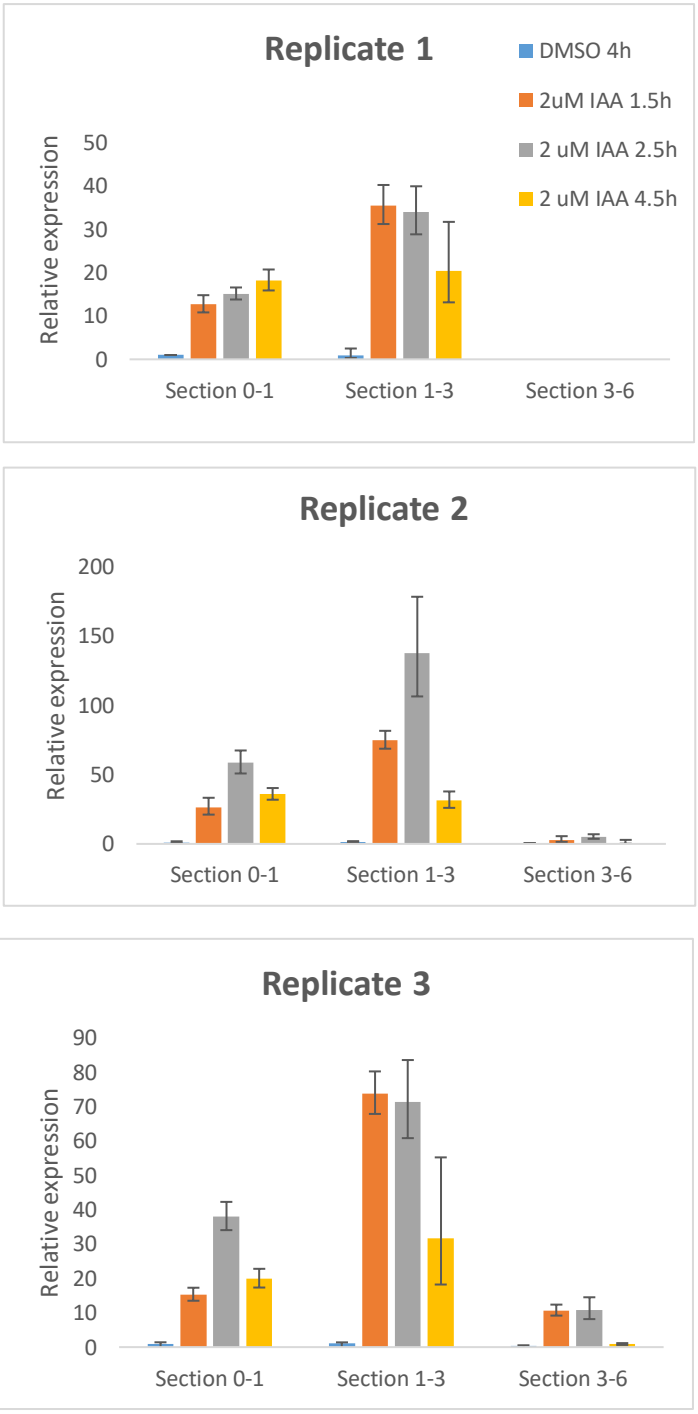


Figure 10. Biological replicates for expression levels determined by qRT-PCR indicate the same trends in gene expression. Replicates show expression of OsRR7 treated with 2uM IAA at time points indicated.

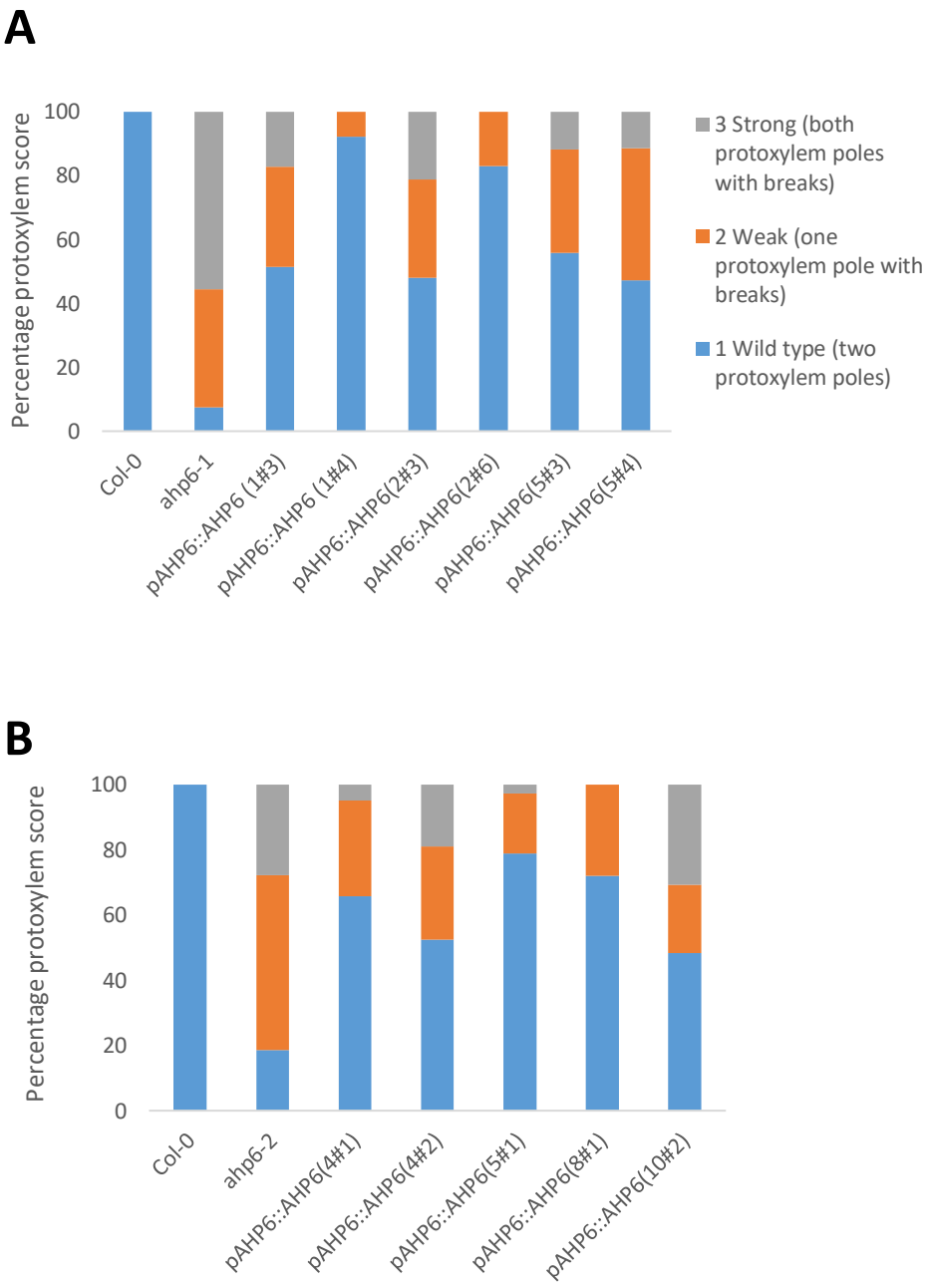


Figure 11. Scoring multiple independent transgenic lines for trans-complementation of *ahp6-1* and *ahp6-2* reveals slight phenotypic differences but the general trends remain the same. Expression of AHP6 CDS under the native promoter with 6 independent transgenic lines in *ahp6-1* (A) and 5 in *ahp6-2* (B) the mutants is displayed.

	AtARR3	AtARR4	AtARR5	AtARR6	AtARR7	AtARR8	AtARR9	AtARR15	AtARR16	AtARR17	OsRR1	OsRR2	OsRR3	OsRR4	OsRR5	OsRR6	OsRR7	OsRR8	OsRR9	OsRR10	OsRR11	OsRR12	OsRR13
AtARR3	100	76.52	64.02	62.42	57.3	47.83	48.92	54.49	51.88	53.64	45	46.91	58.78	50.53	62.88	54.05	56.58	48.76	48.3	48.3	60.29	47.93	47.93
AtARR4	76.52	100	61.24	61.88	54.73	46.23	45.19	50.5	55.28	54.97	44.05	44.79	58.02	47.32	61.36	54.36	56.21	47.93	50.79	49.74	61.03	47.11	47.11
AtARR5	64.02	61.24	100	80.87	63.13	56.05	54.82	64.2	51.95	51.37	44.52	44.52	54.96	51.9	57.25	55.32	51.39	43.8	50.92	51.53	55.22	43.8	44.63
AtARR6	62.42	61.88	80.87	100	63.19	55.35	51.79	62.01	53.59	53.79	43.62	43.24	57.25	51.27	58.78	56.03	50.69	45.45	52.12	52.12	56.72	44.63	45.45
AtARR7	57.3	54.73	63.13	63.19	100	51.81	49.15	70.26	53.29	53.74	37.75	40.67	56.49	48.52	53.44	54.23	50.35	46.28	50.88	49.71	50.38	47.11	47.93
AtARR8	47.83	46.23	56.05	55.35	51.81	100	71.3	49.72	54.23	53.57	38.89	39.33	56.59	56.74	56.25	58.14	57.81	44.63	58.55	58.55	56.25	47.93	46.28
AtARR9	48.92	45.19	54.82	51.79	49.15	71.3	100	44.68	55.56	54.93	40.24	40.22	57.36	55.3	57.03	62.02	58.59	43.8	61.5	61	57.81	47.11	45.45
AtARR15	54.49	50.5	64.2	62.01	70.26	49.72	44.68	100	56.38	58.33	42.21	38.31	55.73	47.22	56.49	57.35	50.36	46.28	50	50.57	52.63	46.28	47.93
AtARR16	51.88	55.28	51.95	53.59	53.29	54.23	55.56	56.38	100	81.7	41.79	41.13	50.38	54.48	50.38	50.34	44.59	43.8	54.86	54.86	48.89	43.8	42.15
AtARR17	53.64	54.97	51.37	53.79	53.74	53.57	54.93	58.33	81.7	100	39.55	39.57	52.67	57.34	53.44	52.86	45.32	43.8	58.45	58.45	51.91	44.63	42.15
OsRR1	45	44.05	44.52	43.62	37.75	38.89	40.24	42.21	41.79	39.55	100	62.67	50	40.99	52.76	50	51.18	42.98	39.13	38.51	55.12	42.15	43.8
OsRR2	46.91	44.79	44.52	43.24	40.67	39.33	40.22	38.31	41.13	39.57	62.67	100	50.79	38.67	51.2	48.41	52	46.28	37.87	37.28	52	44.63	43.8
OsRR3	58.78	58.02	54.96	57.25	56.49	56.59	57.36	55.73	50.38	52.67	50	50.79	100	57.69	71.54	71.32	67.69	48.74	57.36	57.36	70	49.58	50.42
OsRR4	50.53	47.32	51.9	51.27	48.52	56.74	55.3	47.22	54.48	57.34	40.99	38.67	57.69	100	59.69	61.54	58.14	47.11	61.26	60.73	58.91	49.59	48.76
OsRR5	62.88	61.36	57.25	58.78	53.44	56.25	57.03	56.49	50.38	53.44	52.76	51.2	71.54	59.69	100	75.19	73.88	51.26	59.38	59.38	84.33	50.42	52.1
OsRR6	54.05	54.36	55.32	56.03	54.23	58.14	62.02	57.35	50.34	52.86	50	48.41	71.32	61.54	75.19	100	64.02	50.41	58.14	58.14	75.37	50.41	50.41
OsRR7	56.58	56.21	51.39	50.69	50.35	57.81	58.59	50.36	44.59	45.32	51.18	52	67.69	58.14	73.88	64.02	100	49.58	59.38	59.38	70.07	50.42	51.26
OsRR8	48.76	47.93	43.8	45.45	46.28	44.63	43.8	46.28	43.8	43.8	42.98	46.28	48.74	47.11	51.26	50.41	49.58	100	46.28	46.28	51.26	95.04	90.08
OsRR9	48.3	50.79	50.92	52.12	50.88	58.55	61.5	50	54.86	58.45	39.13	37.87	57.36	61.26	59.38	58.14	59.38	46.28	100	98.51	61.72	48.76	47.11
OsRR10	48.3	49.74	51.53	52.12	49.71	58.55	61	50.57	54.86	58.45	38.51	37.28	57.36	60.73	59.38	58.14	59.38	46.28	98.51	100	61.72	48.76	47.11
OsRR11	60.29	61.03	55.22	56.72	50.38	56.25	57.81	52.63	48.89	51.91	55.12	52	70	58.91	84.33	75.37	70.07	51.26	61.72	61.72	100	50.42	50.42
OsRR12	47.93	47.11	43.8	44.63	47.11	47.93	47.11	46.28	43.8	44.63	42.15	44.63	49.58	49.59	50.42	50.41	50.42	95.04	48.76	48.76	50.42	100	91.74
OsRR13	47.93	47.11	44.63	45.45	47.93	46.28	45.45	47.93	42.15	42.15	43.8	43.8	50.42	48.76	52.1	50.41	51.26	90.08	47.11	47.11	50.42	91.74	100

Figure 12. Amino acid sequence similarity between the type-A RRs of *Arabidopsis* and rice. Sequence similarities were calculated using Clustal 2.1.

Primer name	Gene	Sequence	Ta (SensiMix SYBR Hi-ROX)
qRT-OsUbqF	OsUbq	aggctaagatccaggacaagg	58
qRT-OsUbqR	OsUbq	tccttctggatgttgtagtcagc	58
qRT-Os40SF	Os40S	ttgtctttattttcgcttgtgc	58
qRT-OS40SR	Os40S	acaggaagacgatccagtatcc	58
qRT-OsPHP1F	OsPHP1	ggaactgttggtgcctgttt	58
qRT-OsPHP1R	OsPHP1	tgtagatggtaggctgaatgga	58
qRT-OsPHP2F	OsPHP2	tgggttaccttgatgaacagttt	58
qRT-OsPHP2R	OsPHP2	aacaaaattggggcttgattc	58
qRT-OsPHP3F	OsPHP3	aagaaaacgccgaaggatct	58
qRT-OsPHP3R	OsPHP3	cgcaacagctggaagtagg	58
qRT-OsRR1F	OsRR1	ctctgaagccgatcccagt	58
qRT-OsRR1R	OsRR1	tcttcagcaccagcattcat	58
qRT-OsRR2F	OsRR2	aagaaggcgatggagctg	58
qRT-OsRR2R	OsRR2	acgatgtcgatcgcttgat	58
qRT-OsRR3F	OsRR3	cgatctcctcaagagggtca	58
qRT-OsRR3R	OsRR3	gacattagcaccaccggaat	58
qRT-OsRR4F	OsRR4	tgcctgcaaggatcaacag	58
qRT-OsRR4R	OsRR4	gtcagcgagcttgacaggtt	58
qRT-OsRR5F	OsRR5	gaaggtcaaggagtcgtcca	58
qRT-OsRR5R	OsRR5	ggcttcagcaagaaatcctc	58
qRT-OsRR6F	OsRR6	gtgatcatgtcgtcggagaa	58
qRT-OsRR6R	OsRR6	catctgatacggctgcagag	58
qRT-OsRR7F	OsRR7	agcagatgcttggaagaagg	58
qRT-OsRR7R	OsRR7	agcatccggctggttatg	58
qRT-OsRR8F	OsRR8	gcacatctcccggttgtaat	58
qRT-OsRR8R	OsRR8	tcctccatccaagcactttc	58
qRT-OsRR9F	OsRR9	gaacagcagcagcagcacta	58
qRT-OsRR9R	OsRR9	tggggcaaaatttcttcatc	58
qRT-OsRR10F	OsRR10	ccagttgtgatcatgtcatcg	58
qRT-OsRR10R	OsRR10	ccgaactggtttgaggaaaa	58
qRT-OsRR11F	OsRR11	ctcccggtttcgtgtgac	58
qRT-OsRR11R	OsRR11	ccgtgattatcatgctcacatt	58
qRT-OsRR12F	OsRR12	ctagcacatctcccagtggtaa	58
qRT-OsRR12R	OsRR12	gctcctccatccaagcac	58
qRT-OsRR13F	OsRR13	tggtacatctcccggtgataa	58
qRT-OsRR13R	OsRR13	tcctccatcgaagcactttc	58

Table 1. qRT-PCR primers

Table 2.

Primer name	Gene	Sequence	Product size	Ta
g/wOsPHP1F	OsPHP1	GGGGACAAGTTTGTACAAAAAAGCAGGCTgctcccacaagtcatatgttcatca	602	70
g/wOsPHP1R	OsPHP1	GGGGACCACTTTGTACAAGAAAGCTGGGTttacatgacaggcctagtggcag	602	70
g/wOsPHP2F	OsPHP2	GGGGACAAGTTTGTACAAAAAAGCAGGCTattgtgtctcagctctctccacc	773	67
g/wOsPHP2R	OsPHP2	GGGGACCACTTTGTACAAGAAAGCTGGGTgcataagcagggctttacataactt	773	67
g/wOsPHP3F	OsPHP3	GGGGACAAGTTTGTACAAAAAAGCAGGCTggtgatcggcaacctgtgtattc	613	68
g/wOsPHP3R	OsPHP3	GGGGACCACTTTGTACAAGAAAGCTGGGTttacttgcccgcaggccta	613	68
g/wOsRR1F	OsRR1	GGGGACAAGTTTGTACAAAAAAGCAGGCTgtcaccttacttgcttggctact	910	62
g/wOsRR1R	OsRR1	GGGGACCACTTTGTACAAGAAAGCTGGGTtcaagcacaccacaggttg	910	62
g/wOsRR3F	OsRR3	GGGGACAAGTTTGTACAAAAAAGCAGGCTatgtcgacgaagacagtgccg	454	72
g/wOsRR3R	OsRR3	GGGGACCACTTTGTACAAGAAAGCTGGGTtcatttcatgatgacgcggttg	454	72
g/wOsRR6F	OsRR6	GGGGACAAGTTTGTACAAAAAAGCAGGCTattgcaaccgcaaagcctctt	1069	71
g/wOsRR6R	OsRR6	GGGGACCACTTTGTACAAGAAAGCTGGGTgatgcatggttaattggcaagactt	1069	71
g/wOsRR7F	OsRR7	GGGGACAAGTTTGTACAAAAAAGCAGGCTatgagggtgccggcg	691	68
g/wOsRR7R	OsRR7	GGGGACCACTTTGTACAAGAAAGCTGGGTtcactgcagcatccggct	691	68

Table 3.

Primer name	Construct fragment	Sequence	Product size	Ta (Phusion HF)
GibpAHP6F	AHP6 promoter	tatgaccatgattacgccaagctatCAACTTTGTATAGAAAAGTTGG	1649	57.2
GibpAHP6R	AHP6 promoter	tgggagcagcctgCTTTTTTGTACAAACTTGTCC	1649	57.2
GibPHP1QNF	PHP1QN CDS	ttgtacaaaaaagCAGGCTGCTCCCACAAGTC	563	65.9
GibPHP1QNR	PHP1QN CDS	ctaccccactttgtacAAGAAAGCTGGGTTTACATGACAG	563	65.9
GibnosTF	nosT terminator	acccagctttcttGTACAAAGTGGGGTAGCG	315	61
GibnosTR	nosT terminator	tgtaaaacgacggccagtgaattatcaactaTGTATAATAAAGTTGAAGCTTCTGTC	315	61
GibpHMF	pHM34 backbone	TAGTTGATAATTCACTGGC	~8600	56.8
GibpHMR	pHM34 backbone	ATAGCTTGGCGTAATCATGGTCATAG	~8600	56.8

Table 2. Gateway cloning primers

Table 3. Gibson cloning primers

Table 4.

Primer name	Gene	Sequence	Restirction site added	Product size	Ta (Phusion HF)	For cloning into
CDS_OsAHP1f	OsAHP1	cgggatccggaggaATGGCGGCCGCCGCGCTGACC	BamHI	466	72	pGEX-6p1
CDS_OsAHP1r	OsAHP1	gcgtcgacTTAATGTTTAGGGTAACAAGCTTGGATTTGC	SalI	466	72	pGEX-6p1
CDS_OsAHP2f	OsAHP2	cgggatccggaggaATGGCGGCCGCCGCTCTCCGC	BamHI	472	72	pGEX-6p1
CDS_OsAHP2r	OsAHP2	tgactgaattcTTATTGCTGCTTGGGATCATAAGCCTG	EcoRI	472	72	pGEX-6p1
CDS_OsPHP1f	OsPHP1	cgggatccggaggaATGGATTATTCTAATTTGCGTC	BamHI	478	60	pFAST-BAC1-GST
CDS_OsPHP1r	OsPHP1	gcgtcgacTTACATGACAGGCCTAGTGG	SalI	478	60	pFAST-BAC1-GST
CDS_OsPHP2f	OsPHP2	cgtgatcaggaggaATGGAGTATTCAAATTTGCGTC	BclI	471	64	pFAST-BAC1-GST
CDS_OsPHP2r	OsPHP2	gcgtcgacTTACTTCCTTGAGCTCACTGC	SalI	471	64	pFAST-BAC1-GST
CDS_OsPHP3f	OsPHP3	cgggatccggaggaATGGAGTACGGTAATTTGCGACG	BamHI	481	67	pFAST-BAC1-GST
CDS_OsPHP3r	OsPHP3	gcgtcgacTTACTTGCCCGCAGGCC	SalI	481	67	pFAST-BAC1-GST

Table 5.

Primer name	Gene	Sequence	Amino acid substitution	SDM kit
SDM_OsAHP1_Nf	OsAHP1	GGACTCGTATGTGaATCAGCTCAAGGGGAG	H79N	Agilent Quickchange II XL kit
SDM_OsAHP1_Nr	OsAHP1	CTCCCCTTGAGCTGATtCACATACGAGTCC	H79N	Agilent Quickchange II XL kit
SDM_OsAHP1_Qf	OsAHP1	GACTCGTATGTGCAaCAGCTCAAGGGGAGC	H79Q	Agilent Quickchange II XL kit
SDM_OsAHP1_Qr	OsAHP1	GCTCCCCTTGAGCTGtTGCACATACGAGTC	H79Q	Agilent Quickchange II XL kit
SDM_OsAHP2_Nf	OsAHP2	GTCGACGCCTACGTTaATCAGCTCAAAGGCAG	H82N	Agilent Quickchange II XL kit
SDM_OsAHP2_Nr	OsAHP2	CTGCCTTTGAGCTGATtAACGTAGGCGTCGAC	H82N	Agilent Quickchange II XL kit
SDM_OsAHP2_Qf	OsAHP2	GACGCCTACGTTCAaCAGCTCAAAGGCAG	H82Q	Agilent Quickchange II XL kit
SDM_OsAHP2_Qr	OsAHP2	CTGCCTTTGAGCTGtTGAACGTAGGCGTC	H82Q	Agilent Quickchange II XL kit
SDM_OsPHP1_Hf	OsPHP1	GGGATACATATATGCAtCAACTAAAAGGCAGCTGTTCC	Q79H	Agilent Quickchange II XL kit
SDM_OsPHP1_Hr	OsPHP1	GGAACAGCTGCCTTTTAGTTGaTGCATATATGTATCCC	Q79H	Agilent Quickchange II XL kit
SDM_OsPHP2_Hf	OsPHP2	GATTAGATTCTCTTGTGCAtCAACTCAAAGGCAGCGG	Q79H	Agilent Quickchange II XL kit
SDM_OsPHP2_Hr	OsPHP2	CCGCTGCCTTTGAGTTGaTGCACAAGAGAATCTAATC	Q79H	Agilent Quickchange II XL kit
SDM_OsPHP3_Hf	OsPHP3	GGGACACACACATGCAtCAATTGAAAGGCAGCTG	Q79H	Agilent Quickchange II XL kit
SDM_OsPHP3_Hr	OsPHP3	CAGCTGCCTTTCAATTGaTGCATGTGTGTGTCCC	Q79H	Agilent Quickchange II XL kit
SDM_AHP6NQpFASTf	AtAHP6	GAAAATAGGATTACAcCTGAATCAGCTGGTGGGAAG	N83Q	Agilent Quickchange II XL kit
SDM_AHP6NQpFASTr	AtAHP6	CTTCCCACCAGCTGATTCAGgTGTAATCCTATTTTC	N83Q	Agilent Quickchange II XL kit
SDM_AHP6NHpFASTf	AtAHP6	GAAAATAGGATTACACCTGcATCAGCTGGTGGGAAGC	N83H	Agilent Quickchange II XL kit
SDM_AHP6NHpFASTr	AtAHP6	GCTTCCCACCAGCTGATgCAGGTGTAATCCTATTTTC	N83H	Agilent Quickchange II XL kit
SDMneb_PHP1QNf	OsPHP1	TACATATATGaacCAACTAAAAGGCAGC	Q79N	NEB Q5 SDM kit
SDMneb_PHP1QNr	OsPHP1	TCCCACCTGTTGAAATCTC	Q79N	NEB Q5 SDM kit

Table 4. Phosphotransfer assay cloning

Table 5. Site directed mutagenesis primers

Primer name	Gene	Sequence	Restirction site added	Product size	Ta (Phusion HF)
proOsPHP1f_1_XbaI	PHP1	CGTGTCTAGAaggaatcaatcgtgtcggc	XbaI	3055	63
proOsPHP1f_2_XbaI	PHP1	CGTGTCTAGAatttcctatgatgccctttgaaata	XbaI	4092	66
proOsPHP1r_HindIII	PHP1	GCACTAAGCTTttatatgaatgaatgaggaaatatgtgac	HindIII		
proOsPHP2f_1_XbaI	PHP2	CGTGTCTAGAaggaagaatctgtctctctta	XbaI	3052	57
proOsPHP2f_2_XbaI	PHP2	CGTGTCTAGAggtacaagtaaaatgagctca	XbaI	3911	59
proOsPHP2r_SalI	PHP2	AATTGTCGACatatggctaagctttagagatcag	SalI		
proOsPHP3f_1_BamHI	PHP3	TTAAGGATCCatcgaaaaggaggtagcgtat	BamHI	3075	62
proOsPHP3f_2_BamHI	PHP3	TTAAGGATCCgaaattagagcggaagggtt	BamHI	4076	59
proOsPHP3r_SalI	PHP3	AATTGTCGACtcacaagtattgaacagtcagg	SalI		
proOsRR1f_1_SalI	RR1	TTAAGTCGACgagctgtttaacggaaatgtgg	SalI	3079	64
proOsRR1f_2_SalI	RR1	TTAAGTCGACgaggtggatgtggaggatgga	SalI	4059	65
proOsRR1r_PstI	RR1	AGTGCTGCAGctctccctcaccaacaacca	PstI		
proOsRR3f_1_BamHI	RR3	TTAAGGATCCgagggcgagggtaaatagtcc	BamHI	3151	65
proOsRR3r_SalI	RR3	AATTGTCGACgaggcagagaatggagcaga	SalI		
proOsRR6f_1_XbaI	RR6	CGTGTCTAGAtgagaatacagagaagccgaga	XbaI	3084	66
proOsRR6f_2_XbaI	RR6	CGTGTCTAGAgtcacaggtcaatgcaggttta	XbaI	4034	67
proOsRR6r_HindIII	RR6	GCACTAAGCTTtgatcaactcaaaatccaaccca	HindIII		
proOsRR7f_1_XbaI	RR7	CGTGTCTAGAgtgatgctgtactgttggatt	XbaI	3115	62
proOsRR7f_2_XbaI	RR7	CGTGTCTAGAcaagctatgcagtagagaagag	XbaI	3674	61
proOsRR7r_HindIII	RR7	GCACTAAGCTTctccatcgatcaacaacgtta	HindIII		

Table 6. Promoter amplification primers

Table 7.

Oligo name	Gene	Sequence
OsPHP1_283f_1	OsPHP1	aggtctcaggcaAGATGAGCAATTTTGTCAGGgtttagagacca
OsPHP1_283f_2	OsPHP1	tggtctctaaacCCTGACAAAATTGCTCATCTtgcctgagacct
OsPHP1_319f_1	OsPHP1	aggtctcaggcaTGAAGCTAGTCCTAATTTTGgtttagagacca
OsPHP1_319f_2	OsPHP1	tggtctctaaacCAAAATTAGGACTAGCTTCAtgcctgagacct
OsPHP2_55f_1	OsPHP2	aggtctcaggcaGATGAACAGTTTAATCAGCgtttagagacca
OsPHP2_55f_2	OsPHP2	tggtctctaaacGCTGATTAAACTGTTCATCtgcctgagacct
OsPHP2_79r_1	OsPHP2	aggtctcaggcaCGCAACTTCCTCAACAAAATgtttagagacca
OsPHP2_79r_2	OsPHP2	tggtctctaaacATTTTGTTGAGGAAGTTGCGtgcctgagacct
OsPHP3_530f_1	OsPHP3	aggtctcaggcaTGAGCAATTTTGTCAGGTTGgtttagagacca
OsPHP3_530f_2	OsPHP3	tggtctctaaacCAACCTGACAAAATTGCTCAtgcctgagacct
OsPHP3_576r_1	OsPHP3	aggtctcaggcaGGTTGAATCCTTAAAAAACAgtttagagacca
OsPHP3_576r_2	OsPHP3	tggtctctaaacTGTTTTTTAAGGATTCAACCtgcctgagacct
OsRR1_52f_1	OsRR1	aggtctcaggcaTGCACCACCCTCCTGTCCACgtttagagacca
OsRR1_52f_2	OsRR1	tggtctctaaacGTGGACAGGAGGGTGGTGCAtgcctgagacct
OsRR1_182r_1	OsRR1	aggtctcaggcaGGCCTTCTTGGCGCTGTCGAgtttagagacca
OsRR1_182r_2	OsRR1	tggtctctaaacTCGACAGCGCCAAGAAGGCCtgcctgagacct
OsRR6_115f_1	OsRR6	aggtctcaggcaGAAGGTGGTGCCGGTTGTGGgtttagagacca
OsRR6_115f_2	OsRR6	tggtctctaaacCCACAACCGGCACCACCTTCtgcctgagacct
OsRR6_160f_1	OsRR6	aggtctcaggcaGCAGAGCGAGATGCACGTGCgtttagagacca
OsRR6_160f_2	OsRR6	tggtctctaaacGCACGTGCATCTCGCTCTGCtgcctgagacct
OsRR7_137f_1	OsRR7	aggtctcaggcaATGAAGAGTGTCGTCGTCAAgtttagagacca
OsRR7_137f_2	OsRR7	tggtctctaaacTTGACGACGACACTCTTCATtgcctgagacct
OsRR7_163r_1	OsRR7	aggtctcaggcaGCCGATGCGTTGTCGTGCAGgtttagagacca
OsRR7_163r_2	OsRR7	tggtctctaaacCTGCACGACAACGCATCGGCtgcctgagacct

Table 8.

Primer name	Gene	Sequence	Product size	Ta (Phusion HF)
OsPHP1_CRISPR_genoF	OsPHP1	TCCATAGCTCCCACAAGTCAT	675	66
OsPHP1_CRISPR_genoR	OsPHP1	CAGCTGCCTTTTAGTTGCTGC	675	66
OsPHP2_CRISPR_genoF	OsPHP2	GAAGCCTACTCCCTCCATCC	677	61
OsPHP2_CRISPR_genoR	OsPHP2	CACTCTGTGTTCTGGGCATA	677	61
OsPHP3_CRISPR_genoF	OsPHP3	AGGCATATCTGAGACTCTGCA	696	61
OsPHP3_CRISPR_genoR	OsPHP3	GCTTACCTAGAACAGCTGCC	696	61
OsRR1_CRISPR_genoF	OsRR1	AGTCGAGGAGAGATTGCAGT	746	61
OsRR1_CRISPR_genoR	OsRR1	TATCGGTCTCTCGCCTTGTC	746	61
OsRR6_CRISPR_genoF	OsRR6	CACACGACACGCATATCACC	526	64
OsRR6_CRISPR_genoR	OsRR6	ATTACCTTGACGCGCTTGAG	526	64
OsRR7_CRISPR_genoF	OsRR7	GCCCTGCCTTACACCTGATA	597	64
OsRR7_CRISPR_genoR	OsRR7	ACCGAGCCCAATATCTCCAG	597	64

Table 7. CRISPR protospacer oligos

Table 8. CRISPR genotyping primers

Primer name	Gene/plasmid	Sequence
SLN1HKpMALc2x_seqf1	SLN1HK	aacaatttcacacaggaaacagcc
SLN1HKpMALc2x_seqf2	SLN1HK	aataaaggcgaaacagcgatgac
M13f(-40)	Bacmid	GTTTTCCCAGTCACGAC
M13r	Bacmid	CAGGAAACAGCTATGAC
pJET1.2for	pJET1.2 plasmid	CGACTCACTATAGGGAGAGCGGC
pJET1.2rev	pJET1.2 plasmid	AAGAACATCGATTTTCCATGGCAG
pHUbi_seq_f	pHUbi plasmid	tatctctagagaggggcacg
pHUbi_seq_r	pHUbi plasmid	TGTGGTTGGCATGCACATAC
seqpPHP1_1	PHP1 promoter	agcaggatatgaggcaaatagac
seqpPHP1_2	PHP1 promoter	catttatgagaaaggccaaatccc
seqpPHP1_3	PHP1 promoter	ttctgtagtgatgaatgatggacc
seqpPHP1_4	PHP1 promoter	aaagctgatggtattcttcacc
seqpPHP2_1	PHP2 promoter	aaactagggcacgatgcatgac
seqpPHP2_2	PHP2 promoter	caaggaagaatctgtctctcttag
seqpPHP2_3	PHP2 promoter	gtacaattggatgcacacacccac
seqpPHP2_4	PHP2 promoter	catttggtttcagtgtgaaagc
seqpPHP2_5	PHP2 promoter	ctttgaacgaaccagcagagtgc
seqpPHP2_6	PHP2 promoter	tatttgggattactctgtcctggc
seqpPHP3_1	PHP3 promoter	cgaaagcagtgagatccgtc
seqpPHP3_2	PHP3 promoter	cccaatttggatgccactagg
seqpPHP3_3	PHP3 promoter	ccctgagtaaggctgtaagg
seqpPHP3_4	PHP3 promoter	aacgtctgagaggaattgtgttc
seqpPHP3_5	PHP3 promoter	gatgaatagtgagccatgcc
seqpPHP3_6	PHP3 promoter	ttccctatttgattgttcctgc
seqpRR1_1	RR1 promoter	tctagagctgtcgatgcatatc
seqpRR1_2	RR1 promoter	aactaactccgttgttaagctacc
seqpRR1_3	RR1 promoter	agtccacttgtgatgagataatcc
seqpRR1_4	RR1 promoter	ctctctttctctcttcttctacga
seqpRR3-1	RR3 promoter	gagtacaaatgagagagaatctgc
seqpRR3-2	RR3 promoter	atgtgccaaataatgccttgtg
seqpRR3-3	RR3 promoter	ggtactgtgccacatacatgatac
seqpRR3-4	RR3 promoter	gtccagatacagagaaactgac
seqpRR6-1	RR6 promoter	gtaggcacaacttgcttattctc
seqpRR6-2	RR6 promoter	gttattgtgaatccaacaggtgag
seqpRR6-3	RR6 promoter	aatacgtcccagaattatggatgg
seqpRR6-4	RR6 promoter	gggtgtcgattaaaggacgtaaac
seqpRR6-5	RR6 promoter	tggcaacggattgaaccacc
seqpRR6-6	RR6 promoter	gaactgaactaaatcagccaaacc
seqpRR7_1	RR7 promoter	accaaaccaaactggccctatatc
seqpRR7_2	RR7 promoter	gggattcgctacaatgccac
seqpRR7_3	RR7 promoter	gggcaacaagtaggttgagaag
seqpRR7_4	RR7 promoter	aggctaggaacacctgacag
seqpRR7_5	RR7 promoter	tgcgtgtccaactttgactatcc
seqpRR7_6	RR7 promoter	caagcgtatccacgatgctg

Table 9. Sequencing primers

Appendix paper in review

A core mechanism for specifying root vascular pattern can replicate the anatomical variation seen in diverse plant species.

Running title: Vascular pattern in diverse species

Nathan Mellor*, John Vaughan-Hirsch*, Britta MC Kümpers*, Ana Campilho§, John R King$ and Anthony Bishopp*

* Centre for Plant Integrative Biology/School of Biosciences, University of Nottingham, Sutton Bonington Campus, Loughborough, LE12 5RD, UK

§ CIBIO-InBIO, Universidade do Porto, Campus de Vairão, Rua Padre Armando Quintas, 4485-661 Vairão, Portugal.

$ School of Mathematical Sciences/Centre for Plant Integrative Biology, University of Nottingham, University Park, Nottingham, NG7 2RD, UK

Corresponding Author: anthony.bishopp@nottingham.ac.uk

Key words: multiscale modelling, vascular pattern, auxin, cytokinin, developmental biology, root biology

Summary Statement:
We show how a gene regulatory network that generates a diarch vascular pattern in *Arabidopsis* roots can produce the range of patterns seen in flowering plants under different spatial constraints.

Abstract

Pattern formation is typically controlled through the interaction between molecular signals within a given tissue. During early embryonic development, roots of the model plant *Arabidopsis thaliana* have a radially symmetric pattern, but an asymmetric input of the hormone auxin from the two cotyledons forces the vascular cylinder to develop a diarch pattern with two xylem poles. Molecular analyses and mathematical approaches have uncovered the regulatory circuit that propagates this initial auxin asymmetry into a stable cellular pattern. The diarch pattern seen in *Arabidopsis* is relatively uncommon amongst flowering plants, with most species having between three and eight xylem poles. Here, we use multiscale mathematical modelling to demonstrate that this regulatory module does not require an asymmetric auxin input to specify vascular pattern. Instead pattern can emerge dynamically, with its final form dependent upon spatial constraints and growth. The predictions of our simulations compare with experimental observations of xylem pole number across a range of species, as well as in transgenic systems in *Arabidopsis* in which we manipulate the size of the vascular cylinder. Through considering the spatial constraints, our model is able to explain the diversity seen in different flowering plant species.

Introduction

Patterning of organs involves the organization of cell fates within a tissue in space and time. Although the molecular networks that control pattern formation may be considered as deterministic, there is increasing evidence that other factors, including environmental perturbations and stochastic effects, play key roles in the formation of the stable patterns observed. In many processes ranging from floral morphogenesis in plants (Álvarez-Buylla *et al.*, 2008) to flagella length in Chlamydomonas (Kannegaard *et al.*, 2014), stochasticity is required. Alterations in organ growth have also been shown to further the diversity in biological patterns, in systems based on morphogen gradients such as wing patterning in flies (Wartlick and González-Gaitán, 2011) and in polarity-based systems such as floral morphogenesis (Kennaway *et al.*, 2011).

The root vascular cylinder (stele) of the model plant *Arabidopsis* has been exploited as a model for pattern formation as it constitutes a symmetry-breaking event that transforms a near radially symmetric root into a bisymmetric structure, with two xylem poles arranged in a diarch pattern (Fig 1A). This process is driven through an early asymmetry in the signalling domains of two phytohormones, auxin and cytokinin (Mähönen *et al.*, 2006; Bishopp *et al.*, 2011), in which cells with high auxin output differentiate as xylem. Several key interactions between these hormones specify distinct domains of hormonal signalling. Auxin response promotes the transcription of a cytokinin signalling inhibitor *ARABIDOPSIS HISTINE PHOSPHOTRANSFERASE 6* (*AHP6*) (Mähönen *et al.*, 2006; Bishopp *et al.*, 2011). Cytokinin signalling modulates the activity of a group of auxin transport proteins known as PINFORMED proteins (PINs) (Gälweiler *et al.*, 1998; Ruzicka *et al.*, 2009; Bishopp *et al.*, 2011; Pernisova *et al.*, 2016). An additional feedback loop exists in which auxin signalling promotes cytokinin biosynthesis via activation of the *LONELY GUY4* (*LOG4*) enzyme (De Rybel *et al.*, 2014). Although the domain of high auxin response extends throughout the xylem axis, the formation of protoxylem is restricted to the marginal positions. A group of class III HD-ZIP transcription factors, including the gene *PHABULOSA* (*PHB*), act in a dose-dependent manner to prevent protoxylem formation and *AHP6* expression in the central part of the root (Carlsbecker *et al.*, 2010).

A number of theoretical studies have investigated this mechanism for generating stable vascular pattern in *Arabidopsis* roots (De Rybel *et al.*, 2014; Muraro *et al.*, 2014; el-Showk *et al.*, 2015), with a consensus between the three models being drawn recently (Mellor *et al.*, 2016). Collectively, these models support the hypothesis that the nonlinear feedback between auxin and cytokinin can transform an initial asymmetry into the stable diarch pattern seen in *Arabidopsis*. Although different asymmetric inputs have been modelled, experimental evidence points to an asymmetric input of auxin coming from the two cotyledons during embryogenesis (De Rybel *et al.*, 2014). Consistently, mutants with altered cotyledon number have irregular numbers of xylem poles within the embryonic root (Help *et al.*, 2011). This cytokinin-based patterning mechanisms seems specific to the root, as shoot models of periodic auxin distribution can pattern vascular bundles solely via activity of auxin influx and efflux proteins (Fàbregas *et al*., 2015).

Whilst these studies provide a feasible mechanism for generating the root vascular pattern seen in *Arabidopsis*, they cannot explain the patterns seen in many other species. Many dicotyledonous roots typically display three or four xylem poles during primary development (Figure 1B) (Esau, 1965). In contrast monocotyledonous plants typically display five or more xylem poles (Figure 1C-D) (Esau, 1965). Previous studies have focused on deterministic molecular mechanisms in *Arabidopsis* and have not investigated the role spatial constraints play in determining the final pattern; in this paper we show vascular pattern can be set as an emergent property of the interaction between auxin and cytokinin, but that spatial constraints and stochastic elements play a significant role in directing the final pattern.

Results and Discussion

To generate a holistic model that can simulate pattering in a range of species, we consider three essential components (namely auxin, cytokinin and PIN) only, rather than explicitly modelling individual gene products (Fig 2A,C). Auxin represents both the molecule itself and the mechanism through which it is perceived. Rather than explicitly modelling an AHP6-like component that represses cytokinin signalling, we simplify the network so that auxin represses cytokinin signalling directly. Likewise we make the simplification that auxin promotes the production of cytokinin directly, without including any intermediate components (such as the LOG genes). Cytokinin represents only itself, auxin having the dual antagonistic effects of promoting the synthesis of cytokinin while repressing the cytokinin response, which we model through the interaction with PIN. We consider a generic PIN to be induced by cytokinin, with feedback through auxin. Finally, as an auxin efflux transporter, the presence of PIN in a cell enhances the unidirectional transport of auxin out of that cell. Like all previous models, we do not explicitly model the process of vascular differentiation, but interpret spikes of high auxin response as indicators of cells primed to differentiate as xylem.

To approximate the vascular cells immediately adjacent to the pericycle, where xylem poles develop, the spatial domain of the model consists of a ring of cells of equal size that can vary only in cell number between simulations (Fig 2B). In this way, as cell number increases, the size of the ring increases proportionally.

Running the model with uniform initial conditions results in a spatially homogenous steady state for all three components (Fig S1). However, in suitable parameter regimes (see Supplementary Information, Figs S2-6), adding a small amount of noise to the initial level of auxin is sufficient to initiate an instability and produce poles of high auxin response. With a configuration of 10 cells, we see one or two xylem poles forming (Fig 2D), while with 20 initial cells we see either two or three poles (Fig 2E). This suggests that vascular pattern could be set by small stochastic fluctuations rather than specific spatial asymmetries.

To test the relationship between domain size and pole number further, we ran repeated simulations, using templates with between 8 and 26 cells (Fig 3A). In all simulations, the system reached steady state, with diverse patterns generated. Whilst

the smallest template, of 8-cells, only ever has one pole, for most templates, variation in pole number is observed, i.e. a set of possible outcomes rather than a single solution, with increasing cell number increasing the likelihood of generating more poles. This positive relationship between cell number and pole number is consistent for a broad range of parameter values (Figures S2-6).

We investigated whether these observations are representative of the variation seen in plants, using rice, which shows variation in both the size of roots and number of xylem poles, by sectioning roots and comparing the number of xylem poles to root diameter (Fig 3B). Consistent with our simulations, we saw an increased likelihood of more vascular poles in the larger roots. As in the model, we observed considerable overlap of possible xylem patterns within roots of particular sizes. For example, roots with a diameter of 74-76 µm could give 5, 6, 7 or 8 poles (Fig S7). Taken together, these simulations coupled with the biological observations above present a potential mechanism through which distinct patterns could be set depending on the spatial constraints within which the gene regulatory network operates.

Whilst this static model investigates the relationship between stele size and the number of xylem poles, it does not consider how the pattern evolves in a growing root. Although we see some variation of pole number within some species, for others there is none and our static model suggests a greater number of possible outcomes than can be observed experimentally. To address whether organ growth has an effect on stabilizing the patterning process, we incorporated cell growth and division into the model. Division of a given cell is based on the accumulation over time of the product of a generic cytokinin response gene, denoted *R*, modelled in addition to PIN. Once *R* reaches a given threshold the cell is primed for division. To prevent numerous cells dividing simultaneously we assign a fixed duration to the mitosis step.

We used the outcomes of static simulations to provide sets of initial conditions that could then be grown further, allowing pattern to evolve. In simulations starting with 8 cells (which give one pole in 100% of simulations), growing to up to 20 cells resulted in two poles 100% of the time (Fig 4A). By comparison, static simulations with 20 cells resulted in either two poles (around 40%) or three poles (around 60%) (Fig 3A). These predicted differences between the static and dynamic simulations suggest that organ growth can stabilize patterning. We used the model to test this hypothesis further, by running simulations in which the templates grew larger still. Starting with templates of 20 cells, which have either two or three xylem poles, and growing to 54 cells, we found differences in behaviour depending on whether the initial 20 cell template had a two- or a three-pole configuration (Fig 4C): while 69% of simulations starting from a two-pole configuration resulted in a pattern with 4 poles, 19% in 5 poles and 19% in 6 poles, for those starting from a 3-pole initial configuration, only 10% had 4 poles with 43% and 47% having five or six poles respectively. Static simulations for 54-cell templates had between 5 and 9 poles, with 7 poles appearing most commonly (Fig 4B,S8). In all cases, template growth stabilized the patterning process reducing the number of xylem poles, though the morphogenetic history/initial conditions also had a significant effect in directing the final patterning outcome (Fig S8).

To provide experimental evidence testing the effect that altering spatial restraints has on vascular pattern, we exploited the *lonesome highway* (*lhw*) mutant in *Arabidopsis* to develop a system in which we can manipulate stele size: *lhw* mutants have a smaller stele than wild-type plants, with just one xylem pole (Ohashi-Ito and Bergmann, 2007). We engineered an oestrogen inducible rescue line under a stele-specific promoter (*pWOL>>XVE>>LHW*) to rescue this phenotype. It is important to note that LHW protein not only controls cell number but also affects the molecular network controlling cell patterning by promoting cytokinin synthesis via the LOG4 gene (De Rybel *et al.*, 2014; Ohashi-Ito *et al*., 2014).

Whilst in an ideal world, we would separate the processes of growth and cytokinin response, they are so intimately related that this cannot be done experimentally. However, the above modelling approach allows us to do this readily. To simulate the *lhw* mutant and associated rescue via our transgenic rescue line, we ran simulations with maximum cytokinin production set to 50% of the wild type level for an allotted period, then reset cytokinin production to 100% for the remainder of the time course to simulate the transgenic rescue of this mutant. We start from 8 cells as, like the *lhw* mutant, simulations run with the static model in this template always produced just one pole with the chosen parameter set. Though the reduction in cytokinin results in weaker expression of PIN, it is still sufficient to drive auxin into a single pole. When the model is permitted to grow under reduced cytokinin conditions we see no cell divisions; increasing cytokinin production promotes cell division and growth and, if the ring is permitted to grow sufficiently large, a new pole is formed opposite the original one (Fig 4E). Increasing the ring from 8 to 16 or 17 cells resulted in a transition from 1 to 2 poles 100% of the time (Fig S9). Other changes in ring size exhibited the same behaviour, though less robustly.

In our experimental system un-induced *lhw* plants had an average vascular-cylinder diameter of 26.9 µm and 32 of 33 plants analyzed had just one xylem pole. Following induction with 17-β-estradiol, (a synthetic derivative of oestrogen) for 72h, the diameter of the stele increased and a second xylem pole had formed in 54 % of plants (Fig 4D). We divided the induced plants into two categories based on xylem pole number: those with one pole had an average diameter of 29.5 µm and those with two had 35.9 µm. We performed a Student t-test to examine the relationships between stele size and final pattern: there was no statistical difference between root size in the two-pole *lhw* rescue lines and the wild-type control, indicating a clear correlation between pole number and size.

Taken together, our simulations and manipulation of stele size support the hypothesis that a dynamic patterning system exists within roots that can specify vascular pattern as an emergent property of the network based on organ size and growth history. Although vascular pattern is initiated during embryogenesis, as the root grows and the positional information from cotyledons is lost, we propose that the initial pattern can be re-set into one of the many patterns observed experimentally. This re-patterning process provides a mechanism whereby final organ size, growth and morphogenetic history can all influence the final pattern.

While the near radial symmetry of plant roots makes the symmetry break discussed above particularly clear-cut, the types of interaction between genetic regulation, intercellular signalling, physical constraints, growth and stochasticity are undoubtedly much more broadly relevant in developmental biology. Thus the interplay between growth and form so influentially highlighted by D'Arcy Thompson (Thompson, 1917) remains key in the era of molecular biology and we accordingly revisit the role of growth in generating robust patterning, which has been widely recognised in other contexts (see Crampin *et al.*, 2002 for example). As we have seen, xylem-pole formation provides a particularly simple model for this phenomenon: PIN regulation by cytokinin enables existing poles to extract auxin from their neighbourhood, but when the spatial separation between poles exceeds a threshold auxin transport becomes insufficient to suppress the formation of a new pole in the cell most distant from extant poles, growth leading thereby to the regular spacing observed in simulations. This spatially limited inhibition by regulation of active transport thus represents a distinctive mechanism for robust patterning.

Materials and Methods

Mathematical Model

The formulation and implementation of the mathematical models is described in the supplementary materials and methods.

Experimental analyses

The LHW rescue line was created using the oestrogen-inducible gateway system in (Siligato *et al.*, 2016). The full LHW coding sequence cloned from a cDNA template used to generate a second box entry clone. This was combined with the WOL::XVE cassette (Siligato *et al.*, 2016) to give *pWOL>>XVE>>LHW* and introduced into the *lhw* mutant carrying the AHP6::GFP marker (Mähönen *et al.*, 2006). Analyses were performed using a Leica SP5 confocal microscope. For other cross sections, we used a plastic sectioning approach as described in (Mähönen *et al.*, 2000).

References

Alvarez-Buylla, E.R., Chaos, A., Aldana, M., Benítez, M., Cortes-Poza, Y., Espinosa-Soto, C., Hartasánchez, D.A., Lotto, R.B., Malkin, D., Escalera Santos, G.J. and Padilla-Longoria, P. (2008). Floral morphogenesis: stochastic explorations of a gene network epigenetic landscape. *PLoS ONE* **3**, e3626.

Bishopp, A., Help, H., El-Showk, S., Weijers, D., Scheres, B., Friml, J., Benková, E., Mähönen, A.P. and Helariutta Y. (2011). A mutually inhibitory interaction between auxin and cytokinin specifies vascular pattern in roots. *Curr. Biol.* **21**, 917–926.

Carlsbecker, A., Lee, J.Y., Roberts, C.J., Dettmer, J., Lehesranta, S., Zhou, J., Lindgren, O., Moreno-Risueno, M.A., Vatén, A., Thitamadee, S., Campilho, A., Sebastian, J., Bowman, J.L., Helariutta, Y. and Benfey, P.N..(2010). Cell signalling by microRNA165/6 directs gene dose-dependent root cell fate. *Nature.* **465**, 316–321.

Crampin, E.J., Hackborn, W.W. and Maini, P.K. (2002). Pattern formation in reaction-diffusion models with nonuniform domain growth. *Bull Math Biol.* **64**:747-69.

el-Showk, S., Help-Rinta-Rahko, H., Blomster, T., Siligato, R., Marée A.F.M., Mähönen, A.P. and Grieneisen, V.A. (2015). Parsimonious Model of Vascular Patterning Links Transverse Hormone Fluxes to Lateral Root Initiation: Auxin Leads the Way, while Cytokinin Levels Out. *PLoS Comp. Biol.* **11**, 1–40.

Esau, K. (1965). Plant Anatomy 2nd ed. Wiley, New York.

Fàbregas, N., Formosa-Jordan, P., Confraria, A., Siligato, R., Alonso, J.M., Swarup, R., Bennett, M.J., Mähönen, A.P., Caño-Delgado, A.I. and Ibañes, M. (2015). Auxin influx carriers control vascular patterning and xylem differentiation in Arabidopsis thaliana. *PLoS Genet*. **11**:e1005183.

Gälweiler, L., Guan, C., Müller, A., Wisman, E., Mendgen, K., Yephremov, A. and Palme, K. (1998). Regulation of polar auxin transport by AtPIN1 in Arabidopsis vascular tissue. *Science* **282**, 2226–30.

Help, H., Mähönen, A.P., Helariutta, Y and Bishopp, A. (2011). Bisymmetry in the embryonic root is dependent on cotyledon number and position. *Plant Signal. & Behav.* **6**, 1837–40.

Kannegaard, E., Rego, E.H., Schuck, S., Feldman, J.L and Marshall, W.F. (2014). Quantitative analysis and modeling of katanin function in flagellar length control. *Mol. Biol. Cell* **25**, 3686–3698.

Kennaway, R,, Coen, E,, Green, A,, Bangham, A. and Ray, P. (2011). Generation of diverse biological forms through combinatorial interactions between tissue polarity and growth. *PLoS Comp. Biol.* **7**, e1002071.

Mähönen, A.P., Bishopp, A., Higuchi, M., Nieminen, K.M., Kinoshita, K., Törmäkangas, K., Ikeda, Y., Oka, A., Kakimoto, T. and Helariutta, Y. (2006). Cytokinin Signaling and Its Inhibitor AHP6 Regulate Cell Fate During Vascular Development. Supplementary. *Science.* **94**, 94–8.

Mähönen, A.P., Bonke, M., Kauppinen, L., Riikonen, M., Benfey, P.N. and Helariutta, Y. **(**2000). A novel two-component hybrid molecule regulates vascular morphogenesis of the Arabidopsis root. *Genes Dev*. **14**:2938-43.

Mellor, N., Adibi, M., El-Showk, S., De Rybel, B., King, J.,, Mähönen, A.P., Weijers, D. and Bishopp, A. (2016). Theoretical approaches to understanding root vascular patterning: A consensus between recent models. *J. Exp. Bot.* **68**. 5-16.

Muraro, D., Mellor, N., Pound, M.P., Lucas, M., Chopard, J., Byrne, H.M., Godin, C., Hodgman, T.C., King, J.R., Pridmore, T.P., Helariutta, Y., Bennett, M.J. and Bishopp, A. (2014). Integration of hormonal signaling networks and mobile microRNAs is required

for vascular patterning in Arabidopsis roots. *Proc. Natl. Acad. Sci. USA.* **111**, 857–862.

Ohashi-Ito, K. and Bergmann, D.C. (2007). Regulation of the Arabidopsis root vascular initial population by LONESOME HIGHWAY. *Development.* **134**, 2959–2968.

Katayama, H., Iwamoto, K., Kariya, Y., Asakawa, T., Kan, T., Fukuda, H. and Ohashi-Ito, K. (2015). A negative feedback loop controlling bHLH complexes is involved in vascular cell division and differentiation in the root apical meristem. *Curr. Biol*. **25**:3144-50.

Pernisova, M., Prat ,T., Grones, P., Harustiakova, D., Matonohova, M., Spichal, L., Nodzynski, T., Friml, J. and Hejatko, J. (2016). Cytokinins influence root gravitropism via differential regulation of auxin transporter expression and localization in. *New Phytol*. **212**, 497-509.

Ruzicka, K., Simásková, M., Duclercq, J., Petrásek, J., Zazímalová, E., Simon, S., Friml, J., Van Montagu, M.C.E. and Benková, E. (2009). Cytokinin regulates root meristem activity via modulation of the polar auxin transport. *Proc. Natl. Acad. Sci. USA.* **106**, 4284–4289.

De Rybel, B., Adibi, M., Breda, A.S., Wendrich, J.R., Smit, M.E., Novák, O., Yamaguchi, N., Yoshida, S., Van Isterdael, G., Palovaara, J., Nijsse, B., Boekschoten, M.V., Hooiveld, G., Beeckman, T., Wagner, D., Ljung, K., Fleck, C. and Weijers, D.(2014). Integration of growth and patterning during vascular tissue formation in Arabidopsis. *Science* **345**, 1255215–1255215.

Siligato, R., Wang, X., Yadav, S.R., Lehesranta, S., Ma, G., Ursache, R., Sevilem, I., Zhang, J., Gorte, M., Prasad, K., Wrzaczek, M., Heidstra, R., Murphy, A., Scheres, B. and Mähönen, A.P.(2016). MultiSite Gateway-Compatible Cell Type-Specific Gene-Inducible System for Plants. *Plant Physiol.* **170**, 627–641.

Thompson, D.W. (1917). On growth and form. Cambridge University Press.

Wartlick, O. and González-Gaitán, M. (2011). The missing link: implementation of morphogenetic growth control on the cellular and molecular level. *Curr Opin Genet Dev.* **21**:690-5.

Competing interests
There are no competing interests.

Author contributions
NM produced all simulations and mathematical analyses. JV-H and BMK performed experimental analyses. All authors designed experiments/simulations, analysed data and NM and AB wrote the manuscript.

Funding
NM and BMK were funded by a BBSRC New Investigator grant to AB (BB/L023555/1). JV-H was funded through a BBSRC Doctoral training programme. AB was funded by a Royal Society University Research Fellowship.

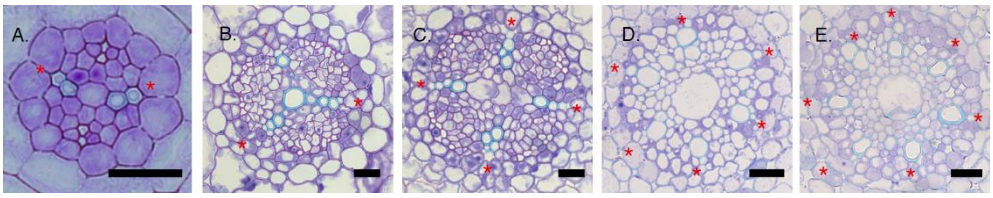


Figure 1. The diversity of vascular pattern in different plant species. (A) The model plant *Arabidopsis thaliana* contains two xylem poles. (B) *Lotus japonica* typically has three xylem poles. (C) *Medicago truncatula* typically has four xylem poles. (D-E) Monocotyledonous plants typically have a greater number, shown here are rice (kitake) primary roots with six and seven poles. Samples have been stained with toluidine blue to highlight cell walls. Xylem poles are indicated with asterisks for additional clarity. Scale bars are 20 µm.

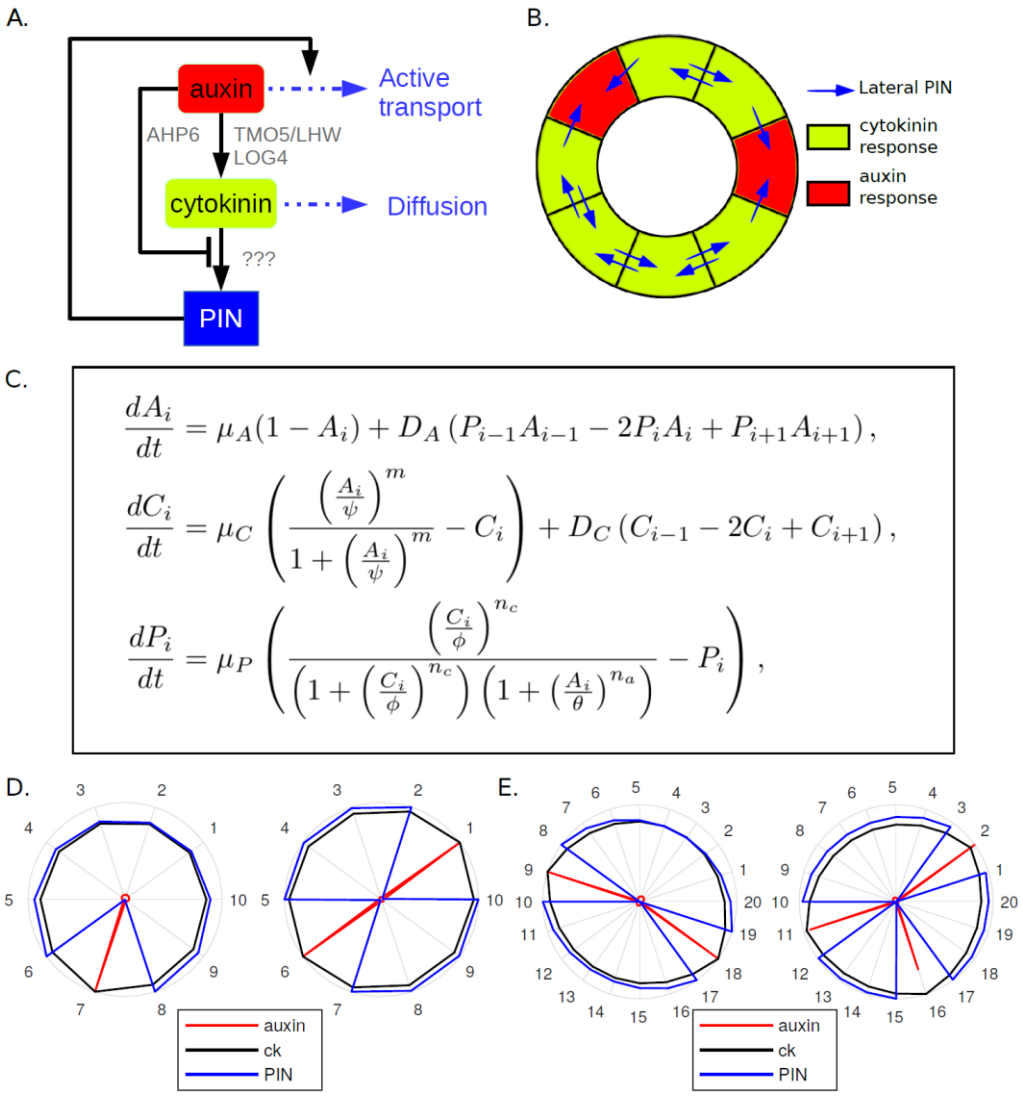


Figure 2. A predictive model of vascular pattern. (A). Schematic diagram showing network configuration. The black lines represent interaction between individual components, and the blue lines represent transport of components between cells. (B) An example model prediction shown in its spatial context, with PIN activity (blue arrows) being dependent on hormonal output. (C) Model equations. A_i represents auxin in cell i, C_i cytokinin in cell i, P_i PIN in cell i. See SI for details and formulation. (D-E). Representative predictions from the static model. The levels of each component is shown on a relative scale between 0-1. Auxin is shown in red, cytokinin in black and PIN in blue. High auxin response is indicative of sites where xylem will form. (D) 10 initial cells results in one or two poles. (E) 20 initial cells results in two or three poles.

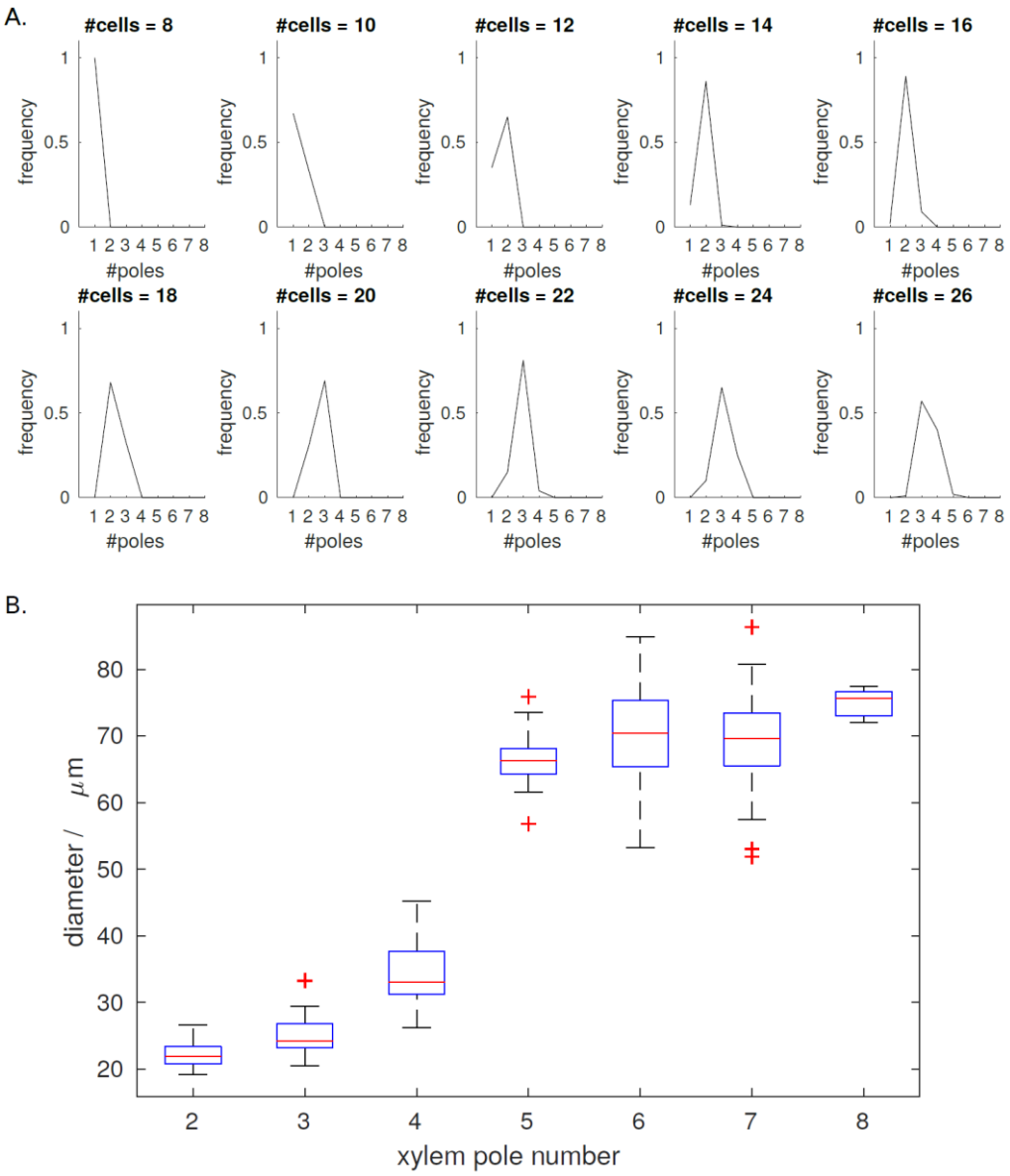


Figure 3. Vascular pattern is dependent on organ size. (A) Pole frequency plots for differently sized templates based on 100 simulations. For some sizes, only one pole number is observed, for others there are multiple possibilities. (B) Experimental data showing an increase in xylem pole number as a relationship to size for rice. Median values are shown with the red bar and the interquartile range is within the blue box

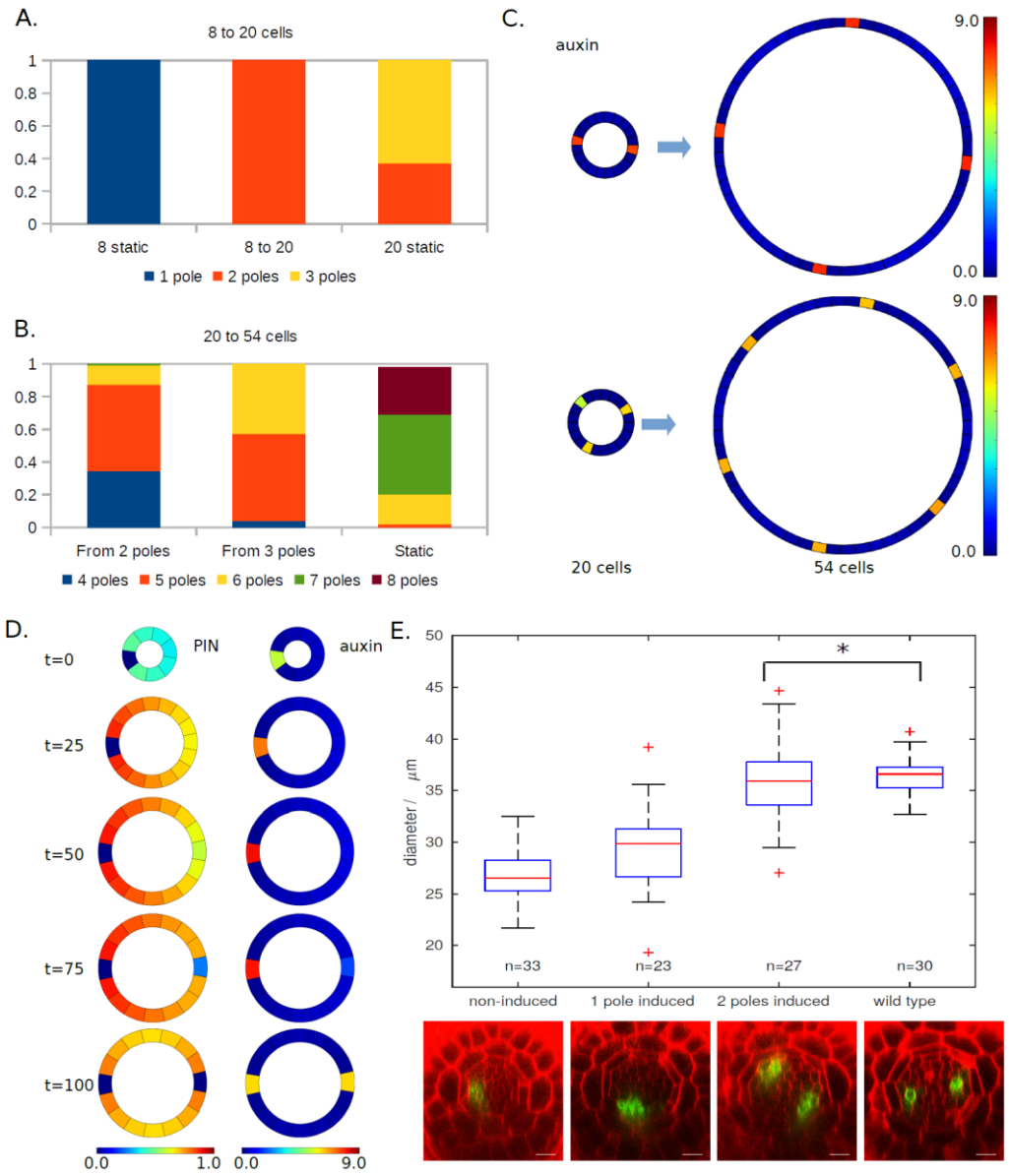


Figure 4. Growth history plays a key role in determining final organ pattern by stabilising the patterning processes. (A-B) Comparison of pole frequency in growing versus static 20-cell (A) and 54-cell (B) templates. (C) An example of different final outcomes (right) from different initial conditions (left) of templates grown from 20 to 54 cells. The heatmap shows auxin. (D) Rescue of the *lhw* phenotype in *pWOL>>XVE>>LHW* following 72h induction with β-estradiol. The graph shows the relationship between diameter and pole number with a representative image shown below. *AHP6::GFP* has been used as a marker for high auxin response and xylem identity.(E) Model simulation of *lhw* rescue line, showing the level of PIN (left) and auxin (right) in the growing template for four time steps post-simulated LHW induction.

SUPPLMENTARY INFORMATION: A core mechanism for specifying root vascular pattern can replicate the anatomical variation seen in diverse plant species.

Nathan Mellor, John Vaughan-Hirsch, Britta M Kümpers, Ana Campilho,
John King and Anthony Bishopp

S1 Introduction

Auxin promotes cytokinin biosynthesis in the Arabidopsis root stele via a linear sequence of transcriptional activation of the transcription factors *ARF5/MP*, *TMO5/LHW* and *LOG4*. While we assume that, due to its small molecular size, cytokinin is free to diffuse from cell to cell, it is known that the movement of auxin depends primarily on the presence of auxin influx and efflux transporters. One such efflux transporter, *PIN7* (which we refer to from now on as the more generic 'PIN'), is known to be up-regulated in response to auxin (though the intermediate transcription factors remain unknown). In addition, auxin promotes transcription of another transcription factor, *AHP6*, that interferes with cytokinin signalling. This network is summarised in Figure 2A, main text.

The net result of this is a system in which auxin simultaneously promotes the production of cytokinin while repressing its response. However, since cytokinin can diffuse into neighbouring cells, cells far enough away from an auxin source may be sufficiently free from the repression of the cytokinin response by auxin to produce PIN7. Given that PIN7 acts by actively transporting auxin out of cells, this further aids the establishment of a domain with low auxin and high expression of PIN7 (Figure 2B, main text).

S2 Model Formulation

S2.1 Dimensional model

To model the production of cytokinin and PIN we use Hill functions. Cytokinin production is an increasing function of auxin, and PIN production is represented by the product of an increasing function of cytokinin and a decreasing function of auxin. We assume a constant production rate of auxin, and linear degradation of auxin, cytokinin and PIN. The movement of cytokinin and auxin between cells is modelled by discretisations of diffusion operators, with auxin transport also dependent on the level of PIN in any given cell.

We denote the concentrations of auxin, cytokinin and PIN in cell i by A_i, C_i and P_i respectively, and use the following dimensional equations:

$$\frac{dA_i}{dt} = \alpha_A - \mu_A A_i + \frac{wD_A}{a_i}\frac{1}{P_{max}}\left(P_{i-1}A_{i-1} - 2P_iA_i + P_{i+1}A_{i+1}\right), \tag{1a}$$

$$\frac{dC_i}{dt} = \alpha_C \frac{\left(\frac{A_i}{\psi}\right)^m}{1+\left(\frac{A_i}{\psi}\right)^m} - \mu_C C_i + \frac{wD_C}{a_i}\left(C_{i-1} - 2C_i + C_{i+1}\right), \tag{1b}$$

$$\frac{dP_i}{dt} = \alpha_P \frac{\left(\frac{C_i}{\phi}\right)^{n_c}}{\left(1+\left(\frac{C_i}{\phi}\right)^{n_c}\right)\left(1+\left(\frac{A_i}{\theta}\right)^{n_a}\right)} - \mu_P P_i, \tag{1c}$$

where $i = 1, 2, ..n$, with n being the number of cells. We set $A_{n+1} \equiv A_0, C_{n+1} \equiv C_0, P_{n+1} \equiv P_0$ so that the model represents a 1-D ring of cells. Production rates are represented by α_A, α_C and α_P with the subscripts A, C and P referring to auxin, cytokinin and PIN respectively. Similarly, degradation rates are represented by μ_A, μ_C and μ_P; ψ, ϕ and θ are binding thresholds, while m, n_c and n_a are Hill coefficients.

The intercellular permeabilities of auxin and cytokinin are represented by D_A and D_C respectively (units ms^{-1}), w is the width of the ring, and a_i is the area of cell i. The constant P_{max} is required for dimensional consistency

and we choose for it the maximum possible steady state value of PIN, i.e.:

$$P_{max} \equiv \frac{\alpha_P}{\mu_P}$$

S2.2 Nondimensional model

Rescaling concentrations according to

$$A_i \to \frac{\alpha_A}{\mu_A}\overline{A}_i, C_i \to \frac{\alpha_C}{\mu_C}\overline{C}_i, P_i \to \frac{\alpha_P}{\mu_P}\overline{P}_i,$$

and setting

$$D_A \to w\overline{D}_A, D_C \to w\overline{D}_C$$

we have (after dropping the bar notation) the following:

$$\frac{dA_i}{dt} = \mu_A(1 - A_i) + \frac{w^2 D_A}{a_i}\left(P_{i-1}A_{i-1} - 2P_iA_i + P_{i+1}A_{i+1}\right), \tag{2a}$$

$$\frac{dC_i}{dt} = \mu_C\left(\frac{\left(\frac{A_i}{\psi}\right)^m}{1 + \left(\frac{A_i}{\psi}\right)^m} - C_i\right) + \frac{w^2 D_C}{a_i}\left(C_{i-1} - 2C_i + C_{i+1}\right), \tag{2b}$$

$$\frac{dP_i}{dt} = \mu_P\left(\frac{\left(\frac{C_i}{\phi}\right)^{n_c}}{\left(1 + \left(\frac{C_i}{\phi}\right)^{n_c}\right)\left(1 + \left(\frac{A_i}{\theta}\right)^{n_a}\right)} - P_i\right). \tag{2c}$$

In the static case, where all cells have equal size, we define w so that $a_i = w^2$ for all i (i.e. we assume the cross-sectional area of each cell is approximately the square of the contact length between them) and we have:

$$\frac{dA_i}{dt} = \mu_A(1 - A_i) + D_A\left(P_{i-1}A_{i-1} - 2P_iA_i + P_{i+1}A_{i+1}\right), \tag{3a}$$

$$\frac{dC_i}{dt} = \mu_C\left(\frac{\left(\frac{A_i}{\psi}\right)^m}{1 + \left(\frac{A_i}{\psi}\right)^m} - C_i\right) + D_C\left(C_{i-1} - 2C_i + C_{i+1}\right), \tag{3b}$$

$$\frac{dP_i}{dt} = \mu_P\left(\frac{\left(\frac{C_i}{\phi}\right)^{n_c}}{\left(1 + \left(\frac{C_i}{\phi}\right)^{n_c}\right)\left(1 + \left(\frac{A_i}{\theta}\right)^{n_a}\right)} - P_i\right). \tag{3c}$$

Two key parameters controlling pole spacing are D_A (increasing this enhances the spatial range over which a pole can deplete auxin from its neighbours, thereby enabling larger spacing between poles) and ψ (increasing this effectively increases the overall production rate of auxin, allowing more cells to exceed the theshold concentration, and hence potentially decreasing the pole spacing).

S2.3 Growth

The increase in the area of cell i over time is based on the following ODE:

$$\frac{da_i}{dt} = \eta(a_{max} - a_i)$$

in which η is the growth rate, and a_{max} the maximum cell area. For simplicity, we implement this using the following difference equation:

$$a_i(t + s) = a_i(t) + \eta\ s(a_{max} - a_i(t)), \tag{4}$$

where s is the timestep, and $a_i(t)$ denotes the area of cell i at time t. This leads to a dilution of auxin and cytokinin as the cell grows:

$$A_i(t + s) = \frac{A_i a_i(t)}{a_i(t + s)},$$

$$C_i(t+s) = \frac{C_i a_i(t)}{a_i(t+s)}.$$

PIN is membrane bound; we assume that its concentration is unchanged during growth and that the size of the dividing walls remain the same.

S2.4 Division

The cell division model is threshold based and driven by an additional model component that, like PIN, is cytokinin responsive and inhibited by auxin. We denote this component R_i for the concentration in cell i, and model its evolution over time by the following:

$$\frac{dR_i}{dt} = \mu_D \left(\frac{\left(\frac{C_i}{\xi}\right)^{n_d}}{\left(1+\left(\frac{C_i}{\xi}\right)^{n_d}\right)\left(1+\left(\frac{A_i}{\theta}\right)^{n_a}\right)} - R_i \right). \tag{5}$$

Using the same form of equation, but distinguishing it from PIN by introducing the new parameters ξ and n_d, allows for a higher cytokinin threshold for its production to be set. This means that in the *lhw* simulations (see below) the lower level of cytokinin is sufficient to drive weak PIN expression, but not cell divisions.

Each cell has two time-based properties determining whether or not they will divide, denoted 'interphase' (I) and 'mitosis' (M), roughly corresponding to the two biological states after which they are named. Both are initially zero for all cells. We first check if the maximum I is bigger than some threshold (λ_I), and that there are no other cells currently dividing (i.e. that no cells have $M > 0$). If so we increment M a small amount for that cell, and reset I for that cell to zero. Then, for each cell, if M is zero and R is above a given threshold (λ_D)

$$I_i(t+s) = I_i(t) + R_i(t) * s;$$

otherwise:

$$M_i(t+s) = M_i(t) + s,$$

so one and only one of I and M is incremented for a given cell at each timestep.

Finally, if any M exceeds a final threshold λ_M, the cell divides. The area of the two new cells is half that of the parent cell, while the concentrations of auxin, cytokinin, PIN and the cytokin response R remain the same. Mitosis and interphase are reset to zero for both new cells.

Division is be stopped when either a certain number of cells is reached or some total circumference is exceeded.

S2.5 Timestep schedule and implementation

The static model is implemented using Matlab, with ODEs solved using the ode15s function. The growing model is implemented using the Python programming language, with the ODEs solved using the 'odeint' function in the Scipy package. The ring representations of model results were plotted using the matplotlib package. For the growing model, at each timestep we run

1. the ODE model
2. the growth model
3. the division model

in that order for the specified timestep. Steps two and three can be skipped if the time is less than some 'embryonic time' parameter, allowing the ODE model to get near to steady state before the ring grows.

To produce the pole frequency plots in Figures 3A, S2-S6, and S8-S9 we used a automated loop during which the number of poles were counted using k-means clustering. The set of values for auxin in each cell is split into two subsets based on their mean values using the kmeans algorithm in Matlab (Figures 3A, S2-S6) and Scipy (Figures S8-S9), with the subset with the higher mean value taken contain only the poles. The size of this subset was used as the pole count for that particular run of the simulation.

S2.6 Simulation of Lonesome Highway (LHW) rescue line

To simulate the LHW induction line prior to induction we insert a multiplier (γ) in the production rate of cytokinin in equation (2b) so that:

$$\frac{dC_i}{dt} = \mu_C \left(\frac{\gamma \left(\frac{A_i}{\psi}\right)^m}{1 + \left(\frac{A_i}{\psi}\right)^m} - C_i \right) + \frac{w^2 D_C}{a_i} \left(C_{i-1} - 2C_i + C_{i+1} \right).$$

Setting $\gamma < 1$ in the *lhw* mutant simulation reduces the maximum cytokinin production rate compared to wild type.

To run the model we add an additional time parameter, the 'induction time', to simulate the induction of LHW at a given point in time. Experimentally this induction of LHW is driven by the introduction of oestrogen. The model runs with γ set to the *lhw* mutant value (< 1) until the 'induction time' is reached. Then, to simulate the induction of LHW, γ is increased to one and the production of cytokinin is as in the wild type model.

S3 Parameters and Initial Conditions

The default parameter values used in the models are given in Table 1. Based on observation, largely through trial and error, the Hill coefficients, m, n_c, and n_a must be set greater than two to see any patterning, so we choose the lowest integer value greater than this as the default value. D_A and D_C are the respective permeabilities of auxin and cytokinin which we assume to be roughly equal (when PIN is present in the case of auxin). In order for patterning to occur D_A needs to be sufficiently large when PIN is present in a particular cell to deplete auxin from neighbouring cells. We choose $D_A = 40$ as, when used in conjunction with the other parameters, this results in two poles more often than not for a 14 cell model, roughly equivalent to experimental observation in Arabidopsis (Figure S2). The sensitivity parameters ψ, ϕ and θ were also chosen so that patterning would occur with a pole spacing roughly equivalent to that seen in Arabidopsis.

Division and growth parameters are selected so that the biochemical model timescales are shorter than those of growth. We assume that the representative division gene is less sensitive to cytokinin than PIN and set $\xi = 0.2$ (compared to $\phi = 0.1$). Finally we assume that peak cytokinin production is reduced by half in the *lhw* mutant so set $\gamma = 0.5$.

Initial conditions of all model components are equal to zero in all cells, except for auxin which has a random distribution of auxin taken from a normal distribution with mean = 1.0 and standard deviation = 0.01. In the growing model the initial size of the cells is also taken from a normal distribution with mean = 1.0 and standard deviation = 0.01.

S4 Supplementary Figures

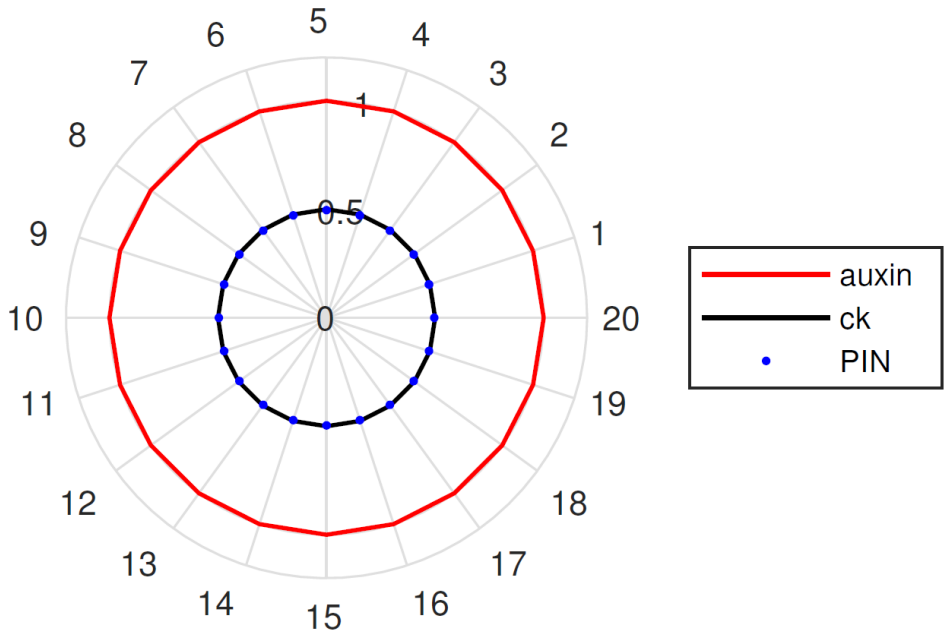


Figure S1: Spatially homogenous steady state of (3a) using parameters in Table 1, with 20 cells and uniform initial conditions (all components equal to one in all cells).

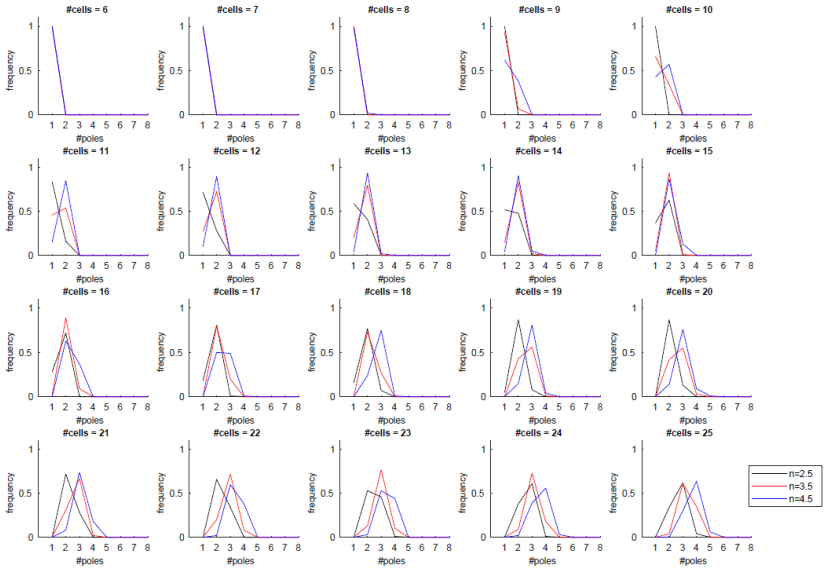


Figure S2: Effect of Hill coefficient n (representing parameters m, n_c, n_a) on pole number frequency distribution with increasing cell number (100 model runs for each cell number with random initial auxin taken from normal distribution with mean=1, s.d.=0.01). All other parameters as in Table 1. In general, increasing n increases the number of poles for a given number of cells. No patterning occurs for $n \leq 2$ (not shown).

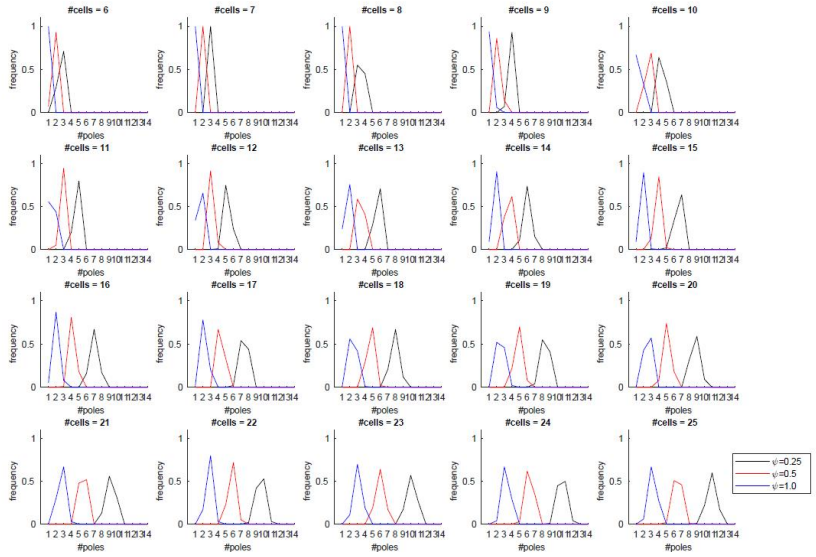


Figure S3: Effect of sensitivity of cytokinin and PIN to auxin (ψ and θ) on pole number frequency distribution with increasing cell number (100 model runs for each cell number with random initial auxin taken from normal distribution with mean=1, s.d.=0.01). All other parameters as in Table 1. In general, decreasing ψ increases the number of poles for a given number of cells. No patterning occurs for $\psi \geq 1.3$ and $\psi \leq 0.1$ (not shown).

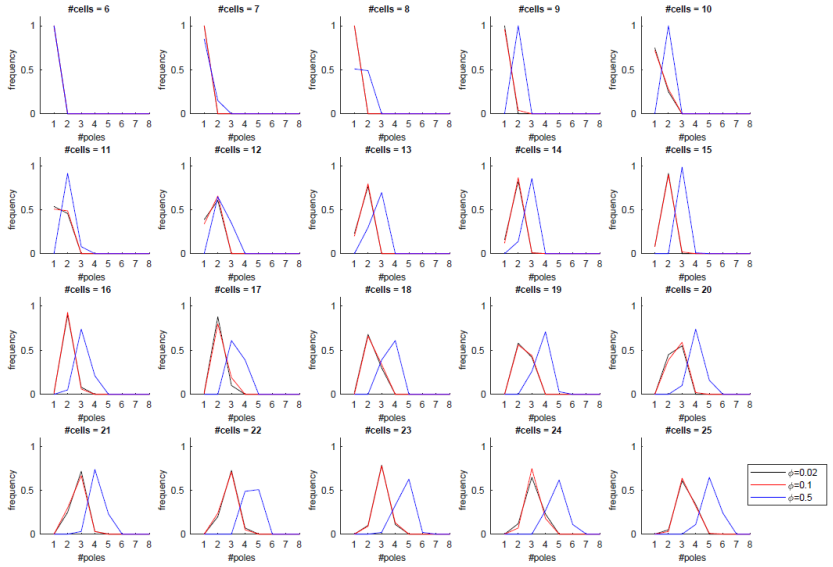


Figure S4: Effect of sensitivity of PIN to cytokinin (ϕ) on pole number frequency distribution with increasing cell number (100 model runs for each cell number with random initial auxin taken from normal distribution with mean=1, s.d.=0.01). All other parameters as in Table 1. In general, decreasing ϕ increases the number of poles for a given number of cells. No patterning occurs for $\phi \geq 1.7$ (not shown).

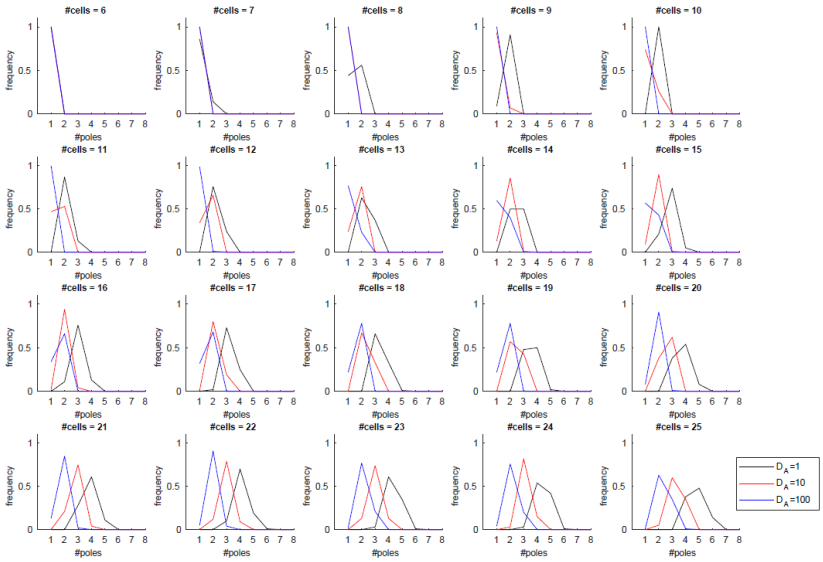


Figure S5: Effect of auxin permeability (D_A) on pole number frequency distribution with increasing cell number (100 model runs for each cell number with random initial auxin taken from normal distribution with mean=1, s.d.=0.01). All other parameters as in Table 1. In general, decreasing D_A increases the number of poles for a given number of cells. No patterning occurs for $D_A \leq 1$ (not shown).

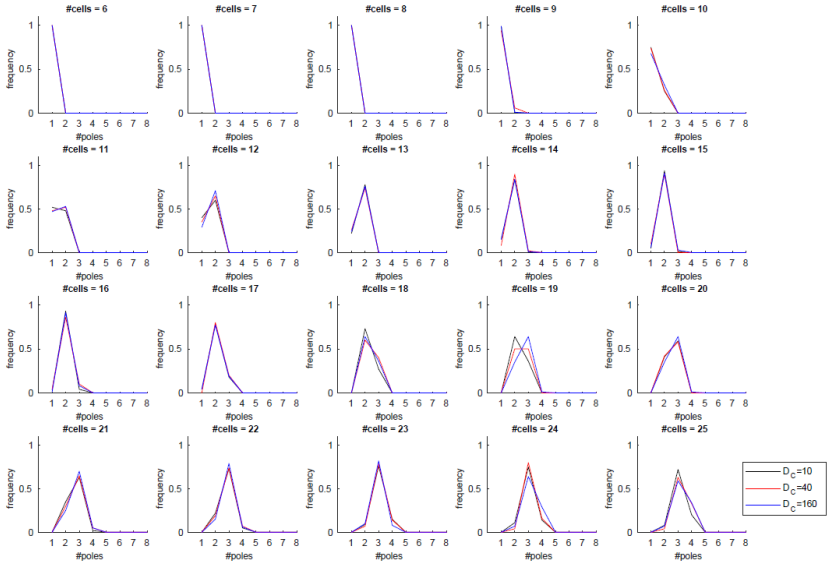


Figure S6: Effect of cytokinin diffusivity (D_C) on pole number frequency distribution with increasing cell number (100 model runs for each cell number with random initial auxin taken from normal distribution with mean=1, s.d.=0.01). All other parameters as in Table 1. In general, changing D_C has no effect on the number of poles for a given number of cells.

Table 1: Nondimensional parameters, with default values.

Biochemical model	
D_A	40
D_C	40
ψ	1.0
ϕ	0.1
θ	1.0
m	3
n_c	3
n_a	3
μ_A	1
μ_C	1
μ_P	1
Growth model	
η	0.1
a_{max}	1.5
w	1
Division model	
ξ	0.2
n_d	2
λ_I	3.0
λ_M	1.0
λ_D	0.25
lhw model	
γ	0.5

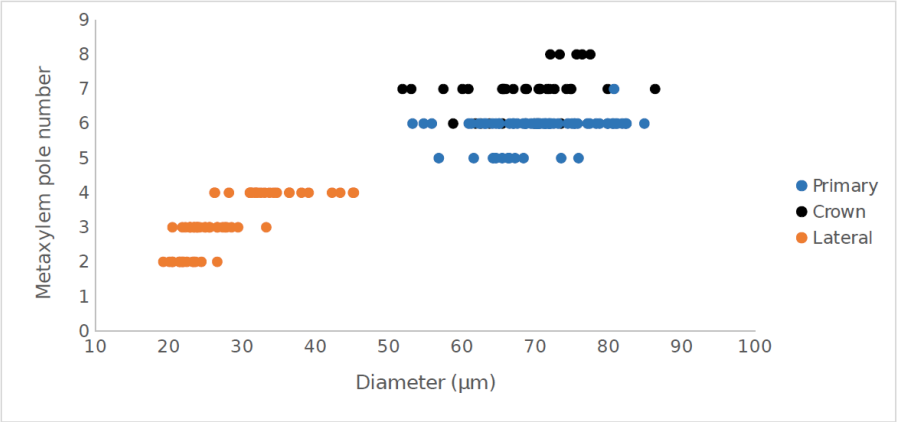


Figure S7: Metaxylem pole number against diameter for each individual lateral, crown and primary assayed (see main text and main text Figure 3B).

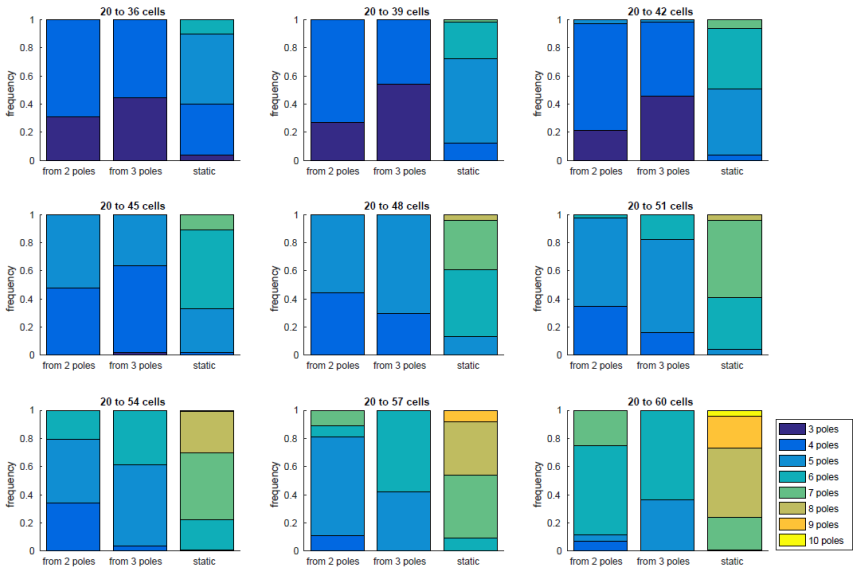


Figure S8: Frequency of poles for the growing ring simulation, starting from a steady state pattern for 20 cells, and growing to a range of final cell numbers (36 to 60 cells). The results are categorised according to whether the initial 20 cell steady had two or three auxin poles. 100 model runs for each subplot. In most cases initial conditions appear to influence the final state of the model.

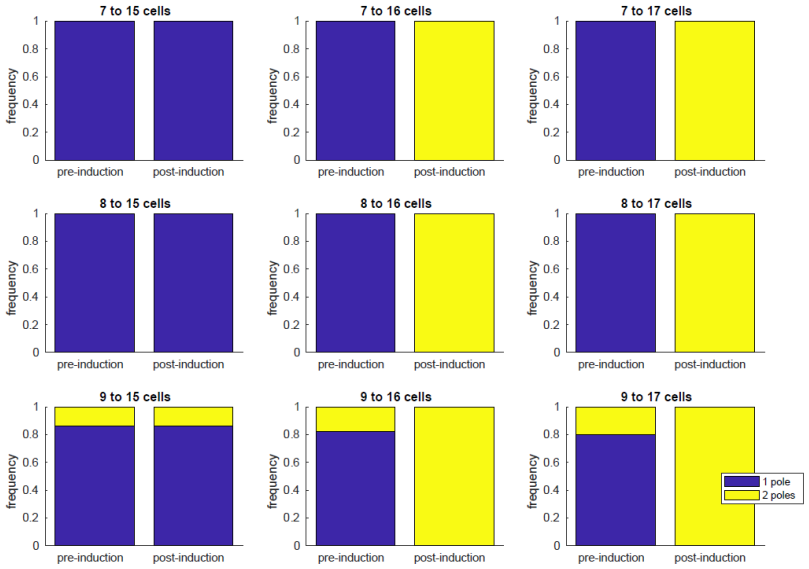


Figure S9: Frequency of poles for the *lhw* rescue simulation (see section S2.6), pre- and post- simulation LHW induction for a range of cell number transitions during growth. 100 model runs for each subplot. Increasing the ring size to 15 cells is insufficient to generate another pole, while starting from 9 cells results in two poles pre-induction around 10-20% of the time. Otherwise the model changes from one to two poles every time.